TRANSPORT OF HYDROPHOBIC ORGANIC COMPOUNDS BETWEEN

WATER AND NATURAL SEDIMENTS

by

Shian-chee Wu

B. S.   National Taiwan University
(1974)

M. E.   National Taiwan University
(1981)

SUBMITTED TO THE DEPARTMENT OF CIVIL ENGINEERING

IN   PARTIAL FULFILLMENT OF THE REQUIREMENTS

FOR THE DEGREE OF

DOCTOR OF PHILOSOPHY

at the

MASSACHUSETTS INSTITUTE OF TECHNOLOGY

June 1986

© Massachusetts Institute of Technology

Signature of Author _____
Department of Civil Engineering
June 23, 1986

Certified by _____
Philip M. Gschwend
Thesis Supervisor

Accepted by _____
Ole S. Madsen
Chairman, Department Committee

TRANSPORT OF HYDROPHOBIC ORGANIC COMPOUNDS BETWEEN

WATER AND NATURAL SEDIMENTS

by

Shian-chee Wu

Submitted to the Department of Civil Engineering

on June 23, 1986 in partial fulfillment of the

requirements for the Degree of Doctor of Philosophy

in Civil Engineering

ABSTRACT

Experimental results support the hypothesis that the rate of sorption of hydrophobic organic compounds on natural sediments and soils is controlled by molecular diffusion of the sorbate in the intraparticle pores and local equilibrium between the sorbed-to-solid species and the dissolved species in the porous sediment aggregates. A radial diffusion sorption kinetic model is developed to describe this sorption behavior. The modelling parameter, effective diffusivity, can be estimated from chemical and physical properties of the environmental system of interest (i.e., octanol-water partition coefficient, molecular diffusivity, sediment organic carbon content, intraparticle porosity, and aggregate bulk density).

This model not only extents our understanding of the sorption process but also enables us to predict sorption behavior a priori. A numerical modelling scheme is formulated to handle a wide particle size distribution and time varying solution concentrations, which are common in field situations. Model simulations are performed to demonstrate the feasibility of incorporating this sorption kinetics description into chemical fate models. The validity of a geometric-mean-size simplification and a first-order exponential approximation for sorption kinetics are evaluated by using the numerical radial diffusion model. The criteria for selecting these alternative solutions are established.

Results of microcosm experiments show that when conveyor-belt type bioturbation by tubificid worms greatly enhances the transport of PCBs between sediment beds and the sediment surface, sorption kinetics controls the transfer of compounds between reworked sediments and the overlying water. Model simulations with an integrated chemical transport model compare favorably with the experimental results.

Thesis Supervisor: Dr. Philip M. Gschwend
            Title: Associate Professor

To my country, my teachers, and my family.

ACKNOWLEDGEMENT

TABLE OF CONTENTS

6

List of Figures

List of Tables

CHAPTER 1 Introduction

Human activities have brought significant amounts of a variety of organic
chemicals into natural water bodies. Polychlorinated biphenyls (PCBs),
pesticides (e.g., kepone), petrochemical products and halogenated solvents are
classic examples (Saleh and Lee, 1978; Lopez-Avila and Hites, 1982; Brown et
al., 1985). Many of these compounds, especially those which are hydrophobic,
are strongly associated with natural particles (Chiou et al., 1979; Karickhoff
et al., 1979).

River and marine environments receiving polluted discharges retain large
amounts of these hydrophobic pollutants in their sediment beds. Typical
examples include PCBs in the Hudson River (Turk, 1980; Bopp et al., 1981),
PCBs in New Bedford Harbor and the nearby coastal area (Brownawell and
Farrington, 1986), and kepone in the James River Estuary (Huggett et al.,
1980). These sediments become the primary supplier of the contaminants long
after the elimination of direct discharge into the water bodies.

The fate of these pollutants is significantly affected by their sorption
behavior. For substances which undergo chemical or biological degradation or
have toxic effects to aquatic organisms, sorption is a competing reaction
lowering the activities of the substances and altering the degradation rate
(Zepp and Schlotzhauer, 1979). The rate of transport of solid-bound pollutant
can be quite different in a quiescent river or during storm events when
erosion of surface soils or sediments occurs (Turk, 1980). The migration and
dispersion of pollutants in sediment beds or groundwater aquifers are greatly
reduced when a significant portion of the substance is sorbed to the immobile

matrix (Schwarzenbach et al., 1983). Consequently, the tendency to sorb, the kinetics of sorption, the transport of pollutants in the sediment beds, and the mass exchange between solids and the aqueous phase at the bed/water interface are all important processes which need to be studied to facilitate the prediction of the fate of these hydrophobic compounds and the human hazard they present.

Attempts have been made to include the sediment bed into chemical fate models in aqueous environments (Onishi and Wise, 1982; Ambrose et al., 1983). The modelling approach is to describe the distribution ratio of a pollutant between the solid phase and the aqueous phase with an equilibrium model. This model is based on the concept of partitioning between the aqueous phase and the organic matter "solvent" phase (Karickhoff et al., 1979; Means et al., 1980, Schwarzenbach and Westall, 1981, and Appendix 1), i.e.:

$$S\text{(mass of compound/g of solid)} = K_p \cdot C \text{ (mass of compound/cm}^3 \text{ of solution)}$$

$$(1.1)$$

in which K_p is the partition constant (cm^3/g).

The equilibrium partition model is often adequate to describe transfer phenomena, particularly when solid-solution contact times are relatively long (days to months). Examples where equilibrium descriptions appear appropriate include organic compound exchange between slowly settling suspended solids in lakes and rivers and to and from aquifer soils and groundwater percolating at common flow velocities.

However, there is evidence that in some situations sorption/desorption transfers are sufficiently slow as to invalidate the use of equilibrium models. Several investigators evaluating the transport of organic compounds through leached soil columns have found both asymmetric distributions of chemical concentrations versus depth and non-sigmoid or tailing breakthrough curves (Kay and Elrick, 1967; van Genuchten and Wierenga, 1976; Rao et al., 1979; Schwarzenbach and Westall, 1981). These observations are best explained by recognizing that the sorptive exchange "reactions" or mass transfers are slow with respect to advective flow of the pore fluids. Investigations of the release of organic pollutants from contaminated sediments also provide evidence for sorptive exchange limiting transport. For example, transfer of phthalates and polychlorinated biphenyls from natural sediments, especially those deposited as fecal pellet aggregates and those exposed to the pollutant for extended times (> months), has been found to occur on timescales of days to months (Freeman and Cheung, 1981; Karickhoff, 1984; Karickhoff and Morris, 1985).

In all of these cases, fluid-solid contact time is short (minutes to days), and mass transfers do not proceed to completion before "new" fluids have displaced incompletely equilibrated "old" fluids. Other situations where sorption kinetics will undoubtedly play a role include storm-derived resuspension of quickly redeposited bed sediments; soils rapidly infiltrated by heavy rains, flooding events, or wastewater applications; and sediment-water mixing associated with dredging and dumping operations. Consequently, to assume equilibrium between solids and aqueous phase may result in significant error in prediction of chemical fate in the

aforementioned situations. Consideration of the need to incorporate a quantitative description of sorption kinetics into the pollutant transport models forms the basis of this thesis.

Although many models have been developed to simulate sorption kinetics, they all contain empirical fitting parameters which are not predictable from given environmental conditions. Studies of the properties of sediments and soils suggest that natural particles are often aggregates of fine mineral grains and natural organic matter (Johnson, 1974; Zabawa, 1978; Chase, 1979; and Stevenson, 1982). Following the approach of modelling sorption of organic compounds by porous activated carbon, synthetic resins, and catalyst pellets (Mathews and Weber, 1976; Prasher and Ma, 1977; and Weber and Liu, 1980), we developed and experimentally verified a sorption kinetic model based on the intraparticle molecular diffusion and phase partitioning processes and the commonly available parameters used to describe them. This work constitutes Chapter Two of the thesis.

Analytical solutions of this intraparticle diffusion model are only available for uniform particle size and simple boundary conditions (i.e., a constant concentration on the particle surface or a well mixed closed system) (Crank, 1975). However, particle sizes in natural waters vary widely and temporal and spatial variation of aqueous concentrations are very common in the environment. In Chapter Three, we formulate a numerical solution based on the retarded radial diffusion mechanism to cope with the kinetic problems in a variety of environmental situations. Model simulations are conducted to test the performance of this numerical model in some hypothetical cases and to establish criteria for the selection of alternative approximate solutions

(i.e., analytical solutions with a geometric-mean size and the first-order approximation).

In order to incorporate sorption kinetic description in the chemical fate model, we extend existing models for mass transport in the sediment bed (Schink and Guinasso, 1978; and Berner, 1980) to include three sorbate species (i.e., free in solution, sorbed on particles, and carried by colloids or macromolecules) and, most importantly, the exchange kinetic or equilibrium relationships among them. Two types of microcosm experiments with different dominant transport processes, molecular diffusion in the pore water and conveyer-belt type biogenic sediment mixing, are performed to demonstrate the predictive capability of this integrated chemical transport model. The model development and experimental results are presented in Chapter Four.

Chapter Five is a summary of this thesis. Additional information of relevance to the body of the thesis are included in the appendices. Appendix 1 is a list of notations used in this thesis. A previous study on the effects of nonseparable microparticles or macromolecules on the observed partition coefficient is shown in Appendix 2. The effects of energy input by stirring or bubbling on the sorption kinetics are discussed in Appendix 3. A computer program for the numerical model of sorption kinetics is listed in Appendix 4. The numerical model and computer program for chemical transport in the sediment bed are described in Appendix 5 and Appendix 6, respectively.

CHAPTER 2

Sorption Kinetics of Hydrophobic Organic Compounds to

Natural Sediments and Soil

2.0 Introduction

Many models have been developed to simulate sorption kinetics. Among

them the one-box model is the simplest model in which the sorption rate is a

first order function of concentration difference between the sorbent (viewed

as a completely mixed box) and the solution, and is quantified by a single

rate constant, k_f, (Figure 2.1) (Lapidus and Amundson, 1952; Oddson et al.,

1970). This mathematical formulation implies that sorptive exchange is

limited by only one of many conceivably important processes including binding

by a single class of sorbing site or mass transfer across a boundary.

However, the one-box model does not fit experimental data well. Sorption

kinetics data always show a rapid initial uptake followed by a slow approach

to equilibrium (Leenheer and Ahlrichs, 1971; van Genuchten and Wierenga, 1976;

Karickhoff, 1980; and this work). The improved modelling approach typically

utilized involves subdividing the sorbent into two compartments. This

conceptualization corresponds to physical situations in where there are two

classes of sorbing sites, two chemical reactions in series, or a sorbent with

an exterior part (easily accessible) and an inner part (exchanging slowly)

(Figure 2.1). Unfortunately, this type of model retains three independent

fitting parameters (i.e., k_1, the exchange rate from the solution to the first

box; k_2, the exchange rate from the first box to the second box; and X_1, the
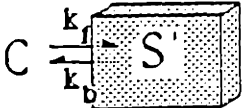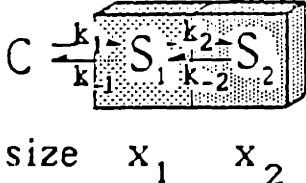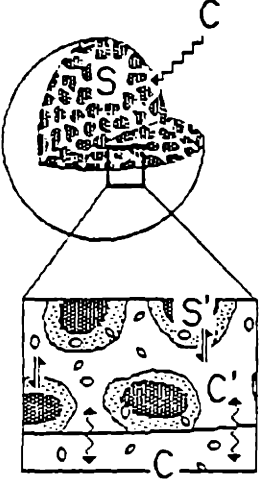
Kinetics Models	Independent Kinetics Fitting Parameters (derived parameters)
One-box model	k_f $$(k_b = k_1 / K_p)$$
Two-box model size x_1 x_2	k_1, k_2, x_1 $$(k_{-1} = k_1/K_p)$$ $$(k_{-2} = k_2)$$ $$(x_2 = 1 - x_1)$$
Diffusion model	D_{eff}

Figure 2.1   Comparison of three sorption kinetics models. K_p is the
partition coefficient.

fraction of total sorbing capacity in the first box) which can not be easily

evaluated or estimated for new combinations of chemicals and solids. Numerous

other mass transfer approaches (e.g., those reviewed in Hendricks and Kuratti,

1982) similarly suffer in having no fundamental basis on which to predict the

values of the model parameters.

Therefore, the objective of this work was to develop and experimentally

verify a model of sorption kinetics which is based on known physical and

chemical processes (i.e., molecular diffusion and phase partitioning) and the

commonly available parameters used to describe them.

2.1 A Radial Diffusion Sorption Kinetics Model

As a point of departure, we assume that the sediment and soil particles

of most concern for hydrophobic organic compound sorption are aggregates of

fine mineral grains and natural organic matter. The aggregate nature of

natural sorbents as they exist in the environment, including suspended solids

(Zabawa, 1978; Chase, 1979), sediments (Johnson, 1974), and soils (Black et

al., 1965; Brady, 1974; Steveson, 1982), is well documented. Therefore,

following the previous suggestion of Leenheer and Ahlrichs (1971) we

hypothesize that the kinetics of solution-solid exchange should be described

as a radial diffusive penetration of organic pollutants into these porous

natural particles. That is, sorbate molecules diffuse through the pore fluids

held in the interstices of natural silt aggregates and their penetration is

"retarded" by microscale partitioning of the compounds between essentially

mobile (i.e., dissolved in intraparticle pore fluids) and immobile (i.e.,

in/on intraparticle solids) states of the organic chemical.

This physical conceptualization suggests that the same approaches used to develop intraparticle diffusion models in synthetic particles may be appropriate for natural sorbents. Chemical engineers have long considered intraparticle diffusion to limit sorption of organic compounds by activated carbon, synthetic resins, and porous catalysts (Mathews and Weber, 1976; Prasher amd Ma, 1977; Sudo et al., 1978; Weber and Liu, 1980). Similarly, separation scientists have used intraparticle diffusion models to explain chromatographic phenomena (Karger et al., 1973). Soil scientists have recently demonstrated the effectiveness of this physical view for transport of conservative chemicals through soils in their natural aggregate state (Rao et al., 1979; Rao et al., 1980). For the following model development discussion, derived from the engineering, soil science, and separation science literature, it will be assumed that the sorbents of interest are spherical and internally homogeneous porous media (Rao et al., 1982). We shall confine our treatment here to instances in which the bulk fluid is sufficiently turbulent that an exterior boundary layer does not limit sorptive exchange. The boundary layer effect in our experimental conditions is discussed in Appendix 3 and has been effectively modelled previously by Connolly (1980).

The time rate of change of sorbed compound per unit volume can be mathematically expressed (Crank, 1975)

$$\frac{\partial S(r)}{\partial t} = D_m n \left[\frac{\partial^2 C'(r)}{\partial r^2} + \frac{2}{r} \frac{\partial C'(r)}{\partial r} \right] \tag{2.1}$$

where

S(r) is the local total volumetric concentration in the porous sorbent, mol/cm^3,

C'(r) is the compound concentration free in the pore fluid and varying with radial distance (r), mol/cm^3,

n is the porosity of the sorbent, cm^3 fluid/ cm^3 total, and

D_m is the pore fluid diffusivity of the sorbate, cm^2/s.

By definition

$$S(r) = (1-n)\rho_s S'(r) + nC'(r) \qquad (2.2)$$

in which

S'(r) is the concentration of the immobile bound state, mol/g, and

ρ_s is the specific gravity of the sorbent, g/cm^3.

If the pore fluid concentration and the solid-bound concentration are locally in equilibrium, a sorption isotherm relating these states applies such as

$$S'(r) = K_p C'(r) \qquad (2.3)$$

where K_p is the equilibrium partition coefficient, $(mol/g)/(mol/cm^3)$. This isotherm relationship can be used to restate the intraparticle diffusion

kinetics in S only

$$S(r) = (1-n)\rho_s K_p C'(r) + nC'(r)$$

$$= ((1-n)\rho_s K_p + n) \, C'(r) \qquad\qquad (2.4)$$

$$\frac{\partial S(r)}{\partial t} = \frac{D_m \, n}{((1-n)\rho_s K_p + n)} \left[\frac{\partial^2 S(r)}{\partial r^2} + \frac{2}{r} \frac{\partial S(r)}{\partial r}\right]$$

$$= D'_{eff} \left[\frac{\partial^2 S(r)}{\partial r^2} + \frac{2}{r} \frac{\partial S(r)}{\partial r}\right] \qquad\qquad (2.5)$$

where D'_{eff} is the effective intraparticle diffusivity, cm^2/s. When K_p is

large (true for hydrophobic compounds), the effective diffusivity, D'_{eff}, is

simply

$$D'_{eff} = \frac{D_m \, n}{(1-n)\rho_s K_p} \qquad\qquad (2.6)$$

One last consideration is that this model of radial diffusive penetration

assumes: (1) the entire surface area is available for mass flux, and (2) the

pathlength of diffusive transfer is straight and radially oriented. Clearly

the D_{eff} appropriate for natural silts must include a correction factor,

$f(n,t)$, which is a function of intra-aggregate porosity and tortuousity (t),

that is

$$\frac{\partial S(r)}{\partial t} = D_{eff} \left[\frac{\partial^2 S(r)}{\partial r^2} + \frac{2}{r} \frac{\partial S(r)}{\partial r} \right] \tag{2.7}$$

where

$$D_{eff} = D'_{eff} \cdot f(n,t)$$

This model of sorption kinetics is quite flexible and physically

reasonable. The compound properties (diffusivity in solution and

hydrophobicity) and those of the natural sorbents (e.g., organic content,

particle size, and porosity) can be used in the model to predict a priori

sorption kinetics for each chemical and/or site of interest.

2.2 Experimental Section

2.2.1 Materials

Four chlorobenzene congeners (1,4-dichlorobenzene; 1,2,4-

trichlorobenzene; 1,2,3,4-tetrachlorobenzene; and pentachlorobenzene) were

purchased from Foxboro/Analabs Co. (North Haven Connecticut) and used as

received. Milli-Q Water (Millipore, Bedford, Massachusetts) was used for

aqueous preparations.

Three natural sediments and soils were used in our experiments.

Sediments taken from river beds were air-dried, sieved through a No. 20

standard sieve (opening = 0.84 mm) and stored at room temperature. Air-dried

soil samples provided to us by Dr. S. Karickhoff of the Environmental Research

Laboratory, U.S. EPA, (Athens, Georgia) were previously treated similarly.

Soil and sediment suspensions used in the kinetics experiments were prepared

by adding about 50 mL of water to air-dried sediments or soils two days in

advance. The suspensions were shaken by hand several times during this two

day period to facilitate wetting and establishment of a natural aggregation

condition.

Some properties of the sediments are listed in Table 2.1. Wet particle

sizes were determined by sieving 2 liters of sediment suspension prepared two

days previously and containing 2 to 3 gm of dry sediments through standard

sieves (openings: 840 μm, 177 μm. and 88 μm) and Nitex® net (openings: 53 μm

and 28 μm). The amount of the smallest size fraction was determined by

measuring the total solid mass left in the suspension after the last sieving.

The dry solid densities were estimated with the specific gravity bottle method

(Black et al., 1965). The organic matter content was estimated by heating the

sample at 550°C for 25 minutes and determining the weight loss (Black et al.,

1965). Contaminated sediments were prepared by equilibrating an aqueous

solution of the test compound with a sediment suspension. Then, sediments

were separated from water by settling for one week and homogenized by

stirring. Water content, size distribution, and combustible loss were

measured as well.

Table 2.1 Properties of sediments and soils

Sample name	Source	Combustible[a] loss (550°C, 25 min) %	Dry density g/cm^3	Wet particle size distribution fraction by weight diameter µm					
				>840	840-177	177-88	88-53	53-28	<28
Charles River sediments	Charles River, MA.	17.0	2.25	0.03	0.34	0.14	0.14	0.17	0.18
contaminated Charles River sediments	prepared in our lab.	17.7	nd(c)	0.0	0.04	0.12	0.22	0.28	0.34
Iowa soils	EPA (EPA-10)	6.5 (f_{oc}=2.1%)[b]	2.6	0.04	0.32	0.15	0.15	0.27	0.08
North River sediments	North River MA.	8.8	2.51	0.01	0.19	0.23	0.18	0.15	0.24
contaminated North River sediments	prepared in our lab.	8.4	nd	0.0	0.02	0.06	0.17	0.43	0.32

(a): Combustible loss includes organic matter and possibly chemically bound water. The organic carbon content (f_{oc}) will be slightly less than one half of combustible loss (Black et al., 1967)

(b): The organic carbon content of Iowa Soils is 2.1 % (Dr. Karickhoff p. c.).

(c): nd = not determined.

2.2.2. Experimental Apparatus

We have developed an apparatus (Figure 2.2) which enabled us to continuously monitor the changing dissolved concentrations of hydrophobic sorbates on timescales of seconds to days without performing solid-solution phase separations which often lead to analytical difficulties (Appendix 2). The setup included a 2-liter reaction vessel which was continuously stirred with a magnetic stirrer. During periods of analysis, stripping air was pumped with a flow rate of 90 cm^3/s by a stainless steel bellows pump (MB-21, Metal Bellows Co., Sharon, Massachusetts) and recycled in a closed-loop all-glass system except that a small part of the flow was diverted through a parallel loop containing a photoionization detector, PID, (PI-52-02, HNU Systems Inc., Newton, Massachusetts). The PID measured the chemical concentration in the gas phase thereby reflecting the activity of the dissolved compound in the solid suspension. With small headspace volume (0.1 of suspension volume) and Henry's Law constants of 0.1 to 0.15 (mole/cm^3 air)/(mole/cm^3 water)) for the compounds studied, this apparatus could respond to changes in solution concentration with a time constant of 4 min^{-1} (i.e., 50% to equilibrium in 10 s) and could be used up to 48 hours without noticeable loss of compounds (e.g., due to leaks or decomposition by the PID). The temperature of the solution was maintained at 25°C ± 3°C with a hot plate. The loop of flow containing the detector was switched to an identical reference system with only water (not shown in Figure 2.2) in order to check the baseline detector response from time to time.

to recorder

photo-ionization
detector

2-liter
reactor

metal bellows
pump

magnetic
stirrer
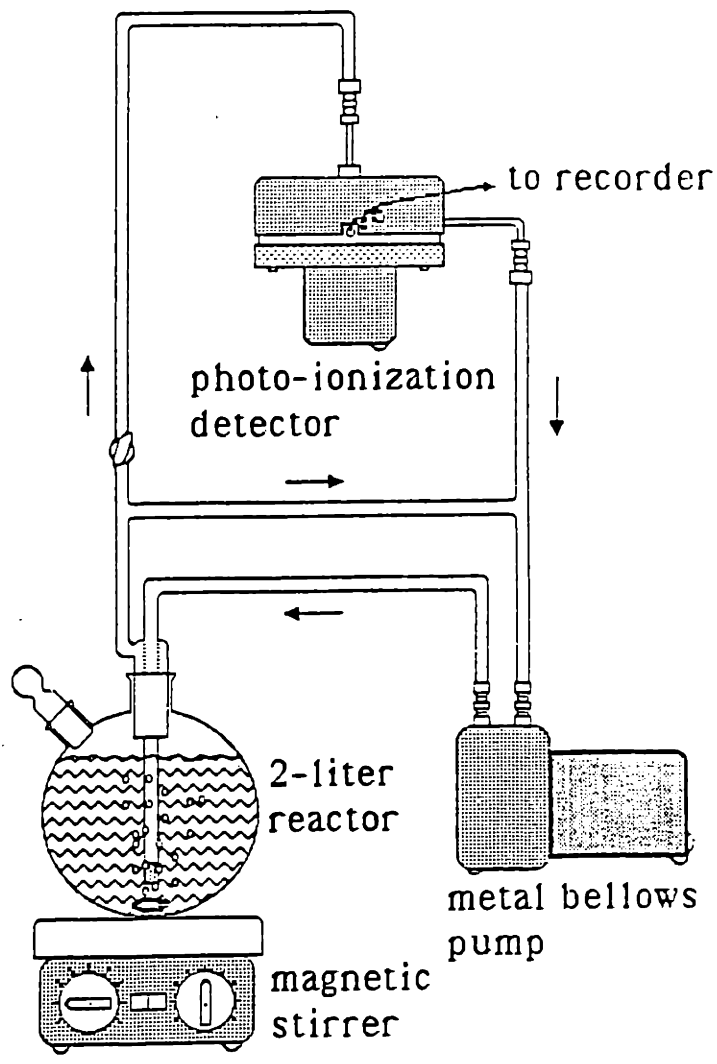
Figure 2.2   Apparatus for sorption-desorption kinetics experiments.

2.2.3. Experimental Procedure for Sorption and Desorption Kinetics

At the beginning of a sorption kinetics experiment only water and clean air were in the experimental system. The responses of the reaction system and the reference system were recorded. In order to dissolve the test compound into the water and avoid inclusion of microscopic crystals in the solution, a small crystal of the compound which had been weighed on a Cahn 25 microbalance (Cahn Instruments, Inc., Cerritos, California) was placed within a bolus of glass wool or carefully melted and recrystallized onto the glass wall of a removable section of tubing of the stripper in the gas path before the bubbler. By recirculating air through the stripper, the crystal sublimed and the compound was transferred to the aqueous solution within two days if the amount put in was smaller than the amount necessary to saturate the solution. If the solution became saturated, the remaining crystalline compound was removed and the concentration in the solution was lowered to 50% of the saturated concentration by stripping with clean air and monitoring the gas phase with the PID.

The sorption experiment was initiated by pouring about 50 mL of sediment or soil suspension into the side mouth of the reaction vessel. Tests showed that opening the side mouth for several seconds did not result in significant loss of compound from the system. The activity of the compound in the solution was monitored continuously during the first hour and was measured intermittently afterward. Typically, there was no measurable change of activity after 1 or 2 days. Therefore, the experiments lasted 2 or 3 days and the last measured activity was assumed to be the equilibrium activity at infinite time. Desorption experiments were similar to sorption experiments

32

except that contaminated sediments were poured into clean water in the reactor.

Since the size of the particle aggregates was expected to be a critical factor in controlling sorptive exchange, we examined the particle size distributions of Charles River sediments under continuous bubbling and stirring for different time periods. The results show that the particle size distribution shifted significantly to smaller sizes with combined bubbling and stirring (Figure 2.3). Therefore, sorption rates would be continuously increased throughout the experiment by shortening the diffusion path and increasing particle surface area. This phenomenon was observed in our early experiments (i.e., Experiments 1, 4, 5 and 6) in which the suspensions were bubbled throughout the experimental periods and the time to reach sorption equilibrium was relatively long. Consequently, we modified our subsequent experimental procedure so that continuous bubbling was used only for the first hour, and then limited to brief periods necessary to monitor the sorption progress at longer times. This procedure lowered energy input into the sediment suspension by about 95% and therefore greatly reduced the shearing causing particle disaggregation (details are described in Appendix 3). Thus, when we observe the size distribution for two days of continuous stirring (Figure 2.3), we observe much more stable particle size distributions.

2.3 Model Simulation

In order to evaluate the effectiveness of the radial diffusion model, model simulations were compared with the experimental results. In the
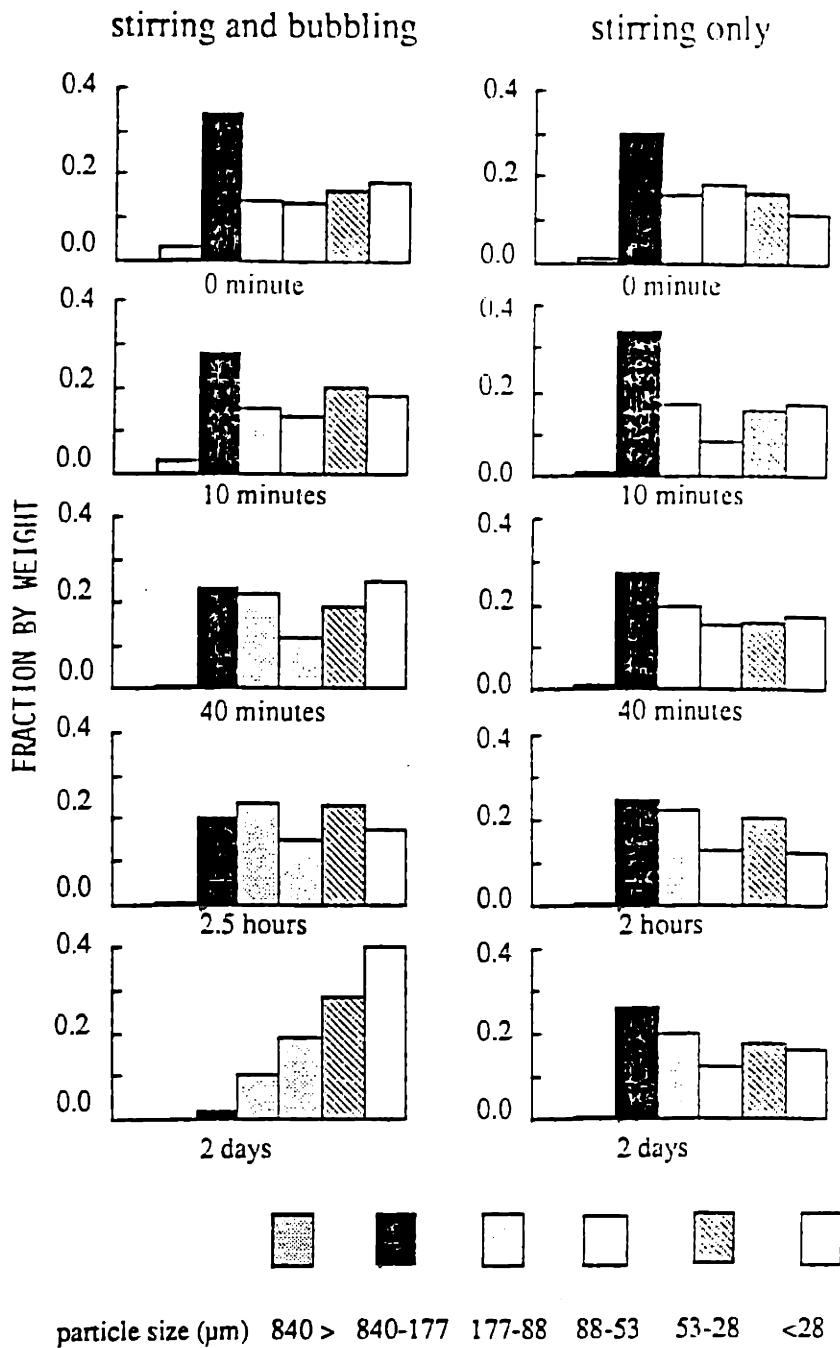
Figure 2.3   Particle size distributions of Charles River sediments during (a) continuous bubbling and stirring or (b) continuous stirring only.

intraparticle diffusion governing equation (Equation 2.7), the intraparticle

diffusivity, D_{eff}, is the only parameter necessary to quantify the process for

given conditions. The boundary condition at the particle surface (r=particle

radius, R) is given by the expression of local equilibrium assuming $K_p \gg$

$n/(1-n)\rho_s$:

$$S\ (r=R)\ =\ (1-n)\ \rho_s K_p C \qquad (2.8)$$

where C is the dissolved concentration in bulk solution. C is not necessarily

a constant. In our experimental conditions (i.e., a well-mixed closed system)

C can be related to S by a mass conservation equation:

$$\frac{V}{V_s}\ C\ +\ \overline{S}\ =\ \frac{V}{V_s}\ C_o\ +\ \overline{S}_o \qquad (2.9)$$

in which V and V_s are the total volume of solution and particles,

respectively. S_o is the average initial sorbed concentration over all

particles. The average concentration at any time, $\overline{S}$, is given by :

$$\overline{S}\ =\ \text{sum of }\{\ \frac{3}{4\pi R^3}\ \int_0^R\ 4\pi r^2\ S(r)\,dr\ \} \qquad (2.10)$$

Analytical solutions are available for this intraparticle diffusion

description of sorption kinetics in which all the particles are assumed to be

the same size and the exterior solution volume, V, is well-mixed (Crank,

1975). Analytical solutions, however, are only valid for simple boundary conditions and for a mix of particles having a very narrow size distribution (i.e., the particle sorption behavior can be represented by a single average diameter if the size distribution spans only about one order of magnitude, Cooney and Adesanya, 1983). In aquatic environments, the particles sizes of sediments and soils in their natural aggregated state span several orders of magnitude, and open systems in which bulk dissolved concentration varies with time are very common. Therefore, a numerical method was developed in which particles were divided into several size classes and the bulk dissolved concentration was allowed to vary. The details of the numerical method are described further in Chapter 3.

The best fit value of D_{eff} was obtained by adjusting the D_{eff} in the model so that the data points at the most rapidly changing section around the midpoint of equilibration, $t_{1/2}$, (i.e., when $(C-C_{equilibrium})/(C_o-C_{equilibrium}) = 0.5$) fell on the predicted curve. This method gives the best results because the predicted curve is very sensitive to the selected D_{eff} at $t_{1/2}$, and the effects of experimental errors at the very beginning and near the end of an experiment where errors are largest can be avoided.

When the time scale of sorption is close to the time scale of the apparatus response ($\ln 2/(4 \text{ min}^{-1})$), there will be significant error in the fit values of D_{eff} because what we measured was the true sorption kinetics response superimposed on an apparatus response. By assuming that the apparatus response to changes in solution activity of sorbates can be described with a first order rate expression and a response rate constant of 4

min^{-1}, we can estimate the extent to which the observed D_{eff} differs from a "true" value. Our worst cases (i.e., shortest time to exchange) involved dichlorobenzene sorption on Charles River ($t_{1/2}$ = 0.8 min, therefore $D_{eff,observed} \simeq 1.48\ D_{eff,true}$), and trichlorobenzene on the same sediments ($t_{1/2}$ = 1.6 min, therefore $D_{eff,observed} = 1.16\ D_{eff,true}$). Apparatus response errors are insignificant (<1%) for our other experimental results.

2.4 Results and Discussion

The experimental conditions and results are summarized in Table 2.2 and are shown in the Figures 2.4 to 2.8 and Figure 2.10. By plotting the ratio of $(C-C_e)$ to (C_o-C_e) in some figures the concentration change in solution is magnified. Two experiments (Figure 2.4) which were performed with the same compound and sediments and similar initial conditions show the reproducibility of this experimental protocol.

2.4.1 Evidence for Intraparticle Diffusion

The results show several very interesting features of sorption consistent with the intraparticle diffusion model. First, large particles show a slower sorption approach to equilibrium than otherwise similar smaller particles when we use the same sorbate (Figure 2.5). When the original sediments (with organic content of 17.7%) are disaggregated (i.e., by sonication) before sorption experiments, they demonstrate an even faster uptake rate. These three types of sediments have similar organic contents (17.7% to 25.5%) and,

Table 2.2 Experimental and model simulation results

sorption

Experiment number	Figure number	Sorbate [a]	C_o μM	C_e/C_o	Sorbent [b]	solid conc. ρ mg/L	Particle size μm	Temp. °C	K_p cm³/g	D_{eff} (from model fits of kinetics data) cm²/s
1	5	P	2.0	0.48	CR	235	mixed	23	4690	$<8.3 \ 10^{-11}$(d)
2	9-a	TR	13.7	0.29	CR	9350	mixed	24	265	$3.3 \ 10^{-10}$
3	9-a	D	4.4	0.39	CR	17900	mixed	22	87	$1.0 \ 10^{-9}$
4	5	TE	1.4	0.46	CR	968	mixed	24	1220	$<2.0 \ 10^{-10}$(d)
5	4	TE	3.2	0.39	CR	1030	96 μm	23	1520	$<2.5 \ 10^{-10}$(d)
6	4	TE,	3.7	0.62	CR	442	232 μm	28	1390	$<3.3 \ 10^{-10}$(d)
7	6	TE	2.5	0.58	CR	1060	mixed	55	684	$<4.2 \ 10^{-10}$(d)
8	6	TE	2.3	0.44	CR	1240	mixed	40	1020	$<4.2 \ 10^{-10}$(d)
9	9-b	TE	2.8	0.63	IS	10200	mixed	22	58	$1.0 \ 10^{-9}$
10	9-b	P	1.6	0.5	IS	4250	mixed	25	239	$2.5 \ 10^{-10}$
11	9-c	TE	2.5	0.54	NR	2050	mixed	23	418	$5.0 \ 10^{-11}$
12	9-c	P	0.4	0.45	NR	770	mixed	26	1560	$8.3 \ 10^{-12}$

desorption

13	9-d	TE	0.0	–	CR	2270	mixed	27	1220(c) 8.3 10^{-11}
14	9-d	TE	0.0	–	NR	2390	mixed	24	418(c) 1.3 10^{-10}

(a) P: pentachlorobenzene, TE: 1,2,3,4-tetrachlorobenzene, TR: 1,2,4-trichlorobenzene, D: 1,4-dichlorobenzene.

(b) CR: Charles River sediments, IS: Iowa soils, NR: North River sediments.

(c) K_p's of sorption cases were calculated from the observed dissolved concentration at the end of the kinetics experiments. K_p's of desorption cases were taken as same as the K_p's of corresponding sorption cases.

(d) The D_{eff}'s in these model simulation results are upper limits because of artificially higher uptake rate caused by bubbling-derived particle breakage.
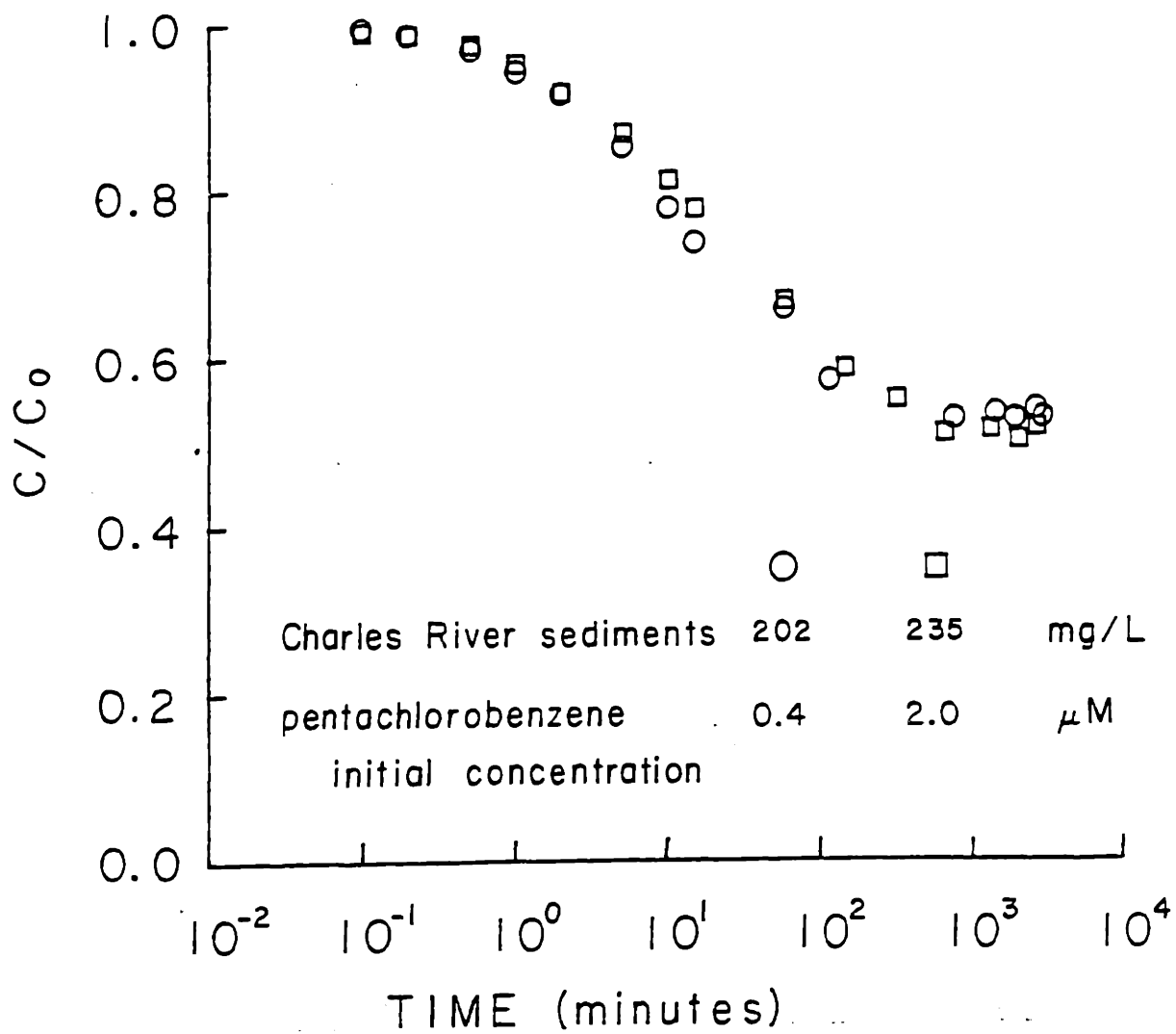
Figure 2.4   Experimental results of two similar treatments showing
reproducibility of the experimental protocol for sorption
kinetics.
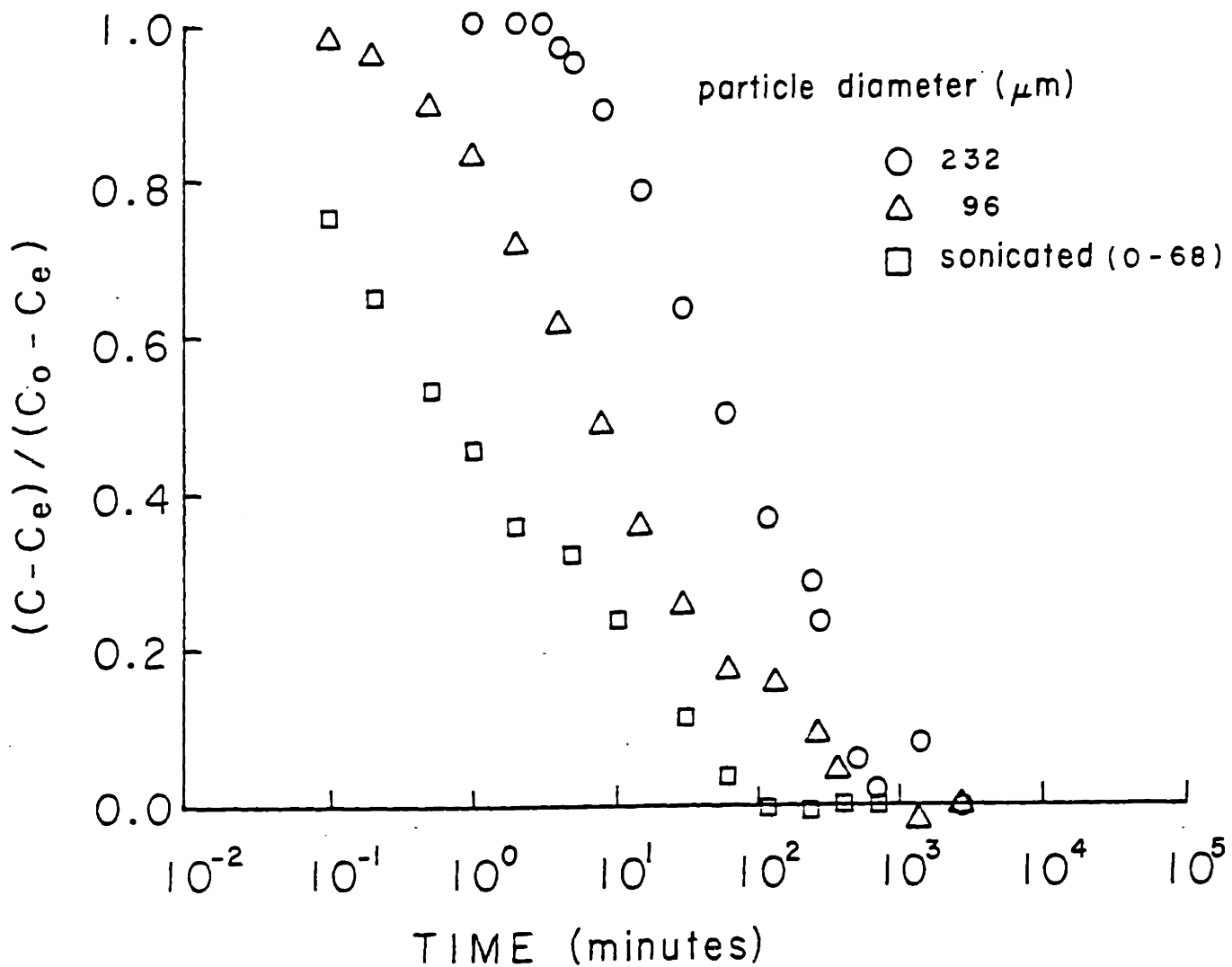
Figure 2.5   Sorption kinetics experimental results for tetrachlorobenzene

on Charles River sediments with two different particle sizes

and the same sediments disaggregated by sonication.

therefore, similar K_p. Clearly by reducing the diffusive pathlength into the interior of the particles and by increasing the exposed sorbent surface area, we can greatly increase sorption rates.

Second, compounds with greater hydrophobicity (i.e., higher K_{ow}) have slower uptake rates into the same sediments (Figure 2.6, K_{ow} from Chiou, 1985). This corroborates the previous results of Karickhoff (1980) who studied polycyclic aromatic hydrocarbons. This finding is important, because if local sorption equilibrium between molecules dissolved in pore fluids and those sorbed locally in the aggregates is always established, the chemicals with higher partition coefficients are predicted to penetrate the natural sorbent aggregates more slowly if diffusive transport occurs primarily in the intraparticle pore fluids. The compounds with higher molecular weight (also higher K_{ow} in this case) will penetrate slower because of lower diffusivities. Since molecular diffusivity is inversely proportional to one third power of molar volume (Satterfield, 1981), differences in the solution diffusivities do not vary greatly among these four compounds. Therefore, the effects of hydrophobicity dominate the variation of sorption rate for the different compounds.

Finally, over a temperature range of 30°C, there is no large change in sorption rates (Figure 2.7). The temperature could potentially affect the sorption rate in two ways in terms of intraparticle diffusion. First, diffusivities in solution and pore water vary directly with temperature. However, a temperature change of 30°C corresponds to only about a 10% range in molecular diffusivities (Satterfield, 1981), and we do not believe our

42
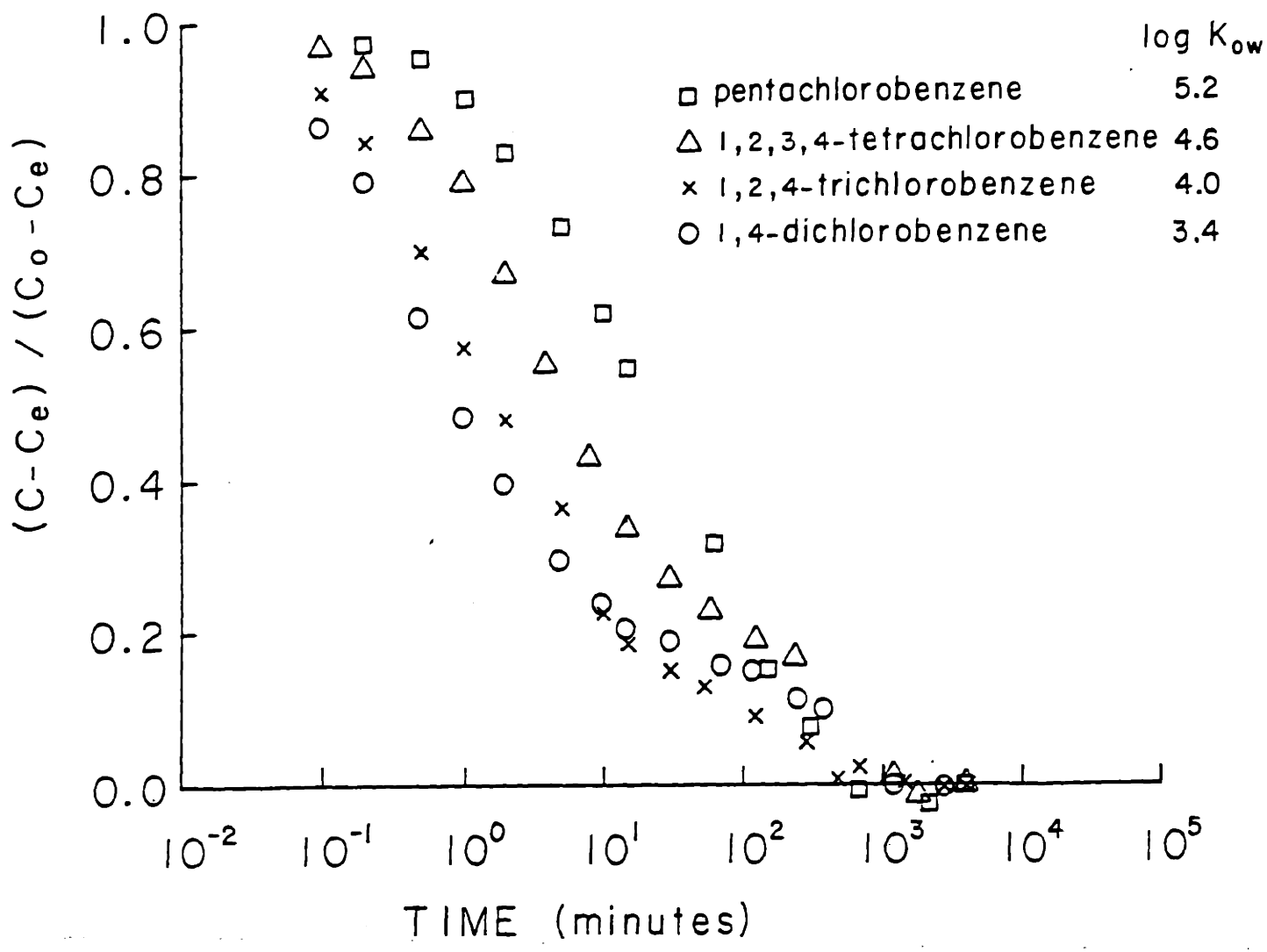
Figure 2.6   Comparision of sorption kinetics experimental results for four

chlorobenzene congeners exhibiting a range of hydrophobicities

(K_{ow} from Chiou, 1985) on Charles River sediments.
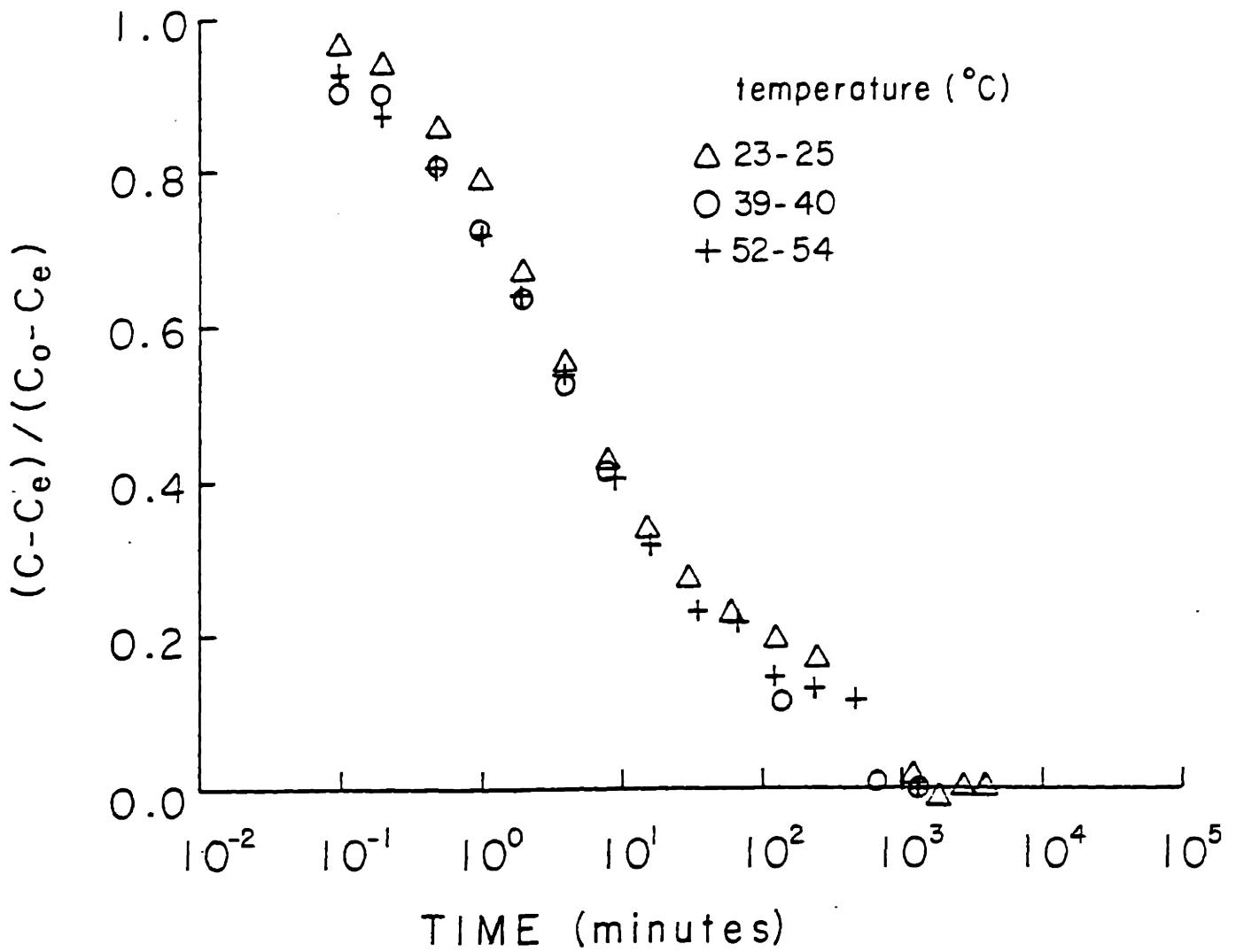
Figure 2.7   Comparison of sorption kinetics experimental results for

tetrachlorobenzene on Charles River sediments at three

different temperatures.

observations are sufficiently precise to show this. Second, temperature can change the partition coefficients and consequently change the effective diffusivities which determine the sorption rates. The sorption partition coefficient of tetrachlorobenzene to Charles River sediments is indeed smaller at 55°C ($K_p = 0.68 \times 10^3$ cm^3/g) than at 40°C ($K_p = 1.0 \times 10^3$ cm^3/g) and at 24°C ($K_p = 1.2 \times 10^3$ cm^3/g) (Table 2.2). This relationship between the partition coefficients and the temperature corresponds to an exothermic sorption heat of about -3.5 Kcal/mole (derived from the Gibbs-Helmholtz equation, see Moore, 1962). Given the observed temperature effect on K_p, we predict from Equation 2.6 the effective diffusivity to vary by a factor of two in these experiments. As shown the Table 2.2 and discussed below, the effective diffusivities needed for model simulations to fit the data for this range of temperatures varied by about this magnitude.

The desorption experiments further confirmed that the reversible processes of intraparticle diffusion and phase partitioning (Chiou et al., 1983; and Appendix 2) may be used to quantify solid-to-solution exchange kinetics. As can be seen in Figure 2.8, the desorption process has a similar time scale as the sorption process for the same combination of sediments and sorbate, although desorption is slightly faster because of the smaller average particle size for contaminated North River sediments used in the desorption experiment. Both sorption and desorption processes were completed in about 2 days in this case which strongly supports the argument that the sorption process is reversible.
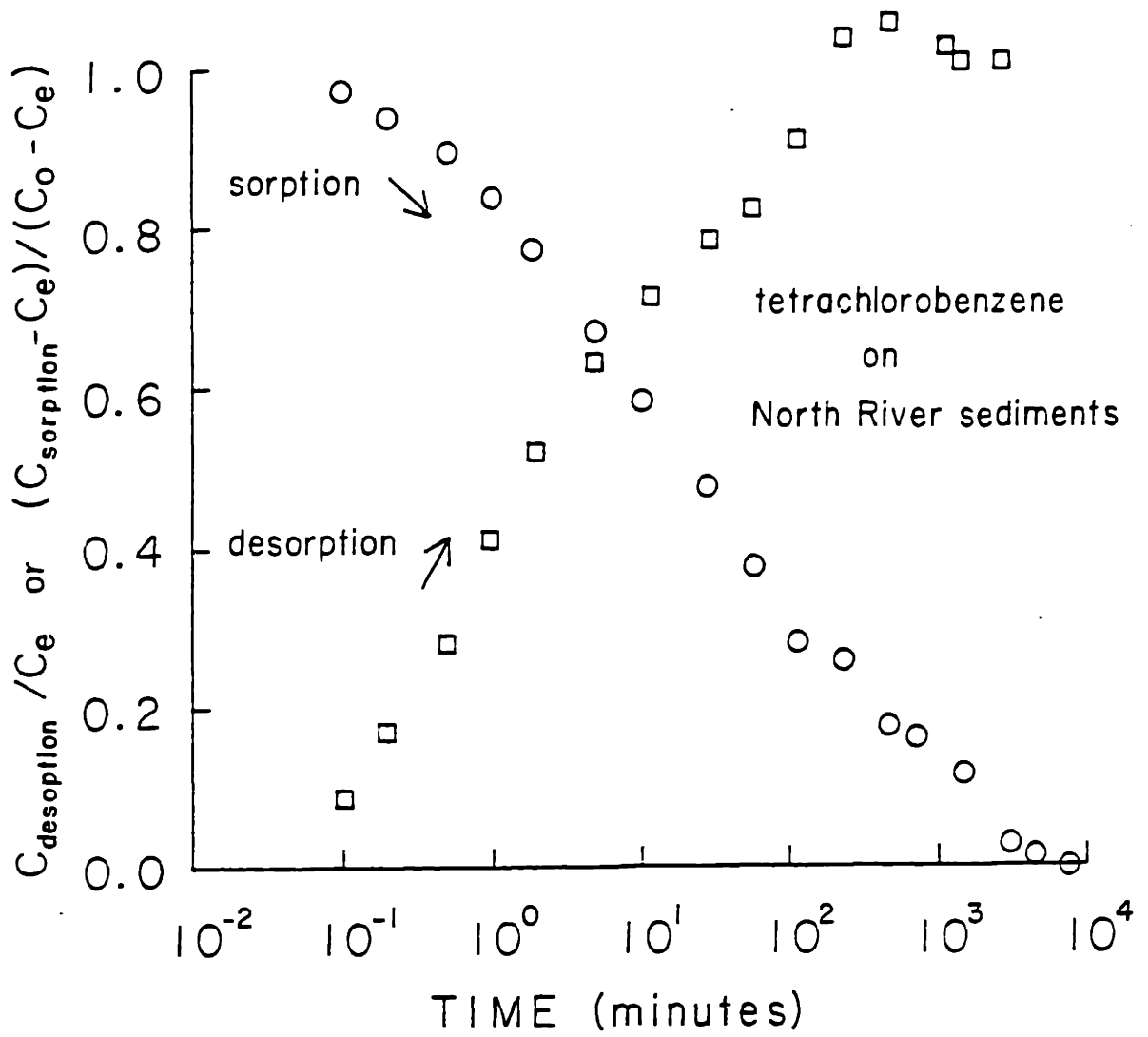
Figure 2.8   Desorption vs. sorption kinetics for tetrachlorobenzene on
North River sediments.

2.4.2 Comparison of Models

We have fit our experimental data with our retarded/radial diffusion model and the two other box models. The diffusion model fits the data quite well. The one-box model simply fails to fit the data well (Figure 2.9). The data shows a more rapid uptake at beginning followed by a slow approach to equilibrium. The two-box modle can be adjusted more closely to the data (Figure 2.9). However, this is not surprising since there are three fitting parameters involved (the two rate constants, k_1 and k_2, and the fraction of the total sorption capacity in the rapid-exchange compartment, X_1). In addition, the primary disadvantage of the two-box model is the difficulty of relating these three parameters to known properties of sediments and sorbates. For example, for two experiments with the same compound (tetrachlorobenzene) and the same sediments (Charles River sediments), however, with different mean aggregate sizes (97 μm and 232 μm), we obtain two totally different sets of parameters ((1) $k_1 = 5.8 \times 10^{-2}$ min^{-1}, $k_2 = 2.8 \times 10^{-3}$ min^{-1}, $X_1 = 0.44$; (2) $k_1 = 8.7 \times 10^{-3}$ min^{-1}, $k_2 = 3.2 \times 10^{-4}$ min^{-1}, $X_1 = 0.67$) by minimizing the fitting residual. This indicates that we have to experimentally estimate these parameters for each type of sediment which is impractical for modelling natural water systems. Consequently, these models limit our understanding of the processes governing sorption kinetics and require recalibration for every new situation in which they are applied.

On the contrary, since the particle diameters can be measured, the retarded/radial diffusion model can be fit to the polychlorobenzene uptake data adjusting only one parameter (the effective intraparticle diffusivity).
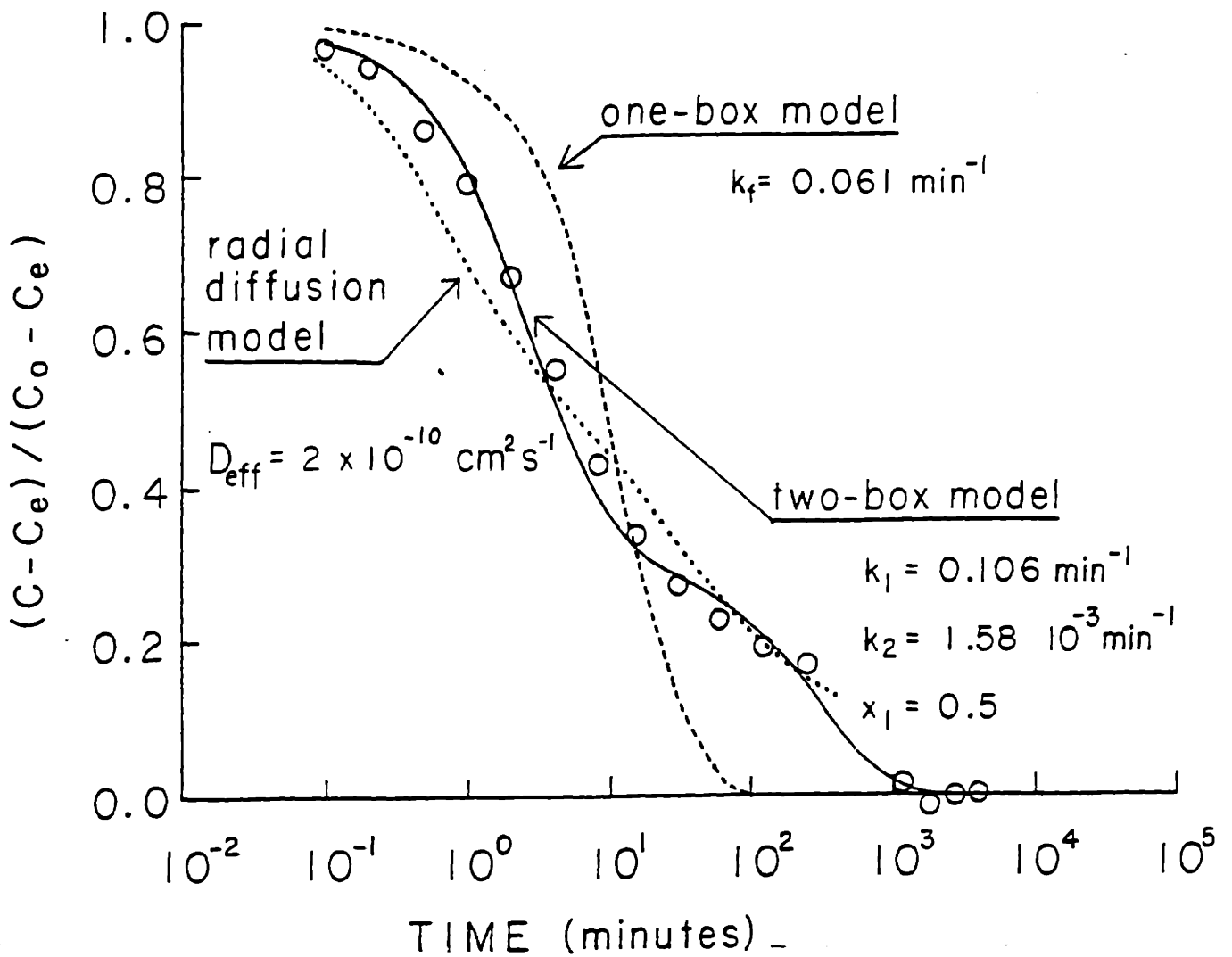
Figure 2.9   Model fitting results (for data of Experiment 4) with one-box, two-box models, and retarded radial diffusion model.

This model fits our results very well (Figures 2.10 a-d). In addition, this model not only extends our understanding of the sorption kinetics, but also offers us the opportunity to estimate the effective diffusivity a priori based on correlations with chemical and sediment properties.

2.4.3 Effective Diffusivity, D_{eff}

Table 2.2 summarizes the values of the fitting parameter, D_{eff}. According to the previous discussion, the effective diffusivety should be inversely related to the partition coefficient, K_p, for strongly hydrophobic compounds if pore fluid diffusion dominates. Figure 2.11 shows the relationship of D_{eff} versus K_p for the various combinations of sorbates and sorbents used. The inverse relationship for these parameters is obvious and consistent with our intraparticle diffusion model. Since the partition coefficient can be estimated from the octanol-water partition coefficient of the compound and the organic carbon content of sediments within a reasonable range (Karickhoff et al., 1979), the molecular diffusivity can be predicted by the Stokes-Einstein equation (Satterfield, 1981), and we can measure the

particle size distribution and dry solid density, ρ_s, the only factors which

we have to know to independently estimate D_{eff} are the porosity and pore

geometry factors, $f(n,t)$.

Ullman and Aller (1982) observed that the pore geometry factor is a function of porosity in sediment beds, i.e.,
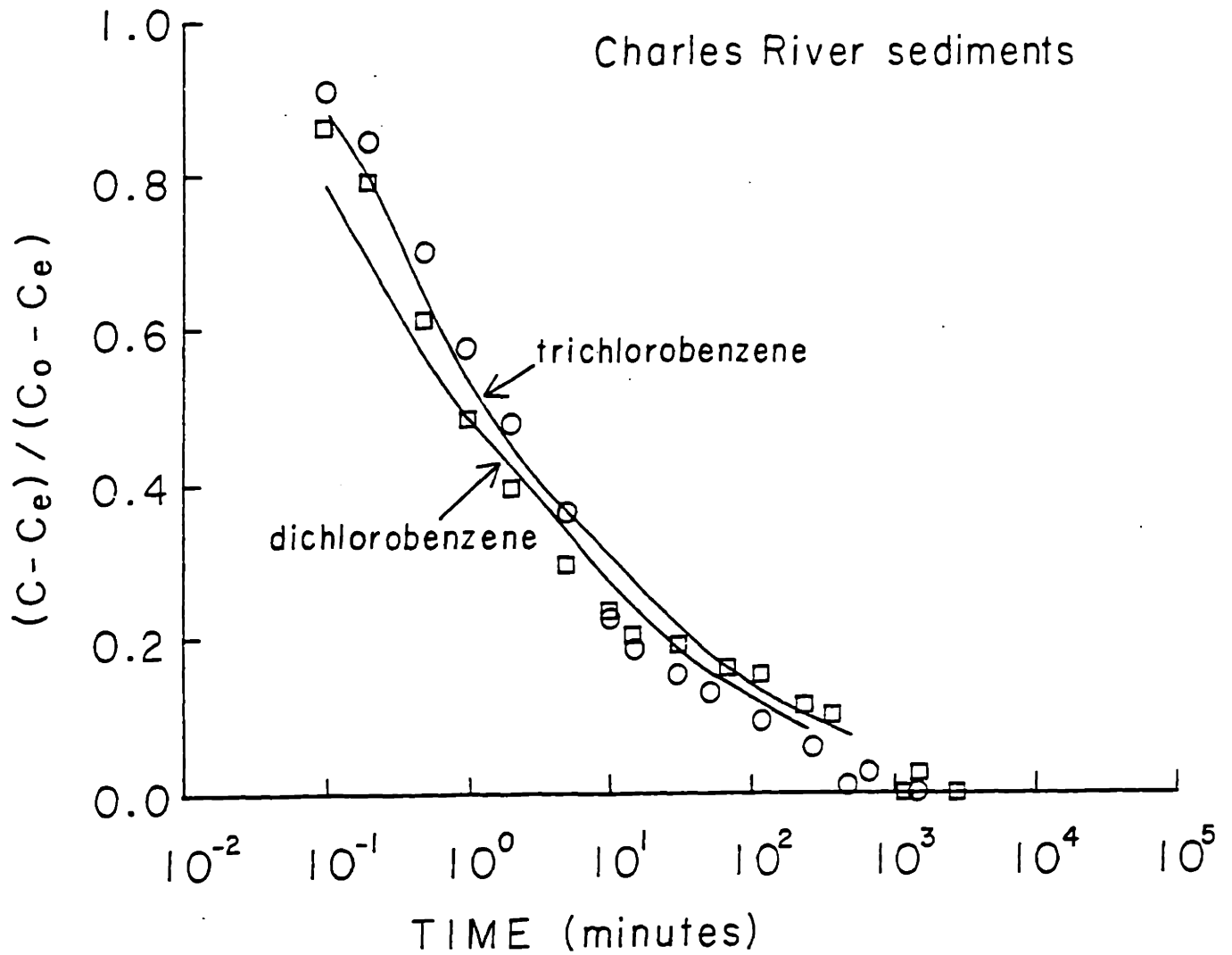
Figure 2.10   Experimental and model fitting results for Experiments (a) No.2

and 3. Lines are fitting results by retarded/radial diffusion model.

Iowa soils (EPA-10)

(b) No.9 and 10

North River sediments

pentachlorobenzene

tetrachlorobenzene
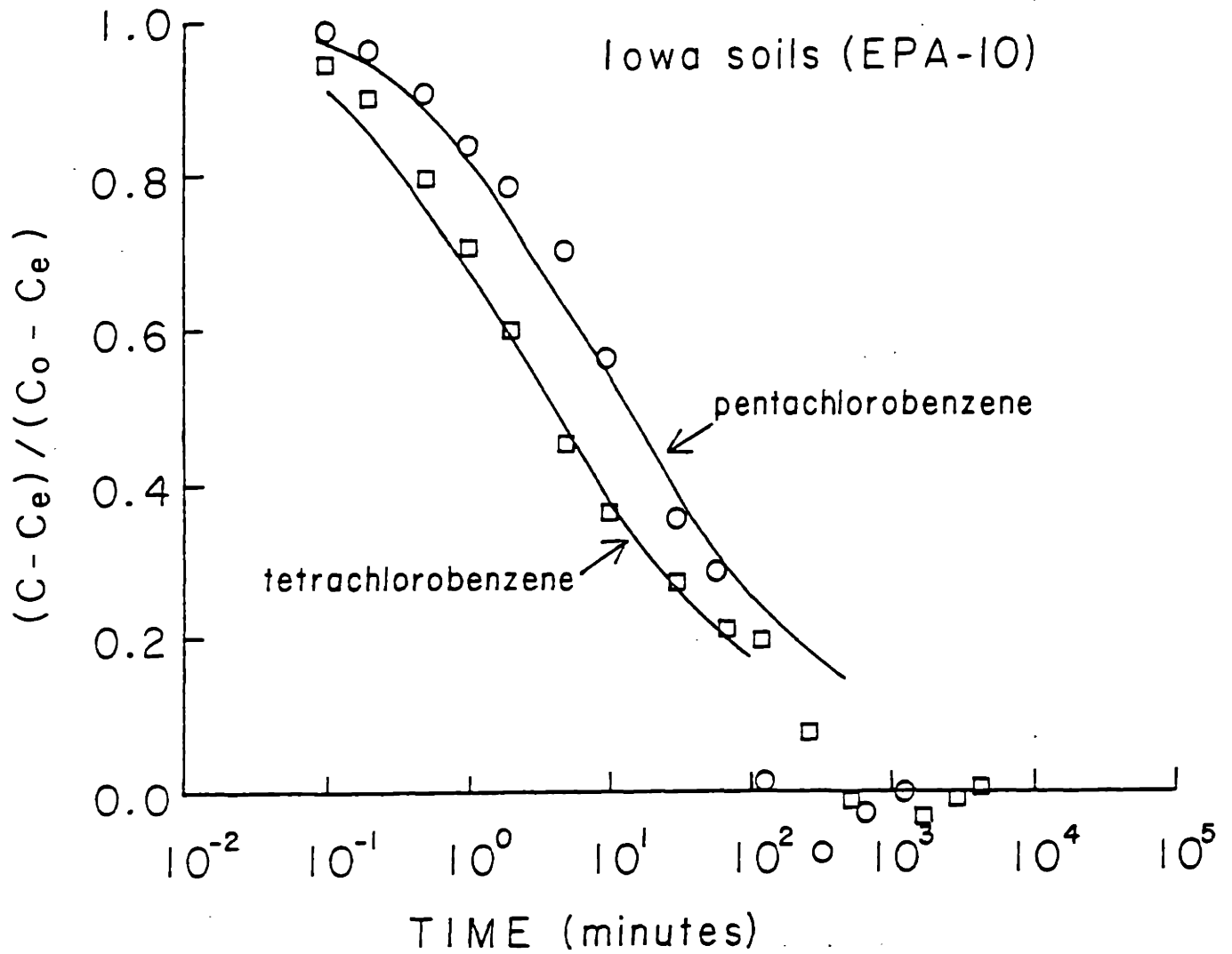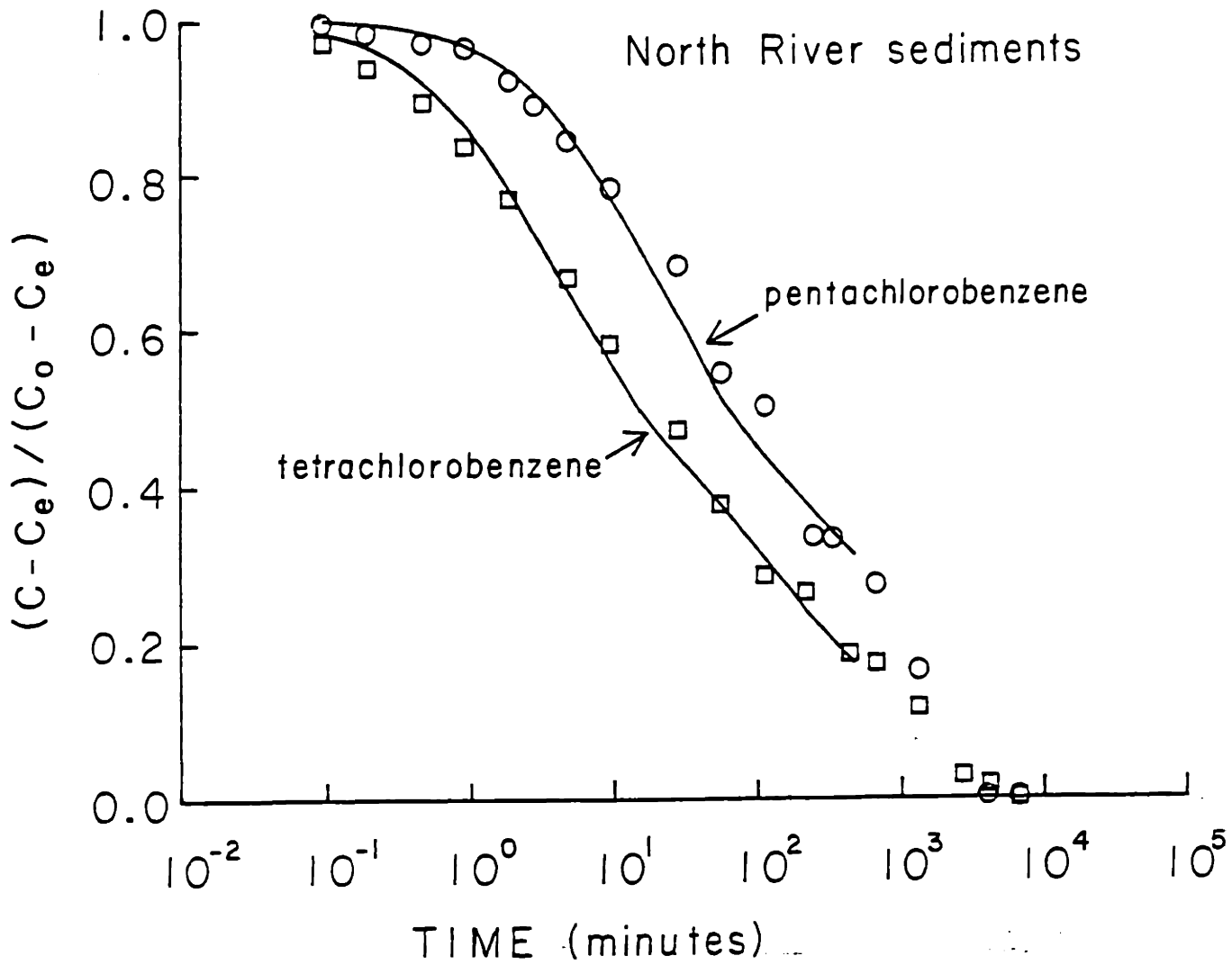
(c) No.11 and 12
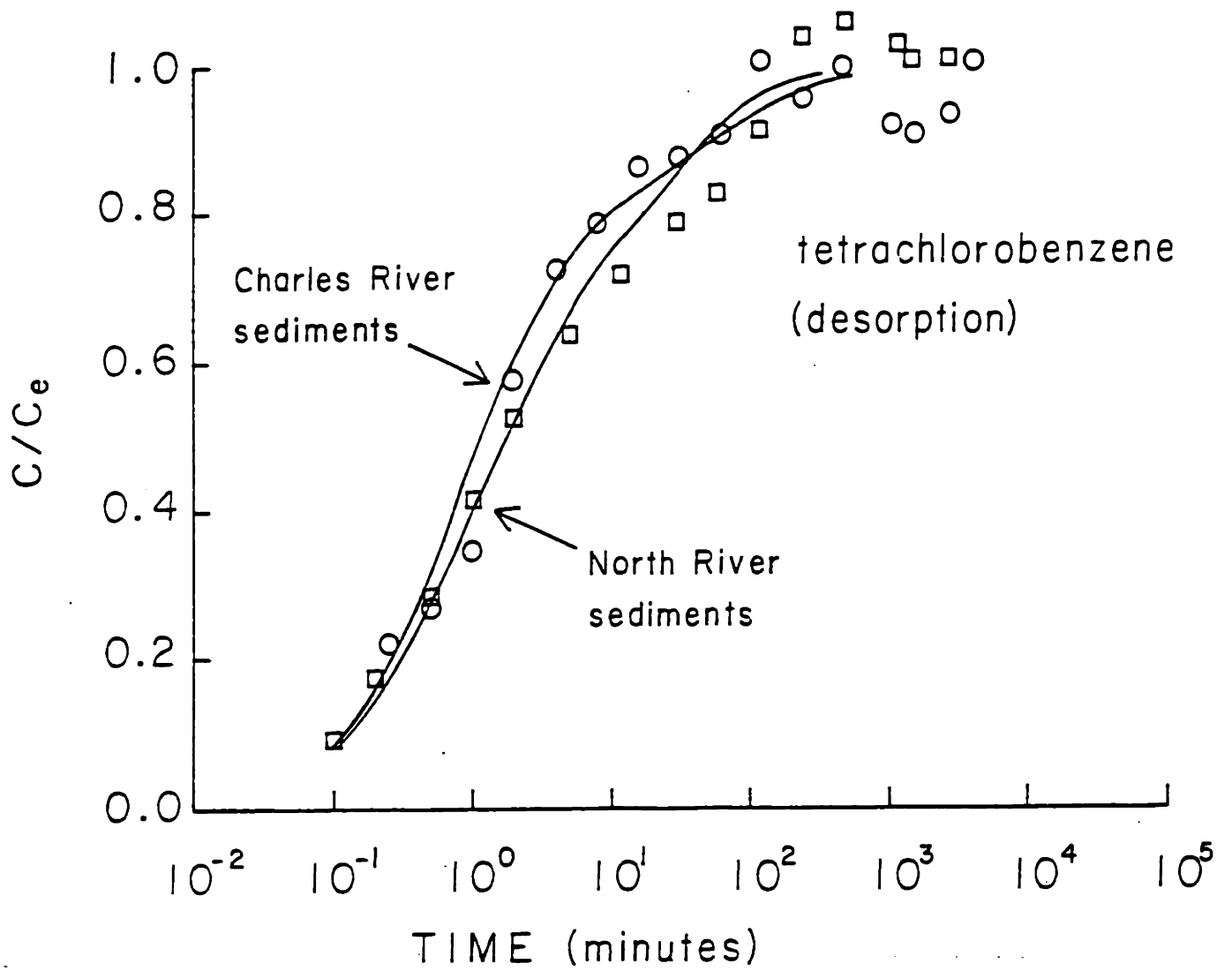
(d) No. 13 and 14
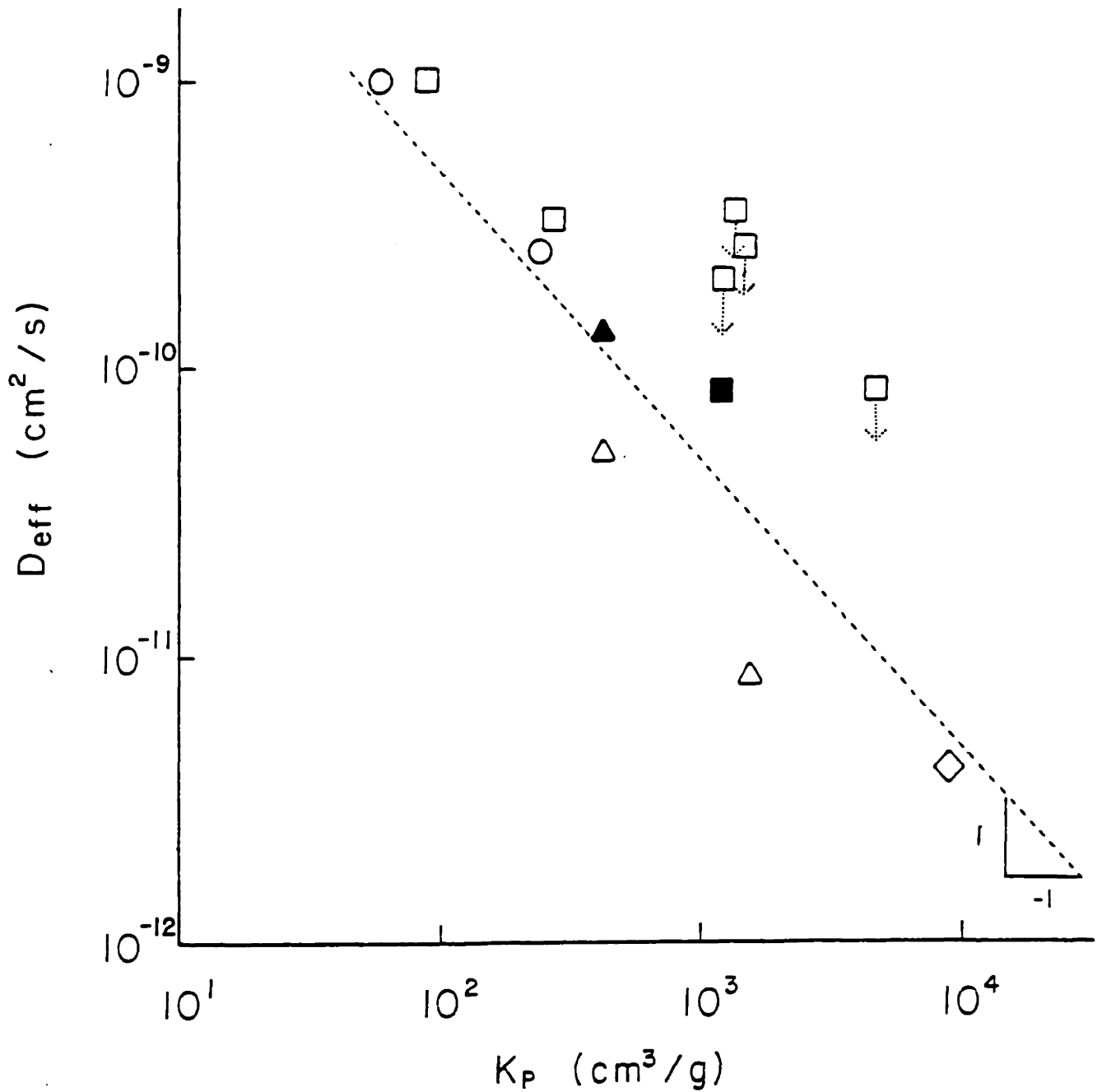
Figure. 2.11   Model fit D_{eff} versus K_p. Squares are data from Charles River
sediments, circles are from Iowa soils, and triangles are from
North River sediments. Diamond is data of kepone sorption in
Range Point sediments by Connolly (1980). Solid symbols
represent desorption results from corresponding sorbents.
Arrows indicate experiments in which continuous bubbling caused
disaggregation and therefore yielded upper limit estimates of
D_{eff}.

$$f(n,t) = n^i \qquad (2.11)$$

where the exponent, i, is between 1 and 2. If we treat intraparticle diffusion similarly and arbitrarily take i to be 1, the effective diffusivity takes the following form:

$$D_{eff} = \frac{D_m n^2}{K_p (1-n) \rho_s} \qquad (2.12)$$

The porosity, n, becomes the only fitting parameter.

We can evaluate what the intraparticle porosities would have to be to yield the observed D_{eff}. The results of this evaluation (Table 2.3) show that for three different types of sediments, the fitting porosities have an average of 0.13 and a standard deviation of 30%, and are very closely reproduced for any one sediment studied with different sorbates (i.e., an average of 0.17 and a standard deviation of 3% for Charles River sediments; an average of 0.1 and a standard deviation of 30% for North River sediments; and the same porosity for Iowa soils in two experiments). In light of our physical picture of sorptive exchange, we would predict that the same intraparticle porosity fraction should apply for desorption as for sorption. Indeed, the fitting porosities, n, for desorption of tetrachlorobenzene from Charles River and North River sediments are similar to the values obtained from corresponding uptake experiments. Connolly (1980) used a comparable approach to study the sorption of kepone on Range Point sediments (salt marsh, Santa Rosa Sound,

55

Table 2.3 Intra-aggregate porosities which yield observed

D_{eff} for i=1 (Equation 2.12).

sediments	compounds		fitting porosity, n
sorption			
CR[a]	P(a)		(0.32)(c)
CR	TR		0.17
CR	D		0.17
CR	TE		(0.26)(c)
CR	TE	96 μm	(0.33)(c)
CR	TE	232 μm	(0.39)(c)
IS	TE		0.15
IS	P		0.15
NR	TE		0.09
NR	P		0.07
Range Point[b]	kepone		0.11
		average	0.13±0.04
desorption			
CR	TE		0.18
NR	TE		0.14

(a). Same notation as in Table 3.

(b). Data from (Connolly, 1980)

(c). These values were not used in averaging due to
changing particle size distributions during experiments
(see Section 2.2.3 and Appendix 3).

Florida). He obtained a D_{eff} of 3.7 x 10^{-12} cm^2/s and K_p of 9100 cm^3/g.

Consequently, we can calculate the value of n to be 0.11, which falls within

the range of n from our experiments. If we choose i=1 and n=0.13 (or i=2 and

n=0.24) as a typical intraparticle porosity for the sorbing silts of our

experiments, all of the observed sorption rates can be fit with reasonable

accuracy.

We know of no data appropriate to judge these intra-aggregate porosity

estimates, yet they appear reasonable. Certainly more research is needed to

develop methods of characterizing natural aggregate particles and to select

key parameters (e.g., n and i) which will enable us to predict a *priori* the

effective diffusivity, D_{eff}, accurately.

Karickhoff and Morris (1985) reported the results of desorption of

hexachlorobenzene from intact tubificid fecal pellets, suspended pellets,

crushed pellets, and parent sediments, separately. Although they reported no

data on size distribution, taking n to be 0.13 we can fit their data quite

well by adjusting only the average particle size in a retarded-radial

diffusion model simulations (Figure 2.12). This analysis indicates that if we

know the pellet sizes, our model can fit the shape of their experimental

results. In addition, the corresponding "simulation sizes" for intact

pellets, suspended pellets, crushed pellets, and parent sediments are 800 μm,

400 μm, 250 μm, and 200 μm, respectively. This sequence of particle sizes

appears appropriate for fecal pellets, pellet debris, and silty natural

particles.
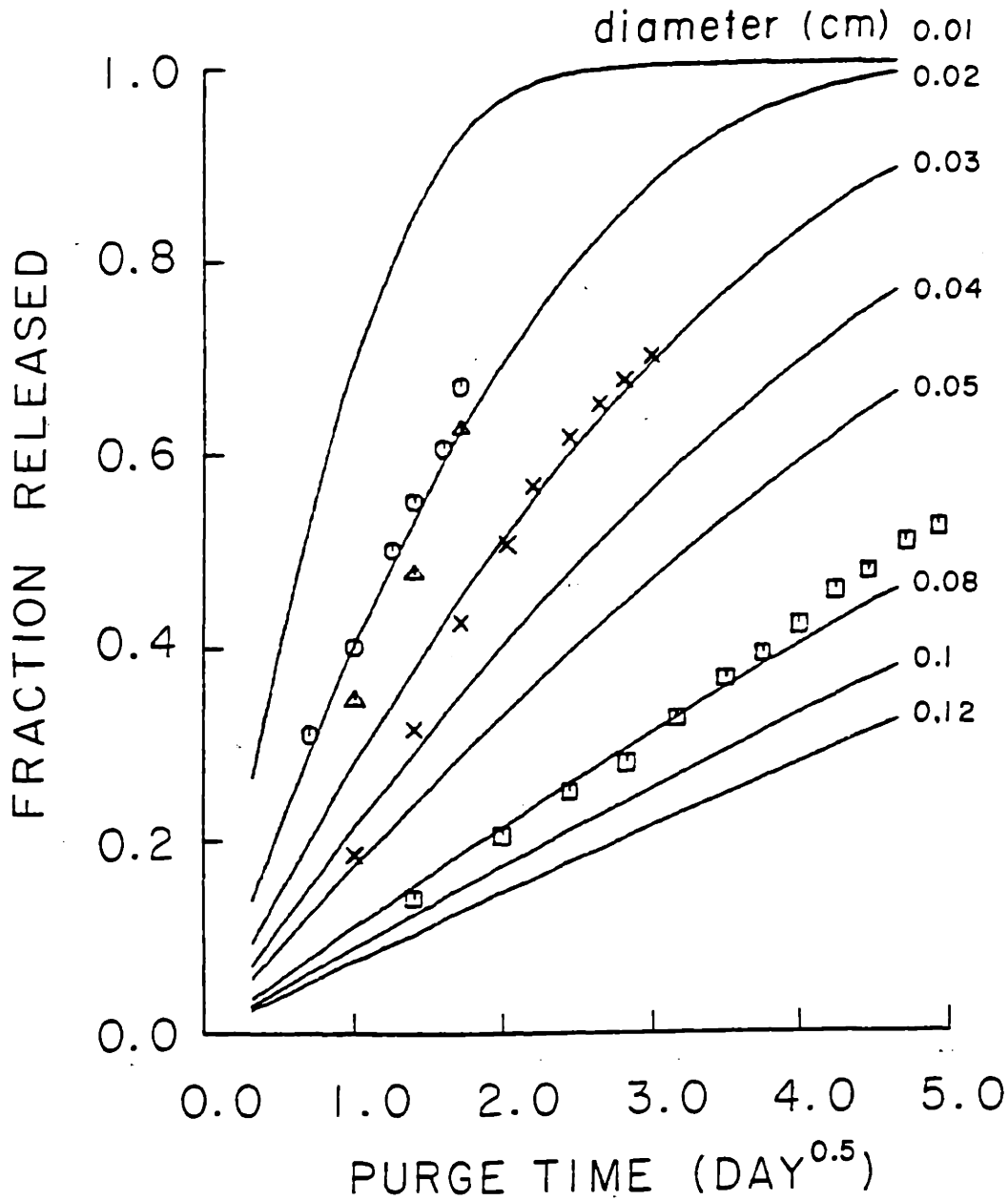
Figure 2.12   Model prediction compared with desorption experimental results by Karickhoff and Morris (1985). The environmental parameters are: i=1, n=0.13, ρs= 2.5g/cm^3, K_p= 2240 cm^3/g and varying diameter. Experimental data were obtained from desorption of hexachlorobenzene from intact pellets (squares), suspended pellets (crosses), crushed pellets (triangles), and parent sediments (circles).

2.5 Applications and Limitations

From the above model analysis it is clear that the radial diffusion sorption kinetics model can be applied to a variety of environmental situations by adjusting the D_{eff} according to easily measured or estimated environmental parameters. Therefore, once it is incorporated in the fate models it will certainly improve our capability to predict the fates of organic pollutants and the related human exposures. In addition, the approximate time scale of sorption and desorption can be easily predicted from analytical solutions to the radial diffusion governing equations if the particle size distribution is sufficiently narrow that we can choose a reasonable average particle size (e.g. method by Rao and coworkers, 1982; or Cooney and Adesanya, 1983). For example, in an open system where desorbed chemicals are flushed away, the released fraction of sorbate reaches 50% at time of 0.03 R^2/D_{eff} and reaches 90% at time of 0.2 R^2/D_{eff} (Crank, 1975). Thus, we propose that this model may serve as a useful tool to quickly estimate the mobility of an organic pollutant from an environmental location.

It has been reported that sorption exchange may require extended times (weeks to months) for complete equilibration (Karickhoff, 1984). Based on our retarded/radial diffusive description, this could be due to very long diffusive pathlengths and/or high microscale retardation. Limited by the present laboratory setup we have not obtained experimental results on sorption kinetics with very large soil or sediment particles (>200 μm) nor with very hydrophobic substances (e.g., $K_{ow} > 10^5$). However, for silty particles of relatively large mean diameter 200 μm and f_{oc} of 3%, we would expect

hexachlorobenzene to show a desorption timescale of 90% release in about 20 days. Longer sorption timescales will be expected for even more hydrophobic compounds. For instance, polychlorinated biphenyls with octanol-water partition coefficients of 10^5 to 10^8 (Rapaport and Eisenriech, 1984) will show timescales of 90% release of up to 280 days from particles with a diameter of 50 μm and a few percent organic carbon content. Some additional factors which may also result in this extended sorption timescale include: (1) a steric effects in which a large sorbate molecule experiences diminished mobility as some intraparticle pore spaces are too small to pass through (Satterfield, 1980); (2) formation of large aggregates and therefore long diffusion pathlengths in situations of high sediment concentration; (3) special pore geometry in some natural particles (e.g., space between expandible clay layers (Brady, 1974) and debris of tissue of dead organisms with very compact structure). More research is needed to shed light on the "highly retarded" sorption process especially based on more understanding on the characteristics of natural particles.

2.6 Conclusions

We have used experimental and model simulation approaches to investigate the kinetics of sorption of organic pollutants on natural sediments. Efforts were made to identify the important factors controlling sorption kinetics and to model the process using measurable system parameters and known physical and chemical processes. The evidence supports the theory that the sorption kinetics is controlled by intraparticle diffusion for natural aggregated sediments and soils. The results demonstrate that the bigger aggregates have

lower uptake rates, that compounds with higher values of K_{ow} show slower sorption, that there is about a factor of two effect on sorption kinetics due to variations in K_p in a temperature range of 30°C (i.e., 25°C to 55°C), and that desorption rates are consistent with a reversible diffusive exchange mechanism. Model simulation analysis indicates that the radial diffusion model is the best among the three tested models because it fits the data as well as the two-box model and much better than the one-box model, and it has only one fitting parameter, the intraparticle diffusivity, rather than three fitting parameters as the two-box model has. The observed effective diffusivity is a function of chemical and particle properties (i.e., $D_{eff}=$

$D_m \cdot n^2 / K_p (1-n) \rho_s$). An empirical choice of n=0.13 could fit all our experimental results and other reported research results with reasonable accuracy. Consequently, this model not only extends our understanding of the sorption kinetics, but also enables us to estimate the effective diffusivity a priori based on correlations with chemical and sediment properties.

CHAPTER 3

Numerical Modelling Of Sorption Kinetics Of Organic Compounds To Natural

Soils And Sediments

3.0 Introduction

The fate of an organic pollutant in aquatic environments is often highly

dependent on its sorption behavior. As part of the larger effort to develop

models to predict the disposition of organic chemicals released to the

environment (Onishi and Wise, 1982; Ambrose et al., 1983), we have focussed on

elucidating and verifying quantitative expressions of the equilibrium

(Appendix 2) and kinetic (Chapter 2) aspects of sorption exchange.

As a result of the sorption kinetics investigations described in Chapter

2, we obtained a governing equation of sorption kinetics:

$$\frac{\partial S(r)}{\partial t} = D_{eff} \left[\frac{\partial^2 S(r)}{\partial r^2} + \frac{2}{r} \frac{\partial S(r)}{\partial r} \right] \qquad (3.1)$$

in which S = total local volumetric concentration (mol/cm^3), r = radial

distance, t = time (s), and (r) denotes the location with distance r from the

center of the natural aggregate particles. S, the total solid associated

concentratio, is given:

$$S = (1-n)\rho_s S' + nC' \qquad (3.2)$$

where S' is the sorbed concentration (mol/g), and C' is the dissolved

concentration (mol/cm^3) in the aggregate pore fluids.

The effective intraparticle diffusivity, D_{eff} (cm^2/s), is defined as

$$D_{eff} = \frac{D_m n^{i+1}}{(1-n)\rho_s K_p + n} \qquad (3.3)$$

where D_m = molecular diffusivity (cm^2/s), n = intraaggregate porosity, ρ_s = dry solid density (g/cm^3), K_p = equilibrium partition coefficient (cm^3/g), and i is an empirical parameter (g/cm^3) between 1 and 2.

Analytical solutions of this retarded intraparticle diffusion description of sorption kinetics are limited to special problems with simple conditions (i.e., uniform size of particles with constant aqueous concentration or in a closed system (Crank, 1975)). Therefore, a numerical solution technique is required to solve sorption problems in the real world in which there are polydisperse particle size distributions and spatially and temporally varying aqueous concentrations. Finite difference approaches have been used to solve the radial diffusion problems in company with mass transfer through a particle surface boundary layer (Weber and Rumer, 1965; Mathews and Weber, 1976). Cooney et al. (1983) also used a Crank-Nicolson finite difference scheme for radial diffusion with particle size groups to show the effects of particle size distribution on adsorption kinetics.

In this chapter, a numerical model based on the retarded radial diffusion mechanism of sorption kinetics is formulated. The numerical model is then used to evaluate the errors associated with (1) treating polydisperse natural suspensions as uni-sized, and (2) assuming a simple first-order sorption kinetics applies. Finally, model simulations are described which test the

applicability of this model in the framework of environmental chemical fate models.

3.1 Numerical Model

Based on the finite difference method and adopting the multi-size approach, we developed a finite difference numerical method to solve problems in which particles have size distributions spanning orders of magnitude and also problems with varying concentration in aqueous phase.

Introducing the two dimensionless variables

$$\tau = D_{eff}t/R^2 \qquad \text{(time scale)} \qquad (3.4)$$

$$x = r/R \qquad \text{(length scale)} \qquad (3.5)$$

in which R = particle radius, and substituting

$$u = xS \qquad (3.6)$$

into the governing equation (Eq. 3.1) yields the dimensionless governing equation:

$$\frac{\partial u}{\partial \tau} = \frac{\partial^2 u}{\partial x^2} \qquad (3.7)$$

The boundary condition at the aggregate surface is given by:

$$u(x=1) = S(r=R) = [(1-n)\rho_s K_p + n]C \qquad (3.8)$$

in which the concentration in aqueous phase, C, can be either a constant or a

function of time which is a given system condition. At the center of the

sphere

$$u = xS = 0, \qquad \text{since } x=0 \qquad\qquad (3.9)$$

In a closed system the aqueous concentration, C, is determined by a mass

balance equation:

$$V \frac{dC}{dt} = - V_s \frac{d\bar{S}}{dt} \qquad\qquad (3.10)$$

in which V = volume of the solution (cm^3), V_s = volume of the solid phase

(cm^3) ($= V \cdot \rho / ((1-n) \cdot \rho_s)$), and ρ = sorbent concentration in the solution

(g/cm^3). The average concentration in one particle, $\bar{S}$, is given by the

integration over a sphere:

$$\bar{S} = \frac{3}{4\pi R^3} \int_0^R 4\pi r^2 S(r) \, dr$$

$$= 3 \int_0^1 xu \, dx \qquad\qquad (3.11)$$

Therefore, the change of concentration in aqueous phase is also given by:

$$\frac{dC}{dt} = - \frac{V_s}{V} \frac{d}{dt} [3 \int_0^1 xu \, dx] \qquad\qquad (3.12)$$

65

The particles in the solution are categorized in n groups according to their sizes. In each particle, the radial coordinates are divided by equally spaced concentric spherical surfaces. The number of these concentric spherical surfaces, m, can be different for different groups. Using a finite difference expression for the second derivative in Eq. 3.7 and an explicit Euler method for integration in each time-step yields the following governing equations (Eq. 3.13, 3.14 and 3.15). For the ith particle size group (total n groups), there are m_i grid points equally spaced along the radial axis. At the center

$$u_{i,1}^{k+1} = u_{i,1}^{k} = 0 \qquad\qquad i=1 \text{ to } n \qquad\qquad (3.13)$$

The superscript, k+1, denotes the time step following the time step k. At the jth grid point

$$\frac{u_{i,j}^{k+1} - u_{i,j}^{k}}{\Delta\tau_i} = \frac{1}{(\Delta x_i)^2} [\, u_{i,j+1}^{k} - 2u_{i,j}^{k} + u_{i,j-1}^{k} \,] \qquad\qquad (3.14)$$

$$i = 1 \text{ to } n$$
$$j = 2 \text{ to } m_i-1$$

i and j are subscripts referring to size group and grid point number, respectively. $\Delta\tau_i$ and Δx_i are dimensionless time and distance step sizes for

66

size group i ($\Delta x_i = 1/(m_i-1)$). The $\Delta \tau_i$ is set to let all $\Delta \tau_i/(\Delta x_i)^2$ be less

then 0.5 in order to obtain stable integration.

At the surface,

$$u_{i,m_i}^{k+1} = K_p \cdot (1-n) \rho_s c^{k+1} \qquad\qquad i=1 \text{ to } n \qquad\qquad (3.15)$$

in which the aqueous concentration at time step k+1, c^{k+1}, is set according to

the previously given boundary conditions. If it is a closed system, the

aqueous concentration at time step k+1 will be given by:

$$c^{k+1} = c^k - \sum_{i=1}^{n} f_i \frac{V_s}{V} \left(3\int_0^1 x_i u_i^{k+1} dx_i - 3\int_0^1 x_i u_i^k dx_i \right) \qquad (3.16)$$

in which f_i = mass fraction of size group i. Replacing the integrals with

Simpson's 1/3 rule such that:

$$\int_0^1 x_i u_i dx_i = \frac{\Delta x_i}{3} (x_{i,1} u_{i,1} + 4x_{i,2} u_{i,2} + 2x_{i,3} u_{i,3} + 4x_{i,4} u_{i,4} + \ldots$$

$$+ 2x_{i,m_{i-2}} u_{i,m_{i-2}} + 4x_{i,m_{i-1}} u_{i,m_{i-1}} + x_{i,m_i} u_{i,m_i}) \qquad (3.17)$$

and substituting all u_{i,m_i}^{k+1} by $K_p(1-n)\rho_s c^{k+1}$, and $x_{i,j}$ by $\Delta x_i(j-1)$, we obtain

the updated aqueous concentration, c^{k+1}, in which:

67

$$C^{k+1} = \frac{1}{(1+a)} \left\{ C^k - \sum_{i=1}^{n} \frac{f_i V_s (\Delta x_i)^2}{V} \left[\left(\sum_{j=2}^{m_i-1} (3+(-1)^j)(j-1)(u_{i,j}^{k+1}-u_{i,j}^k) \right) \right. \right.$$

$$\left. \left. - (m_i-1) u_{i,m_i}^k \right] \right\} \tag{3.18}$$

where:

$$a = \sum_{i=1}^{n} \frac{f_i V_s (\Delta x)^2}{V} (m_i-1) K_p (1-n) \rho_s$$

Also, the average concentration sorbed to the solids can be calculated by an integration:

$$\overline{S}^{k+1} = \sum_{i=1}^{n} (\Delta x_i)^2 \left[\sum_{j=2}^{m_i-1} (3+(-1)^j)(j-1) u_{i,j}^{k+1} + (m_i-1) u_{i,m_i}^{k+1} \right] \tag{3.19}$$

For the convenience of comparisons later in this paper, we define the fraction of completion of equilibration, M_t/M_∞, in Eq. 3.20 to unify the expressions of the progress of sorption and desorption processes:

$$M_t/M_\infty = (C_o-C)/(C_o-C_e) \quad \text{(in closed system only)}$$

$$= (\overline{S}_o-\overline{S})/(\overline{S}_o-\overline{S}_e)$$

$$= (\overline{S}_o'-\overline{S}')/(\overline{S}_o'-\overline{S}_e') \tag{3.20}$$

in which subscript, o, denotes initial state; subscript, e, denotes equilibrium state at infinite time; the bar denotes average property over the whole aggregate. The equilibrium concentration, C_e, $\overline{S}_e'$, and $\overline{S}_e$ can be

determined from the following equations:

$$\overline{S}_e' = K_p \cdot C_e \quad (mol/g) \quad (in \ equilibrium) \tag{3.21}$$

$$\overline{S}_e = [(1-n) \cdot \rho_s \cdot K_p + n] \cdot C_e \quad (mol/cm^3) \tag{3.22}$$

$$initial \ total \ mass = C_o + \overline{S}_o'\rho \tag{3.23}$$

$$final \ total \ mass = C_e + \overline{S}_e'\rho = C_e + C_e \cdot K_p \cdot \rho \tag{3.24}$$

in which ρ = solid concentration (g/cm^3). In a closed system the final mass

is equal to the initial mass. As a result, the final equilibrium

concentration in the aqueous phase is given by:

$$\therefore C_e = \frac{C_o + \overline{S}_o'\cdot\rho}{(1 + K_p \cdot \rho)} \tag{3.25}$$

Under the condition of a constant aqueous concentration (i.e., in an infinite

bath), the equilibrium concentration is the initial concentration:

$$C_e = C_o \tag{3.26}$$

A BASIC computer program which solicits the chemical and environmental

parameters of interest, calculates D_{eff}, sets the system boundary conditions

according to the user's situation of concern, and solves the time course of

concentration change is listed in Appendix 4. Such a program can be used as a

subroutine in global fate models (Onishi and Wise, 1982; Ambrose et al.,1983).

3.2 Model Accuracy

In order to demonstrate the accuracy of this numerical model formulation, the results of simple cases of sorption kinetics in which analytical solutions are available were compared to numerically generated simulations. Assuming a well mixed closed reactor as an example initially with no pollutant in the uniform solid particles and homogeneous concentration in the water, some numerical solutions obtained as a function of how finely we subdivide the distance intervals in the aqgregate particles are compared to the analytical solution in Fig. 3.1-a. There is significant error at early times due to the extra weight given to the concentration at the surface grid point (assumed to be immediately equilibrated at t=0) when performing numerical integration. The error decreases quickly with increasing grid number and dimensionless time $(D_{eff} \cdot t/R^2)$. A grid number of 50 results in an error less than a factor of 2 when $D_{eff} \cdot t/R^2$ is greater than 10^{-5} (Fig. 3.1-b). By knowing D_{eff} and the aggregate radius, we can choose a grid number which satisfies the required accuracy at a specific time of concern, t, from Fig.3.1-b. On the other hand, in some particular situations we may be able to save computation time by using fewer grid subdivisions by checking to see that the solution converges to the analytical solution before the time of concern (e.g., 1 minute).

Extremely long computation time is required when the particle size distribution is wide. The sorption progress is fast for small size groups which need short time steps to maintain stable iterations. However, the progress for large particles is very slow. Long simulation time is necessary to show the actual sorption behavior. For a size distribution spanning two
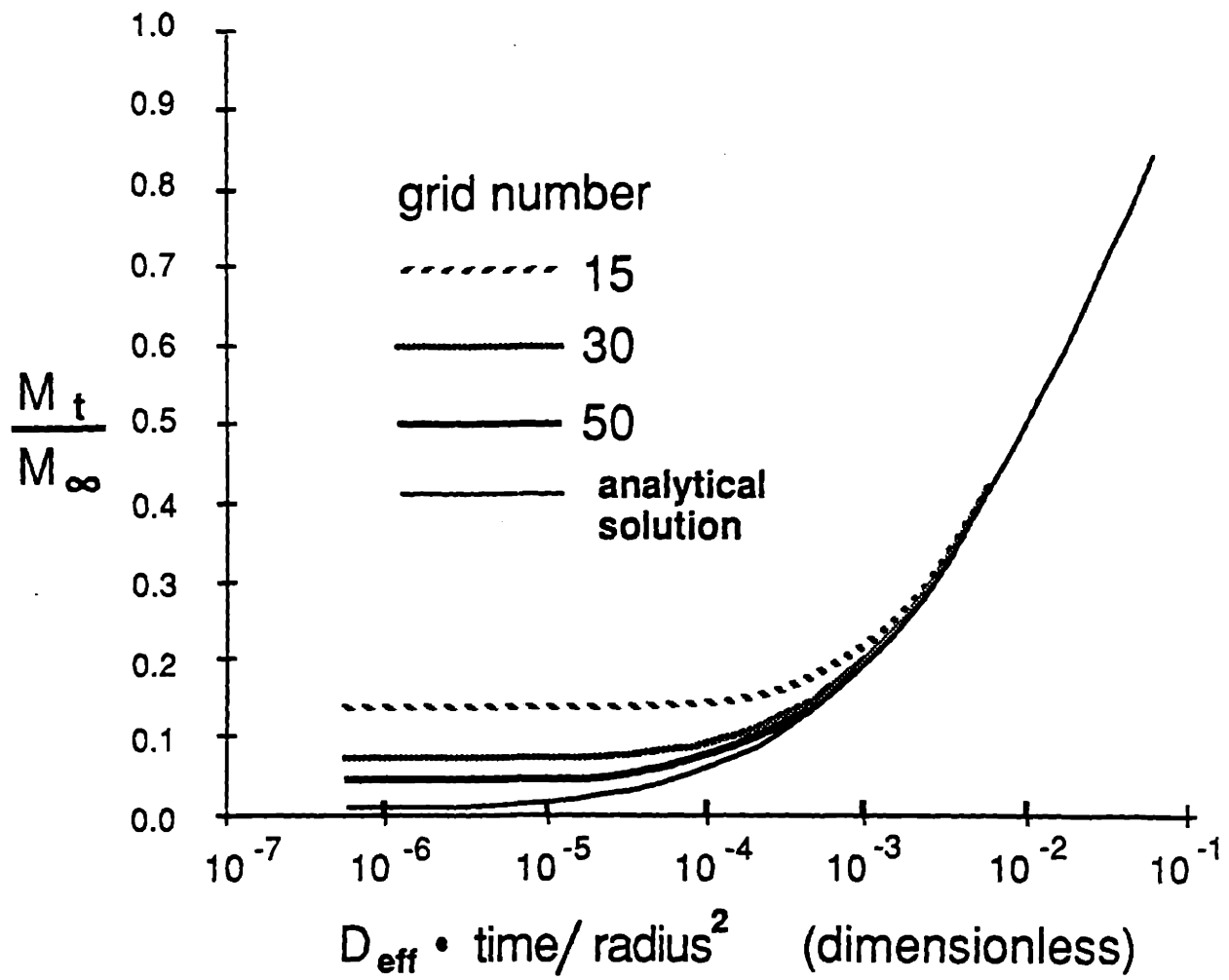
Figure 3.1-a   Numerical solutions with different grid numbers compared with

the corresponding analytical solution for sorption kinetics in

a closed system in which $K_p \rho = 1$.
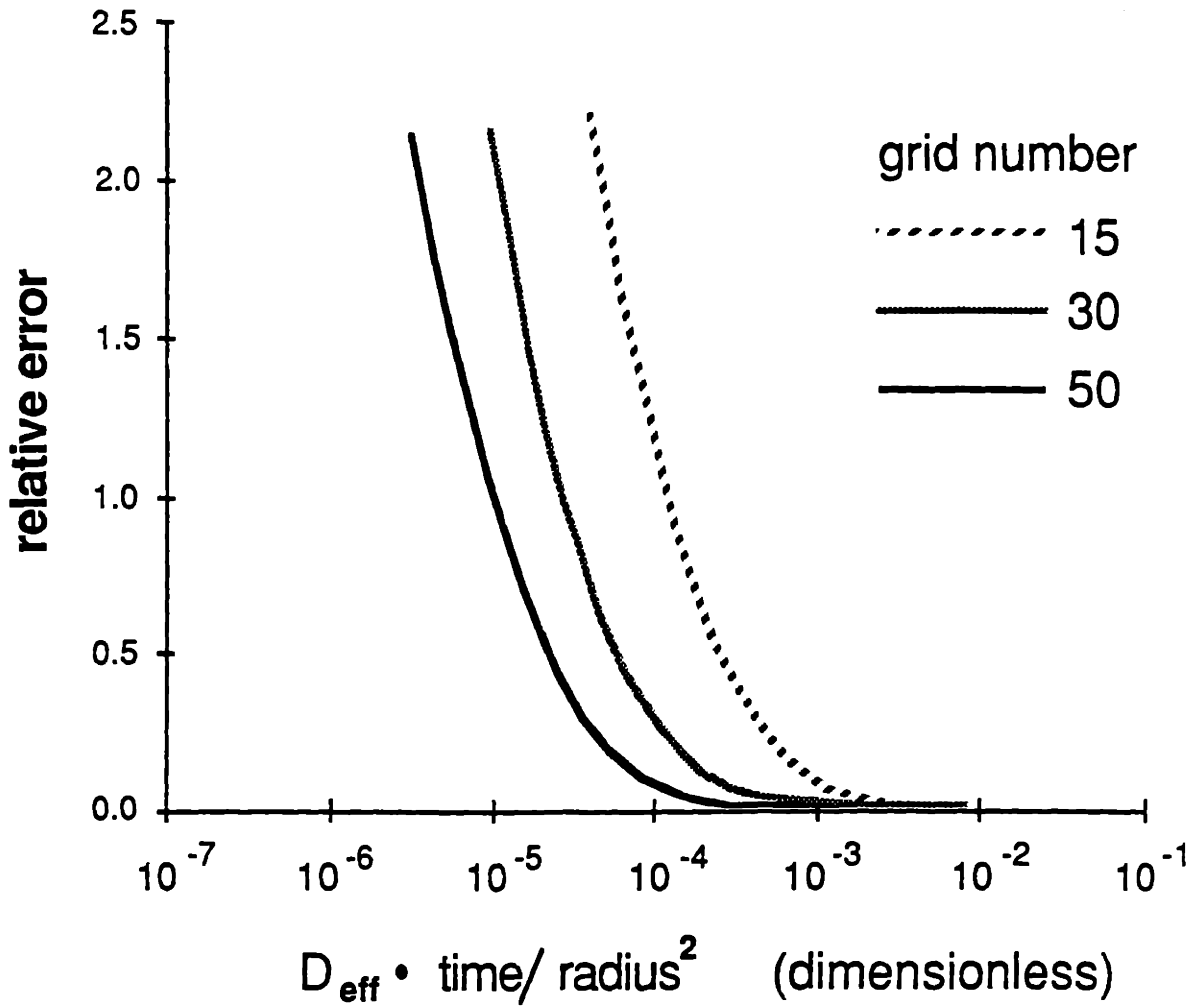
Figure 3.1-b   Error of the numerical method for different choices of grid

numbers. The relative error is calculated from the solution in

Fig. 3.1-a as: relative error = (numerical solution-analytical

solution)/analytical solution.

orders of magnitude, the computation time for a 90% equilibration is several

days with a Macintosh® personal computer. To partly overcome this stiff

numerical problem, our computer program allows different grid numbers for

different size groups. If detailed sorption behavior at the beginning is not

of interest, we can simply reduce the grid number for small particle groups.

3.3 Potential for Modelling Simplification

3.3.1 Approximating The Particle Size Distribution With Single Geometric Mean
       Size

The particle size of the sorbent aggregates has a dramatic effect on the

sorption uptake rates (Chapter 2). These effects have been ignored by most

sorption kinetics modellers. In the radial diffusion model the factor of

particle size was included as a dimensional boundary condition. Eq. 3.4

indicates that increasing particle size by one order of magnitude will

decrease the uptake rate by two orders of magnitude (i.e., the $t_{1/2}$ of 100 μm

particles is 100 times of the $t_{1/2}$ of 10 μm particles). Fig. 3.2 shows the

sensitivity of sorption kinetics to particle size.

Due to the importance of the particle size to sorption kinetics, we used

the numerical model to evaluate the impact of size distribution to this

process. Very often it would be convenient to use a uniform size to replace a

size distribution in prediction or model simulation because of, for instance,

the availability of simple analytical solutions or the requirement of a

particle size to represent all particles between two sieve cuts. Our

numerical method can be used to examine the validity of such uniform-size

73
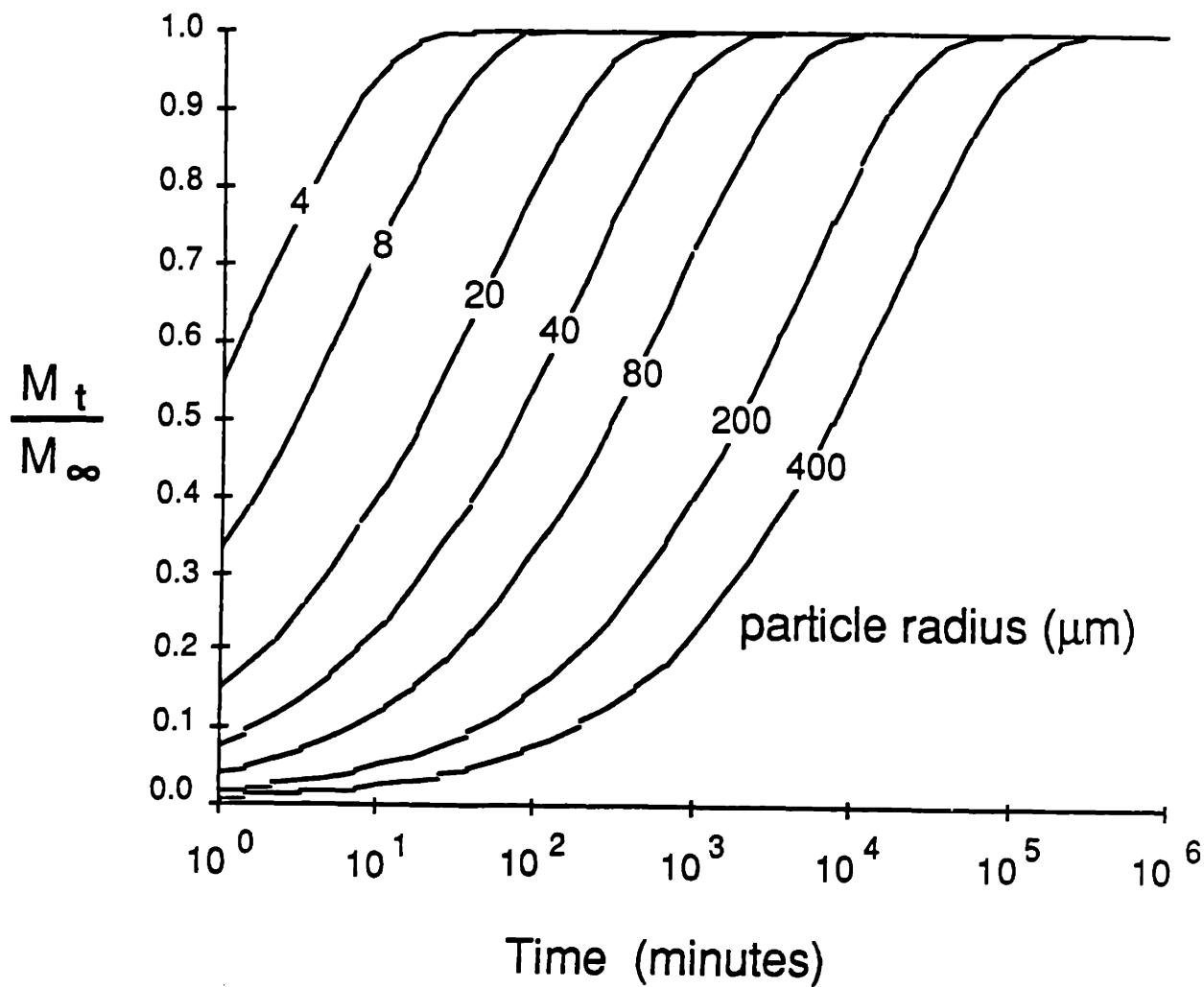
Figure 3.2   The effects of particle size on the rate of sorption. The

simulation parameters are: n=0.13, ρ_s=2.5 g/cm^3, D_m=6x10^{-6}

cm^2/s, f_{oc}=0.02, and K_{ow}=10^5. K_{oc} is calculated by using: log

K_{oc} = log K_{ow} - 0.21, and solid concentration, ρ, is adjusted

so that $K_p\rho$=1...74

approximations. Cooney et al. (1983) discussed the significance of the error

due to replacement of several different types of particle size distribution

(from 0.1 mm to 0.4 mm) with uniform sizes. Significant errors were found for

highly non-Gaussian particle size distributions or at late periods of uptake.

We examined the problem by treating the cases where natural soil or sediment

size distributions span from one to two orders of magnitude. For a block-log

distribution spread over one order of magnitude (size distribution #1 in Fig.

3.3), Fig. 3.4 shows that use of the geometric mean of the largest size and

the smallest size gives an analytical solution lower than the exact solution

by a factor of 2 at $t_{10\%}$, within 20% around $t_{1/2}$, and very close to the exact

solution near the completion of equilibration (i.e., 6% error at $t_{90\%}$). This

choice of representative size is consistent with the approach by Mathews

(1983). For a wider size distribution in which aggregate size spans over two

orders of magnitude (size distribution #2), the uniform size approximation

underestimates the sorption behavior by a factor of 3 at beginning, a factor

of 2 at $t_{1/2}$ and still has an error of 10% at $t_{90\%}$ (Fig.3.4). The geometric

mean of a size distribution appears to be a reasonable choice only if the size

distribution is within one order of magnitude.

3.3.2 First-Order Approximation for Sorption Kinetics

    It has been suggested that the sorption kinetics is similar to

first-order chemical reactions and can be modelled accordingly (Oddson et al.,

1970; van Genuchten et al., 1974). The model is described mathematically as:

$$\frac{dS'}{dt} = k_{-1}C - k_1 S'$$ (3.27)

75
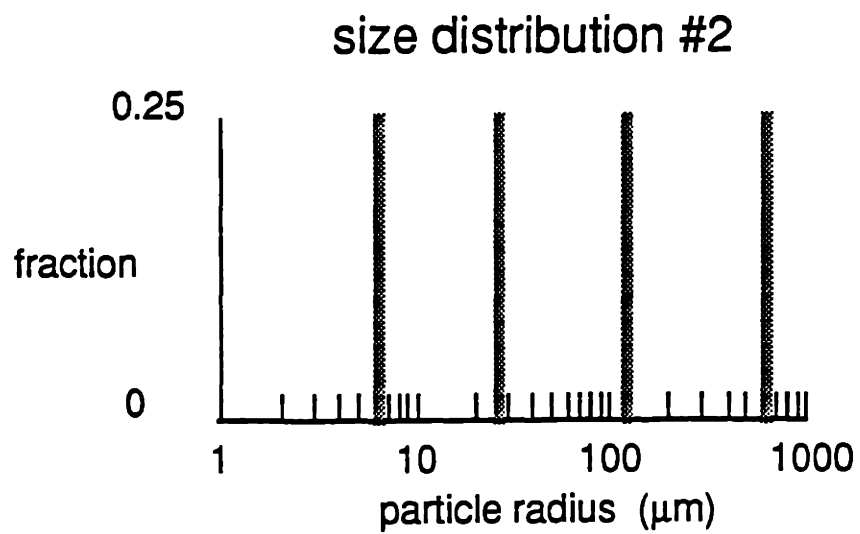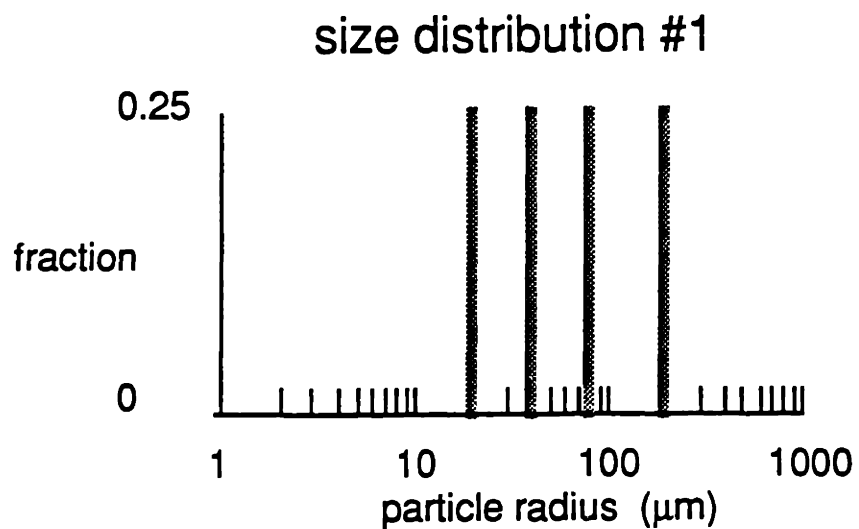
Figure 3.3   Two hypothetical size distributions (with same geometric mean
              size of 63 μm) used in the model simulations to represent
              narrow and wide particle size range.
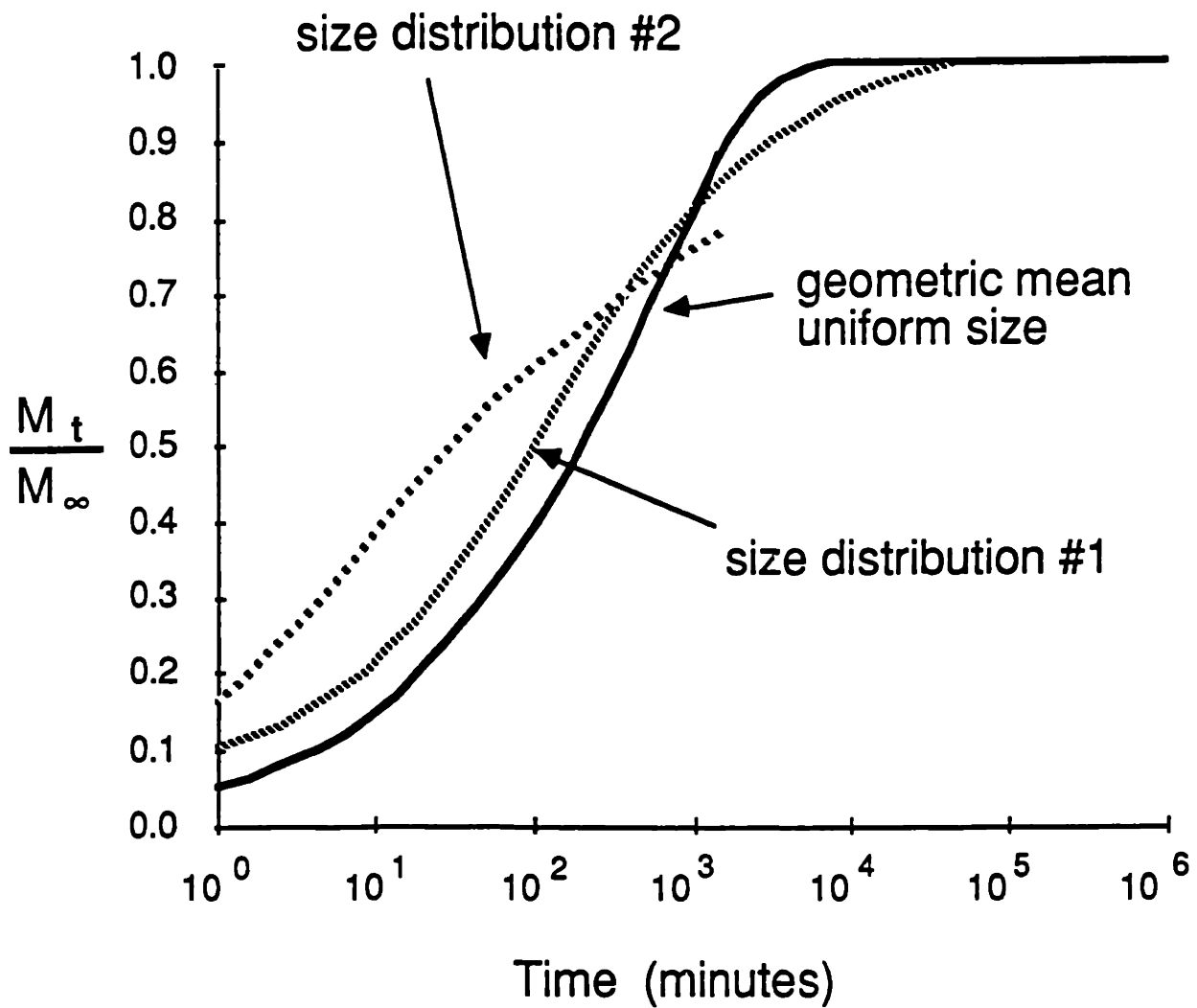
Figure 3.4   An analytical solution using a geometric-mean single size to represent polydisperse particles is compared with solutions obtained by using the numerical method and knowledge of the size distribution. The simulation parameters are the same as those in Fig. 3.2. The geometric mean uniform size is 63 μm.

and

$$\frac{dC}{dt} = k_{-2}S' - k_2C \qquad (3.28)$$

in which k_1, k_{-1}, k_2 and k_{-2} are first-order reaction rate constants. k_{-1} and

k_{-2} are related to k_1 and k_2, respectively, by the partition coefficient, K_p:

$$k_{-1} = k_1 K_p \qquad (3.29)$$

$$k_{-2} = k_2/K_p \qquad (3.30)$$

which are obtained by letting $dS'/dt = dC/dt = 0$ and $S' = K_p \cdot C$. By

substituting Eq. 3.29 and 3.30 into the next mass balance relationship, Eq.

3.31, we reduced the number of independent parameters to 1 (i.e., k_1).

$$\frac{dC}{dt} = -\rho \frac{dS'}{dt} \qquad (3.31)$$

$$\therefore k_2 = k_1 \cdot \rho \cdot K_p \qquad (3.32)$$

This model has been widely used to model sorption kinetics for two major

reasons. First, it has only one fitting parameter, k_1, and a very simple

solution:

$$M_t/M_\infty = 1-\exp[-k_1(K_p \cdot \rho+1)t] \qquad (3.33)$$

In the special case of an infinite bath system in which

$$\rho \cdot K_p \ll 1$$

or

$$C = C_o \ (\text{constant})$$

the solution is

$$M_t/M_\infty = 1-\exp(-k_1 t) \qquad (3.34)$$

Second, most environmental chemical fate models use compartment (box) models in which water bodies, air, sediment beds, suspended particles, themselves or their segments are represented as homogeneous compartments (e.g., SERATRA, (Onishi and Wise, 1982); and TOXIWASP, (Ambrose et al., 1983)). Diffusion and advection processes are translated into fluxes across the boundaries of the compartments and the governing equations are composed of first order exchange terms

i.e., $\quad \Delta C = \Delta t \cdot [\sum_i (\sum_j k_i \cdot C_j) - \sum k_{-i} \cdot C] \qquad (3.35)$

in which k_i = exchange rate constant, i denotes different transport processes,

and j denotes different adjacent compartments. Consequently, the first-order kinetic model can be easily fit into the typical chemical fate models by inserting the terms on the right-hand-side of Eq. 3.27 and 3.28 into the governing equations of appropriate compartments.

This model does not fit experimental results as well as the retarded radial diffusion model (Chapter 2). The error is due to the attempt to fit an infinite series of exponential terms by only one exponential term (see analytical solutions of radial diffusion model, (Crank, 1975)). However, compared to the uncertainty in the parameter estimates used in fate models and the error inherent in the modelling approaches, this error may be acceptable in some modelling situations.

In spite of its simplicity and wide adaptability, a primary drawback of the first-order sorption kinetics model is its lack of correlation between the parameter k_1 and environmental chemical properties. Comparing the solution of the first-order model with the analytical solutions of the retarded radial diffusion model, we found that a reasonable approximation of the value of k_1 is D_{eff}/R^2 multiplied by a correction factor, α, i.e:

$$k_1 = \alpha \cdot D_{eff}/R^2 \tag{3.36}$$

If we match the first-order solution with the radial diffusion model at half-equilibration time, $t_{1/2}$ (i.e., $M_t/M_\infty = 0.5$), we minimize the error of the first-order solution at the most rapidly changing period. From the analytical solution chart (Fig. 3.5), the correction factor, α, for the infinite-bath
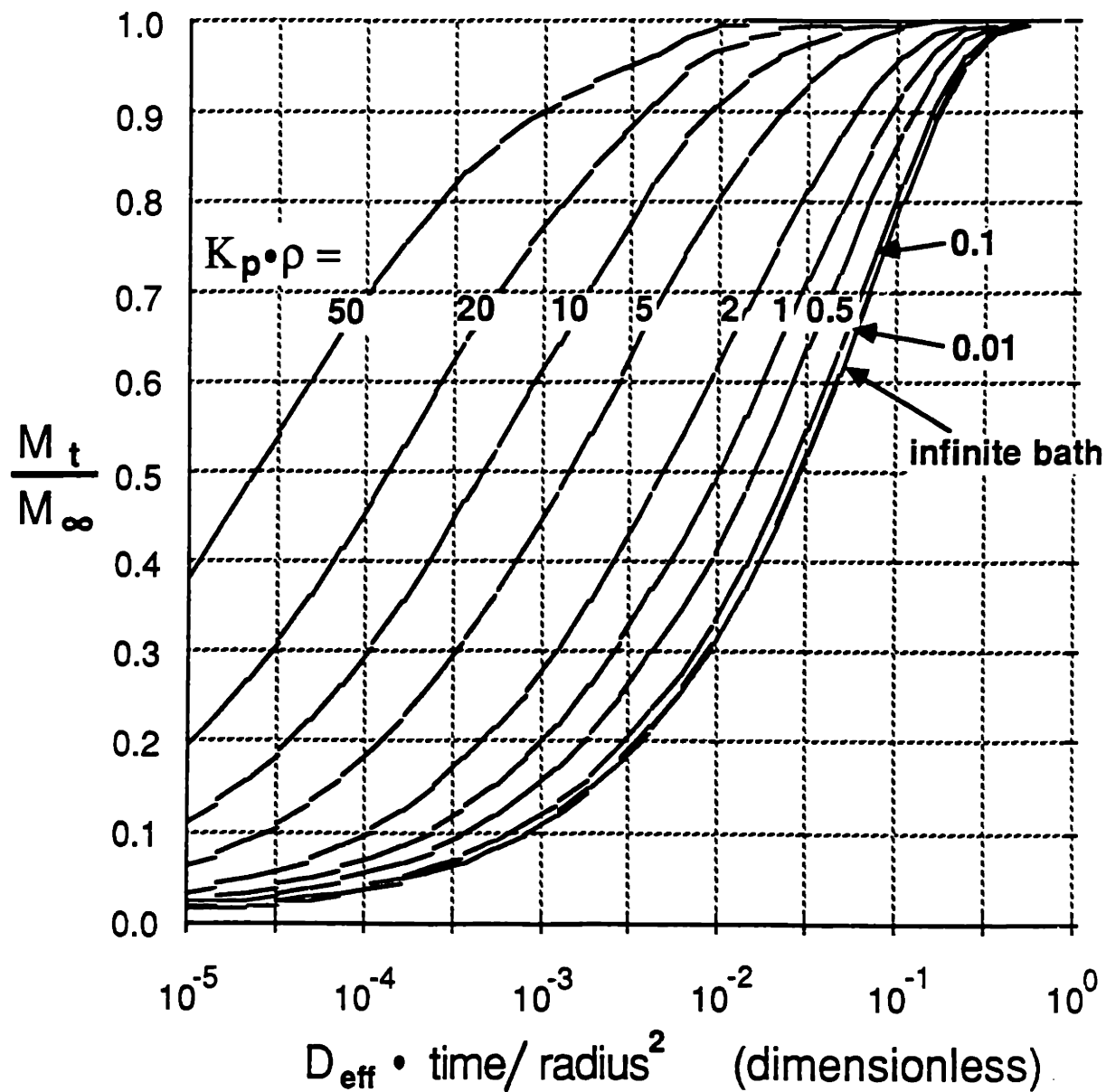
Figure 3.5   Analytical solutions for the radial diffusive uptake or release by spherical particles suspended in a closed system. The numbers on curves show the final ratio of the mass sorbed on solids to the mass dissolved in the solution.

system is found to have a constant value, 22.7. That is,

$$k_1 = 22.7 \, D_{eff}/R^2 \qquad (3.37)$$

For finite bath systems, the correction factor is a function of $K_p \cdot \rho$, i.e.,

$$\alpha = 10.56 \, K_p \cdot \rho + 22.7 \qquad (3.38)$$

By introducing these correlations of k_1 with D_{eff}/R^2 and $K_p \cdot \rho$, we are able to predict an optimal value of k_1 from environmental and chemical properties. In effect, by adjusting the first-order sorption rate constant according to the particle size of interest, the D_{eff}, and the sorbing capacity, $K_p \cdot \rho$, we incorporate most of the solution to the retarded radial diffusion description of sorption kinetics (whose solution is an infinite series of exponential terms with arguments of $D_{eff} \cdot t/R^2$ multiplied by coefficients including functions of $K_p \cdot \rho$ (Crank, 1975)).

The simulation curves of this modified first-order model are compared with those of the radial diffusion model in Fig. 3.6. Obviously, first-order solution curves defined in this manner match the radial diffusion solution exactly at $t_{1/2}$ since we set k_1 according to this criterion. The deviation from the radial diffusion solution is moderate for the infinite bath system

82
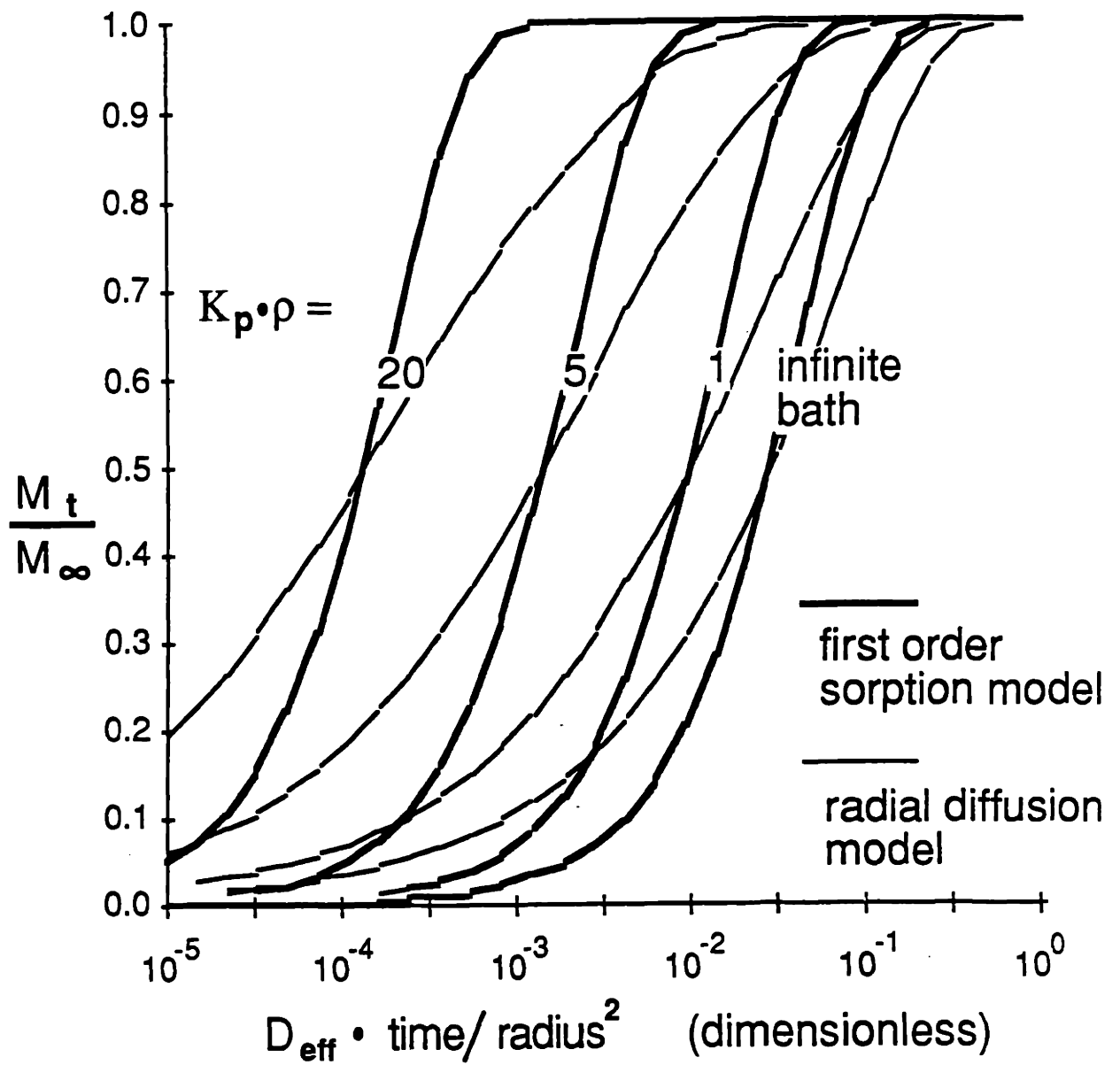
Figure 3.6   Comparison of the solution of the first-order sorption model
                with the analytical solution of the radial diffusion model.
                The numbers on curves show the final ratio of the mass sorbed
                on solids to the mass dissolved in the solution.

and increases with $K_p \cdot \rho$ for finite-bath system.

3.4 Simulation Results

3.4.1 Time Varying Aqueous Concentration

Two hypothetical cases were used to demonstrate how particulate concentrations respond to variations of aqueous solute concentration. In the first case, we can imagine that one reach of a river starts to receive waste discharge during the daytime. The concentration in the aqueous phase, to which the surface of the river bed will be exposed, changes repeatedly with constant concentration for 12 hours and zero concentration for another 12 hours (Fig. 3.7). The time course of the concentration in the solid phase for a compound with K_{ow} of 10^4 is predicted to follow the source strength variation closely, reaching 90% of equilibration in 12 hours. If the chemical exhibited a greater hydrophobicity (K_{ow} of 10^5), only 60% of equilibration would be reached in the first cycle. The change in solid phase concentrations between periods of uptake and periods of release is predicted to be smaller. Sorption kinetics would still be fast enough to result in a significant discrepancy from a time-averaged equilibrium treatment. For a compound with still higher K_{ow} (i.e., 10^6), there would be even smaller sorbed concentration variation and slower approach to the mid-point (i.e., slower approach to a quasi-steady state with an average concentration equal to the average equilibrium concentration, $S = 0.5 \, K_p C_o$). The environmental implication is that if a pollutant takes a long time (days to weeks) to exchange, the

84

diurnally varying source strength ——————

sorbed concentration response $K_{ow} = 10^4$ ﹉﹉﹉﹉

$= 10^5$ ﹀﹀﹀﹀

$= 10^6$ ——————
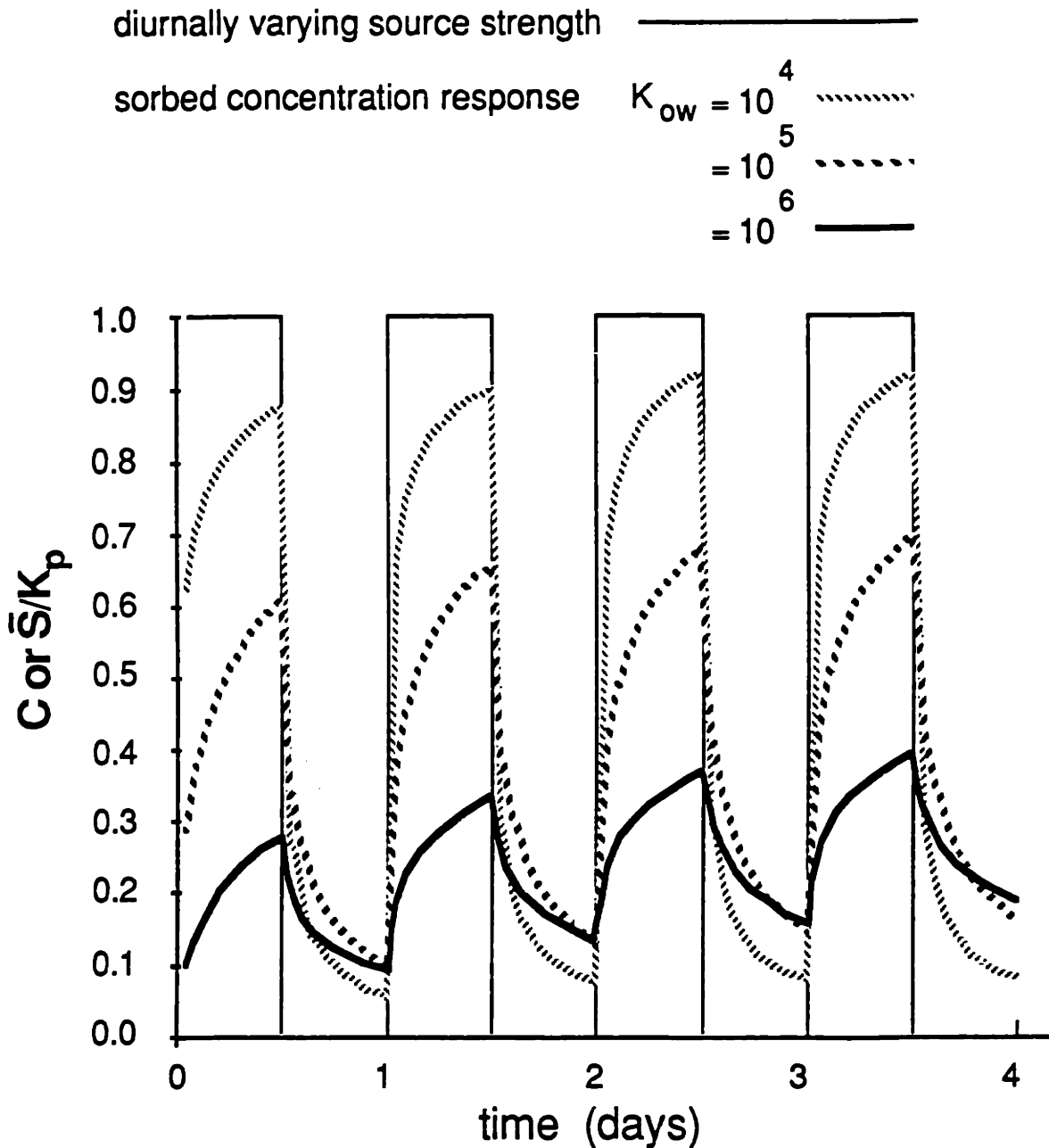
Figure 3.7   Time course of predicted concentration in the solid phase with diurnally varying source strength. The simulation parameters are: $n=0.13$, $\rho_s=2.5$ g/cm^3, $D_m=6\times10^{-6}$ cm^2/s, $f_{oc}=0.02$. K_{oc} is calculated using: $\log K_{oc} = \log K_{ow} - 0.21$. Size distribution #1 is used.

variation of the dissolved concentration and the total amount of a pollutant in a water body would be damped due to the chemical's high hydrophobicity and resultant slow sorption kinetics.

The performance of the first-order model with or without uniform size approximation in simulating this transient aqueous concentration is investigated too. With particle size distribution #1, the first-order model operated for each size class yields a prediction which is very close to the radial diffusion model for a sorbate with K_{ow} of 10^5 (Fig.3.8b). If a single (geometric mean) size is assumed, the prediction deviates somewhat. For sorbates with lower K_{ow} (i.e., 10^4), the first-order model overpredicts the equilibration progress (Fig.3.8a), while for more hydrophobic substances (e.g., K_{ow} of 10^6) the first-order model lags behind the radial diffusion model and underestimates the progress of approach to equilibrium (Fig.3.8c). Assuming a geometric mean size distribution exaggerates these effects. The reason for these model successes and failures is clear. When the sorbate K_{ow} is 10^5, the time scale of sorption/desorption kinetics (i.e., 9 hours) is close to the concentration fluctuation time scale (i.e., half day) and the first-order model is tuned to match the radial diffusion model at this range; therefore, we obtain a good simulation result even with the first-order model. In case in which the system has not reached ($K_{ow} = 10^6$) or already passed ($K_{ow} = 10^4$) the half equilibration point (i.e., $t_{1/2}$), when the aqueous concentration changes, the first-order model will underestimate or overestimate the progress as illustrated in Fig. 3.6. This prediction error

$K_{ow} = 10^4$
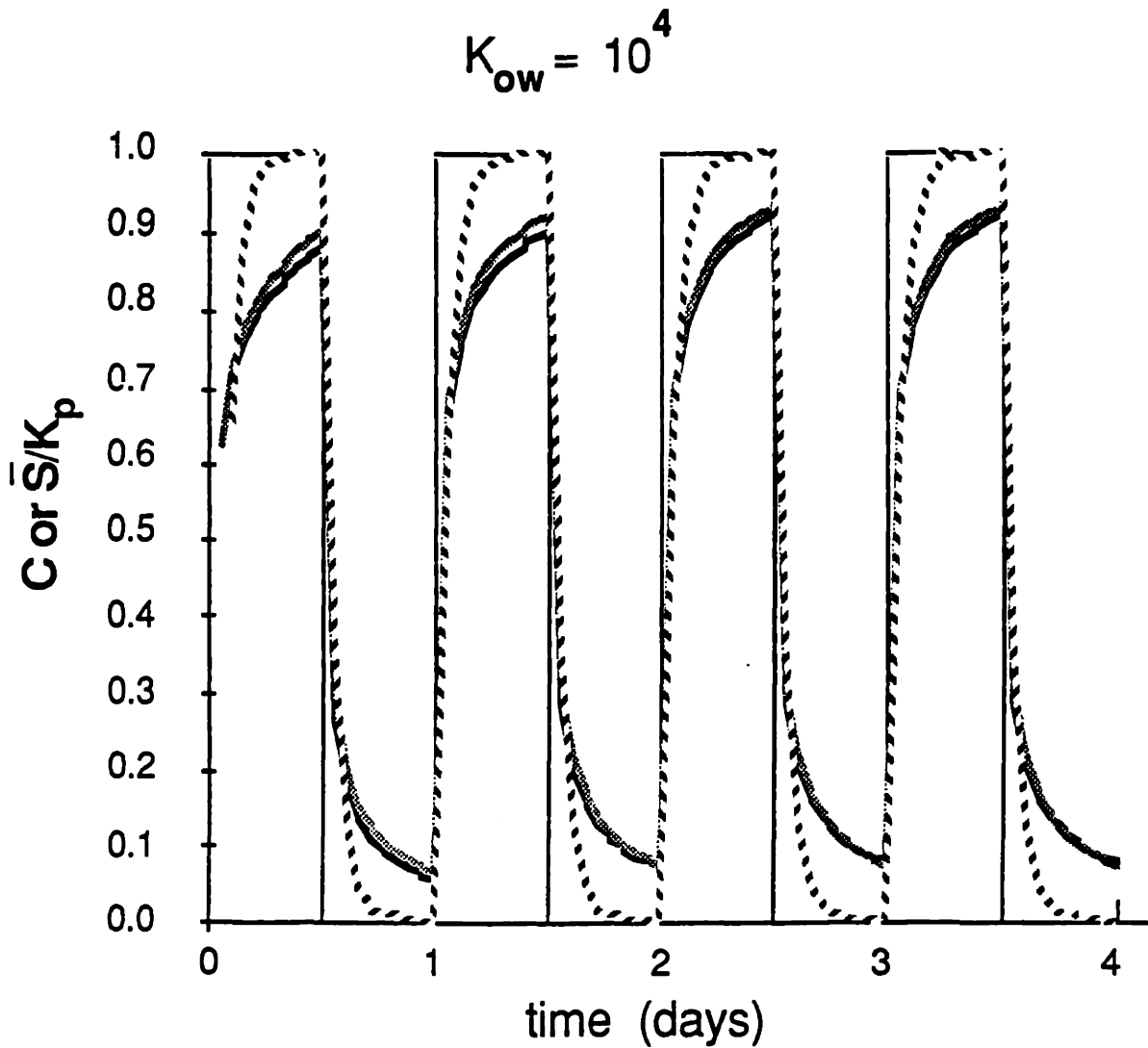
Figure 3.8-a   Comparison of the numerical radial diffusion model (solid

line), the first-order model with geometric mean uniform size

(dotted line), and the first-order model with actual particle

size distribution (distribution #1) (gray line) by simulations

of the response of the sorbed concentration to a transient

aqueous concentration condition.   The simulation conditions are

the same as those in Fig. 3.7. $K_{ow}=10^4$.
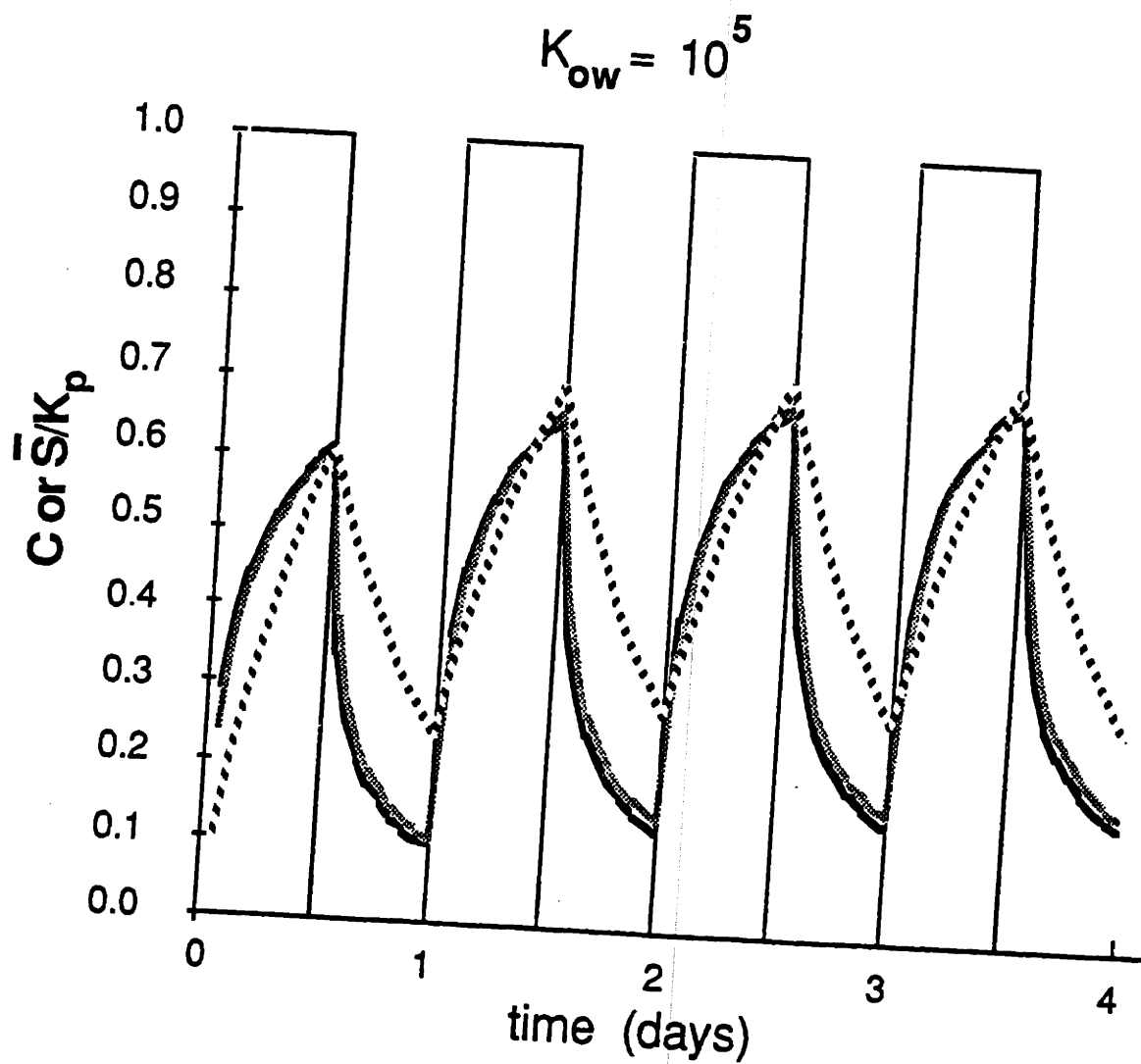
$$K_{ow} = 10^5$$

Figure 3.8-b   The same as Fig. 3.8-a except that $K_{ow}=10^5$.
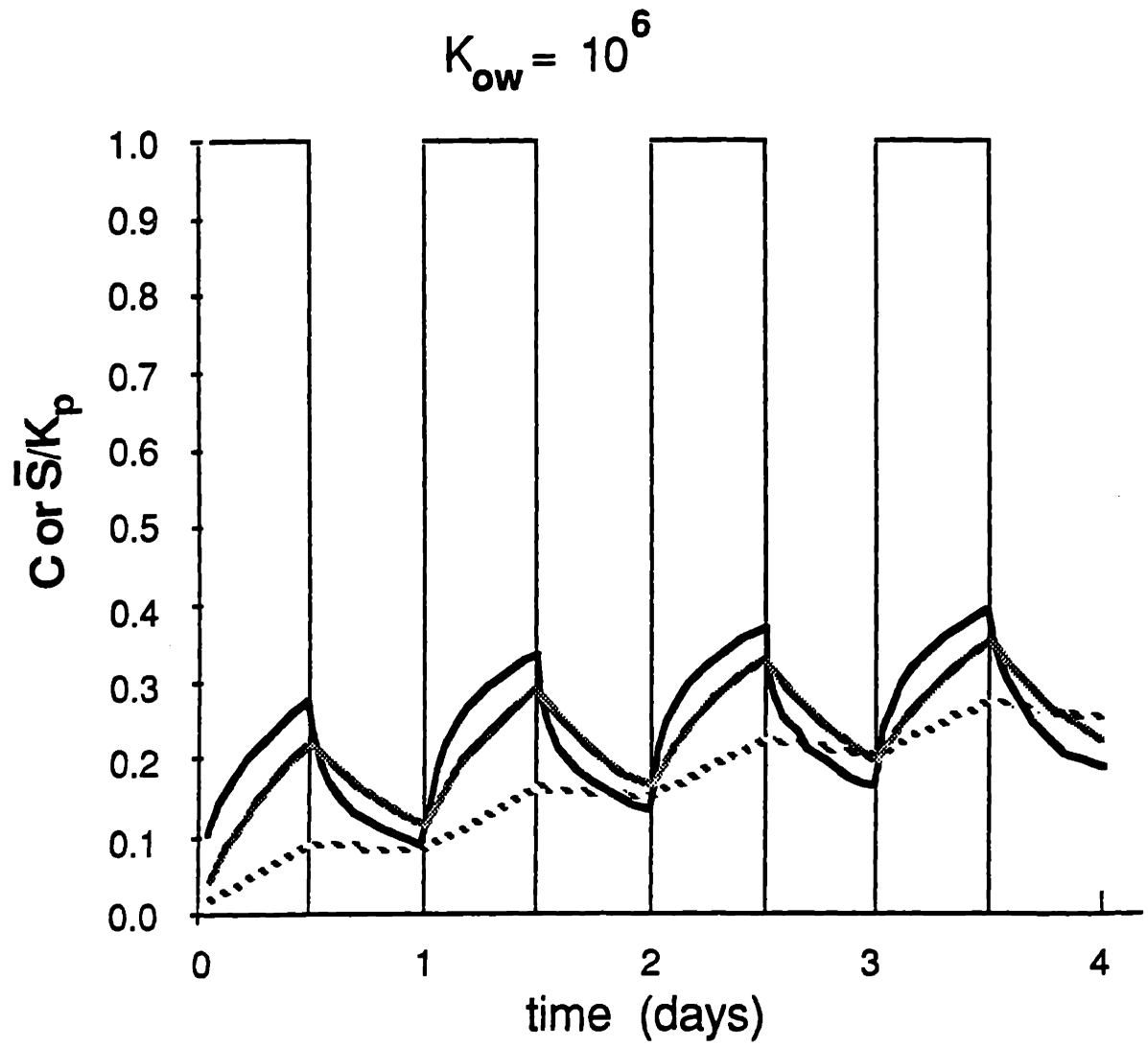
$$K_{ow} = 10^6$$

Figure 3.8-c The same as Fig. 3.8-a except that $K_{ow}=10^6$.

is inherent in the correction factor, α, which is obtained by fitting the first order solution to the $t_{1/2}$ point. Correlations are also possible at any other equilibration point (e.g., $t_{90\%}$, or $t_{10\%}$). If we establish a relationship between the coefficients in Eq. 3.36 and the equilibration progress points, by knowing the fluctuation time scale in the system we can choose an appropriate correction factor, α, and improve our prediction.

Another interesting example involves the consecutive desorption experiments performed in laboratories which may have artifacts due to incomplete equilibration (Fig. 3.9-a). Clean water is assumed to be equilibrated with previously equilibrated contaminated soil. Before reaching complete desorption equilibration, the aqueous phase is replaced by clean water and the procedure repeated. For a compound with K_p of 10^4, we can see that desorption for 1 day could easily be incomplete; thus replacing the insufficiently equilibrated water could cause a kinetic artifact. Using the dissolved and sorbed concentrations predicted by our sorption kinetics model, it is obvious that in these circumstances we would observe increasing K_p with each subsequent desorption experiment. By plotting the "equilibrium" concentrations in the solid phase versus that in aqueous phase at the end of each desorption cycle we see that the model predicts the desorption points will deviate from the sorption isotherm (Fig.3.9-b). Such kinetic effects could contribute to the observed "desorption isotherms" which other workers have interpretted as sorption irreversibility or hysteresis (Swanson and Dutt, 1973; Peck et al., 1981).
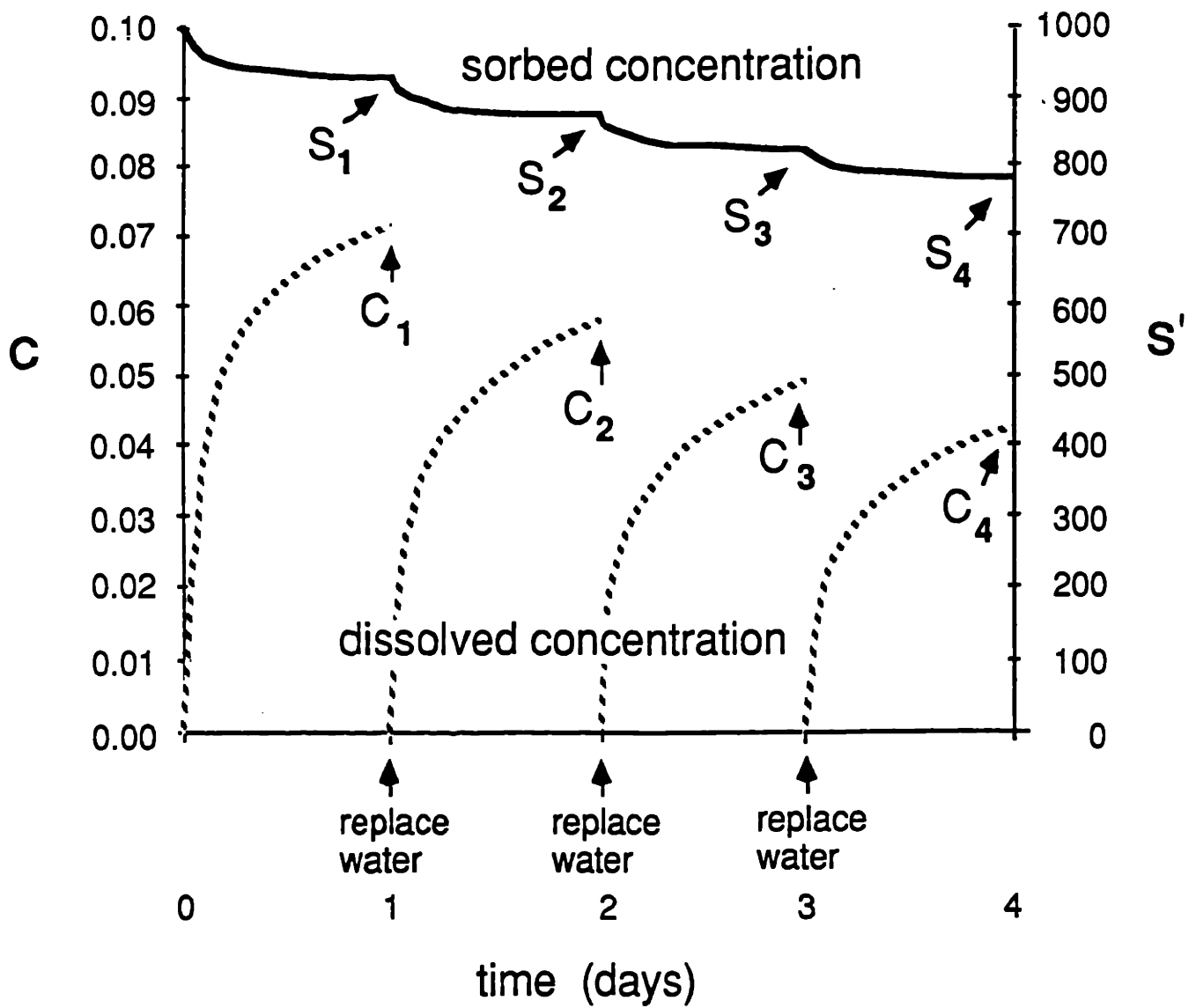
Figure 3.9-a   Time course of the predicted concentration in the solid phase

(S) and in the aqueous phase (C) during a hypothetical

consecutive desorption experiment. The simulation parameters

are: $n=0.13$, $\rho_s=2.5$ g/cm^3, $D_m=6\times10^{-6}$ cm^2/s, $\rho=1000$ mg/L, and

$K_p=10^4$ cm^3/g. Size distribution #1 is used.
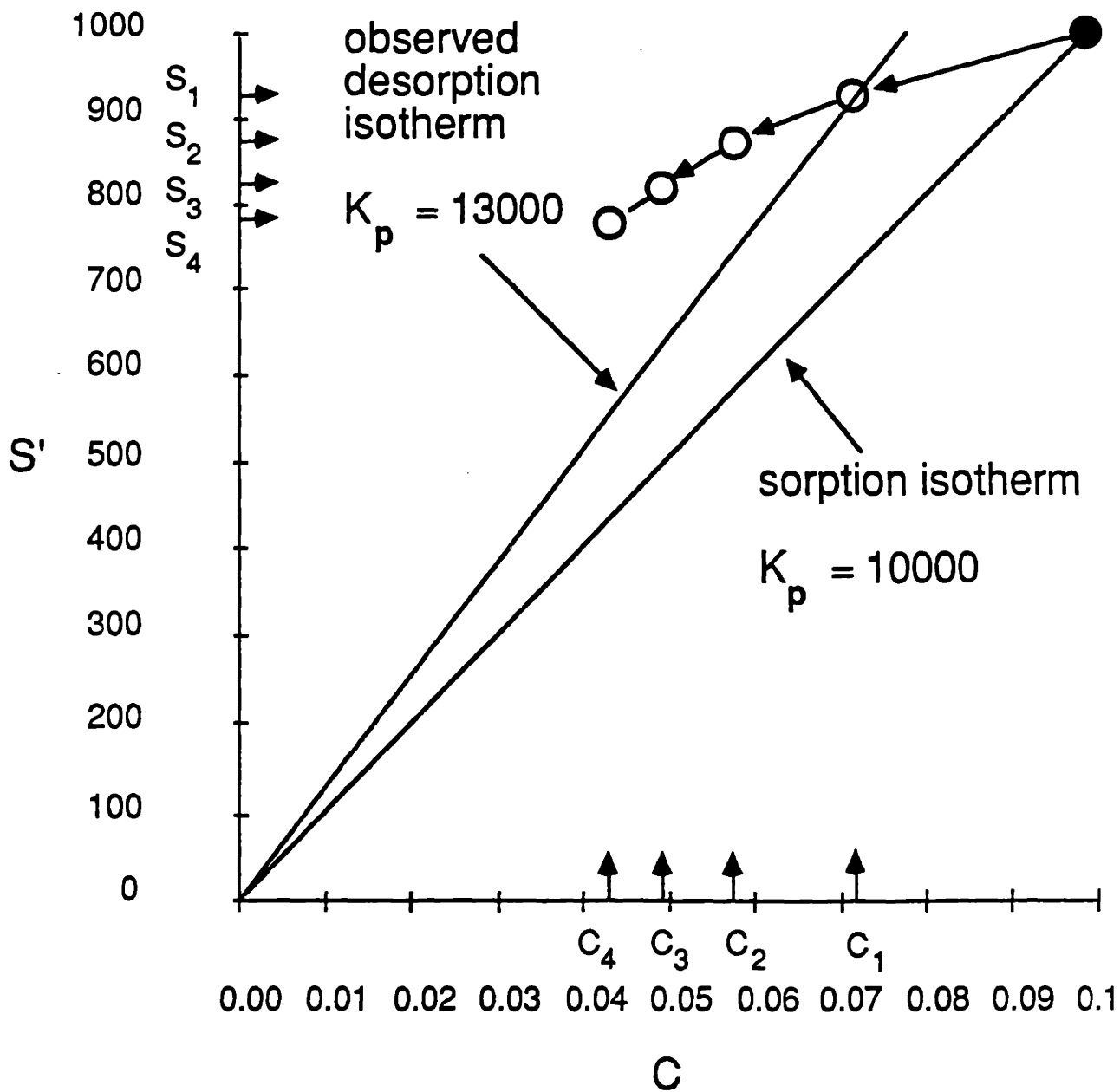
Figure 3.9-b   Sorption and the first desorption isotherms derived from the

hypothetical consecutive desorption experiment shown in Figure

3.9-a.

3.4.2 Coupling the Movement of Particles and Sorption Kinetics

In the previous examples, all particles were in a homogeneous well mixed system. The movement of particles between solutions of differing dissolved concentrations was not considered. Theoretically, this numerical method could solve problems with moving particles as long as the initial conditions (including the local concentrations in the particles) could be well defined and the fate of each particle could be traced. It becomes impractical when the movement of the particles are random and there are infinite patterns of the histories of the particles to be remembered. However, when we can describe particle transport, we may use the numerical model to predict the importance of sorption kinetics to pollutant transport. In the next example, we assume that an instantaneous input load of particle-bound pollutant is introduced into a water body by a storm-induced soil erosion or bed sediment resuspension event. The particles are well-mixed vertically; and they are subsequently gradually depleted due to settling. The first-order disappearance rate of a particle class is given by its settling velocity divided by the depth of the water column.

$$\frac{d\rho_i}{dt} = \frac{v_{si}}{L} \rho_i \qquad\qquad (3.39)$$

in which ρ_i = solid condentration of ith particle group g/cm^3, v_{si} = settling velocity of particles in i^{th} group (cm/s), and L = water depth (cm). While these solids reside in the water column, they releasesorbed pollutants as described by Eq. 3.12.

In this case, the fate of the input solid particles is well defined. The total solid concentration in the water column decreases gradually, and with the particular particle size distribution (#1 in Figure 3.3) and water column depth of 10 m, only 1/4 of the original amount, mostly small-size particles, remains suspended after 3 days (Fig.3.10-a). For a compound with K_{ow} of 10^5, the aqueous concentration is predicted to build up due to compound desorption from the solid particles remaining in the water column, and reach a nearly steady state in about 1 day (Fig.3.10-b). The total concentration (dissolved plus solid-bound compound) in the water column drops due to removal of particles still containing significant loads of sorbate. However, the dissolved concentration no longer changes much after one day because desorption would be nearly complete. The solid-bound sorbate contributes very little to the total concentration after the second day. Fig.3.10-c shows a similar case in which the sorbate has a greater hydrophobicity ($K_{ow} = 10^6$). In spite of the same solid disappearance rate, the total pollutant depletion process lasts longer and results in a lower aqueous concentration because of the slower kinetics arising from the higher partition coefficient. At the end of the third day, the solid-bound form of sorbate still contributes about 30% of the total concentration in the water column.

This example demonstrates the importance of including kinetics in chemical fate models. We can readily see that the aqueous concentration of pollutants in the water column after similar events (e.g., sediment bed resuspension by a storm, pulse input of contaminated sils carried by a strong run off episode, sludge discharge from abarge, and spillage during dredging events) is determined by the competition between settling depletion of the
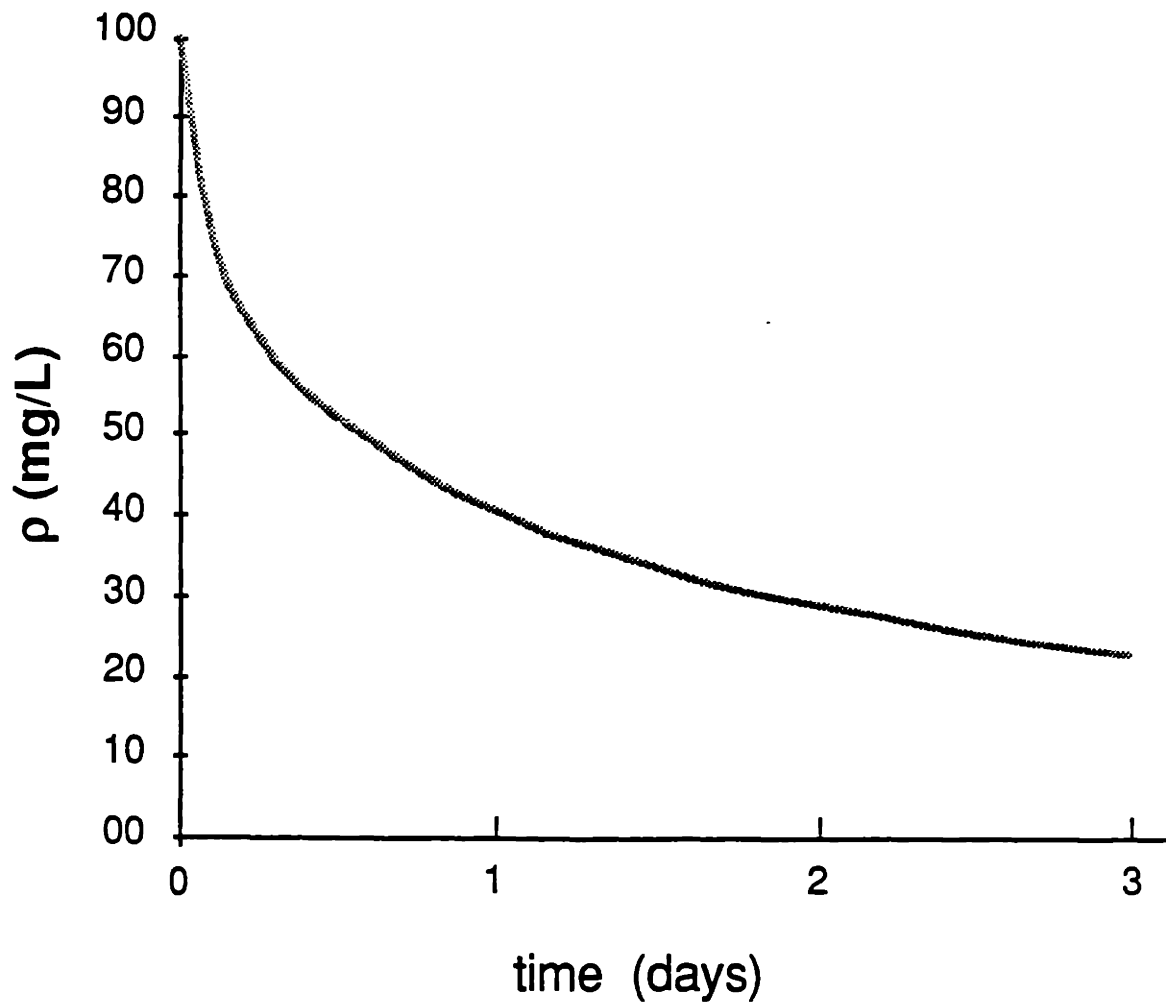
Figure 3.10-a   The suspended solid concentration in the water column versus

time after a pulse input by a storm.   The initial solid

concentration has concentration of 100 mg/L and particle size

distribution #1.   The depth of the water column is 10 m.   Bulk

density of aggregates is 2 g/cm³.
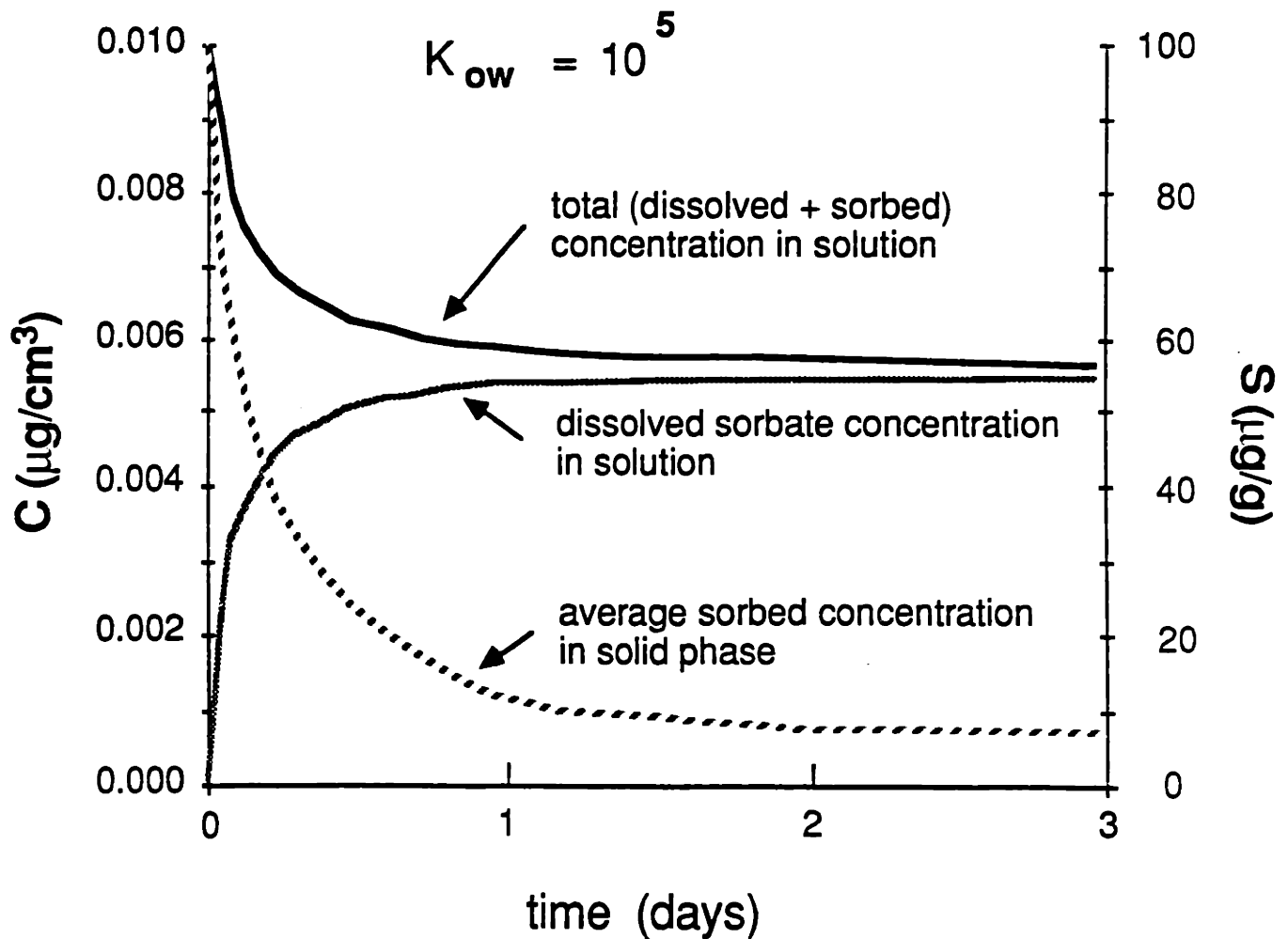
Figure 3.10-b   The total concentration in the water column, the dissolved

concentration, and the average sorbed concentration in the

solid phase after a pulse input of contaminated solids by a

storm.   The initial sorbed concentration is 100 $\mu g/g$.   The

simulation parameters are: $n=0.13$, $\rho_s=2.5$ g/cm^3, $D_m=6\times10^{-6}$

cm^2/s, $f_{oc}=0.02$, and $K_{ow}=10^5$ cm^3/g. K_{oc} is calculated by using:

$\log K_{oc} = \log K_{ow} - 0.21$.
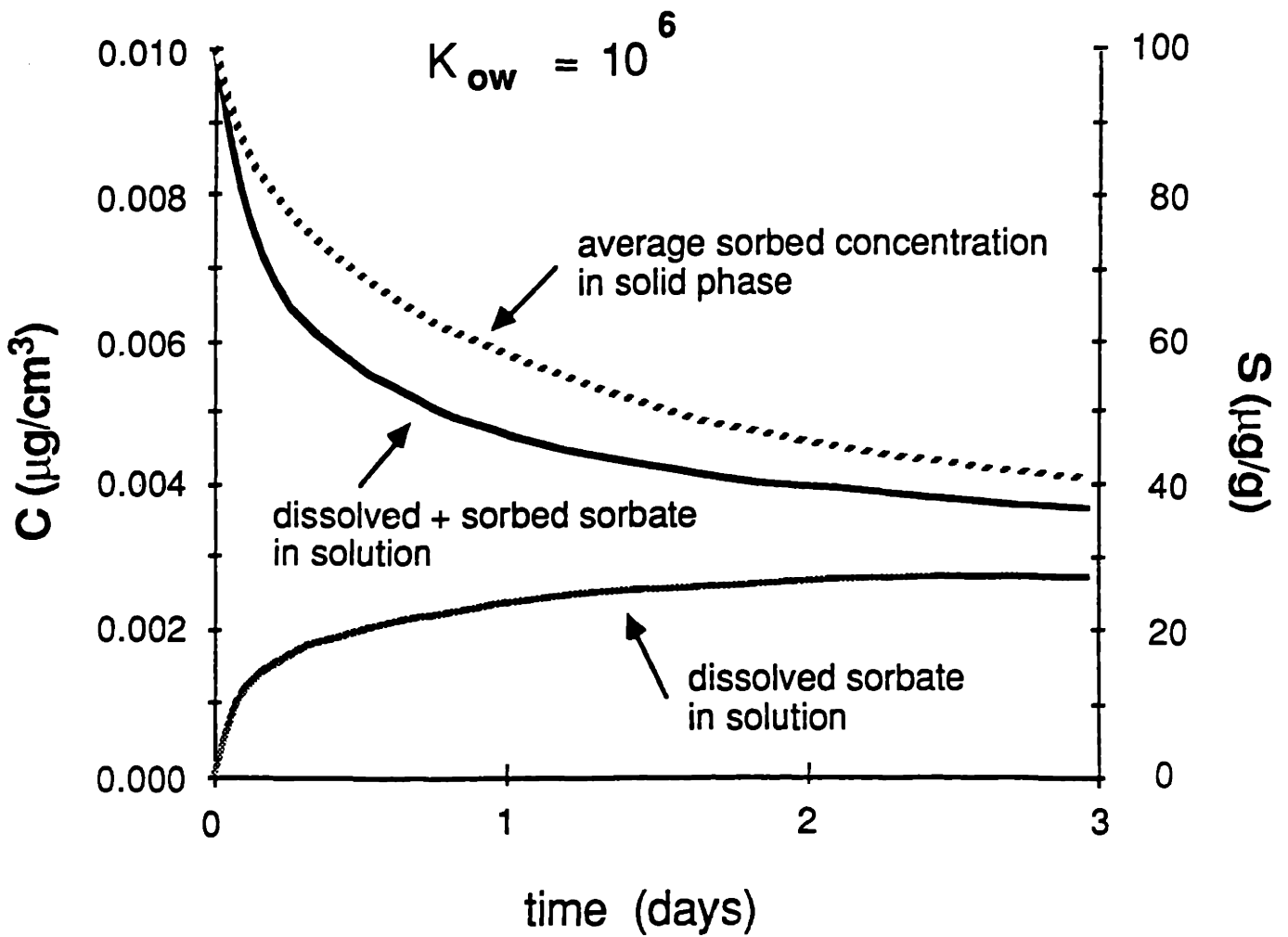
Figure 3.10-c   The total concentration in the water column, the dissolved

concentration, and the average sorbed concentration in the

solid phase after a pulse input of contaminated solids by a

storm. All simulation conditions are the same as in Fig.

3.10-b except that $K_{ow}=10^6$.

particles and the chemical release kinetics. Ultimately, the capability of prediction including the effects of sorption kinetics will depend on our understanding of particle fates in aqueous environments and the availability of modelling techniques (e.g., Stokes settling in the example above) for this particle transport.

3.5 Selecting An Approximation Scheme For Use In Chemical Fate Modelling

In light of the model simulation results, it is clear that a variety of sorption kinetics problems can be solved by using the numerical approach. However, the long computation time required for wide particle size distributions is a disadvantage of this numerical scheme. The analytical solution with a geometric-mean size and the first-order model are the two alternative methods which provide a reasonable approximation for the actual solution under certain conditions.

Analytical solutions can be used for simple boundary conditions (i.e., constant aqueous concentration or closed system with mass conserved) and narrow particle size distribution (i.e., within one order of magnitude) which can be represented by a uniform geometric-mean size.

Narrow size distribution is also required for the first-order kinetics model to be accurate. Because the modified first-order model only fits the radial diffusion solution at the half-equilibrium point, $t_{1/2}$, our choice to use this model should be based on the characteristic time scale of the system, t_c, which is the contact time between the water and the particles (e.g., the residence time of particles in the water column, or the time scale of the aqueous concentration fluctuation). When the expected $t_{1/2}$ (=$0.693 \cdot R^2/$

$[\alpha \cdot D_{eff} \cdot (K_p \cdot \rho + 1)])$ is far from the t_c (i.e., $t_c/t_{1/2} \ll 10^{-0.5}$ or $t_c/t_{1/2} \gg$ $10^{0.5}$), the numerical method should be used. Multi-size treatment in the first-order model simulation will greatly increase the accuracy of the solution. However, we should examine $t_{1/2}$ for each size group to insure the appropriateness of using this simple first-order approximation.

Analytical solutions for radial diffusion and first-order models also provide a means to quickly evaluate the significance of sorption kinetics. By calculating the dimensionless system characteristic time, $D_{eff} \cdot t_c/R^2$, and finding the intersection of the corresponding result with the solution curve of the appropriate $K_p \cdot \rho$ in Fig. 3.5, we see the extent of sorptive exchange completion, the value of $t_c/t_{1/2}$ (i.e., calculated $D_{eff} \cdot t_c/R^2$ divided by $D_{eff} \cdot t_{1/2}/R^2$ at $M_t/M_\infty = 0.5$ in chart), and whether the assumption of equilibrium can be applied. In addition, we can estimate the error due to replacing the radial diffusion model with the first-order model at different value of $t_c/t_{1/2}$ from Fig. 3.6.

For example, the relative rapidity of approach to equilibrium for systems with the same chemical properties (i.e., D_{eff} and K_p), the same particle sizes, but different solid concentrations is visualized in Fig. 3.5. For sediment beds or soils with solid concentration near 1 g/cm^3, and quite high values of K_p, we may expect sorption exchange timescales to be over 100 to 1000 times shorter than for suspended solids with concentrations from several milligrams per liter to 1000 mg/L. This has dramatic implications for

the assumption of sorption equilibrium, for example, in groundwater transport modelling. With flow in the interstitial pores at moderate velocity (lower than 1 m/day), the contact time between the flowing water and an aggregate with 0.1 cm diameter will be longer than 1 mimute, and most compounds in the aqueous phase can reach equilibrium with their sorbed components.

3.6 Conclusion

A numerical model, capable of describing sorptive exchange in aqueous systems containing a spectrum of particle sizes and time-varying solution conditions, has been developed. This model can handle a variety of environmental situations which we encounter in attempting pollutant fate predictions. The feasibility of incorporating the radial diffusion model into the global fate models depends on our ability to describe the fates of the particles. A simple example in which a water body receives a pollutant load from a sudden input of contaminated solids can be handled by coupling particle settling and sorption kinetics. Using this sorption kinetics model also demonstrates our ability to predict the fates of chemicals in a dynamic environment without assuming aqueous/solid equilibrium.

Two other solution techniques (i.e., analytical solutions for a single geometric-mean size and the first-order approximation) were tested by using the numerical model in this work. Simulation results indicate that neglecting size distribution effects is the major source of prediction error. Users with an adequate understanding of the limitations of these two approximate approaches should be able to use them to simulate sorption kinetics. Additionally, use of these simplifications can help investigators judge the importance of sorption kinetics in a particular situation.

100

CHAPTER 4

Transfer of Hydrophobic Organic Pollutants Between Bottom Sediments and Water

4.0 Introduction

Many organic pollutants are brought into water bodies by surface runoff or wastewater discharge. Some of these chemicals, especially those which are hydrophobic, have a strong tendency to become associated with particulate matter and consequently are accumulated in sediment beds. Polychlorinated biphenyls in the Hudson River (Bopp et al., 1981) and kepone in the James River Estuary (Huggett et al., 1980) are typical examples. In these water bodies, pollutants are still found in the water column and aquatic biota several years after the elimination of direct discharge of these compounds (Huggett et al., 1980; Brown et al., 1985). This is because the sediment beds act as reservoirs for these persistent organic subtances and continuously release these pollutants to the water column.

Many processes are involved in the transfer of pollutants between bottom sediments and the overlying water. Sediment resuspension and bed-load transport on the bed surface dominate the transport of sorbed compounds under high flow conditions in rivers (Turk, 1980). However, under low energy conditions (i.e., rivers or side embayments with low flow rate, lakes, or deep sea floors) molecular diffusion of dissolved species or colloid-bound species through sediment pore fluids may be important (Brownawell, 1986). Activities of benthic animals may also enhance the transport of chemicals in the bed. In this chapter, we focus on only the transport processes in quiescent water and,

especially, on the effects of the sorption equilibrium and kinetics on these processes (i.e., molecular diffusion, colloid-mediated diffusion, and bioturbation).

Molecular diffusion through the pore water is important in cases without mixing or resuspension of sediment solids. For hydrophobic compounds, diffusion is retarded because a high fraction of the sorbate is bound to the solid matrix in the bed and is nonmobile. A retarded-diffusion model, which uses a linear partition equilibrium model for hydrophobic compounds to predict the retardation factor, has been developed and substantiated by experimental results of various workers (Di Toro et al., 1985; and Karickhoff and Morris, 1985).

When large amounts of colloids or macromolecules exist in the pore fluid phase, additional transport and partitioning phenomena may need to be considered (Brownawell, 1986). The presence of nonfilterable organic matter in the sediment pore water has long been recognized (Starikova, 1970; Krom and Sholkovitz, 1977; Henrichs and Farrington, 1984; Brownawell and Farrington, 1986). The concentrations of dissolved organic carbon in the sediments have been reported to range from 10 mg/L to 40 mg/L in aerobic sediment beds and up to 90 mg/L in anoxic bed regions. These organic macromolecules or microparticles in the sediment beds are likely to sorb organic compounds (Means and Wijayaratne, 1982; Carter and Suffet, 1982; Landrum et al., 1984; Gschwend and Wu, 1985; Brownawell and Farrington, 1986). Substantial evidence in the literature indicates that the sorption of organic compounds to colloids follows the thermodynamically based partitioning model previously developed for soils and sediments (Carter and Suffet, 1982; Wijayaratne and Means, 1984;

Chiou et al., 1986; and Appendix 2). If one ignored the presence of colloids, the obvious consequence would be higher apparent dissolved concentrations of compounds in the pore fluid, lower observed partition coefficients (Brownawell and Farrington, 1986), and higher apparent diffusivities due to the additional load carried by diffusing colloid particles. However, if we include a third phase, the moving colloids, in the transport models, we will be able to model this colloid-mediated transport and retain the predictive capabilities of the chemical fate models.

When animals live in sediment beds, these organisms can mix the sediment material in many ways (Foster-Smith, 1978; Robbin et al., 1979; Fisher et al., 1980) and enhance the release of pollutants from the beds (Karichhoff and Morris, 1985). These biological mixing activities include: plowing, burrowing, particle collecting and transport, and porewater irrigation. By continuously exposing previously buried sediments to the water column, sorption exchange between the bed and overlying waters can be enhanced. Further, by promoting porewater exchange with the water column, dissolved and colloid-bound contaminants are more effectively released from the bed. All these activities can be approximately described by an advection process or a eddy-diffusion type mixing process or their combination (Guinasso and Schink, 1975; Schink and Guinasso, 1978; Robbins et al., 1979; Fisher et al., 1980; Berner, 1980). This diffusion/advection parameterization approach allows us to quantify these mixing processes and to include them into the chemical fate models. In this chapter, one of these biogenic activity (i.e., conveyer-belt type sediment mixing) will be investigated to illustrate the importance of the biogenic enhancement of chemical transport.

In order to examine the importance of sorption kinetics to the processes involved with the transfer of hydrophobic organic pollutants between bottom sediments and water, the purposes of this work were: (1) to extend currently available transport models between beds and the water column to include sorption kinetics, (2) to perform experiments to test the validity of the expanded models in laboratory (i.e., quiescent water column with or without bioturbation), and (3) to illustrate the range of fluxes entering the water column with different extreme conditions of beds (e.g., no bioturbation, and bioturbation with surface equilibrated with water) by doing model simulations for hypothetical cases.

4.1 Model Development

4.1.1 Diffusion Through Porewater in the Sediment Bed

Without water flow or solid phase movement, dissolved pollutant molecules may still be transported by molecular diffusion in the interstitial pore water in sediment beds. The vertical flux of mass is given by (Berner, 1971; Larsson, 1983; Fisher et al., 1983):

$$\text{flux by molecular diffusion} = -\, n_b D_p \frac{\partial C}{\partial z} \tag{4.1}$$

where C = concentration in the pore fluid (mol/cm^3), z = vertical distance (cm), D_p = diffusivity of pollutant molecules in pores (cm^2/s), and n_b = bed porosity.

Due to the increase of diffusion path by the curvature of interstitial

pores around particles, investigators estimate D_p by multiplying the molecular diffusivity (D_m (cm^2/s)) of the compound of interest with a tortuosity factor which is a function of porosity (i.e., $n_b{}^i$):

$$D_p = D_m \cdot n_b{}^i \qquad (4.2)$$

where i = empirical parameter ranging from 1 to 2 and depending on the magnitude of n_b (Aller and Ullman, 1982). Consequently, the flux becomes:

$$\text{flux by molecular diffusion} = - D_m n_b{}^{i+1} \frac{\partial c}{\partial z} \qquad (4.3)$$

4.1.2 Diffusion Mediated by Colloid Movement

An extra load of sorbate may be associated with colloids in pore water. The concentration of this colloid-bound pollutant is $\rho_c S_c$, in which S_c = mass of pollutant per unit mass of colloidal material (mol/g), and ρ_c = colloid concentration (g/cm^3). The transport of the colloid-bound species is controlled by the diffusion of the colloids in the interstitial solution. If the spatial and temporal variation of ρ_c can be specified, we are able to model the transport of pollutants mediated by the moving colloids:

$$\text{flux of colloid-bound pollutant} = -D_c n_b{}^{i+1} \frac{\partial S_c \rho_c}{\partial z} \qquad (4.4)$$

105

where D_c = diffusivity of colloids in pores (cm^2/s). For very small particles whose sizes are less than a few micrometers, the dominant transport in the pore fluid is via Brownian motion of the particles (Yao et al., 1971) and is characterized by D_c, (originally derived by Einstein, 1905, cited in Friedlander, S. K., 1977):

$$D_c = \frac{k_B T}{3\pi\mu d_c} \qquad (cm^2/s) \qquad\qquad (4.5)$$

where k_B = Boltzmann constant, T = absolute temperature, μ = fluid dynamic viscosity, and d_c = colloidal particle diameter. For a 1 μm diameter spherical particle in water at 20°C, D_c is 4.3 x 10^{-9} cm^2/s. For a 0.001 μm diameter particle, D_c is 4.3 x 10^{-6} cm^2/s.

4.1.3 Mixing of Sediments

An advection-diffusion model has been used to represent the transport of conservative tracers by biological mixing in sediment beds (Schink and Guinasso, 1978; Berner, 1980; Fisher et al., 1980):

$$\frac{\partial S_b}{\partial t} + \frac{\partial w(z) S_b}{\partial z} = \frac{\partial}{\partial z} D_b \frac{\partial S_b}{\partial z} + f(z) S_b \qquad\qquad (4.6)$$

where S_b = total concentration of the tracer in the sediment bed by volume

(mol/cm^3), $w(z)$ = sedimentation and bioturbation induced sediment velocity at depth z (cm/s), and D_b = eddy-diffusion type sediment mixing coefficient (cm^2/s). The feeding activity, $f(z)$, reflects an apparent removal and generation mechanism at depth z due to ingestion of particles there, and this parameter is the derivative of the vertical velocity created by bioturbation (Fisher et al., 1980):

$$f(z) = \frac{dw_r(z)}{dz} \qquad (4.7)$$

in which $f(z)$ = volume of sediment material removed from a unit volume per unit time at depth z (negative) (sec^{-1}), and $w_r(z)$ = sediment velocity due to advective biological mixing (cm/s). Sediment material ejected by animals forms a source usually on the bed/water interface which has concentration determined by the feeding activity function and the concentration profile:

$$S_b(z=0) = \int_0^\infty f(z) S_b(z) dz \qquad (4.8)$$

Since feeding styles vary from species to species, $f(z)$ depends on the population of interest. For example, tubificid worms exhibit a maximum of $f(z)$ at the depth of a few centimeters where most feeding occurs. At this depth, these conveyor-belt type feeders can still respire in the aerobic zone of sediments or overlying water. The feeding activity of surface-deposit feeders (e.g., the clam, Yoldia) which collect surficial sediments and eject fecal pellets on the bed surface may be characterized by a peak of $f(z)$ at the

bed-water interface. Some benthic organisms (e.g., crustaceans) simply due to their movements about the bottom, mix the sediment material randomly but do not create net sediment advection. This so-called plow-like mixing activity is quantified by the eddy-diffusion type mixing coefficient, D_b, and a zero $f(z)$.

4.1.4 A General Model for Pollutant Transfer Between Water and Sediment Beds

From the previous model development sections in this Chapter, one can combine the expressions of the several physical and biological processes of pollutant transfer (Figure 4.1) in terms of diffusion or advection in a general form of transport equation. This approach has been taken by Schink and Guinasso (1978) and Berner (1980) to model diagenetic physical and biological processes including sediment deposition, compaction, molecular diffusion, and eddy-diffusion type benthic mixing.

In the following governing equation constructed to describe the vertical transport of chemicals in a sediment bed, we include three chemical species (i.e., sorbed, freely dissolved, and bound-to-colloid species), and four transport processes (i.e., sediment advection, eddy-diffusion type sediment mixing, molecular diffusion in the pore water, and colloid-mediated transport):

$$\frac{\partial S_b}{\partial t} + \frac{\partial}{\partial z} w(z) S_b$$

$$= \frac{\partial}{\partial z} [D_b \frac{\partial S_b}{\partial z} + D_m n_b^{i+1} \frac{\partial c}{\partial z} + D_c n_b^{i+1} \frac{\partial \rho_c S_c}{\partial z}] + f(z) S_b \quad (4.9)$$
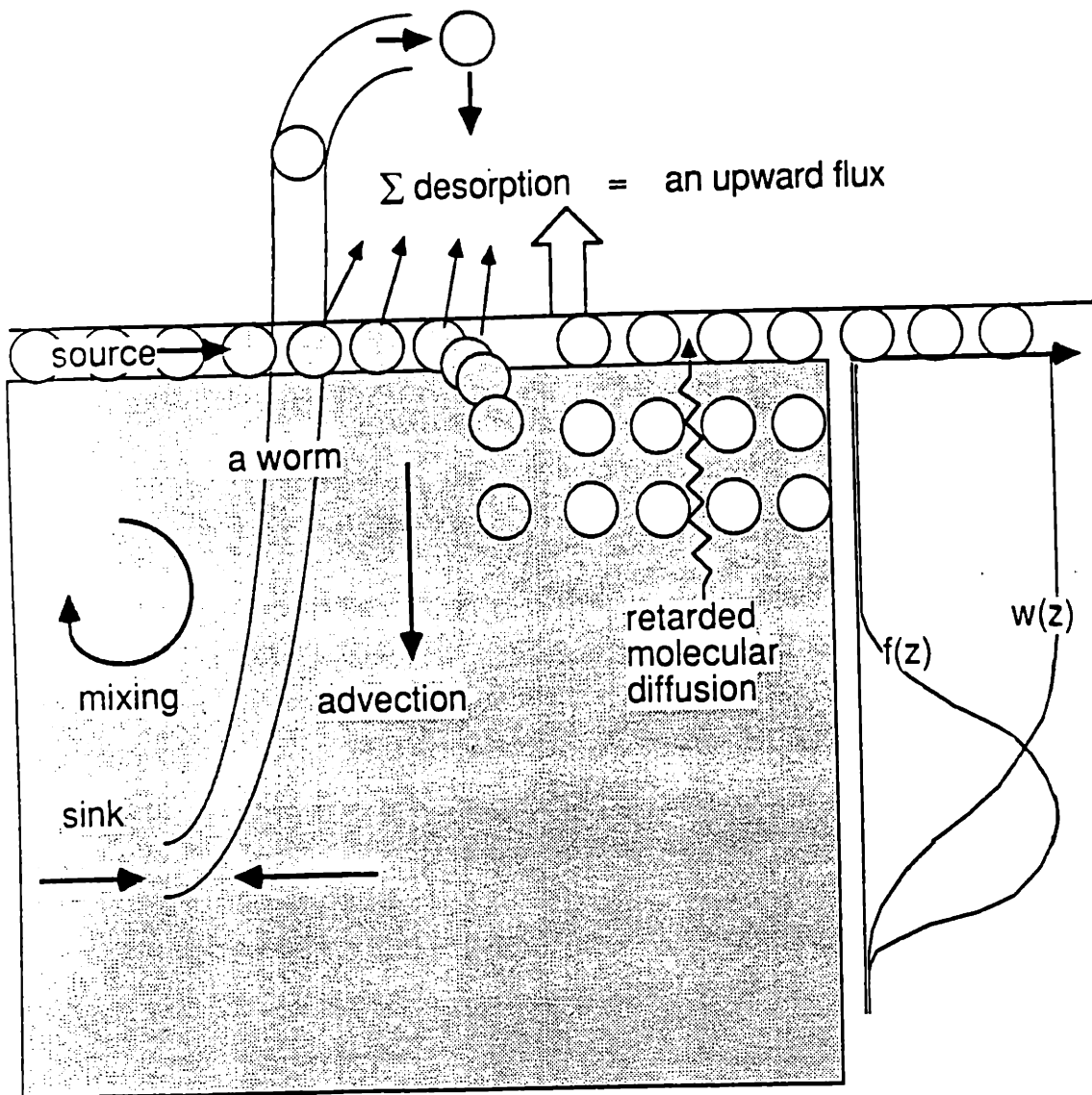
Figure 4.1   A schematic diagram of transport processes between the water
              column and sediment beds (colloids-mediated transport is not
              included). w(z) is the vertical velocity of sediments. f(z)
              is the feeding activity function of depth derived from w(z).

Where the total concentration by volume in the bed, S_b, is defined as:

$$S_b = n_b C + \rho S + n_b \rho_c S_c \qquad (4.10)$$

and where ρ is the solid concentration (g/cm^3) and S is the sorbate concentration in solid phase (mol/g).

Two additional equations combined with Equation 4.9 are required to specify the three concentration variables. The equations of local sorption equilibrium or sorption/desorption kinetics provide the necessary relationships between these species; and these equations and the conditions under which they are appropriate are discussed below.

Additional sink or source terms should be included in the governing equation if the substance undergoes chemical or biological reactions. Most hydrophobic pollutants of concern are stable in the environment during the period of interest here (i.e., months or years). Therefore, we neglect these reaction terms in this model development.

When any one of the three media (i.e., the solid phase, the pore water phase, or the colloids) is subject to transport processes, its concentration is a variable too. For example, we may need the following governing equation to account for the temporal and spatial variation of colloids:

$$\frac{\partial n_b \rho_c}{\partial t} + \frac{\partial w(z) n_b \rho_c}{\partial z}$$

$$= \frac{\partial}{\partial z} (D_b \frac{\partial n_b \rho_c}{\partial z} + D_c n_b^{i+1} \frac{\partial \rho_c}{\partial z}) + f(z) n_b \rho_c$$

+ terms quantifying processes causing the rate of

generation or disappearance of colloids   (4.11)

4.2 Mass Transfer Between Solids, Colloids and Aqueous Phase

4.2.1 Mass Transfer Controlled by Local Equilibrium

In some situations, we can, based on the conclusions in Chapter 2 and Chapter 3, apply local equilibrium relationships and reduce the number of system variables to 1 (i.e., only S_b). First, we consider the relationship between S_c and C. For hydrophobic compounds which are primarily sorbed in the organic matter associated with colloidal particles, the intraparticle penetration mechanism of sorption can be used to estimate times to equilibrium (see Chapter 2). Due to the small sizes of the colloid particles (< 1 µm), sorbates in the colloid-bound phase are predicted to reach equilibrium with solutes in the dissolved phase in less than 1 minute for sorbate/sorbent combinations of K_p less than 10^4. Since the diffusion length scale of colloids moving for 1 minute is between 5 and 200 µm, equilibrium can be assumed. Thus we have:

$$K_c = S_c/C \qquad (4.12)$$

111

Generally, we can also assume equilibrium between S and C for locations away from the surface of the bed. The sorbent concentration in the sediment bed is always about 1 g/cm^3. At this high sorbent concentration, the progress of equilibration will be extremely fast in terms of the dissolved concentration in the pore water. According to the analysis in Chapter 3, we expect the half equilibration time ($t_{1/2}$) to be smaller than 1 minute with an aggregate size of about 0.1 cm, which is the largest size we observed for natural sediment aggregates in suspensions (see Section 3.5). Consequently, if the relative velocity of these sorbent and sorbate phases (e.g., porewater advective velocity) is smaller than 0.1 cm/min, it will be appropriate to assume an equilibrium in the sediment bed. As a result, the following equilibrium equation will apply:

$$K_p = S/C \qquad\qquad (4.13)$$

Third, under bioturbation mixing situations, both solids and the adjacent pore water are subject to the same reworking event. Generally, the contact between these two phases will not be interrupted. In addition, when the solid material and liquid in the sediment beds are ingested by deposit feeders, these two phases will be mixed and form fecal pellets in the guts of the animals (Lee and Swartz, 1980; Karickhoff and Morris, 1985). In this case, to assume equilibrium between porewater and reworked sediments or even equilibrium inside pellets will be a proper choice. Also, since these animals usually reworked large amounts of sediment material in one day compared to

112

their body weight, equilibrium between the animal biomass and the sediment bed

environment should be quickly reached.

If we can use the two local eqilibrium relationships (Eq. 4.12 and 4.13)

to couple the three sorbate species, we can rewrite our expression for total

chemical concentration by volume in the bed:

$$S_b = n_b C + \rho S + n_b \rho_c S_c = (n_b + \rho K_p + n_b \rho_c K_c) \cdot C \tag{4.14}$$

$$\therefore \ C = S_b / R_d \tag{4.15}$$

and $\quad \therefore \ S_c = K_c S_b / R_d \tag{4.16}$

in which R_d is a fraction factor defined as:

$$R_d = (n_b + \rho K_p + n_b \rho_c K_c) \tag{4.17}$$

By substituting Eq. 4.15 and 4.16 in Eq. 4.9, we obtain the governing equation

in terms of S_b only:

$$\frac{\partial S_b}{\partial t} + \frac{\partial}{\partial z} \, w(z) \cdot S_b$$

$$= \frac{\partial}{\partial z} \, [D_b \frac{\partial S_b}{\partial z} + D_m n_b^{i+1} \frac{\partial (S_b / R_d)}{\partial z} + D_c n_b^{i+1} \frac{\partial (K_c \rho_c S_b / R_d)}{\partial z}] + f(z) S_b$$

$$\tag{4.18}$$

This expression applies for all depths in the bed where the equilibrium

assumptions discussed above are appropriate. When the medium concentration,

n_b, ρ, and ρ_c are all constant, S_b is the only variable, i.e.,

$$\frac{\partial S_b}{\partial t} + \frac{\partial w(z) S_b}{\partial z} = D_{app} \frac{\partial^2 S_b}{\partial z^2} + f(z) S_b \qquad (4.19)$$

where $\quad D_{app} = D_b + (D_m n_b{}^{i+1} + D_c n_b{}^{i+1} \rho_c K_c)/R_d \qquad (4.20)$

This apparent mixing coefficient, D_{app}, reflects the simultaneous effects of

porewater diffusion of solute species and colloid-carried species, as well as

the vertical mixing due to organism activities. When there is no

bioturbation, we can set $D_b = 0$. When colloids are absent, $\rho_c = 0$ and the

terms quantifying their impact drop out. In the simplest case (no organisms

or colloids), the apparent diffusivity reduces to:

$$D_{app} = D_m n_b{}^{i+1}/R_d \qquad (4.21)$$

which is the retarded diffusivity in porewater diffusion model (Karickhoff and

Morris, 1985).

4.2.2 Mass Transfer Controlled by Sorption Kinetics

At some locations and some times, it is not appropriate to assume

sorption equilibrium between phases. For example, Karickhoff and Morris

114

(1985) demonstrated that tubificid fecal debris deposited on the bed surface were reburied before establishing sorptive equilibrium of the hexachlorobenzene they contained with the overlying waters. In such cases, we need to define the sorption/desorption rates to couple the dissolved and sorbed components.

We have already described these exchange rate functions by using an intraaggregate diffusion model in Chapter 2. In fact, the exchange rates are determined by the instantaneous dissolved concentration, C, and the intraaggregate concentration distribution, S(r), which is a function of the previous exposure to dissolved concentrations. Therefore, one can include the kinetic model in a transport model when the history of movement of each aggregate can be defined. Examples of successful coupling of these two different diffusion length scales can be found in modelling fixed-bed activated carbon sorption (Crittenden and Weber, 1978a; Crittenden and Weber, 1978b; Weber and Liu, 1980) and modelling diffusion in sediment bed with biogenic microenvironments (Aller, 1978). However, in these cases, the solid phases are stationary. Sorption rates are computed from the concentration in the adjacent solution and the concentration in the aggregates which is determined by the history of the exposured concentration at the location of interest.

When movement of aggregates is involved in the chemical transport processes, our ability to specify the concentration in an aggregate and to calculate the sorption rate depends on whether there is an available technique to model the path of each aggregate. The conveyer-belt type bioturbation by tubificid worms provides a special case in which the sediment is mixed and the

history of each aggregate is still well defined.

Tubificid worms are widely distributed in natural water bodies with significant abundance (e.g., up to 12 worms/cm^2 in Toronto Harbor, Brinkhurst and Cook, 1974). These worms burrow head down to ingest sediments at depth in the bed and expel these materials as fecal pellets at the sediment-water interface (Figure 4.1). Therefore, the bed surface is continuously renewed by sediment materials from the deep bed, and sorption or desorption of pollutants will occur if there is a chemical activity gradient between the pellets and the water.

As discussed in 4.2.1, we can assume equilibrium in the deep sediment bed. However, one particular region where we can not ignore sorption kinetics is the sublayer within one grain width beneath the water/sediment interface. We assume that the dissolved concentration in this layer is the same as the concentration in the overlying water due to turbulence induced dispersion. Therefore, deposited fecal pellets are essentially exposed to the overlying water.

During the period of residence in the bed surface layer, sorbed pollutants will desorb to an extent quantified with our intraaggregate retarded radial diffusion model. The total travel time through a depth of one particle diameter (d) can be estimated from the reworking rate, w_r:

$$t_r = d/w_r \tag{4.22}$$

Using the dissolved concentration in the overlying water, C_w, we can estimate the sorbed concentration, S, in the pellets when they are leaving the

116

sublayer, i.e.,

$$S(z=d) = S(z=0) - (S(z=0)-K_pC_w) \cdot M(t=t_r)/M_\infty \qquad (4.23)$$

in which $M(t=t_r)/M_\infty$ is the fraction of release at $t=t_r$. The concentrations of dissolved and colloid-bound species are quickly replaced by the concentrations in the overlying water due to high dispersivity in the water column, i.e.,

$$C(z=d) = C_w \qquad (4.24)$$

$$S_c(z=d) = K_cC_w \qquad (4.25)$$

$$\rho_c = \rho_c(in\ water) \qquad (4.26)$$

Consequently, the mass exchange between the reworked sediments and the overlying water is simply the sum of materials sorbed/desorbed to/from the pellets plus the dissolved and colloid-bound loads interchanged with the water column. This continuous flux across the bed/water interface is given by:

$$Flux(z=0) = [S_b(z=d)-S_b(z=o)] \cdot w_r$$

$$= \{ (n_b+\rho_cK_c)C_w + \rho[S(z=0)-(S(z=0)-K_pC_w) \cdot M(t=t_r)/M_\infty]$$

$$- (n_b+\rho_cK_c)C(z=0) - \rho S(z=0) \} \cdot w_r$$

$$= \{(n_b+\rho_cK_c) \cdot (C_w-C(z=0)) - \rho[S(z=0)-K_pC_w] \cdot M(t=t_r)/M_\infty\} \cdot w_r$$

in which ρ_c is assumed to be a constant.

When $S \gg C$ (which is true if $K_p \gg 1$ and $\rho K_p \gg \rho_c K_c$) and $\rho > \rho_c$, $\rho S \approx S_b$ and we may express the flux in terms of parameters easily measured in contaminated muds:

$$\text{Flux}(z=0) \approx k_b \cdot [\rho K_p C_w - S_b(z=0)] \tag{4.28}$$

where $\quad k_b = w_r \cdot M(t=t_r) / M_\infty \tag{4.29}$

The bioturbation rate constant is a function of the biological activity, the hydrophobicity of the pollutant, and the particle size and organic content of the sediments. This result provides a boundary condition which is a flux for Eq. 4.19 at $z=0$.

For other types of deposit-feeders, as long as we can describe their activities with the reworking rate, w_r, we will be able to use the same approach to model the integrated transport processes in the sediment beds. Plow-like benthic animals do not generate net sediment advection (i.e., $w_r=0$). However, the mixing activity has been parameterized by using an eddy-diffusion type mixing coefficient, D_b, (Guinasso and Schink, 1975; Aller, 1978; and Lee and Swartz, 1980). Making use of this quantitative description, we can estimate the residence time of the sediment material in the sublayer by:

$$t_r = d^2 / D_b \tag{4.30}$$

and use the same modelling approach as well.

To test the effectiveness of this model, we performed microcosm experiments. Aquariums containing a layer of contaminated sediments with or without tubificid worms were used to simulate polluted natural water bodies in which either porewater diffusion or bioturbation dominated the mass transport between beds and the water column.

4.3 Experimental Section

4.3.1 Materials and Analytical Methods

Five polychlorinated biphenyl (PCB) congeners (4,4'-dichlorobiphenyl; 3,4,2'-trichlorobiphenyl; 2,5,2',5'-tetrachlorobiphenyl; 2,4,5,2',5'-pentachlorobiphenyl; and 2,4,5,2',4',5'-hexachlorobiphenyl) purchased from Foxboro/Analabs Co. (North Haven, Connecticut) were used as received. Freshwater river sediments were obtained from the North River (Marshfield, Massachusetts). Sediment suspensions were wet sieved through a No. 20 standard sieve (opening = 0.84 mm) and stripped with clean air for one month in a 30 L glass carboy to eliminate unknown organic substances originally sorbed in the sediments. About 1 mg of each PCB (except 2,5,2',5'-tetrachlorobiphenyl) dissolved in a total of 1 mL acetone was added into a 20 L sediment suspension containing about 2 kg of dry solid. The suspension was mixed occasionally for 1 month. After concentrating by settling, the wet sediments were stored in a refrigerator at 5°C before experiments. Other sediments obtained from the Charles River (Boston, Massachusetts) were

air-dried and sieved through a No. 20 standard sieve. The same procedure was taken to prepare contaminated Charles River sediments with 4,4'-dichlorobiphenyl, 3,4,2'-trichlorobiphenyl, and 2,5,2',5'-tetrachloro-biphenyl, except they were not stripped. Milli-Q Water (Millipore, Bedford, Massachusetts) was used for aqueous preparations.

A stock of tubificid worms was obtained from a small stream 200 m downstream of a sewage treatment plant outfall 2 years before the experiments. Sediments with worms were kept in the laboratory in a 20 L aquarium with aeration and enriched with several small pieces of bread once a week. Before any particular experiment began, bottom mud with worms were sieved with a No. 20 sieve. Worms retained on the sieve were picked with tweezers and used in the experiments immediately.

Some sediment properties were determined by the following methods. The dry solid density was estimated with the specific gravity bottle method (Black et al., 1965). The organic matter content was determined by heating the sample at 550°C for 25 minutes and measuring the weight loss (Black et al, 1965). The solid content (also the porosity) of the wet sediments was determined by drying the sediments at 105°C for 24 hours. Some properties of the sediments and PCBs used in this work are listed in Table 4.1.

The concentrations of PCBs in the contaminated sediments were determined by extracting small aliquots of the sediments with 2 mL of 1:1 pentane and acetonitrile mixtures in 12 mL centrifuge tubes for 1 week. Sonication was applied at the beginning to destroy the sediment aggregates. After extraction, the pentane layer was withdrawn from the tube and saved. The extraction and separation was repeated twice with only 1 mL pentane added into

120

Table 4.1 Properties of sediments and PCBs

a. Sediment properties

| Sediments | dry solid density | porosity | organic matter content (as combustible loss) | solid conc. |
	g/cm^3	cm^3/cm^3	% of dry mass	g/cm^3
Charles River	2.25	0.73	17.0	0.61
North River	2.51	0.78	8.8	0.55

b. PCB properties

PCBs	$\log K_{ow}$ (a) (cm^3/g)	$\log K_{om}$ (c) (cm^3/g)	molecular diffusivity(d) (cm^2/s)
4,4'-dichloro biphenyl	5.33	4.04	5.8×10^{-6}
3,4,2'-tri-chlorobiphenyl	(5.57) (b)	4.26	5.5×10^{-6}
2,5,2',5'-tetra-chlorobiphenyl	6.05	4.69	5.3×10^{-6}
2,4,5,2',5'-pentachloro-biphenyl	6.49	5.07	5.0×10^{-6}
2,4,5,2',4',5'-hexachloro-biphenyl	7.36	5.87	4.8×10^{-6}

(a) : K_{ow} values are average of observed values from Rapaport and

Eisenreich, 1984; Woodburn et al., 1984; Bruggeman, 1982; Chiou et

al., 1977; Chiou, 1985; Miller et al., 1985 (reviewed by Brownawell,

1986).

(b): This value is K_{ow} of 2,3,3'-trichlorobiphenyl. K_{ow} value of 3,4,2'-trichlorobiphenyl is not known.

(c): K_{om} is the partition coefficient normalized by organic matter content. Valus are obtained from the correlation between the values of K_{ow} and K_{om} developed by Chiou et al., 1983, (log K_{om} = 0.904 log K_{ow} - 0.779), (13 compounds including 4 PCBs and 5 chlorinated benzenes). These K_{om}s are used to estimate the K_ps used in this work by multiplying K_{om} with the organic content.

(d): The molecular diffusivity is estimated by using the method of Hayduk and Laudie (1974).

the tube each time. All pentane extracts were combined and an external standard (tetrachlorobiphenyl or pentachlorobiphenyl whichever was not added into the contaminated sediments) was added. The PCB contents of the extracts were determined by gas chromatography with electron capture detection. The instrument was a Carlo Erba HRGC 5160 Mega Series, equipped with a ^{63}Ni electron capture detector. The 12 m long by 0.32 mm i.d. fused silica capillary column coated with cross-linked SE-54 (Analabs, Inc., North Haven, CT) was operated with H_2 carrier gas at 0.5 m/s linear velocity and was programmed from 40 to 240°C at 8°C/min. Splitless injections were made. The detector was operated at 275°C with 5% CH_4-Ar in the constant current mode with 0.5-µs pulse intervals and a differential electrode potential of 50 V. The recovery by this extraction approach has been shown to be between 80 and 90% in our previous report (Appendix 2). The analytical imprecision was about ±20%.

4.3.2 Procedures of Microcosm Experiments

Microcosm experiments were performed to investigate: (A) diffusion in pore water, (B) modification of the sediment bed by tubificid worms, and (C) bioturbation-enhanced mass transport in the sediment bed. Some experimental parameters are listed in Table 4.2. Sediments were homogenized by mixing with a spatula and samples were taken for sediment property and PCB content measurements. A layer of sediment mud with thickness of 1 cm to 8 cm was laid on the bottom of a gas stripping bottle, which was 10 cm tall and 8.5 cm in diameter (Fig. 4.2-a, and 4.2-b). A depth of 5 cm to 8 cm water was carefully added into the bottle by siphon with capillary tubes. Resuspended sediments

Table 4.2 Experimental parameters

Experiments	A	B	C
Treatment	pore diffusion	bioturbation activity	bioturbation and transport
Initial conc. in sediments (ng/cm3)			
4,4'-dichlorobiphenyl	92	0	480
3,4,2'-trichlorobiphenyl	31	0	340
2,5,2',5'-tetrachloro-biphenyl	38	0	standard
2,4,5,2',5'-pentachloro-biphenyl	standard	0	350
2,4,5,2',4',5'-hexa-chlorobiphenyl	0	0	200
Sediment type	Charles R.	North R.	North R.
Thickness of the sediment layer (cm)	1	8	5
Depth of water (cm)	9	5	8
stripping rate (cm^3/s) (by air)	10	−	−
flushing rate (cm^3/min) (by water)	−	−	40
Worm population (cm^{-2})	0	7.1	13.5
Reworking rate (cm/day)	0	0.07	0.13
Bed surface area (cm^2)	57	61	57
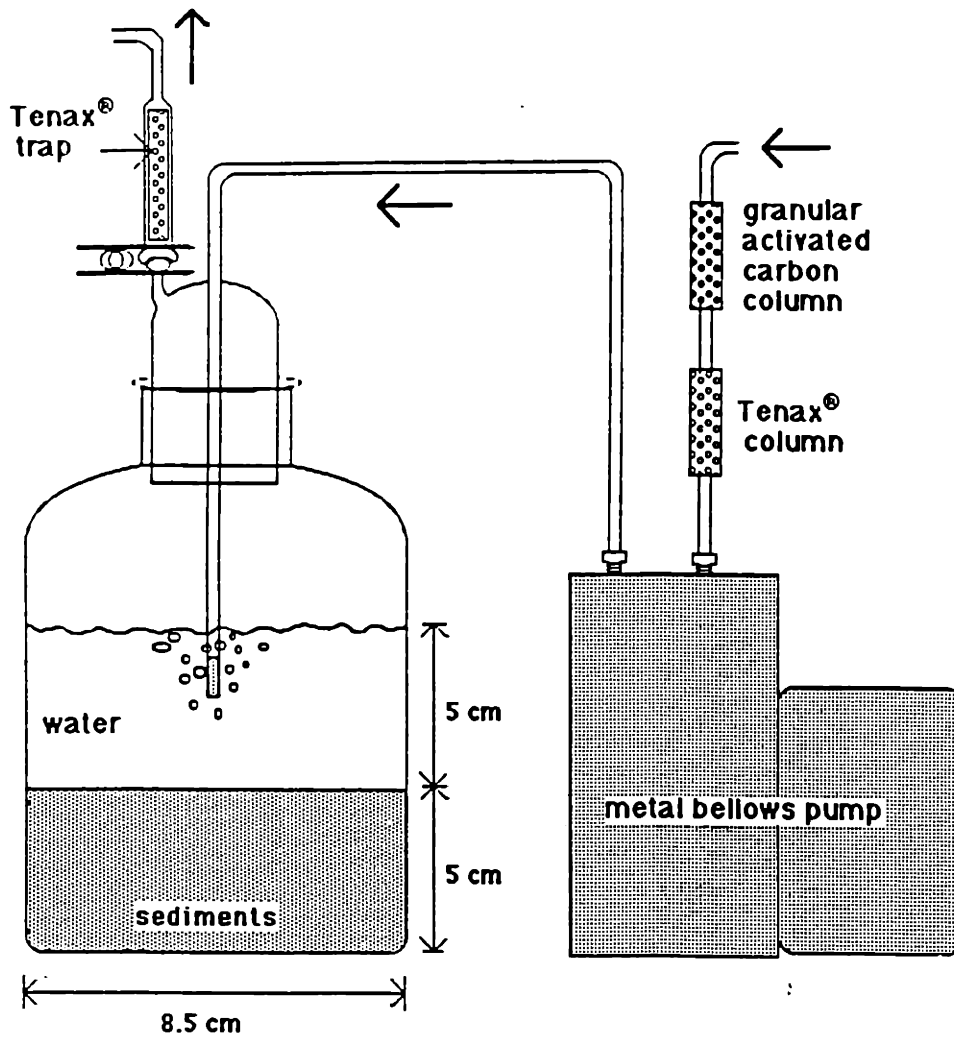
Figure 4.2-a   Microcosm for porewater diffusion experiment (Experiment A).

inflow →

effluent

8 cm

water

5 cm

sediments

8.5 cm
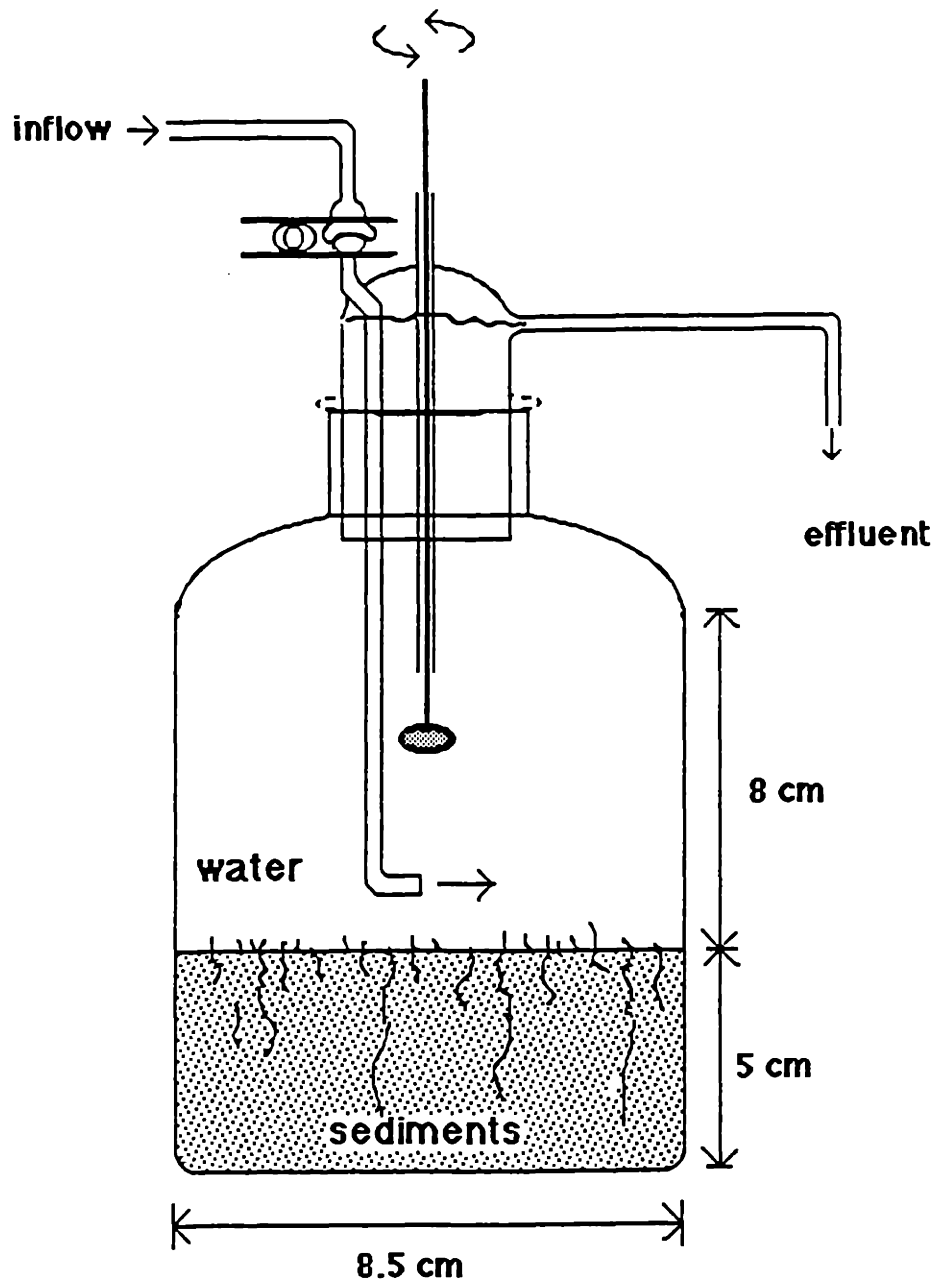
Figure 4.2-b   Microcosm for bioturbation experiment (Experiment C).

were sucked out until the water column was free of visible suspended materials. In Experiment A, clean air was continuously pumped by a stainless steel bellows pump into the water column with a flow rate of 10 cm^3/s (Fig. 4.2-a). The gas flow was recycled in a all-glass closed loop during chemical flux measurements. An organic vapor trap containing 0.1 g Tenax[®] beads (4 cm length and 0.4 cm diameter) was installed in the effluent gas line to collect chemicals released from the sediment bed into the water column. After each period of vapor collection, an external standard dissolved in 1 μl pentane was added to the Tenax[®] trap. PCBs collected in the trap were thermally desorbed after inserting the trap into the GC injection port (Pancow and Kristensen, 1983). The temperature of the GC column was held at 40°C for 20 minutes during desorption and the chromatography was commenced by heating to 240°C at 8°C/min.

A wide mouth jar was used for the experiments on bioturbation activity observations (Experiment B). Sediment cores were taken during the bioturbation activity observation for solid content and organic matter content profile measuremant.

During Experiment C, the water column was flushed with water and gently stirred to ensure low water column chemical concentrations. The flushing rate was chosen to yield aqueous concentrations which were always less than 20% of that equilibrated with the corresponding sorbed concentrations (Fig. 4.2-b). Worms were weighed for wet biomass after they had been put on a tissue for 2 seconds to eliminate excess water. The number of worms in another sample was counted to estimate the average weight of a single worm. It was found that the average body weight was 1.56 mg per worm. Dead worms were removed from

the bottle during the first 2 days and their wet weight was subtracted from

the total added weight to estimate the true input biomass. No significant

change of total wet biomass of input worms (< 10%) was found 30 days after the

experiment started.

4.4 Experimental Results and Discussion

4.4.1 Diffusion Through Porewater

Results of the porewater diffusion experiment (Experiment A) are shown in Figure 4.3-a, b, and c. The fluxes of PCBs from the sediment beds, estimated from the mass collected in the Tenax® trap, decrease with progress of time. The analytical imprecision in the observed fluxes is about 15% based on triplicate analyses and is primarily due to variations in the trapping procedure and analyses by gas chromatography. If all fluxes are normalized with the initial concentrations (about 3 : 1 : 1.5 for dichlorobiphenyl : trichlorobiphenyl : tetrachlorobiphenyl), dichlorobiphenyl which has the lowest hydrophobicity (K_{ow}) has the highest flux, which is predictable by the retarded diffusion model. However, the fluxes of tri- and tetra-chlorobiphenyls are not significantly different.

A blank stripping efficiency test (i.e., only PCBs and water in the bottle) showed that 50% of the original tri- and tetrachlorobiphenyls remained in the spiked water after 4 hours of purging. This half-life time corresponds to a stripping rate constant of 4 day^{-1}. To the extent that the stripping treatment does not remove compounds from the water column efficiently, the flux across the bed/water interface will be reduced due to smaller concentration gradient. Therefore, we have to evaluate the effects of stripping efficiency on the observed fluxes by using a model simulation including a varying concentration in the water column.

A transport model can be readily formulated to describe the concentration change in the water column:

129

4,4'-dichlorobiphenyl

flux

$(ng/cm^2/d)$

time (days)
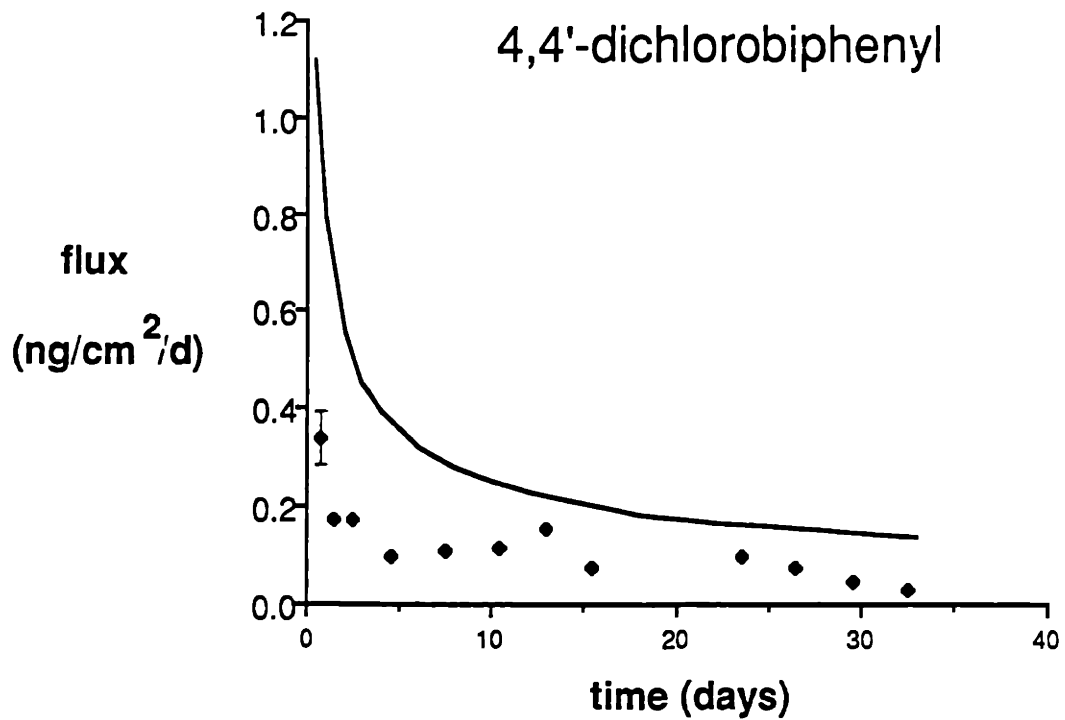
Figure 4.3-a   Results of porewater diffusion experiment. Fluxes of

4,4'-dichlorobiphenyl across the bed surface (squares) compared

to the predicted fluxes (solid line).

3,4,2'-trichlorobiphenyl

flux

$(ng/cm^2/d)$
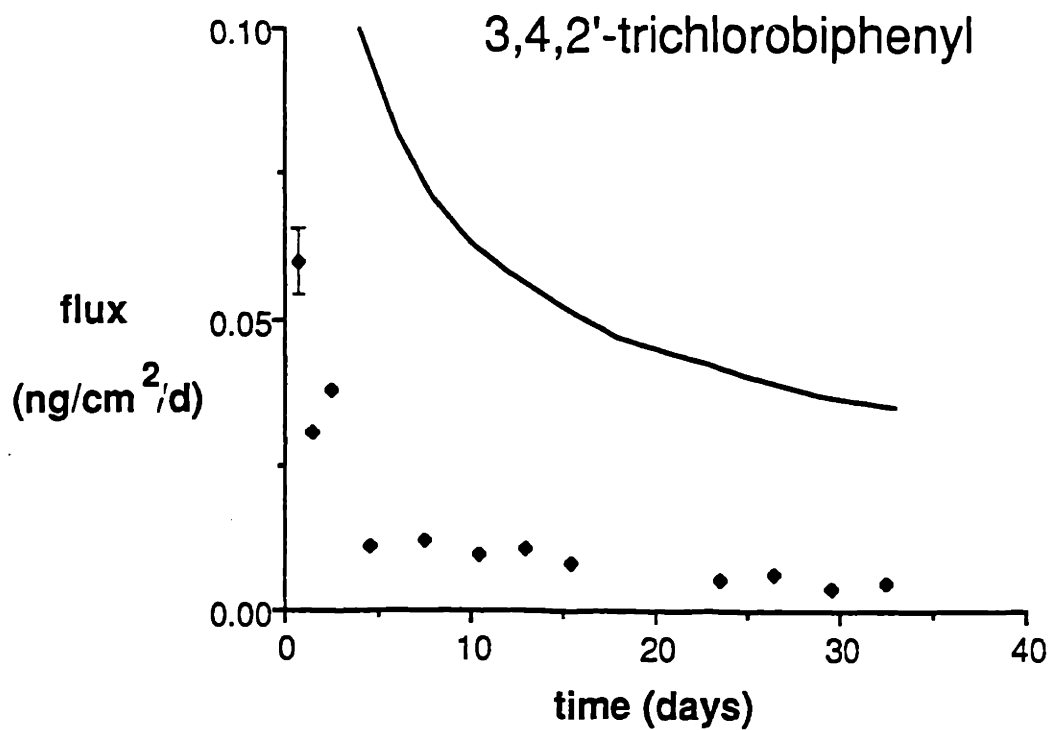
Figure 4.3-b   The same as Figure 4.3-a for 3,4,2'-trichlorobiphenyl.

2,5,2',5'-tetrachlorobiphenyl
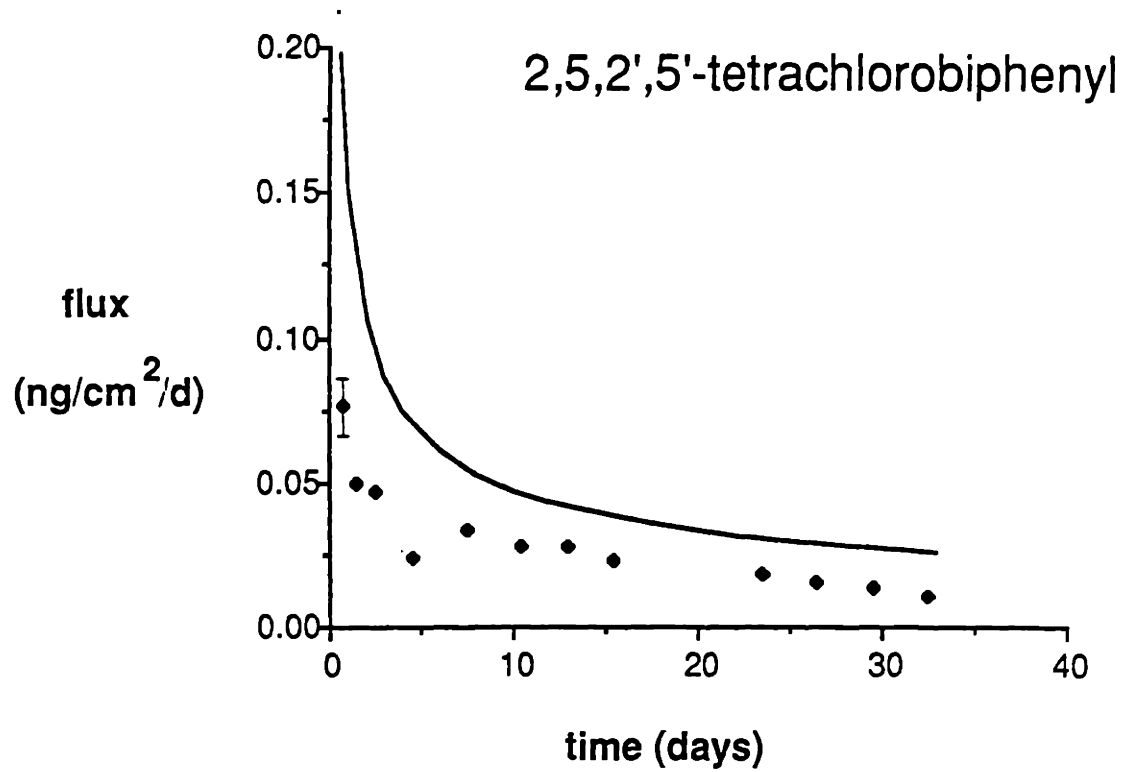
Figure 4.3-c   The same as Figure 4.3-a for 2,5,2',5'-tetrachlorobiphenyl.

$$\frac{dC_w}{dt} = \frac{A}{V} \text{ (flux across the bed surface)} - kC_w$$

$$= \frac{D_{app}}{L_w} \left(\frac{\partial S_b}{\partial z} \right)_{z=0} - kC_w \qquad (4.31)$$

in which A = bed surface area (cm^2), V = volume of the water column (cm^3), k = stripping rate constant (d^{-1}), and L$_w$ = depth of the water column (cm). Since the concentration gradient at z=0 is given by Eq. 4.19 with a time-varying boundary concentration of C$_w$, we have to solve the problem with a numerical approach. Following the modelling approach by Peng et al. (1979), Santschi et al. (1980), and Ambrose et al. (1983), we divide the sediment bed into horizontal compartments. Finite difference approximations are used to replace the concentration gradients in the governing equations. Local equilibrium between sediments and the overlying water is assumed at z=0. Details of the numerical model are described in Appendix 5.

The simulation result indicates that the actual flux across the bed/water interface is greatly reduced during the first several hours (dotted line in Figure 4.4), however, converging to the predicted flux with 100% stripping efficiency (solid line in Figure 4.4) gradually. For all times after one day, the observed flux which is slightly diminished by the accumulated concentration in the water layer but is very close to (greater than 80% of) the predicted flux assuming efficient stripping. Because all fluxes were measured after the second day of the experiment, the data are not significantly affected by the effects of incomplete stripping.
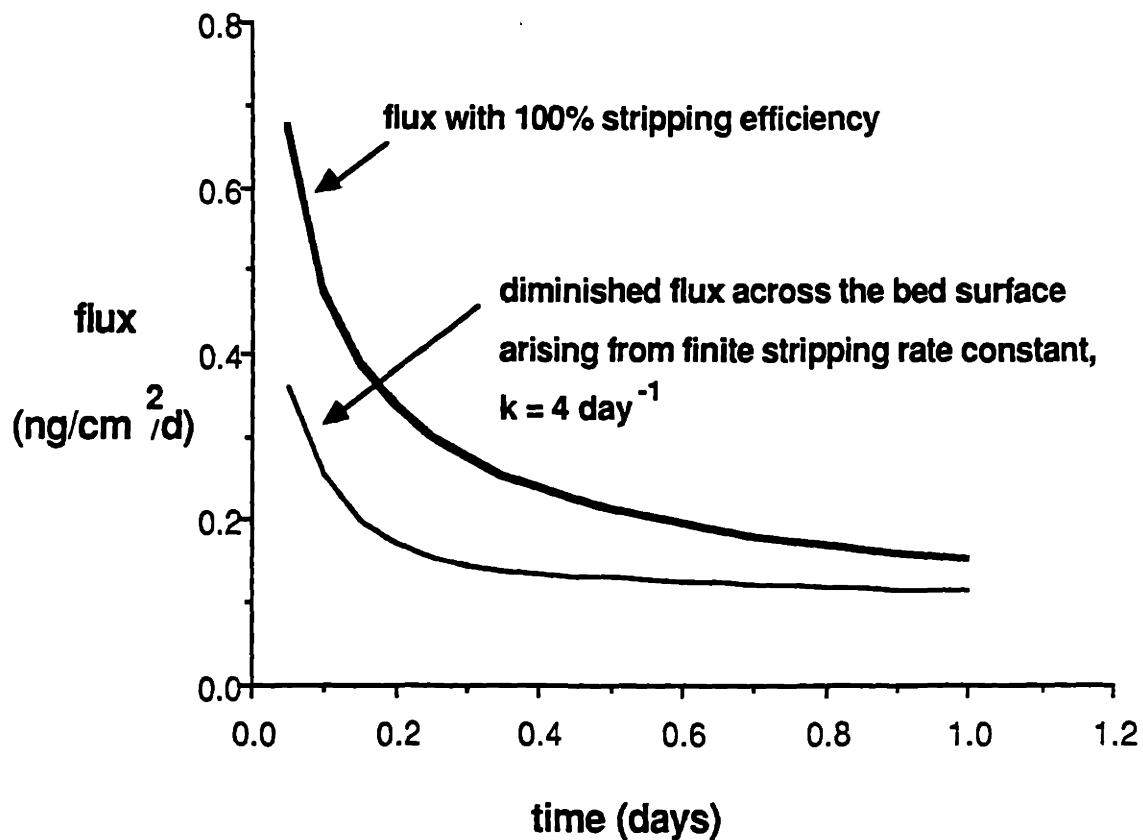
Figure 4.4 Simulation results to show the impact of stripping efficiency on the fluxes from the bed due to porewater diffusion. The simulation conditions are the same as the experiment shown in Fig. 4.3-c, but with very short time.

Neglecting the water column buildup of sorbate due to inadequate stripping, we obtain predictions of the PCB flux by using the retarded molecular diffusion model (Eq. 4.19 with $w(z)=0$, $f(z)=0$, $K_p = K_{om}$ x organic content, $D_{app} = D_m n_b^{i+1}/(n_b + \rho K_p)$, and assuming $i=1$). Solutions are solid lines in Figure 4.3-a, b, and c (from the analytical solution by Crank, 1975). The predictions are within a factor of 2 of the observed fluxes for dichlorobiphenyl and tetrachlorobiphenyl, and a factor of 5 for trichlorobiphenyl. The discrepancies between model simulations and experimental observations are most likely due to the errors in predicting the apparent diffusivities or to neglect of important transport processes. Since the molecular diffusivity of a compound and the solid density of the sediment material are well known parameters, error primarily comes from estimates of the other components in the apparent diffusity, the geometric factor and the partition coefficient. The geometric factor, n^i, varies by about a factor of 2 (Ullman and Aller, 1982). There is also an uncertainty in estimating partition coefficients from octanol water partition coefficients (e.g., a factor of 2 to 3, Karickhoff et al., 1979). Therefore, a propagation error of about 3.5 in the calculated fluxes is expected which may explain the higher fluxes predicted by the model.

Another process possibly controlling the transport of PCBs in the bed is colloid-mediated diffusion. The contribution of colloids to the apparent diffusivity can be estimated from Eq. 4.20. The diffusion rate of colloid-bound species is directly related to the concentration of these microparticles or macromolecules (ρ_c) and the partitioning tendency of the

compound to these small particles (K_c). Assuming that the size of the moving colloids is 10 nm (i.e., $D_c = 4.3 \times 10^{-7}$ cm^2/s) and that a dissolved organic carbon (DOC) concentration of 15 mg/L, typical in the natural sediment beds (Brownawell, 1986; Martin, 1985; McNichol, 1986) also exists in our microcosm, we can predict D_{app} from DOC and K_{oc} (representing ρ_c and K_c respectively) by assuming $K_{oc} = 2 \cdot K_{om}$ (i.e., 50% of the organic content is organic carbon). It is found that the D_{app} (an approximately constant value of 4×10^{-11} cm^2/s) is about 1/10 of the estimated retarded molecular diffusivity for tetrachlorobiphenyl and even smaller for tri- and di-chlorobiphenyls. Therefore, colloids are not likely to contribute to the PCB transport in these cases.

The general agreement between predictions by the retarded diffusion model and observed data is good and corroborates the observations by Di Toro et al. (1985) and Karickhoff and Morris (1985). The effects of the diminished diffusivity by local equilibrium in the sediment beds is clearly demonstrated by these experimental results.

4.4.2 Sediment Bed Modification by Tubificid Worms

At the beginning of Experiment B, tubificid worms (about 430 individuals) were introduced into an aquarium with a sediment column which had 8 cm depth and 61 cm^2 surface area (i.e., about 7.1 worms/cm^2). In the first few days after introducing the worms, the reworking activity was not homogeneously distributed horizontally. Fecal pellet patches appeared on the bed surface. The original surface was not totally covered until 4 days later. The pellet

dunes developed to a maximum size of 4 mm in diameter then stopped growing.

The vertical profiles of organic matter content in the bed show the selective feeding habit of tubificids (Fig. 4.5). The worms not only feed on small particles (Aller, 1978) but also appear to prefer those enriched in organic matter. The 9% combustible loss of the original sediments was increased to 12% in the fecal pellets corresponding to an enrichment factor of 1.3. This phenomenon has been reported in the literature (Karickhoff and Morris, 1985 (factor of 3.5); Aller, 1978 (factor of 1.1 by Yoldia)). Therefore, an enrichment of hydrophobic pollutants in the fecal pellets relative to the remaining bed particles is likely because sorbed compounds are primarily associated with organic matter. In addition, there should be layers with low organic matter to indicate the actively feeding zone. In fact, we found one or a few sections of the sediment core beneath the reworked zone have lighter color and sandy texture as well as low organic content shown by Figure 4.5.

The reworked materials were packed into cylindrical pellets with cross-sectional diameter of about 150 μm (Fig. 4.6). These rigid cylinders greatly increased the porosity in the reworked layer by a card-house-like structure. The solid content is only 0.25 g/cm^3 on the bed surface (Fig. 4-7). High solid content as a result of high fraction of sands left behind after feeding clearly show the actively working layer too.

The boundary of the low solid layer was used to identify the depth of the front of the reworked layer (Fig. 4-8). The movement of the front indicates a steady downward velocity (0.07 cm/day) of sediment in the first 3 cm, but this sediment advection rate is diminished below 3 cm and stops before 5 cm. There
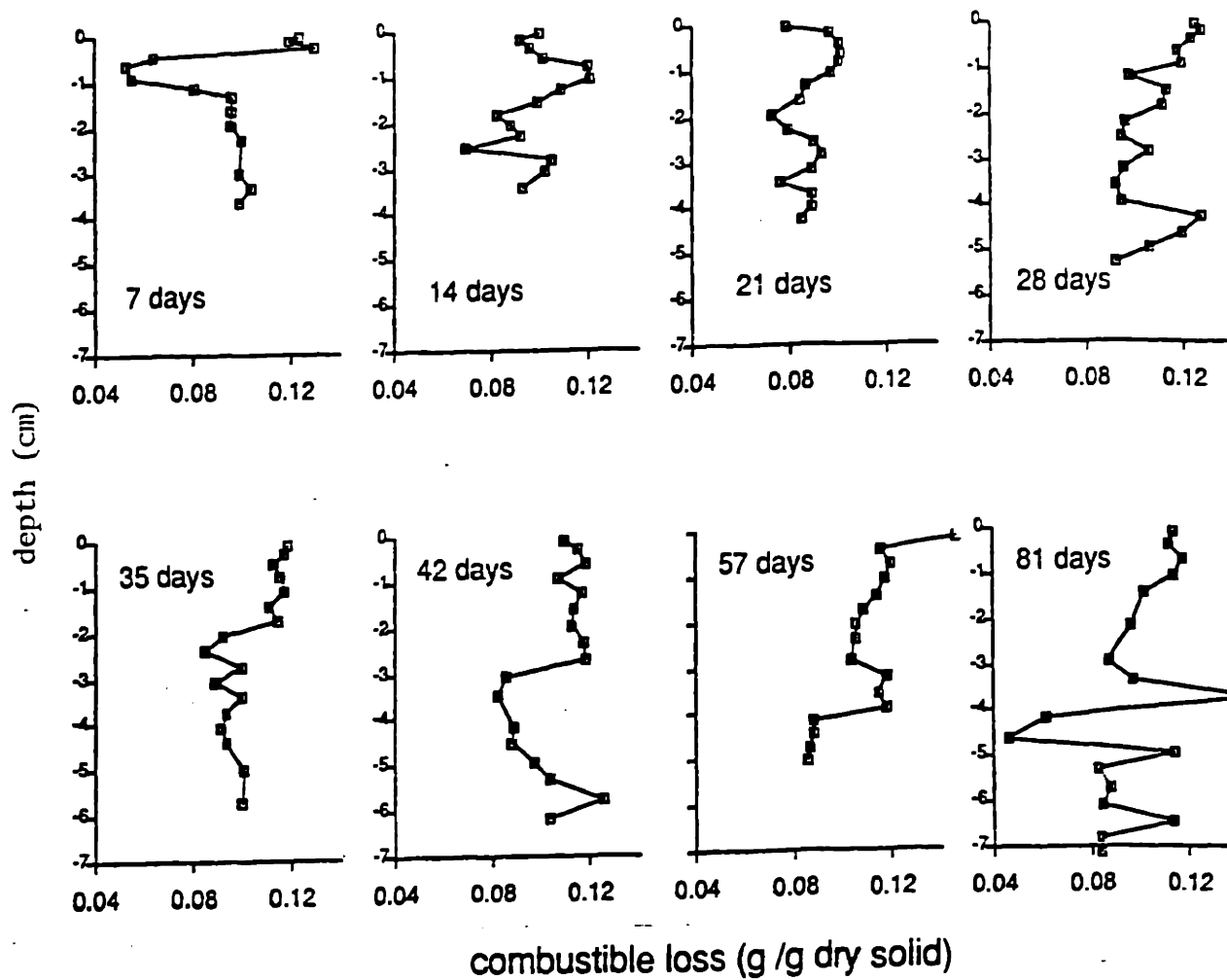
Figure 4.5   Organic matter (shown as combustible loss) profiles in the
sediment bed during Experiment B.

100 μm

Figure 4.6   Fecal pellets of tubificid worms (x100).
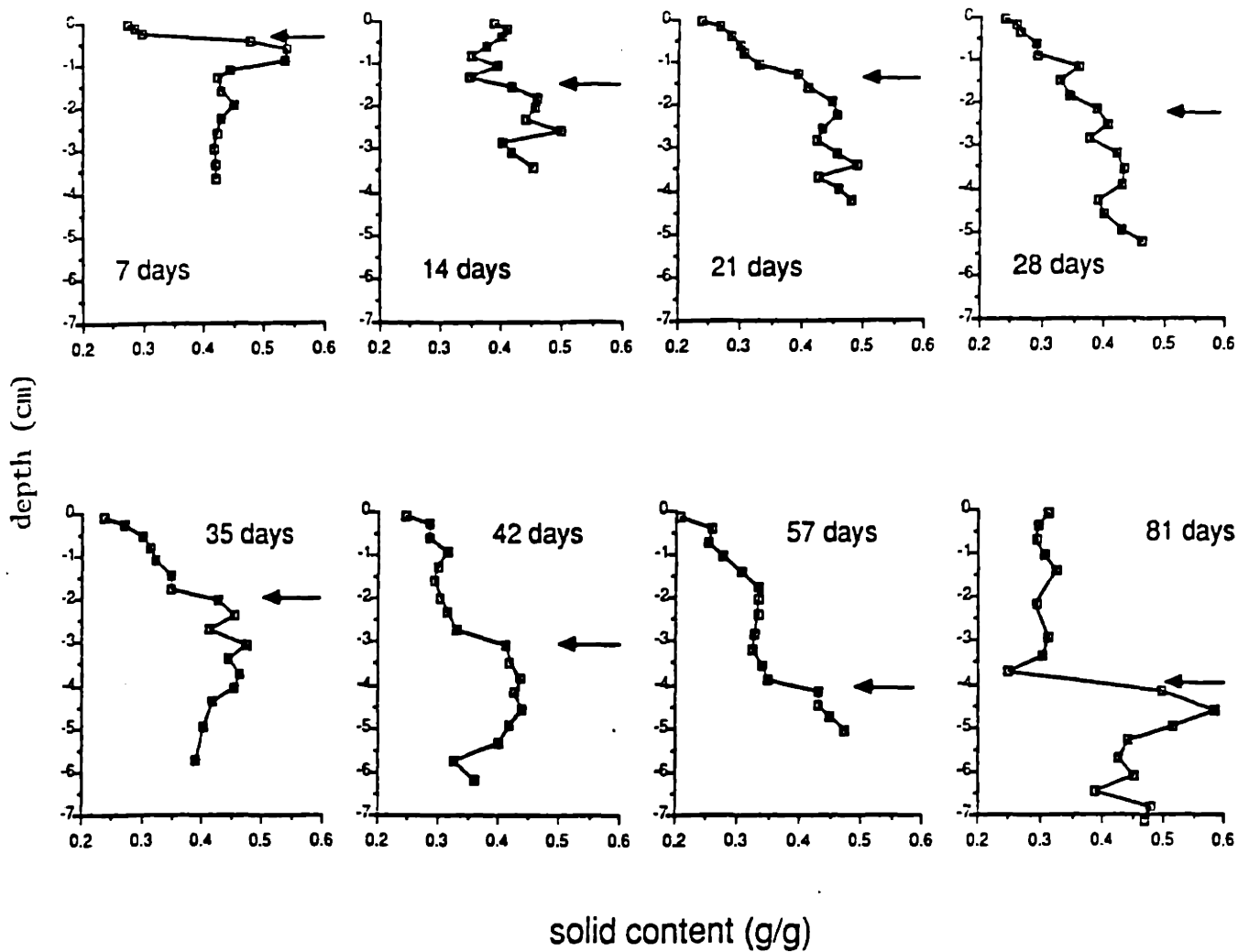
Figure 4.7   Solid content profiles in the sediment bed during Experiment B.
Arrows point out the locations of the lower boundary of
reworked layer which has solid content lower than 0.42 (i.e.,
the original solid content).

4.6 tubificid worms / cm^2
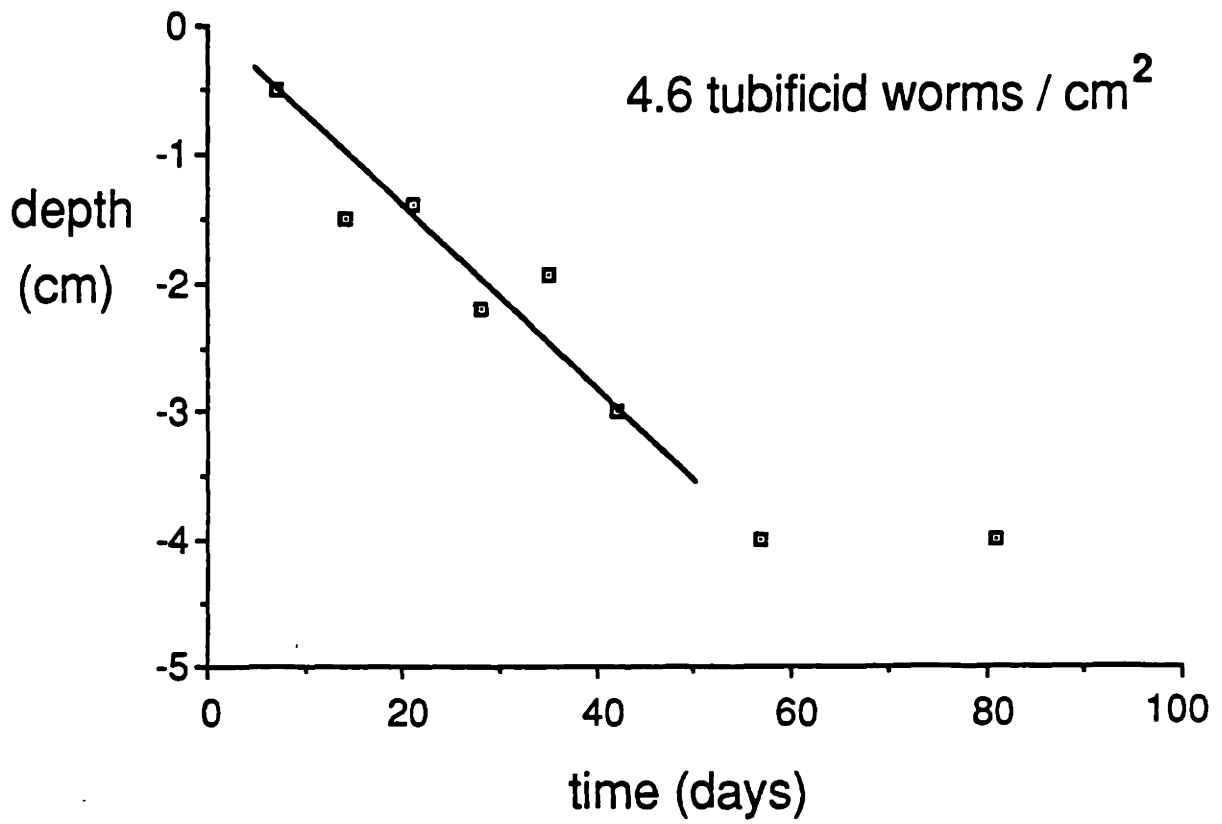
Figure 4.8   The location of the lower boundary of the reworked sediment

layer during Experiment B.

are only few small channels made by worms below 5 cm based on observations from the side of the aquarium. The calculated individual reworking rate (= w_r (cm/d) / worm density (#/cm^2)) is very close to the values in the literature (i.e., 0.014 cm^3/d from Fisher et al., 1980; 0.013 cm^3/d from Karickhoff and Morris., 1985; and 0.01 cm^3/d from this work).

The sediment sinking velocity can be translated into feeding activities if the parameterization approach by Fisher et al. (1980) (Eq. 4.7) is correct. Investigators obtained good velocity profiles by using tracers (i.e., ^{137}Cs sorbed on clays or glass beads) laid on the original bed surface. The feeding activity profiles derived from their results are different. The activity peaks span from 3 cm to 6 cm (Robbins et. al., 1979, with 5 worms/cm^2), 6 cm to 8 cm (Fisher et. al., 1980, with 10 worms/cm^2), and 2.5 cm to 3.5 cm (Karickhoff and Morris, 1985, with 4 worms/cm^2), compared to 3 cm to 5 cm by this work (with 4.6 worms/cm^2). Higher population density seems to drive worms to feed deeper. It has been suggested that the feeding depth may vary with the distribution of tubificid length (which is affected by the worm separation procedure), the species composition of the population, and the population density (Fisher et. al., 1980). Most importantly, according to our experimental results, the maximum feeding activity occurs beneath the front of the reworked layer. Labelling the original bed surface may not yield feeding distribution as a function of depth. We believe that a low organic content region or a sandy zone (with high solid content) in the sediment bed can show the actual feeding activity better. Based on the observations in this sediment modification experiment, a uniform feeding activity zone from 3 cm to 5 cm deep is used in the following model analyses.

4.4.3 Transport of PCBs in the Bed with Bioturbation

The fluxes of PCBs across the surface of the sediment column during

Experiment C are shown in Figure 4-9. Error bars on the data indicate the

relative standard deviations of four measurements of the concentration of PCBs

in the same effluent (i.e., ±30%, ±17%, ±33%, and ±60% for di-, tri-, penta-,

and hexa-chlorobiphenyls, respectively). The PCB fluxes of the more

hydrophobic congeners are relatively low at the beginning but approach nearly

constant values after 6 days. These initial low fluxes could be due to the

low activity of worms in a starting period after their transferral into the

experimental system at time 0. Also, worms burrowing was clustered in the

first few days. The whole bed surface was not entirely covered by fecal

pellets until 4 days after the experiment started. This heterogeneous

distribution of deposition could shorten the exposure time of fecal pellets to

the overlying water and diminish the PCB transport. Apparently, a steady

state situation was not reached until 6 to 8 days after the microcosm

inoculation with worms.

It was found that microcosm flushing with water was necessary to keep the

concentrations of PCBs in the water lower than 20% of the sediment-water

equilibrium concentrations. This could not be achieved with water column

stripping in these bioturbation experiments due to much higher mass fluxes

from the bed than those in the pore water diffusion experiments.

Since no resuspension of fecal pellets or sediment particles was observed

during the experiment, the processes which may contribute to the pollutant

fluxes across the bed surface are retarded molecular diffusion, colloid-
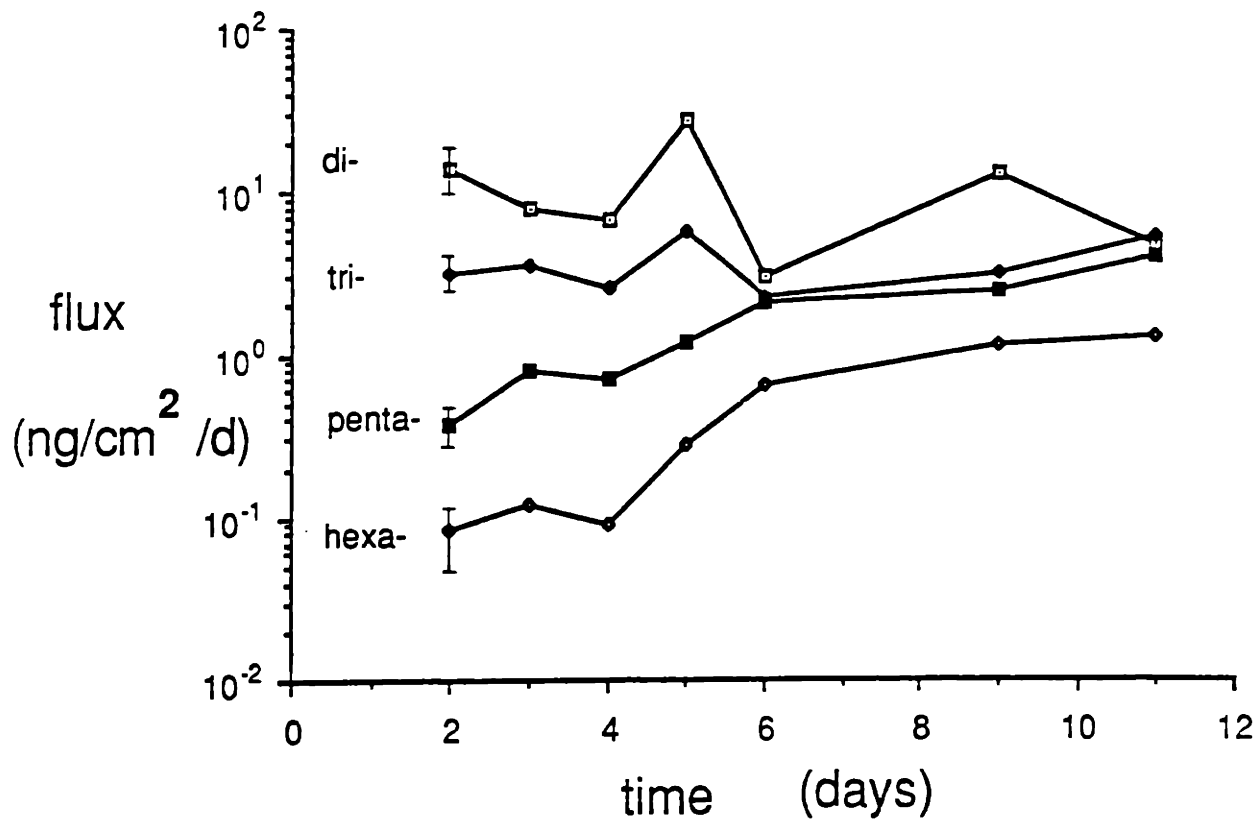
Figure 4.9   PCB fluxes of 4,4'-dichlorobiphenyl (open squares), 3,4,2'-trichlorobiphenyl (solid diamonds), 2,4,5,2',5'-pentachlorobiphenyl (solid squares), and 2,4,5,2',4',5'-hexachlorobiphenyl (open diamonds) in bioturbation enhanced transport experiment (Experiment C).

mediated diffusion, and bioturbation. Simulation analyses show that molecular

diffusion of PCBs in pore water does not contribute significantly to the total

flux (dotted lines in Figure 4.10-a to d compared to the observed fluxes shown

by open squares; note the logarithmic scale). Following the discussion in

Section 4.4.1, we can also neglect the effects of colloid-mediated transport

for di-, tri-, and tetra-chlorobiphenyls. According to a similar model

analysis, the pentachlorobiphenyl flux may be enhanced about 30% by colloids,

and by about a factor of two for hexachlorobiphenyl. Consequently, the

biogenic mixing activities seem to dominate the chemical transport in these

experimental system.

Based on the observation of worm activities (see section 4.4.2), we may

estimate the total mass flux of pollutant brought onto the bed surface by

worms. If one assumes that equilibrium between the reworked pellets and the

water column is rapidly achieved, this total mass flux brought onto the bed

surface is also the flux released to the water column. Using the sediment

advection model with the assumption of instantaneous sorption equilibrium at

the bed-water interface, one predicts the fluxes shown as the dashed lines in

Fig. 4-10 a to d. Clearly, these predicted fluxes are much higher than the

measured fluxes. Therefore, sediment-water equilibration is not likely, and

we must incorporate sorption kinetics to improve the predictions.

Since the initial concentrations of PCBs in the sediment bed are nearly

the same, the magnitude of fluxes can be compared to each other directly. The

flux of 4,4'-dichlorobiphenyl is the highest and that of 2,4,5,2',4',5'-

hexachlorobiphenyl is the lowest. The sequence of the flux intensities for

PCBs is exactly the inverse of the sequence of their hydrophobicities. This
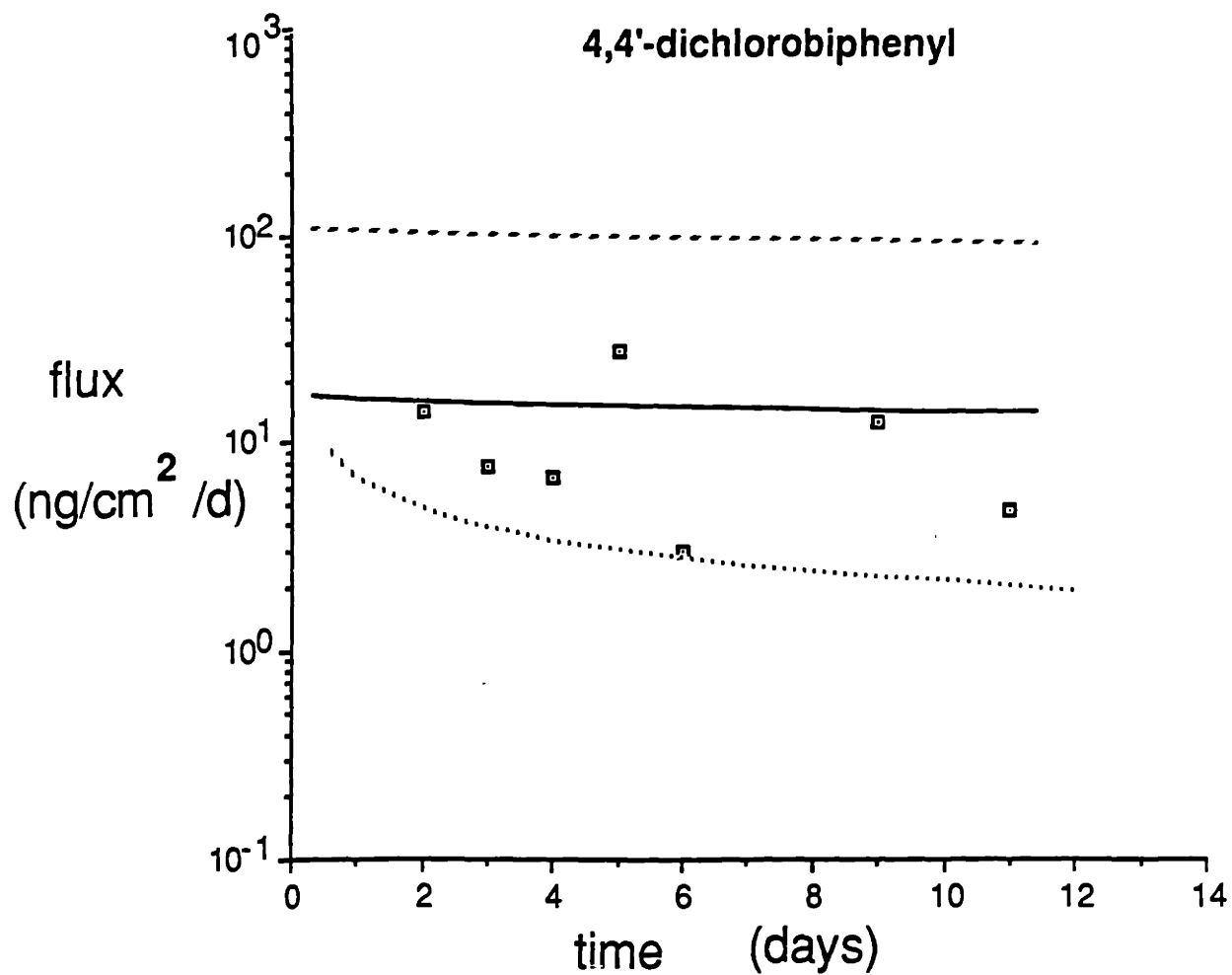
Figure 4.10-a Fluxes of 4,4'-dichlorobiphenyl compared to fluxes predicted by the integrated transport model with kinetics controlled mass transfer (solid line), fluxes predicted with assumption of equilibrium between reworked sediments and the overlying water (dashed line), and fluxes estimated from pore water molecular diffusion only (dotted line).

3,4,2'-trichlorobiphenyl

flux

$(ng/cm^2/d)$

time   (days)
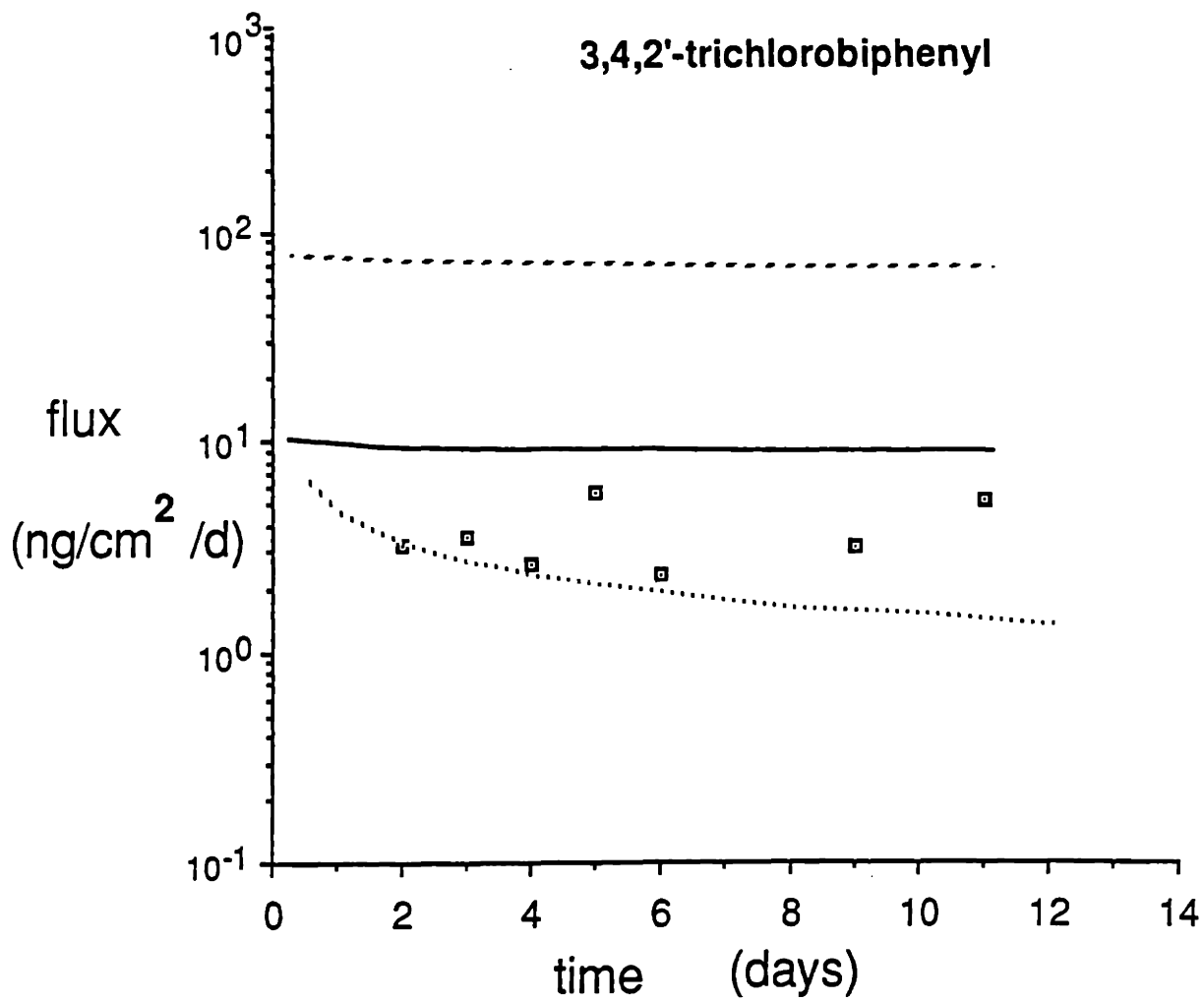
Figure 4.10-b   The same as Figure 4.10a for 3,4,2'- trichlorobiphenyl.

2,4,5,2',5'-pentachlorobiphenyl
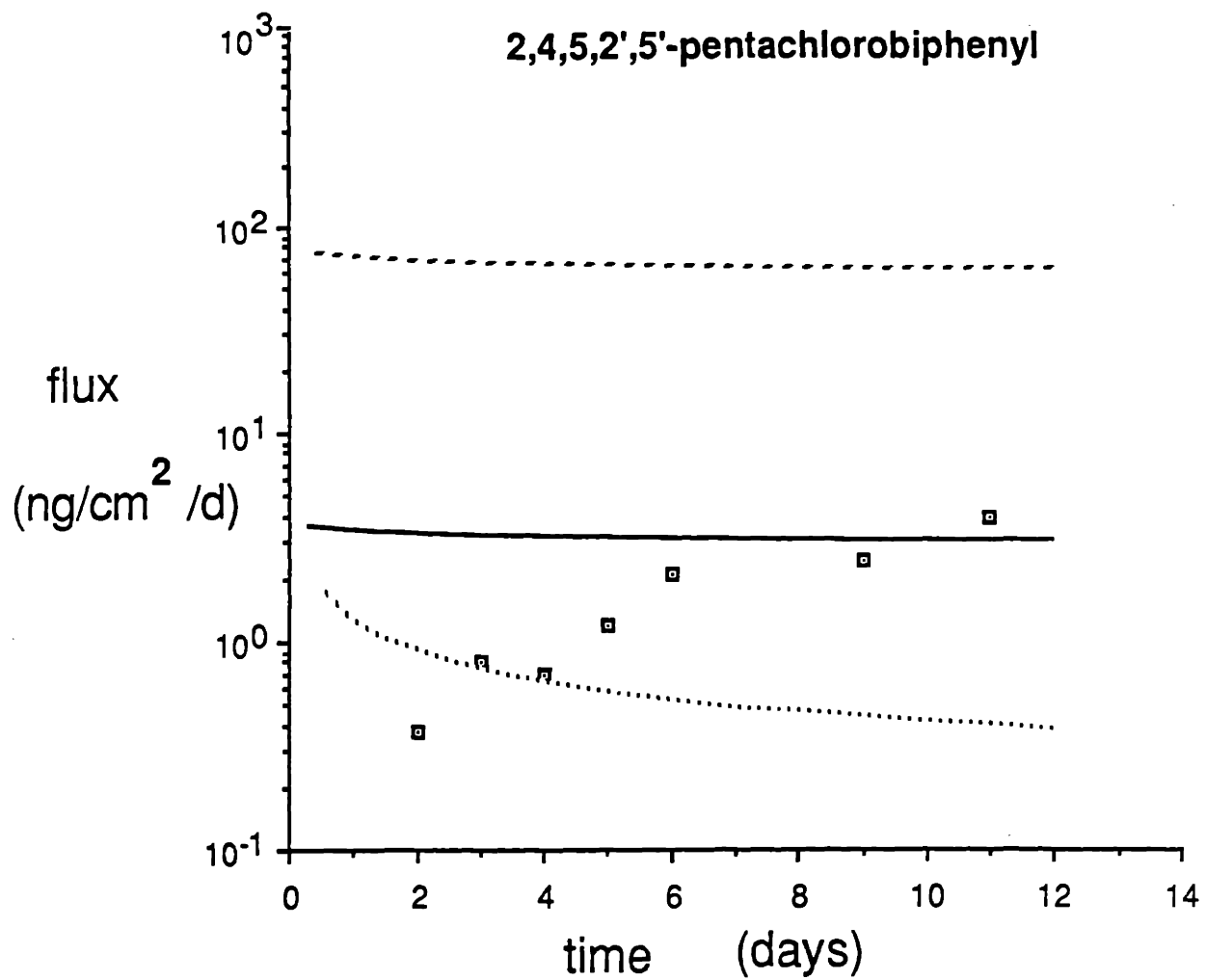
Figure 4.10-c   The same as Figure 4.10a for 2,4,5,2',5'-pentachlorobiphenyl.

2,4,5,2',4',5'-hexachlorobiphenyl
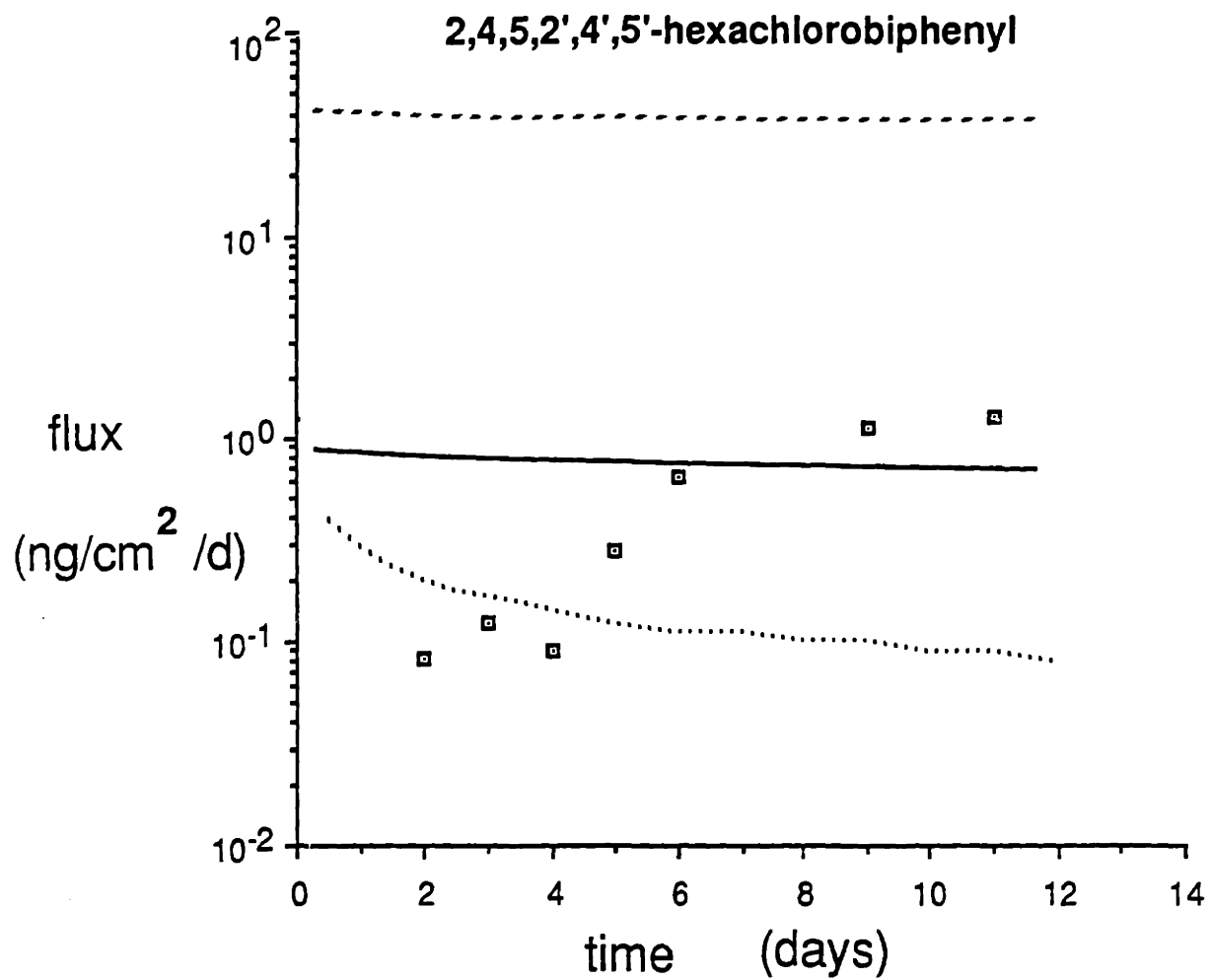
Figure 4.10-d   The same as Figure 4.10a for 2,4,5,2',4',5'-hexachlorobiphenyl.

may be evidence that the desorption rate from fecal pellets to water column, which is high for less hydrophobic compounds and low for more hydrophobic compounds (see Chapter 2), is the limiting factor for the release of these compounds from the bed.

Assuming that the reworked pellets are evenly spread on the bed surface, we obtain a residence time of 2.7 hours for reworked pellets in the bed surface sublayer. Kinetic effects are introduced into the transport model by calculating the fraction of sorbed concentration released from a cylindrical pellet to the overlying water in 2.7 hours. In the model simulations, the effect of the selective feeding which increases the organic content in the

.pellets is taken into account. We use organic content and K_{om} instead of ρ and K_p for the concentration of stationary sorbent phase and partition coefficient, and apply an enrichment factor e (=1.3) to increase the f_{oc} in the pellets.

A numerical approach is necessary to perform model simulations. Instead of an assumption of equilibrium concentration at the bed-water interface, we use mass flux as a boundary condition, which is evaluated at each time step by using the sorption kinetics description (see Appendix 5). The predictions of PCB flux by using our integrated transport model (including a flushing rate constant of 125 day^{-1}) are shown in Figure 4.10-a to 4.10-d as solid lines. The predicted fractions of PCBs released from the reworked sediments are indeed quite small (i.e., M_t/M_∞ is from 17% for dichlorobiphenyl to 2% for hexachlorobiphenyl). Microcosm data obtained after more than 6 days are generally within a factor of three of the predictions. Considering the

uncertainty in the estimates of modelling parameters (e.g., the retarded diffusivities as discussed previously), this agreement between the model predictions and experimental data is reasonably good.

Karickhoff and Morris (1985) also investigated this kinetics controlled mass transfer between reworked fecal pellets and the overlying water by doing similar experiments. They estimated the M_t/M_∞ by performing desorption experiments of polluted fecal pellets in suspension and found that the M_t/M_∞ is only 0.15 for hexachlorobenzene after 2 days. The corrected initial flux (by multiplying the initial reworked mass flux, $S_b(z=0)w_r$, with M_t/M_∞) matched the experimental results very well. The results of our bioturbation transport experiments are consistent with their investigations. In addition, since we can predict M_t/M_∞ *a priori* from the given environmental conditions, there is no need for additional empirical estimation of parameters when this transport model is incorporated into the pollutant fate models. This treatment introduces the sorption kinetics into the transport model and eliminates the invalid assumption of equilibrium at the bed/water interface.

Since we made some assumptions and neglected many processes in our model simulations, compensating errors might have caused the false good fit. Good agreement between model predictions and observed fluxes does not prove the validity of this integrated model. Certainly, we need more study to evaluate the appropriateness of the assumptions made in the model analyses. For example, two important modelling parameters, thickness of the one-grain-size sublayer and the cylinder geometry of intraparticle diffusion, were based on the assumption that the surface of the grains in the first layer are entirely exposed to the

overlaying water. However, the pellets on the bed-water interface may have close contact with the immediate lower layer. The lack of complete exposure could alter the diffusion path and lower the desorption rate. For example, the desorption rate from one end of a plane sheet is about 1/4 of the rate from a cylinder with similar width (Crank, 1975). It is likely that the assumption of a one-diameter thickness of the sublayer and a complete exposure of the pellets overestimated the fluxes by factors substantially greater than 1. However, whenever the turbulence in the water column is high in the environment, the overlying water might penetrate deeper than one-grain depth, and fecal pellets on the surface might be subject to bed load transport and expose the pellets underneath; therefore, the assumption of one-grain size sublayer would underestimate the PCB fluxes in that case. More study is needed to accurately extimate the geometry of the sublayer.

In the simulation, we also neglect many processes which are likely enhanced by bioturbation activities and only consider the conveyer-belt type sediment mixing. Two other biological activities, eddy-diffusion type sediment mixing and biogenic irrigation, might also contribute significantly to the total chemical fluxes. The eddy-diffusion type mixing by tubificid worms has been reported to be 2.8×10^{-9} cm^2/s in a similar condition (Robbins et al., 1979). This diffusivity corresponds to a residence time in the sublayer of about 1 day. Compared to the conveyer-belt type mixing with a residence time of 2.7 hours in the sublayer, this random mixing by worm bodies is not important in our experimental situations.

During this experiment (C) we found that the effluent had an average absorbance of 0.028 at a wavelength of 500 nm compared to 0.000 of the flushing

water. Stopping the flushing flow allowed the water to build up materials released from the bed as indicated by an increase of absorbance to 0.122 after 30 minutes, 0.309 after 2 hours, and 1.382 after 15 hours. This phenomenon which was not been observed in Experiment A indicates that there is a flux of absorbent colloidal material coming out of the sediment bed due to animal activities. Some benthic species exchange large amounts of overlying water with the sediment porewater (Foster-Smith, 1978; Lee and Swartz, 1980). When the oxygen in the sediment is limited, tubificid worms can recycle water through their bodies to facilitate oxygen transport (Grzimek, 1968). Also, these animals make many channels in the mud. These irrigation and channelling processes will certainly accelerate the release of dissolved substances and colloids into the overlying water.

Clymenella torquata, one of the conveyer-belt type reworking animals in the sea, has an irrigation rate which exchanges about 50 volumes of water for each volume of solids reworked (Lee and Swartz, 1980). If tubificid worms have similar irrigation-to-reworking ratio, the total mass of dissolved species pumped through their bodies will be much less than the reworked sorbed species because of the very high sorbed-to-dissolved ratio of pollutant species in the sediment bed (i.e., the partition coefficients of tested compounds are all higher than 10^3 cm^3/g). However, when local equilibrium can be assumed, the amount of pollutants transported by moving colloids will only depend on the concentration of DOC in the moving fluid and the compound concentration in the bed. The colloid-mediated PCB transport will be very important for more hydrophobic PCBs because this process overcomes the transport limitation due to retardation by local partitioning equilibrium, which is more significant for

more hydrophobic compounds.

This biological colloid transport may be one possible reason for the observed increasing of fluxes during the first 6 days of the experiment. For example, assuming that the DOC concentration in the porewater is 30 mg/L and the individual irrigation rate for tubificid worms is 0.5 cm^3/worm/d (i.e., 50 times of the sediment reworking rate), the total flux of DOC per unit area will be 2×10^{-4} g/cm^2/d. The PCB fluxes carried by colloids will be 4 ng/cm^2/d, 3 ng/cm^2/d, 3 ng/cm^2/d, and 1.7 ng/cm^2/d for di-, tri-, penta-, and hexa-chlorobiphenyls, respectively, which are much lower than the observed fluxes of di- and tri-chlorobiphenyls, but similar to the highest flux observed for penta- and hexa-chlorobiphenyls. If this biogenic irrigation rate is zero at the beginning of the experiment and reaches the maximum after 6 days, this significant contribution to transport for more hydrophobic compounds by biological colloid generation may explain the dramatic start-up increase of fluxes for penta- and hexa-chlorobiphenyls.

Apparently, desorption kinetics is an important factor governing pollutant transfer between beds and the water column under our experimental conditions. However, other biological processes (e.g., biogenic irrigation and colloid generation) may contribute significantly to the overall flux. More studies are necessary to identify and quantify these biological enhanced transport processes.

4.5 Conclusion

The work described in this chapter set forth a general modelling approach for the transport of hydrophobic compounds associated with pore water, solid

material, and moving colloids between the sediment beds and the water column. Several conclusions can be drawn from the model analyses and the experimental results:

1. Three phases are considered in our model (i.e., pore water, solid, and colloids). The effects of colloids in the transport of pollutant can be clearly specified without using an empirical formula for the partition coefficient.

2. In addition to the equilibrium partitioning model we incorporate the sorption kinetic model in the fate model to handle problems with kinetic limited pollutant transport (e.g., quick renewal of sediment surfaces by bioturbation). This approach eliminates invalid assumptions of equilibrium between solid and aqueous phases

3. The results of the pore diffusion experiment show that the diffusion of PCBs is diminished by local equilibrium in the sediment bed. Model predictions are generally higher than the experimental data by a factor of 2 to 5.

4. Observations of the bioturbation behavior show that the individual reworking rates are quite constant among different observations. The selective feeding habit of tubificid worms increases the organic matter content in the fecal pellets and, consequently, will increase the concentration of hydrophobic pollutants in the fecal pellets. Organic matter content and solid content profiles provide information on the reworking rates and the location of the active feeding zones.

5. Transport of PCBs in the bed is greatly enhanced by bioturbation. However, the mass transfer between the reworked sediments and the overlying water is controlled by sorption kinetics. The predictions of the model are within a reasonable range (a factor of 5) from the data. Colloids are released

from the sediment layer during the bioturbation experiment and therefore might contribute to the overall flux of pollutants entering the water column.

6. This integrated transport model is developed based on known chemical, physical, and biological processes. All parameters in this model can be easily measured or derived from system properties. The retarded diffusivity in the interstitial pores or in the intraparticle pores can be predicted from the known chemical properties (i.e., octanol-water partition coefficient (K_{ow}), and molecular diffusivity (D_m)) and sediment or particle characteristics (i.e., organic carbon content (f_{oc}), and porosity (n or n_b)). A survey at the field site of interest will be able to supply information on the types and population of the benthic animals, and the organic content (or porosity) profile which will indicate the actively reworked zone in the beds. Also, the size distribution of aggregates or fecal pellets can be obtained from the sediment samples. The information on animal feeding behavior and individual reworking rate in the literature (reviewed by Lee and Swartz, 1980) will help us to estimate the two important parameters, the sediment reworking rate and the eddy-diffusion type mixing coefficient.

1. In this thesis, a predictive description of sorption kinetics for hydrophobic organic compounds on natural solids is introduced into the chemical transport model to handle a variety of environmental situations in which the assumption of equilibrium between solid and aqueous phases may not be valid.

2. A sorption kinetics model developed and experimentally verified based on the intraparticle diffusion process and local phase partitioning forms the basis of this work. The only adjustable model parameter, the intraparticle diffusivity, can be estimated from the chemical and physical properties of the compound and the natural sorbents of interest.

3. A numerical model capable of describing sorption exchange in an aqueous system, containing a spectrum of particle sizes and time-varying solution conditions, has been developed. Simulation examples demonstrate our ability to predict the fates of chemicals in a dynamic environment without assuming aqueous/solid equilibrium.

4. Colloids, a moving sorbent phase in the solution, are included in an integrated chemical transport model. Concentrations of the three sorbate species (i.e., dissolved, sorbed, and colloid-bound species) are coupled by the equilibrium relationships or the kinetics expressions. Microcosm experiments have shown the predictive capability of this model.

5. This thesis presents useful approaches to parameterize sorption exchange processes and sediment mixing process. The results of this work will improve our ability to predict the fate of hydrophobic chemicals in

natural water bodies.

6. Future studies on the sorption controlled mass transport are suggested:

a. to verify the sorption kinetics model under the situations in which there are highly hydrophobic compounds, a variety of natural particles (e.g., aggregates formed by clayey material, and microorganism debris or live bodies), or high solid concentrations;

b. to develop methods to measure the intraaggregate porosity in the aggregates;

c. to study the dynamic change of particle size distributions in the nature;

d. to elucidate the generation and fate of colloids in order to specify the temporal and spatial variation of the concentration of colloids in the environment;

f. to develop parameterization techniques to quantify the impacts of a variety of bioturbation activities (e.g., plowlike bioturbation, and biogenic irrigation) on the transport of pollutants sorbed-on-sediment;

g. to formulate a predictive model coupling sorption kinetics with the sediment resuspension processes.

REFERENCES

Aller, R. C., "Experimental Studies of Changes Produced by Deposit Feeders on Pore Water, Sediment, and Overlying Water Chemistry," *Americal Journal of Science*, Vol. 278, 1978, pp. 1185-1234.

Ambrose, R. B. Jr., Hill, S. S. and Mulkey, L. A., "User's Manual for The Chemical Transport and Fate Model TOXIWASP Version 1," U. S. Environmental Protection Agency, Athens, Georgia, EPA-600/3-83-005, 1983, p. 13.

Berner, R. A., *Principles of Chemical Sedimentology*, McGraw-Hill Book Co., New York, 1971, p. 98.

Berner, R. A., *Early Diagenesis: A Theoretical Approach*, Princeton University Press, Princeton, N. J., 1980.

Black, C. A., Evans, D. D., White, J. L., Ensminger, L. E. and Clark, F. E., "Methods of Soil Analysis", No. 9 in the series Agronomy, American Society of Agronomy, Madison, Wisconsin, 1965.

Bopp, R. F., Simpson, H.J., Olsen, C. R. and Kostyk, N., "Polychlorinated Biphenyls in Sediments of the Tidal Hudson River, New York," *Environmental Science and Technology* , Vol.15, 1981, pp. 210-216.

Brady, N. C., *The Nature and Properties of Soil*, 8th ed., MacMillan Publishing Co., Inc., New York, 1974, p. 58.

Brinkhurst, R. O. and Cook, D. G., "Aquatic Earthworm (Annelida: Oligochaeta)," in *Pollution Ecology of Freshwater Invertebrates*, Hart, C. W. Jr. and Fuller, S. L. H. eds., Academic Press, New York, 1974, pp. 143-156.

Brown, M. P., Werner, M. B., Sloan, R.J., and Simpson, K. W., "Polychloronated Biphenyls in the Hudson River," *Environ. Sci. Technol.* Vol. 19, 1985, pp. 656-664.

Brownawell, B. J., *The Role of Colloidal Organic Matter in the Marine Geochemistry of PCBs*, Ph.D. thesis, Joint Program in Oceanography, Massachusetts Institute of Technology and Woods Hole Oceanographic Institution, 1986.

Brownawell, B. J. and Farrington, J. W., "Biogeochemistry of PCBs in Interstitial Waters of a Coastal Marine Sediment," *Geochimica et*

Cosmochimica Acta, Vol. 50, 1986, pp. 157-169.

Bruggeman, W. A., van der Steen, J. and Hutzinger, O., "Reversed-Phase Thin-Layer Chromatography of Polynuclear Aromatic Hydrocabons and Chlorinated Biphenyls," *Journal of Chromatography,* Vol. 238, 1982. pp. 335-346.

Chase, R. R. P., "Settling Behavior of Natural Aquatic Particulates," *Limnology and Oceanography,* Vol. 24, 1979, pp. 417-426.

Carter, C. W. and Suffet, I. H., "Binding of DDT to Dissolved Humic Materials," *Environmental Science and Technology,* Vol. 16, No. 11, 1982. pp. 735-740.

Chiou C. T., "Partition Coefficients of Organic Compounds in Lipid-Water Systems and Correlations with Fish Bioconcentration Factor," *Environmental Science and Technology,* Vol. 19, 1985. pp.57-62.

Chiou C. T., Freed, V. H., Schmedding, D. W. and Kohnert, R. L., "Partition Coefficient and Bioaccumulation of Selected Organic Chemicals," *Environmental Science and Technology,* Vol. 11, 1977. pp. 475-478.

Chiou, C. T., Malcolm, R. L., Brinton, T. I., and Kile, D. E., "Water Solubility Enhancement of Some Organic Pollutants and Pesticides by Dissolved Humic and Fulvic Acids," *Environmental Science and Technology,* Vol. 20, 1986, pp. 502-508.

Chiou, C. T., Peters, L. J., and Freed, V. H., "A Physical Concept of Soil-Water Equilibria for Nonionic Organic Compounds," *Science,* vol. 206, 1979, pp. 831-832.

Connolly, J. P., "The Effect of Sediment Suspension on Adsorption And Fate of Kepone," Ph.D. diss., University of Texas at Austin, 1980.

Cooney, D. O., Adesanya, B. A. and Hines, A. L., "Effect of Particle Size Distribution On Adsorption Kinetics in Stirred Batch System," *Chemical Engineering Science,* Vol. 38, No. 9, 1983, pp. 1535-1541.

Crank, J., *The Mathematics Of Diffusion,* 2nd ed., Clarendon Press, Oxford, England, 1975.

Crittenden, J. C. and Weber, W. J. Jr., "Predictive Model for Design of Fixed-Bed Adsorbers: Parameter Estimation and Model Development," *J. of the Environmental Engineering Division,* ASCE, Vol. 104, No. EE2, 1978. pp.185-196.

Crittenden, J. C. and Weber, W. J. Jr., "Predictive Model for Design of
    Fixed-Bed Adsorbers: Single-Component Model Verification," *J. of the
    Environmental Engineering Division*, ASCE, Vol. 104, No. EE3, 1978. pp.
    433-443.

Di Toro, D. M., Jeris, J. S. and Ciarcia, D., "Diffusion and Partitioning of
    Hexachlorobiphenyl in Sediments," *Environmental Science and Technology*,
    Vol. 19, No. 12, 1985, pp. 1169-1176.

Fisher, J. B., Lick, W. J., McCall, P.L. and Robbins, J. A., "Vertical
    Mixing of Lake Sediments by Tubificid Oligochaetes," *J. of Geophysical
    Research*, Vol. 85, No. C7, 1980. pp. 3997-4006.

Fisher, J. B., Petty, R. L., and Lick, W. J., "Release of Polychlorinated
    Biphenyls from Contaminated Lake Sediments: Flux and Apparent
    Diffusivities of Four Individual PCBs," *Environmental Pollution* (B), Vol.
    5, 1983, pp. 121-132.

Foster-Smith, R. L., "An Analysis of Water Flow in Tube-Living Animals," *J.
    Exp. Mar. Biol. Ecol.*, Vol. 34, 1978, pp. 73-95.

Freeman, D. H. and Cheung, L. S., "A Gel Partition Model for Organic
    Desorption From a Pond Sediment," *Science*, 214, 1981, pp. 790-792.

Friedlander, S. K., *Smoke, Dust and Haze: Fundamentals of Aerosol Behavior*,
    John Wiley & Sons, Inc., 1977. p. 31.

Grzimek, B., *Grzimek's Animal Life Encyclopedia*, Vol. 1, van Nostrand
    Reinhold Company, New York, 1968, pp. 370-372.

Gschwend, P. M., and Wu, S. C., "On the Constancy of Sediment-Water
    Partition Coefficients of Hydrophobic Organic Pollutants," *Environmental
    Science and Technology*, Vol. 19, No. 1, 1985, pp. 90-96.

Guinasso, N. L. Jr., and Schink, D. R., "Quantitative Estimates of
    Biological Mixing Rates in Abyssal Sediments," *Journal of Geophysical
    Tesearch*, Vol. 80, No. 21, July, 1975. pp. 3032-3043.

Hassett, J. P. and Milicic, E., "Determination of Equilibrium and Rate
    Constants for Binding of a Polychlorinated Biphenyl Congener by Dissolved
    Humic Sbustances," *Environmental Science and Technology*, Vol. 19, No. 7,
    1985. pp. 638-643.

Hayduk, W., and Laudie, H., "Prediction of Diffusion Coefficients for
    Non-electrolysis in Dilute Aqueous Solutions," American Institute of

Chemical Engineers, Journal, Vol. 20, 1974, pp. 611-615.

Hendricks, S. W. and Kuratti, L. G., "Derivation of an Emperical Sorption Rate Equation by Analysis of Experimental Data," *Water Research* Vol. 16, 1982, pp. 829-837.

Henrichs, S. M. and Farrington, J. W., "Peru Upwelling Region Sediments Near 15'S. 1. Remineralization and Accumulation of Organic Matter," *Limnology and Oceanography*, Vol. 29, 1984, pp. 1-19.

Huggett, R. J., Nichols, M. M. and Bender, M.E., "Kepone Contamination of the James River Estuary," in *Contaminants and Sediments*, Vol. 1, R. A. Baker, ed., Ann Arbor Science : Ann Arbor, Mi, 1980. pp. 33-52.

Jaffe, P. R. and Ferrara, R. A., "Modeling Sediment and Water Column Interactions for Hydrophobic Pollutants, Parameter Discrimination and Model Response to Input Uncertainty," *Water Research*, Vol. 18, 1984, pp. 1169-1174.

Johnson, R. G., "Particulate Matter at the Sediment-Water Interface in Coastal Environments," *Journal of Marine Research*, Vol. 32, No. 2, 1974, pp. 313-330.

Karger, B. L., Snyder, L. R. and Horvath, C. *An Introduction to Separation Science*, Wiley and Sons: New York, 1973, p. 80-81.

Karickhoff, S. W., Brown, D. S. and Scott, T. A., "Sorption of Hydrophobic Pollutants on Natural Sediments," *Water Research*, Vol. 13, 1979, pp. 241-248.

Karickhoff, S. W., "Sorption Kinetics of Hydrophobic Pollutants in Natural Sediments," in *Contaminants and Sediments*, vol. 2, *Analysis, Chemistry, and Biology*, R. A. Baker ed., Ann Arbor Science: Ann Arbor, Mi, 1980, pp. 193-205.

Karickhoff, S. W., "Organic Pollutant Sorption in Aquatic Systems," *Journal of the Hydraulic Engineering Division*, ASCE, Vol. 110, No. 6, June, 1984, pp. 707-735.

Karickhoff, S. W. and Morris, K. R., "Impact of Tubificid Oligochaetes On Pollutant Transport in Bottom Sediments," *Environmental Science and Technology*, Vol. 19, No. 1, 1985, pp. 51-56.

Kay, B. D. and D. E. Elrick, "Adsorption and Movement of Lindane in Soils," *Soil Science*, 104, 1967, pp. 314-322.

Krom, M. D. and Sholkovitz, E. R., "Nature and Reactions of Dissolved Organic Matter in the Interstitial Waters of Marine Sediments," *Geochimica et Cosmochimica*, Vol. 41, 1977, pp. 1565-1573.

Landrum, P. F., Nihart, S. Q., Eadie, B. J. and Gardner, W. S., "Reverse-Phase Separation Method for Determining Polutant Binding to Aldrich Humic Acid and Dissolved Organic Carbon of Natural Waters," *Environmental Science and Technology*, Vol. 18, 1984,. pp. 187-192.

Lapidus, L. and Amundson, N. R., "Mathematics of Adsorption in Beds. VI. The Effect of Longitudinal Diffusion in Ion Exchange and Chromatographic Columns," *J. Phys. Chem.* 56, 1952, pp. 984-988.

Larsson, P., "Transport of ^{14}C-Labelled PCB Compounds from Sediment to Water and from Water to Air in Laboratory Model System," *Water Research*, Vol. 17, 1983, pp. 1317-1326.

Lee, H. II, and Swartz, R. C., "Biological Processes Affecting The Distribution of Pollutants in Marine Sediments, Part II. Biodeposition and Bioturbation," in *Contaminants and Sediments*, Vol. 2, *Analysis, Chemistry, and Biology*, R. A. Baker, ed. Ann Arbor Science, Ann Arbor, MI, 1980, pp. 555-606.

Leenheer, J. A. and Arlrichs, J. L. *Soil Science* Soc. Amer., J., vol. 35, 1971, pp. 700-704.

Lopez-Avila, V., and Hites, R. A., "Organic Compounds in an Industrial Wasterwater, Their Transport into Sediments," *Environ. Sci. Technol.*, Vol. 14, 1980, pp. 1382-1390.

Lyman, W. J., Reehl, W. F. and Rosenblatt, D. H., *Handbook of Chemical Property Estimation Methods*, McGraw-Hill Book Company, New York, 1982, pp. 17-1.

Martin, W. R., *Transport of Trace Metals in Nearshore Sediments*, Ph.D. thesis, 1985, Joint Program in Oceanography, Woods Hole Oceanographic Institute/Massachusetts Institute of Technology.

Mathews, A. P., "Adsorption In An Agitated Slurry of Polydisperse Particles," American Institute of Chemical Engineers, Symposium Series, No. 230, Vol. 79, 1983, pp. 18-25.

Mathews, A. P. and Weber, W. J. Jr., "Effects of External Mass Transfer and Intraparticle Diffusion on Adsorption Rates nn Slurry Reactors," American

Institute of Chemical Engineers, Symposium Series, No. 166, Vol. 43, 1976, pp. 91-98.

McCarthy, J. F. and Jimenez, B. D., "Interactions between Polycyclic Aromatic Hydrocarbons and Dissolved Humic Material: Binding and Dissociation," *Environmental Science and Technology*, Vol. 19, No.11, 1985, pp. 1072-1076.

McNichol, A. P., *A Study of the Remineralization of Organic Carbon in Nearshore Sediments Using Carbon Isotopes*, Ph.D. thesis, 1986, Joint Program in Oceanography, Woods Hole Oceanographic Institute/Massachusetts Institute of Technology.

Means, J. C., Wood, S. G., Hassett, J. J. and Banwart, W. L., "Sorption of Amino- and Carboxy-Substituted Polynuclear Aromatic Hydrocarbons by Sediments and Soils," *Environmental Science and Technology*, Vol. 16, No. 2, 1982, pp. 93-98.

Means, J. C. and Wijayaratne, R., "Role of Natural Colloids in Transport of Hydrophobic Pollutants," *Science*, Vol. 215, 1982. pp. 968-970.

Menzel, D. W. and Vaccaro, R. F., "The Measurement of Dissolved Organic and Particulate Carbon in Seawater," *Limnol. Oceanogr.*, Vol. 9, 1964, pp. 138-142.

Miller, M. M., Wasik, S. P., Huang, G-L, Shiu, W-Y. and Mackay, D., "Relationships Between Octanol-Water Partition Coefficient and Aqueous Solubility," *Environmental Science and Technology*, Vol. 19, 1985. pp. 522-529.

Moore, W. J., *Physical Chemistry*, 3rd ed., Pretice-Hall Inc.:Englewood Cliffs, N. J., 1962.

Oddson, J. K., Letey, J. and Weeks, L. V., "Predicted Distribution of Organic Chemicals in Solution and Adsorbed as a Function of Position and Time for Various Chemical and Soil Properties," Soil Science Society of American, *Proceedings*, Vol. 34, 1970, pp. 412-417.

Onishi, Y. and Wise, S. E., "Mathematical Model, SERATRA, for Sediment-Contaminant Transport in River and Its Application to Pesticide Transport in Four Mile and Wolf Creeks in Iowa," U.S. Environmental Protection Agency, *Athens*, Georgia, EPA-600/3-82-045, 1982, p.7.

Orem, W. H., Hatcher, P. G., Spiker, E. C., Szeverenyi, N. M. and Maciel, G.

E., "Dissolved Organic Matter in Anoxic Pore Waters From Mangrove Lake, Bermuda," Geochim. et Cosmochim. Acta, in press.

Pankow, J. F., and Kristensen, T. J., "Effects of Flow Rate and Temperature on Thermal Desorbability of Polycyclic Aromatic Hydrocarbons and Pesticides from Tenax-GC," *Analytical Chemistry*, Vol. 55, No. 13, 1983, pp. 2187-2192.

Peck, D. E., Corwin, D. L. and Farmer, W. J., "Adsorption-Desorption of Diuron by Freshwater Sediments," *Journal of Environmental Quality*, Vol. 9, No. 1, 1980, pp. 101-106.

Peng, T. -H., Broecker, W. S. amd Berger, W. H., "Rates of Benthic Mixing in Deep-Sea Sediment as Determined by Radioactive Tracers," *Quaternary Research*, Vol. 11. 1979. pp.141-149.

Prasher, B. D. and Ma, Y. H., "Liquid Diffusion in Microporous Alumina Pellets," *American Institute of Chemical Engineers Journal*, Vol. 23, No. 3, 1977, pp. 303-311.

Rao, P. S. C., Davidson, J. M., Jessup, R. E. and Selim, H. M., "Evaluation of Conceptual Models for Describing Nonequilibrium Adsorption-Desorption of Presticides During Steady-Flow in Soils," *Soil Science*, Society of America, Journal, 43, 1979, pp. 22-28.

Rao, P. S. C., Jessup, R. E., Rolston, D. E., Davidson, J. M. and Kilcrease, D. P., "Experimental and Mathematical Description of Nonadsorbed Solute Transfer by Diffusion in Spherical Aggregates," *Soil Science*, Society of America, Journal, Vol. 44, 1980, pp. 684-688.

Rao, P. S. C., Jessup, R. E. and Addiscott, T. M., "Experimental and Theoretical Aspects of Solute Diffusion in Spherical and Nonspherical Aggregates," *Soil Science*, Vol. 133, 1982, pp. 342-349.

Rapaport, R. A. and Eisenreich, S. J., "Chromatographic Determination of Octanol-Water Partition Coefficients (Kow's) for 58 Polychlororinated Biphenyl Congeners," *Environmental Science and Technology*, Vol. 18, 1984, pp. 163-170.

Robbin, J. A., McCall, P. L., Fisher, J. B. and Krezoski, J. R., "Effect of Deposit Feeders on Migration of ^{137}Cs in Lake Sediments," *Earth and Planetary Science Letters*, Vol. 42, 1979, pp. 277-287.

Saleh, F. Y., and Lee, G. F., "Analytical Methodology for Kepone in Water

and Sediment," *Environmental Science and Technology*, Vol. 12, 1978, pp. 297-301.

Santschi, P. H., Li, Y.-H., Bell, J. J., Trier, R. M. and Kawtaluk, K., "Pu in Coastal Marine Environments," *Earth and Planetary Science Letters*, Vol. 51, 1980, pp. 248-265.

Satterfield, C. N., *Mass Transfer in Heterogeneous Catalysis*, Robert E. Krieger Publishing Co., Huntington, New York, 1982.

Satterfield, C. N., *Heterogeneous Catalysis in Practice*, McGraw-Hill, Inc., U. S. A. 1980.

Schink, D. R. and Guinasso, N. L. Jr., "Redistribution of Dissolved and Adsorbed Materials in Abyssal Marine Sediments Undergoing Biological Stirring," *American Journal of Science*, Vol. 278, May, 1978, pp. 687-702.

Schöne, (1970) quoted in Dempsey, H. P., "The Effects of Turbulence on Three Algae: Skeletonema costatum, Gonyaulax tamarensis, Heterocapsa triquetra," M.S. theses, Massachusetts Institute of Technology, 1982.

Schwarzanbach, R. P., Giger, W., Hoehn, E. and Schneider, J. K., "Behavior of Organic Compounds during Infiltration of River Water to Groundwater, Field Study," *Environmental Science and Technology*, Vol. 17, 1983. pp. 472-479.

Schwarzenbach, R. P. and Westall, J., "Transport of Nonpolar Organic Compounds from Surface Water to Groundwater. Laboratory Sorption Studies," *Environmental Science and Technology*, Vol. 15, No. 11, 1981, pp. 1360-1367.

Starikova, N. D., "Vertical Distribution Patterns of Dissolved Organic Carbon in Sea Water and Interstitial Solutions," *Oceanology*, Vol. 10, 1970, pp. 796-807.

Stevenson, F. J., *Humus Chemistry, Genesis, Composition Reactions*, John Wiley and Son, New York, 1982, p. 374.

Sudo, Y., Misic, D. M. and Suzuki, M., "Concentration Dependence of Effective Surface Diffusion Coefficients in Aqueous Phase Adsorption on Activated Carbon," *Chemical Engineering Science*, Vol. 33, 1978, pp. 1287-1290.

Swanson, R. A. and Dutt, G. R., "Chemical and Physical Processes That Affect Arazine and Distribution in Soil System," *Soil Science*, Society of

America, Proceedings, Vol. 37, 1973, pp. 872-876.

Turk, J. T., "Applications of Hudson River Basin PCB-Transport Studies," In: *Contaminants and Sediments*, Vol. 1, Edited by R. A. Baker, Ann Arbor Science, Ann Arbor, MI, 1980, pp. 171-183.

Ullman, W. J. and Aller, R. C., "Diffusion Coefficients in Nearshore Marine Sediments," *Limnology and Oceanography*, Vol. 27, No. 3, 1982, pp. 552-556.

van Genuchten, M. T., Davidson, J. M. and Wierenga, P. J., "An Evaluation of Kinetic and Equilibrium Equations for the Prediction of Pesticide Movement Through Porous Media," *Soil Science*, Society of America, Proceedings, Vol. 38, 1974, pp. 29-35.

van Genuchten, M. T. and Wierenga, P. J., "Mass Transfer Studies in Sorbing Porous Media. I. Analytical Solutions," *Soil Science*, Society of America, Journals, vol. 40, 1976, pp. 473-480.

Weber, W. J. Jr. and Liu, K. T., "Determination of Mass Transport Parameters for Fixed-Bed Adsorbers," *Chemical Engineering Communication*, Vol. 6, 1980, pp. 49-60.

Weber, W. J. Jr. and Rumer, R. R. Jr., "Intraparticle Transport of Sulfonated Alkylbenzenes in a Porous Solid: Diffusion with Nonlinear Adsorption," *Water Resources Research*, Vol. 1, No. 3, 1965, pp. 361-373.

Weber, W. J. Jr. and Liu, K. T., "Determination of Mass Transport Parameters for Fixed-Bed Adsorbers," *Chemical Engineering Communication*, Vol. 6, 1980, pp. 49-60.

Wijayaratne, R. D., and Means, J. C., "Affinity of Hydrophobic Pollutants For Natural Estuarine Colloids in Aquatic Environments," *Environmental Science and Technology*, Vol. 18, 1984, pp. 121-123.

Wilson, J. T., Enfield, C. G., Dunlap, W. J., Cosby, R. L., Foster, D. A., and Baskin, L. B., "Transport and Fate of Selected Organic Pollutants in a Sandy Soil," *Journal of Environmental Quality*, Vol. 10, No. 4, 1981, p. 501.

Woodburn, K. B., Doucette, W. J. and Andren, A. W., "Generator Column Determination of Octanol/Water Partition Coefficients for Selected Polychlorinated Biphenyl Congeners," *Environmental Science and Technology*, Vol. 18, 1984, pp. 457-459.

Wu, S. C. and Gschwend, P. M., "Sorption Kinetics of Hydrophobic Organic Compounds to Natural Sediments and Soils," *Environmental Science and Technology*, in print.

Yao, K., Habibian, M. T. and O'Melia, C. R., "Water and Wastewater Filtration: Concepts and Applications," *Environmental Science and Technology*, Vol. 5, 1971, pp. 1105-1112.

Zabawa, C. F., "Microstructure of Agglomerated Suspended Sediments in Northern Chesapeake Bay Estuary," *Science*, Vol. 202, Oct. 1978, pp. 49-51.

Zepp, R. G., and Schlotzhauer, P. F., "Photoreactivity of Selected Aromatic Hydrocarbons In Water," In: *Polynuclear Aromatic Hydrocarbons*, edited by P. W. Jones and P. Leber, Ann Arbor Science Pub. Inc., Ann Arbor, MI, 1979, pp. 141-158.

Appendix 1 Notations

A = surface area of a sediment bed, cm^2;

a = coefficient in Eq. 3.18;

C = concentration of dissolved sorbate in bulk aqueous phase, mol/cm^3;

C_w = concentration of dissolved sorbate in the water column, mol/cm^3;

C' = concentration of dissolved sorbate in pore fluid, mol/cm^3;

D_{app} = apparent diffusivity in sediment beds, cm^2/s;

D_b = eddy-diffusion type biological sediment mixing coefficient, cm^2/s;

D_{eff} = effective intraparticle diffusivity, cm^2/s;

D_m = molecular diffusivity, cm^2/s;

D_p = diffusivity in pores, cm^2/s;

d = particle or pellet diameter, cm;

d_c = colloid particle diameter, cm;

f_i = mass fraction of particle-size group i;

f_{oc} = fraction of organic carbon content;

$f(n,t)$ = geometric factor as a function of porosity and tortuosity;

$f(z)$ = feeding activity function, s^{-1};

i = empirical exponent in the expression of pore geometry in Eq.2.11;

k = stripping rate constant, s^{-1};

k_1, k_{-1}, k_2, k_{-2}

        = reaction rate constants in the first-order kinetics model, s^{-1};

k_B = Boltzmann constant;

k_b = bed surface mass transfer rate constant, cm/s;

169

K_c = equilibrium partition coefficient with colloids, cm^3/g;

K_{oc} = partition coefficient normalized to the organic carbon content,

cm^3/g;

K_p = equilibrium partition coefficient, cm^3/g;

L = water depth, cm;

m = number of grids on the radial axis in spherical particles;

M_t/M_∞ = fraction of completion of equilibration defined in Eq. 3.20;

n = intraparticle porosity, cm^3/cm^3; or number of size groups;

n_b = bed porosity, cm^3/cm^3;

r = radial coordinates, cm;

R = particle radius, cm;

R_d = a fraction factor defined in Eq. 4.17;

S = local total volumetric concentration in the aggregates, mol/cm^3;

S' = local sorbed concentration by weight in the solid phase, mol/g;

$\overline{S}$ = average volumetric concentration over the whole aggregates, mol/cm^3;

S_c = colloid-bound concentration, mol/g;

T = absolute temperature, °K;

t = time, s;

$t_{1/2}$ = half-equilibration point at $M_t/M_\infty=0.5$, s;

t_c = characteristic water/solid contact time or aqueous concentration

fluctuation time scale of the system, s;

t_r = residence time of a pellet in the bed surface sublayer, s;

u = substitute of local concentration in the aggregates in the

numerical method, mol/cm^2;

V = volume of the solution, cm^3;

V_m = molar volume of the sorbate, cm^3;

V_s = volume of the solid phase, cm^3;

v_s = particle settling velosity, cm/s;

w = sediment vertical velosity, cm/s;

w_r = sediment reworking rate, cm/s;

x = dimensionless radial coordinates in the numerical method;

z = vertical distance in sediment beds, cm;

α = correction factor of the first-order rate constant;

μ = fluid dynamic viscosity;

ρ = solid concentration in the solution, g/cm^3;

ρ_c = colloid concentration in the solution, g/cm^3;

ρ_s = density of solid phase, g/cm^3;

τ = dimensionless time in the numerical method;

Ψ = geometric correction factor.

subscripts

i = size group;

j = grid number;

o = initial concentration;

e = equilibrium concentration at infinite time;

s = solid phase;

superscript

k   = time step.

APPENDIX 2

On The Constancy Of Sediment-Water Partition Coefficients Of

Hydrophobic Organic Pollutants

On the Constancy of Sediment-Water Partition Coefficients of
Hydrophobic Organic Pollutants

by

Philip M. Gschwend* and Shian-chee Wu
Ralph M. Parsons Laboratory
Department of Civil Engineering
Massachusetts Institute of Technology
Cambridge, MA 02139

ABSTRACT

If precautions are taken to eliminate or account for nonsettling (or
nonfilterable) microparticles or organic macromolecules which remain in the
aqueous phase during laboratory sorption tests, the observed partition
coefficients (K_p or K_{oc}) for a group of model hydrophobic organic
compounds (PCBs) are found to remain constant over a wide range of
solids-to-solution ratios. Further, the partition coefficients for either
sorptive uptake or desorptive release are indistinguishable and confirm the
reversible nature of hydrophobic sorption. It is proposed that descriptions
of the "speciation" of hydrophobic compounds in natural waters should
include not only dissolved and sorbed-to-suspended-sediments fractions, but
also a component sorbed to nonsettling microparticles or organic
macromolecules.

* to whom correspondence should be addressed.

INTRODUCTION

One of the fundamental processes controlling the fate of hydrophobic organic compounds in aquatic environments is the exchange of these chemicals between dissolved and sorbed states. Many studies have shown that it is essential to distinguish dissolved from sorbed concentrations to describe either equilibrium conditions or kinetic rates. The tendency of hydrophobic organic compounds to associate with natural particles has been modelled by various workers (1-3) using an equilibrium expression for sorption: S(mass of compound/g solid) = K_p x C(mass of compound/ml solution). Further, the equilibrium constant in this relation generally can be predicted as a product, $K_p = f_{oc} \times K_{oc}$, where f_{oc} is the organic carbon weight percent in the solids of interest, and K_{oc} quantifies the hydrophobic partitioning tendency of the compound of interest to "generic" natural organic matter. K_{oc}'s are typically found to be constant within about a factor of two for sorption of a given hydrophobic compound to a variety of soils and sediments (eg. 2). This simple partitioning model implies that sorption is reversible and that isotherms are linear. Based on our present "physical picture" of this process of sorption (4, 5) as a phase equilibration in which only weak attractive forces (no covalent bonds or ion exchange) between organic solutes and natural organic matter are involved, these qualities (i.e. linearity and reversibility) are expected.

However, two sets of observations have been made which challenge this view of sorption. The first involves the results of several studies showing that the equilibrium partition coefficient (K_p or K_{oc}) decreases as the ratio of solids-to-water increases (eg. ref. 6 and references therein; 7).

The second set of results suggests that sorption is not a reversible process; that is, some organic molecules sorbed to natural particles are not free to be released when the exterior water concentrations decline (8-10). Both of these results conflict with the view described above of hydrophobic organic sorption as a partitioning process between two immiscible "solvents", and both suggest that using the associated linear isotherm approach for predicting the fate of organic pollutants will be inaccurate.

Since it is difficult to envision mechanistic explanations for these complex sorptive phenomena, we initiated this study to determine if they resulted from artifacts associated with the common phase separation techniques employed in batch equilibration sorption experiments. If the phase separations in these experiments were incomplete, noncentrifugable or nonfilterable microparticles or organic macromolecules released from the solids remained in the aqueous phase. Carter and Suffet (11) and Voice et al. (7) have recently suggested the possibility that dissolved organic materials may cause the decline in partition constants with higher suspended solids loading, but they provided no direct evidence to support this assertion. In this report, we demonstrate that these nonsettling organic materials have a major impact on observed partition constants. Our results strongly suggest that this analytical consideration can fully explain the "solids concentration effect" and irreversible sorption phenomena observed in laboratory batch equilibration experiments. Moreover, we suggest that similar concepts must be employed in any discussion of truly dissolved hydrophobic pollutants in the "real world".

METHODS

Materials

Several polychlorinated biphenyl isomers (Analabs Inc., North Haven, Ct.) were used as model nonpolar organic compounds for sorption studies. Isomers, containing two to seven chlorines (2Cl-PCB to 7Cl-PCB) to provide a range of hydrophobic tendencies (log K_{ow} of 5 to 7), were utilized as received. Lake Superior bottom sediment solids, obtained from Dr. Steven Eisenreich (box core S78-11 Bx, ref. 12), had a 2.5% organic carbon content and were generally clayey in nature. The Missouri River sediments were supplied by Dr. Samuel Karickhoff (EPA-6, ref. 2), exhibited an f_{oc} of 0.72% and were of a silty-clay composition. Milli-Q water (Millipore, Bedford, MA.) was used for aqueous preparations.

General Batch Equilibration Protocol

Several microliters of our stock PCB solution (@ 2 to 90 ng individual PCB isomers per μl acetone) were spiked into 40 ml of water in 45 ml glass graduated centrifuge tubes with teflon-lined screw caps. A pre-weighed portion of solids was then added to each tube to yield various, but known, solids-to-water ratios (ρ_s). The tightly capped tubes were then agitated with a wrist-action shaker for 48 hours to allow sorption equilibration. Subsequently, the tubes were centrifuged at either 760g for 20 minutes or 1700g for 60 minutes (corresponding to complete settling of particles having density 1.2 g/cm^3 and 1.0 μm or 0.4 μm diameter respectively, based on Stokes settling velocities) to separate the solid and aqueous phases. If desorption experiments followed, the supernatant was carefully withdrawn, replaced with clean water, agitated again, and finally re-centrifuged.

After centrifugation, the supernatant was transferred with a pasteur pipette to a clean centrifuge tube; the pellet was resuspended in a minimum of Milli-Q water and transferred by pipette to a second centrifuge tube. The original cap and tube used for equilibration, the tube containing the water, and the tube with the sediments were each spiked with an internal standard (4-Cl PCB) and then were individually extracted overnight by shaking with 2 ml 1:1 pentane-acetonitrile. The organic phase was collected from each sample, and the three fractions were each shaken briefly 2 additional times with 1 ml pentane which was combined with the appropriate first extracts. The resultant organic extracts were spiked with a second internal standard (6-Cl PCB) and reduced to approximately 0.2 ml by evaporating under a N_2 gas stream.

The PCB contents of these extracts were ultimately determined by glass capillary gas chromatography with electron capture detection. This GC approach allows quantitation of several isomers simultaneously and provides direct evidence that biodegradation of sorbates had not occurred even over prolonged equilibrations. The instrument was a Carlo Erba Fractovap model 2100 equipped with a Ni-63 electron capture detector. The 15 m long by 0.32 mm i.d. fused silica capillary column coated with SE-54 (Analabs, Inc., North Haven, Ct.) was operated with H_2 carrier at 0.5 m/sec linear velocity and was held isothermally at 70°C for 2 minutes, and then programmed from 70° to 250°C at 6°C/minute; splitless injections were made. The detector was operated at 300°C with 5% CH_4 – Ar in the constant current mode with 0.5 μsec pulse intervals, a differential electrode potential of 50V, and a standing current of about 250 nA.

PCB peak heights were used for quantitation and results were not corrected for losses as both standards were consistently recovered with

about 95% efficiency. Some losses of 2-Cl and 3-Cl compounds were commonly observed (80% and 85% average recoveries, respectively, while more highly chlorinated PCB's were always recovered at >90%) and these were traced to losses during evaporation under N_2. Losses of PCB's to the glass walls of the equilibration tubes plus teflon liners of the screw caps proved to be less than 4% of the dissolved PCB load in all cases. Analytical reproducibility for concentration determinations in each phase from replicate equilibration experiments was +10%, which indicates a precision on our K_p determinations of better than +15% due to propagation of errors. Since f_{oc} could be measured to within ±5%, calculated K_{oc} errors were ±15%.

In some cases, the sediments used for equilibrations were "prewashed" to remove nonsettling microparticles and macromolecules. This washing was done by suspending the sediments in 40 ml water in the 45 ml graduated centrifuge tubes, shaking for 48 hours, centrifuging at 760g for 20 minutes, and discarding the supernatant. After several (≈5) washes, the solids were used in the batch experiments.

In order to assess the impact of prewashing sediments, the quantities of solids lost with the discarded supernatants were determined in three ways. Small aliquots of the supernatant were carefully evaporated on small preweighed aluminum pans and the dry weight was determined with a Cahn micro-balance. Additionally, turbidity of the supernatant was monitored by measuring the absorbance of the solution in a 10 cm cell at 500 nm in a spectrophotometer. Finally, dissolved organic carbon (DOC) measurements were made on the supernatants by persulfate wet oxidation of acidified CO_2-free aliquots (13) and subsequent CO_2 determination with a Shimadzu

GC 8A (Columbia, Maryland) equipped with a thermal conductivity detector. The organic carbon content of the non-centrifugable microparticles and macromolecules is the ratio of the "DOC" to the dry weights.

RESULTS AND DISCUSSION

Nonsettling Microparticles or Macromolecules in the Supernatant

All three measures of "dissolved" sorbing phase (weight of "dissolved" solids, turbidity, and "dissolved" organic carbon) demonstrated the increased loading of nonsettling microparticles or macromolecules (NSPs) in the supernatants of batch equilibrium experiments as the solids-to-water (ρ_s) ratio increased (Figure 1). The NSPs were seen to increase in a fixed proportion to the total solids. For the Missouri River sediment this fraction (wt. NSP/wt. solids) was 5.6%, while the Lake Superior solids maintained a 4.9% NSP fraction under the conditions of our phase separations. At suspended solids concentrations less than 500 mg/l, we were unable to measure NSPs by dissolved organic carbon methods due to blank problems. Voice et al. (7) also attempted to assess NSPs by turbidity and DOC measurements of supernatants recovered from equilibrations with 10-200 mg solids/l and had poor success, concluding that the methods were insufficient. Nonetheless it is clear from our data that NSPs vary regularly with suspended solids concentration.

That this occurs should not be particularly surprising. First, particle size distributions of natural sediments and soils are undoubtably continuous and do not drop to zero abundance in the region of typical centrifugation or filtration separation capabilities. Additionally, there is some evidence to indicate that the DOC and POC (particulate organic

180
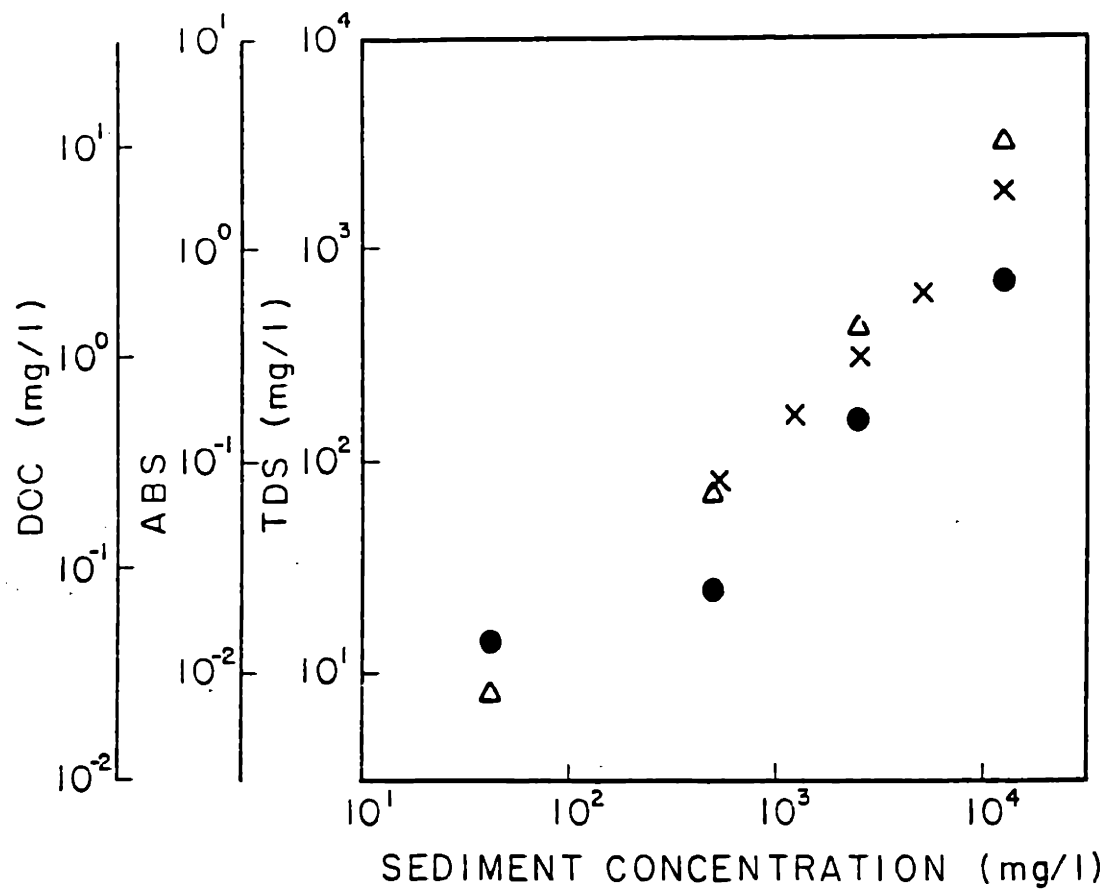
Figure 1. Nonsettling particles in the first wash supernatants
versus varying Missouri River solids concentrations
as determined by DOC (crosses), light absorption
(triangles), and total dissolved solids (solid circles).

carbon) in natural waters are in dynamic equilibrium causing new particles or new "dissolved" molecules to be formed when others are removed (14, 15). Finally, experiments with soil columns have shown that natural soils can release large quantities of DOC into percolating fluids (16). Consequently, since there are NSPs remaining in the aqueous phase, we should take their effects into account.

One approach to diminish the NSPs effect is to try to reduce their abundance, for example by washing the sediments. Figure 2 shows the decrease in NSP content of supernatants after successive washes of 12,000 mg/l Lake Superior sediment. The NSP content dropped by about an order of magnitude, yet remained at an amazingly high level of 100 mg/l even after five washes. As a result, if K_p for readily settled particles is desired, we recommend the strategy of centrifuging washes relatively weakly (eg. 760g for 20 min.) and discarding the supernatant containing microparticles and macromolecules which may be incompletely settled during subsequent phase separation operations (eg. 1700g for 60 min.).

Using the quotient of the observed DOC and NSP weight results, we calculated the f_{oc} values for the NSPs in our experiments. Lake Superior NSPs contained 2.5% organic carbon and Missouri River NSPs had 0.83% organic carbon. Both results are indistinguishable from the f_{oc} values of the parent solids, and as a result we did not find that washing significantly affected the sediment f_{oc}. Thus at least for these laboratory-derived microparticles and macromolecules, it may be reasonable to assign to them a similar affinity for hydrophobic compounds as that exhibited by the larger mass of solids (i.e. $K_{NSP} = K_p$ or $K_{oc-NSP} = K_{oc}$). This assumption is reasonable if the organic matter of the NSPs is of similar composition as
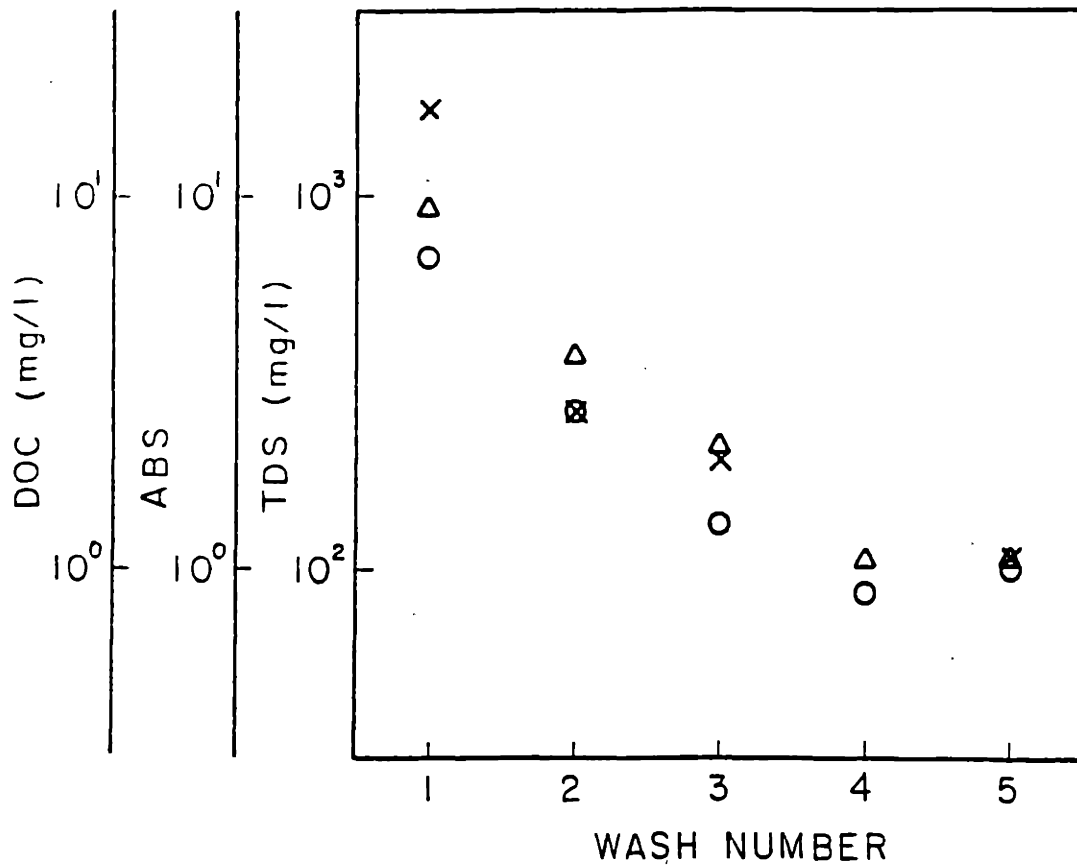
Figure 2. Nonsettling particles in successive washes of Lake
Superior sediment (12,000 mg/l) as determined by DOC
(crosses), light absorption (triangles), and total
dissolved solids (circles).

that in the settling solids and if sorption is truly a partitioning process.

Other recent studies have provided mixed insights to this last assumption. Means and Wijayaratne (17) found that atrazine and linuron sorbed 10-35x more strongly on natural colloids than on soils and sediments, suggesting that small particles or macromolecules should be treated with enhanced K_{oc}'s. If sorption entails an adsorption process to the "surface" exposed by organic macromolecules, then K_{oc}'s associated with colloids could reasonably be expected to be greater than those for soil and sediment organic matter since colloidal organic matter has a greater surface area per mass of organic carbon. However, it is known that nitrogen-containing organic compounds may "sorb" by ion exchange (18, 19) or by condensation reactions (18, 20 - 22) in addition to hydrophobic interactions. Since the sorption constants observed for atrazine and linuron varied with pH (17), these nonhydrophobic sorption mechanisms were likely operating. Thus these enhanced K_{oc}'s may simply reflect the greater reactive nature of colloidal organic matter than that in sediments and soils. In contrast, Carter and Suffet (11) have focussed on DDT (nonionizable and unable to participate in condensation reactions) sorption to natural humic acids and found carbon normalized partition constants (log K_{oc} = 4.8 to 5.7) which were similar to values previously reported for soils (log K_{oc} = 5.3; ref. 23). Finally, at least for some components of the DOC, one could reasonably expect the phase equilibrium partition coefficients to be less than those of the organic matter on particles since macromolecules in solution must be relatively hydrophilic in nature to maintain favorable aqueous interactions. This view is supported by the reports describing heteroatom compositional differences between fulvic and

humic acids recovered from natural waters. The smaller, more water soluble
fulvic acids have higher oxygen-to-carbon ratios compared to the larger
humic compounds (24). Presumably the sequence of "defunctionalization"
continues into condensed phases (25). Thus smaller, more water soluble
macromolecules may be expected to be more polar sorbents (ie. exhibit
relatively lower K_{oc}'s) than related larger macromolecules and particulate
organic matter. Clearly more work is needed to understand these
possibilities.

Effect of Suspended Solids on Observed Partition Coefficients

The observed sorption partition coefficients (determined with no
precautions against NSP effects) were found to diminish with suspended
solids loadings as reported previously by many workers (Figure 3). This
effect was strongest for the sediment with the greatest organic carbon
content (i.e. Lake Superior) and for hydrophobic compounds with the
strongest tendencies to sorb (i.e. 7-Cl > 5-Cl). This result is precisely
as predicted if the observed ratio is viewed:

$$K_P^{obs} = \frac{P/\text{mass particles}}{(D + N)/\text{volume water}} \qquad (1)$$

where P is the mass of compound sorbed to settleable particles, D is the
mass of compound dissolved, and N is the mass of compound sorbed to NSPs.
At sufficiently low suspended solids loadings, the volume of water to weight
of NSPs is great enough that the D >> N; under these conditions the
K_P^{obs} could be considered the "true" value for the compound of
interest. This is the value which should be used to quantify sorption to
settling particles irrespective of the suspended solids concentration.
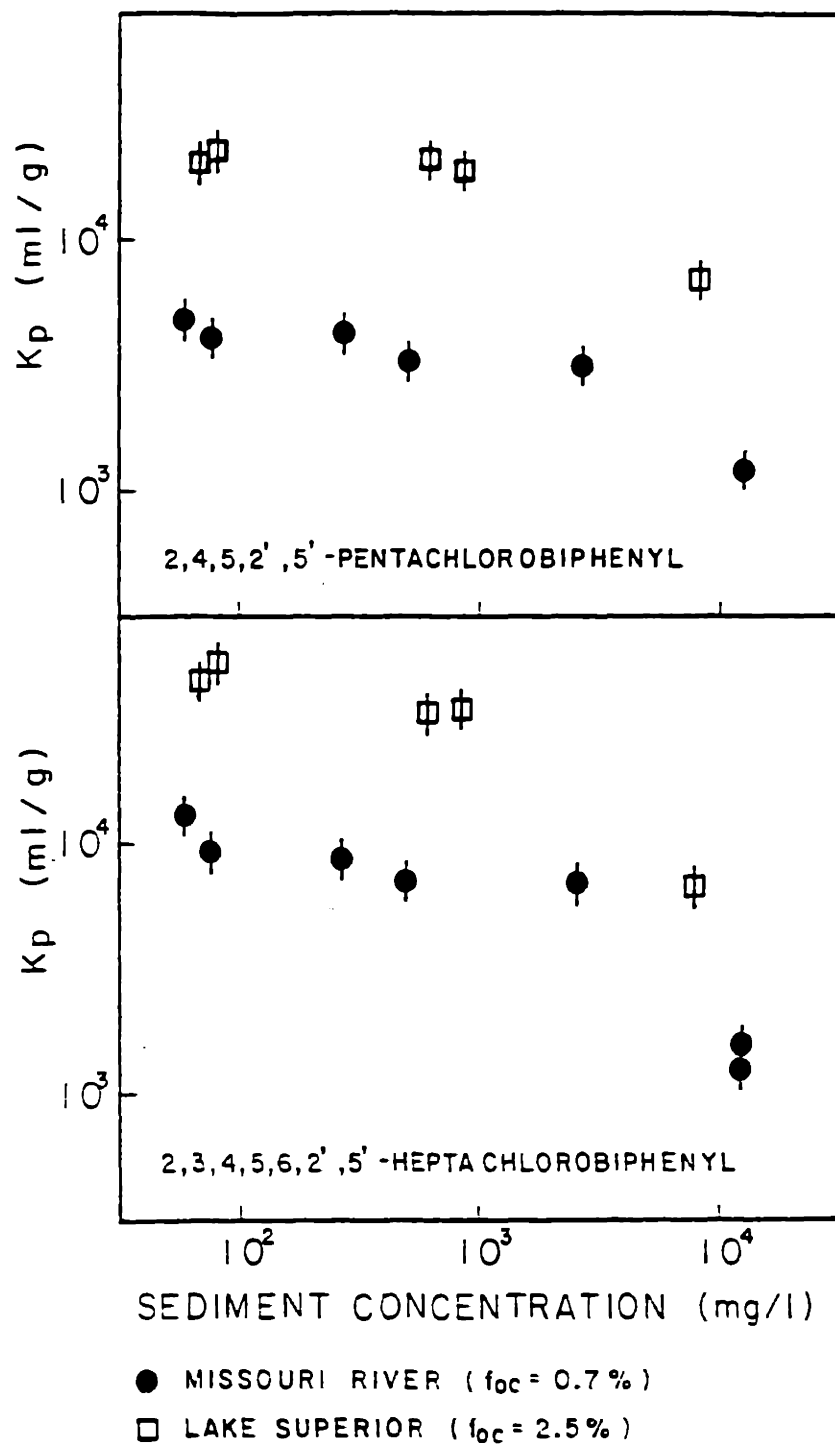
Figure 3. K_p for two PCB isomers versus initial sediment concentration when no precautions are taken for NSPs. Missouri River (solid circles) and Lake Superior (squares).

However, as the suspended solids loadings are increased and the NSPs increase concommitantly and/or as the hydrophobicity of the compounds of interest increase, then D will no longer greatly exceed N and the K_p^{obs} will decline accordingly. This observed partitioning constant has no real phase equilibration meaning.

Utilizing the simple approach of centrifuging with greater settling forces for longer periods to reduce the abundance of NSPs, it can be readily seen that the K_p^{obs} remains unchanged at low ρ_s and increases somewhat in equilibrations with high ρ_s especially with the more hydrophobic 7-Cl PCB (Figure 4). Nonetheless, as indicated by these results and those of other workers (7), more stringent centrifugal conditions still do not eliminate NSPs completely, and the observed partition constants are inaccurate.

In order to greatly reduce the effect of the NSPs, a succession of prewashing treatments is necessary. This was particularly true for Lake Superior and Missouri River solids since they contained a significant proportion of fine clay grains, and the vigorous mixing provided by our wrist-action shaker undoubtedly continuously released these particles from larger aggregates. When prewashed sediments were used for batch equilibration experiments, the observed K_p remained virtually constant over the range of suspended solids tested (Figure 5). This is most dramatically shown for the partitioning of the most hydrophobic compound, 7-Cl PCB, and the difference in K_p^{obs} with and without prewashing clearly reflects the great sensitivity of very strongly sorbed compounds to small NSP loadings in the aqueous phase.

Utilizing the measured NSP loadings in batch equilibrations with no prewashings, we can predict the K_p^{obs} (or K_{oc}^{obs}) versus ρ_s.
By definition:
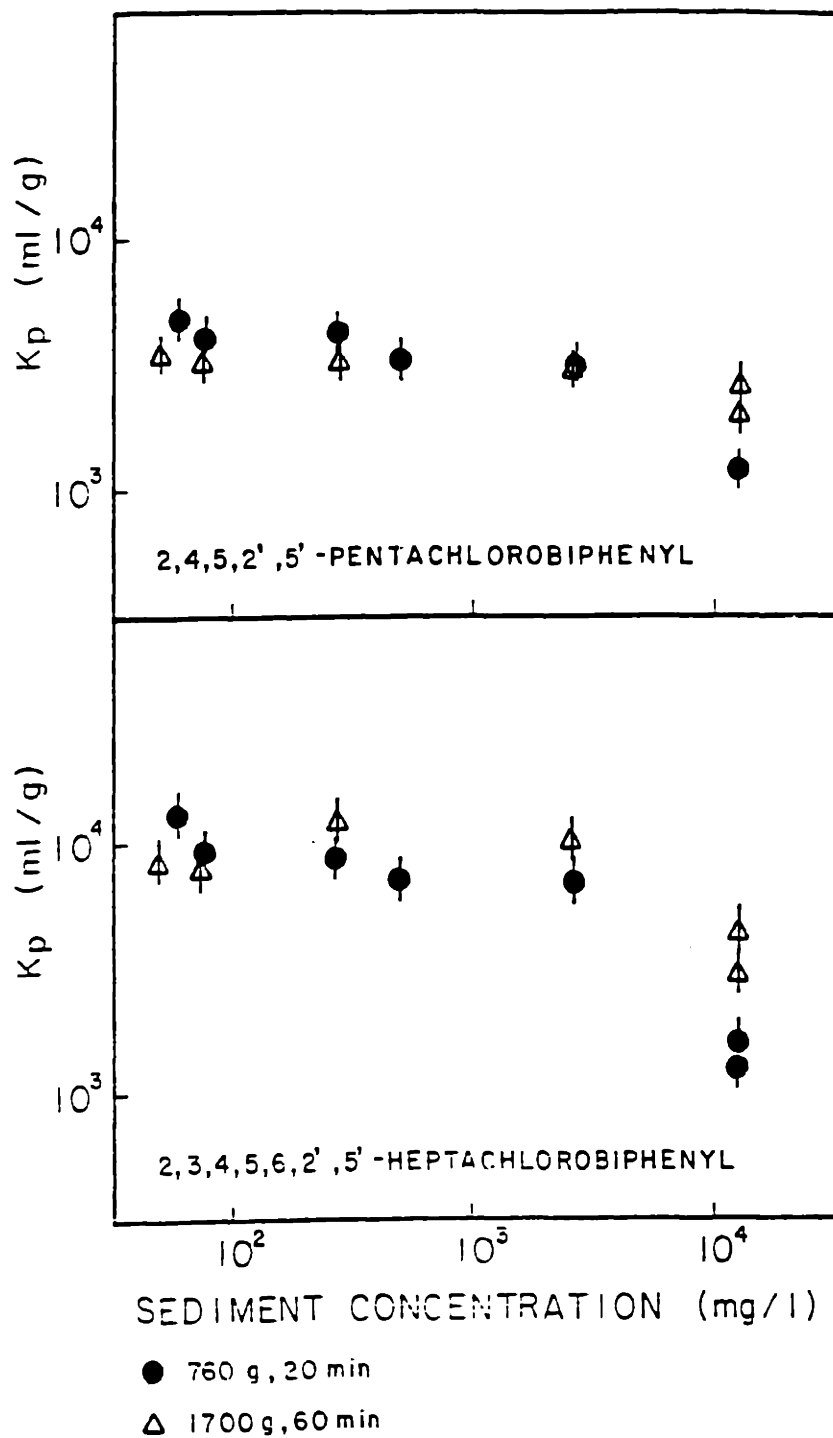
Figure 4. K_p for two PCB isomers versus initial sediment (Missouri River) concentration when different centrifugation conditions are used. 760g for 20 min. (solid circles) and 1700g for 60 min. (triangles)
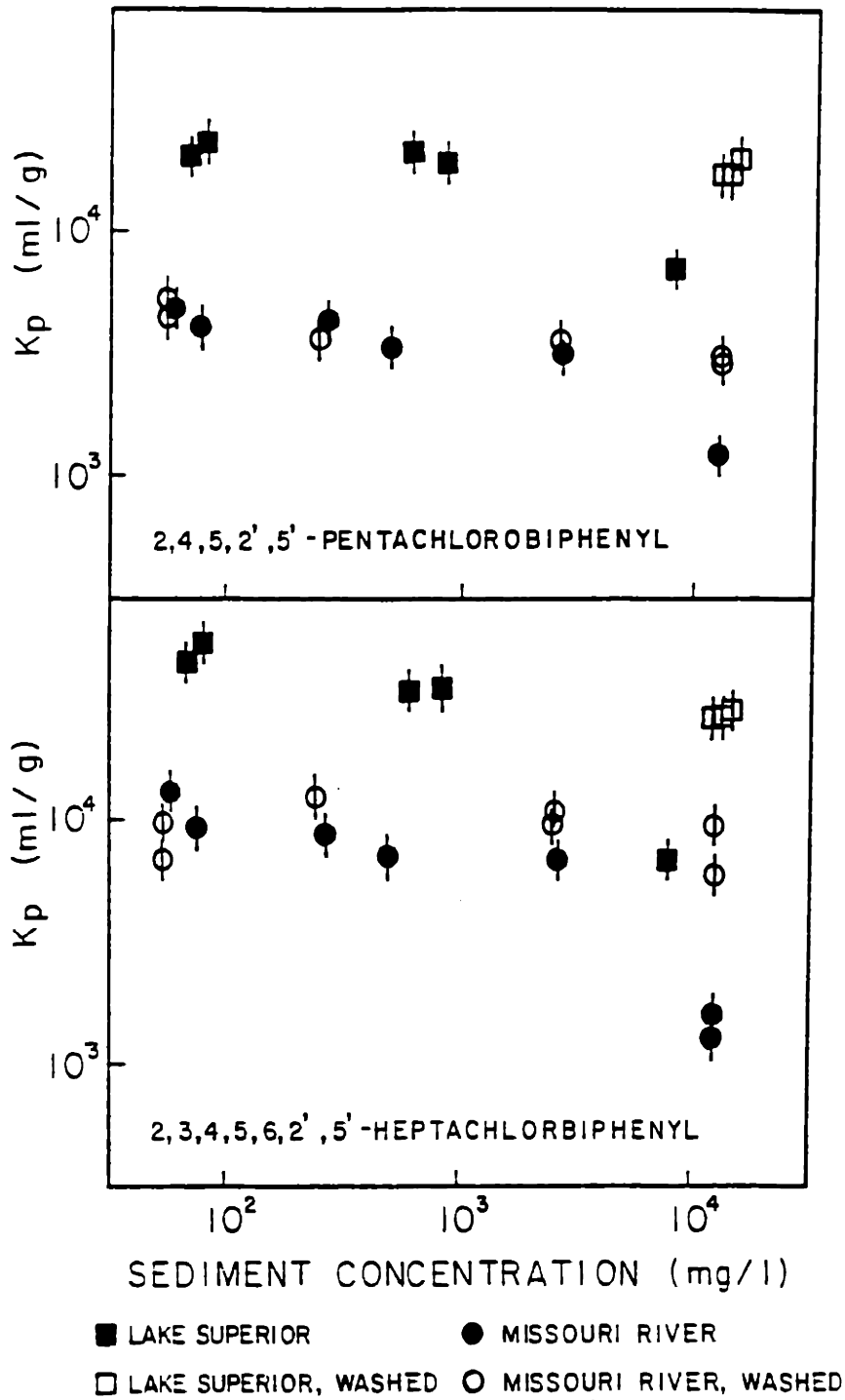
Figure 5. K_p for two PCB isomers versus initial sediment concentration with (open symbols) and without (closed symbols) prewashing to remove NSPs. Missouri River (circles) and Lake Superior (squares)

$$K_p^{true} = \frac{P/\text{Mass Settleable Particles}}{D/\text{Vol. Water}} \qquad (2)$$

By incorporating the hypothesis that some sorption to NSPs occurs in the supernatant (as suggested by this work and previous studies, 7, 11), we have:

$$K_p^{obs} = \frac{P/\text{Mass Settleable Particles}}{D + N/\text{Vol. Water}} \qquad (3)$$

Combining (2) and (3):

$$K_p^{obs} = K_p^{true} \left(1 + \frac{N}{D}\right)^{-1} \qquad (4)$$

Now defining

$$K_{NSP}^{true} = \frac{N/\text{Mass NSPs}}{D/\text{Vol. Water}} \qquad (5)$$

then

$$K_p^{obs} = K_p^{true}\left(1 + K_{NSP}^{true} \cdot \frac{\text{Mass NSPs}}{\text{Vol.Water}}\right)^{-1} \qquad (6)$$

Recalling $K_p = f_{oc} \cdot K_{oc}$ (and correspondingly $K_{NSP} = f_{oc-NSP} \cdot K_{oc-NSP}$), then we may write:

$$K_{oc-p}^{obs} = K_{oc-p}^{true}\left(1 + K_{oc-NSP}^{true} \cdot \frac{f_{oc-NSP} \cdot \text{Mass NSPs}}{\text{Vol. Water}}\right)^{-1} \qquad (7)$$

Finally, since the f_{oc-NSP} was determined in our experiments by utilizing DOC measurements, then

$$DOC = \frac{f_{oc-NSP} \cdot \text{Mass NSP}}{\text{Vol. Water}}, \qquad (8)$$

and

$$K_{oc-p}^{obs} = K_{oc-p}^{true}\left(1 + K_{oc-NSP}^{true} \cdot DOC\right)^{-1} \qquad (9)$$

Expressions (6) and (9) allow us to predict the observed change in partition coefficients due to varying suspended solids concentrations, if the values of K_{NSP} or K_{oc-NSP} can be estimated. For example, using our measured fixed proportions of NSP mass to suspended solids (for Lake Superior 4.9% and for Missouri River, 5.6%), recalling that the organic carbon contents of the settleable and nonsettleable particles were identical, allowing K_p^{true} to be just high enough to fit the data at the lowest solids loads, and assuming $K_p^{true} = K_{NSP}^{true}$, we have predicted the observed K_p for the batch equilibrations with untreated suspended solids (Figure 6). The fit for the Missouri River solids for the entire range of hydrophobic compounds tested is excellent. Although the model shows the correct trend for experiments using Lake Superior solids, it overpredicts the decline in K_p^{obs} by about a factor of two at the highest ρ_s. This may indicate that the K_{oc-NSP} is lower than the K_{oc-p} for these solids from Lake Superior. Despite this minor misfit, we conclude that the NSPs were the primary cause of declining observed K_p's, and therefore that K_{oc} remains constant irrespective of the proportion of solids-to-solution. Interestingly, this result predicts that at high NSP masses the K_p's for all the PCBs collapse to the same values which are simply the Vol. of water/ Mass NSPs.

Effect of Suspended Solids on Observed Sorption Reversibility

It has been suggested (8) that hydrophobic organic compound sorption to natural sediment particles may be irreversible to some degree. Unless either some unusual chemical bond between these nonreactive compounds (eg. PCB's or PAH) and natural organic matter or mineral surfaces is forming or some deformation of the natural organic matter around the sorbates to form a

191
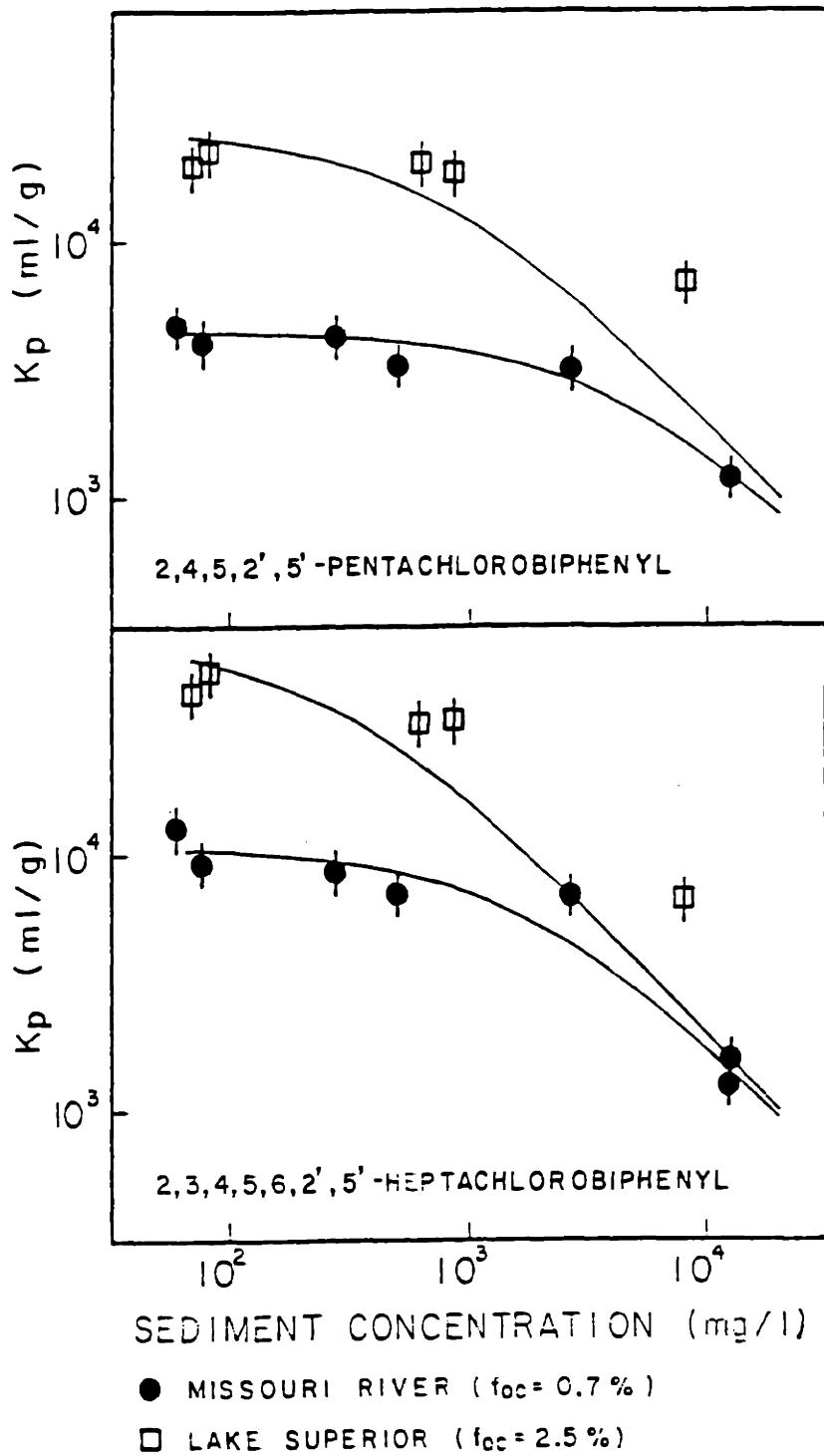
Figure 6. Model predictions of K_p versus initial sediment concentrations assuming wt. NSPs/wt. solids is 5% and $K_{NSP} = K_p$.

"cage-like" structure is occurring, we do not understand how such an apparently irreversible uptake could take place (especially on the timescale of hours to days). Consequently, we hypothesized that irreversible sorption behavior could also be due to washing out the NSPs during sequential sorption and desorption experiments.

In typical desorption protocols, a sorptive batch equilibration is performed by first establishing a sorption equilibrium between the solid and aqueous phases. In preparing to establish desorption equilibrium, the initial aqueous layer is discarded and with it the first wash load of NSPs, and clean water is added to take its place. After shaking and allowing hydrophobic compounds in the solids to exchange back into the aqueous phase, the solids and aqueous phases are separated again and concentrations determined in each. However, unlike the initial sorptive uptake experiment, the NSPs in this inadvertently prewashed condition are reduced in quantity and the resultant aqueous load contains proportionately less NSP-sorbed material. Hence the <u>observed</u> K_{oc}desorption is greater than the previous K_{oc}sorption. Further successive desorption tests will continue to be effected by NSPs less and less.

When we performed sorption and desorption experiments with prewashed sediments, our uptake and release isotherms were indistinguishable (Figure 7). This result was more easily obtained with less hydrophobic compounds, with solids containing lower organic contents, and with lower initial solids-to-water ratios as in these cases the resulting NSP-sorbed contents in equilibrations were more readily diminished relative to the dissolved concentrations.

Given our data on the NSP abundance in successive wash solutions of Lake Superior and Missouri River solids (NSPs sequentially declined to the
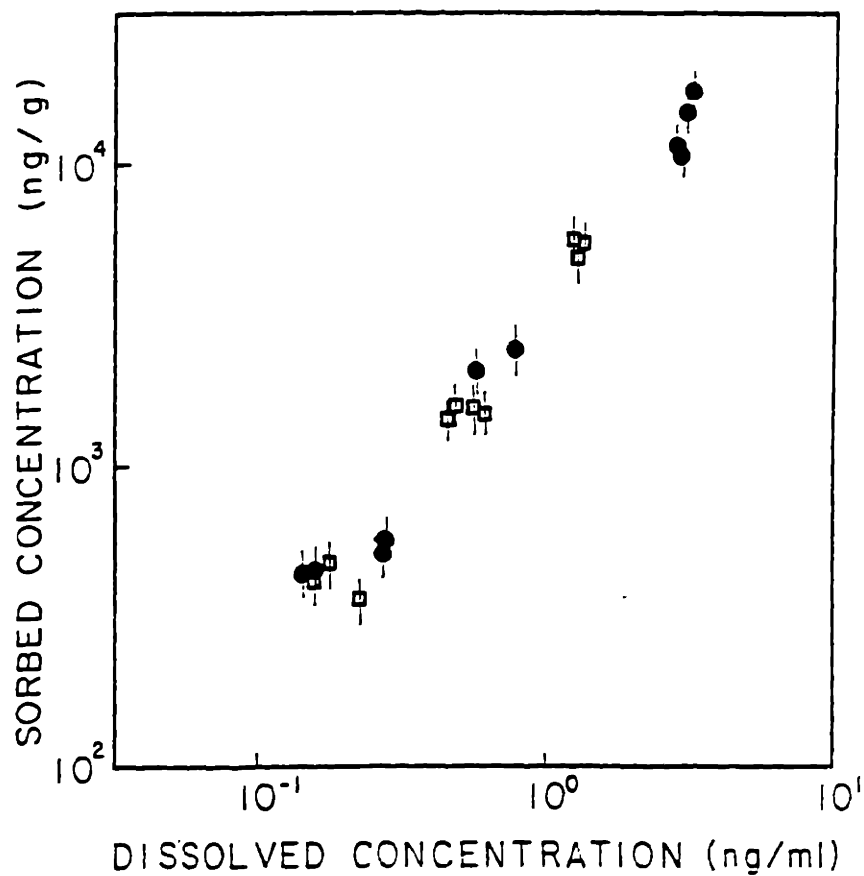
Figure 7. Dissolved versus sorbed concentrations for penta-
chlorobiphenyl in sorption (solid circles) and desorption
(squares) tests using prewashed Lake Superior solids.

following percentages of the solids: 5%, 2%, 1%, ≈ 0.6% each wash thereafter), we can estimate the impact of these nonsettling sorbents in a typical succession of sorption-then-desorption equilibrations with ρ_S = 1000 mg/L. For example, DiToro and Horzempa (8) have studied the desorptive behavior of a hexachlorobiphenyl from Saginaw Bay sediments (f_{oc} ≈ 2.3%). Using equation 7, their observed K_p, and assuming an NSP loading of 5% in the first equilibration, we can calculate a "true" K_p = 2.0 x 10^4 ml/g. By combining this result and our observed decline in NSPs with successive washes, and by maintaining a mass balance for the hexachlorobiphenyl (ie. system load of equilibration $\underline{n}$ equals system load of equilibration $\underline{n-1}$ minus the amount discarded with the aqueous phase), we can predict the desorptive isotherm points shown in Figure 8. These results are remarkably similar to those observed experimentally by DiToro and Horzempa, as well as in other studies (9, 10) particularly when large solids-to-solution ratios were used. The isotherm predicted by using the first desorption equilibration data indicates a higher K_{oc}desorption than K_{oc}sorption. These results would lead to the erroneous conclusions that irreversible binding was occurring and that there was a hysteretic effect in the extent of irreversibly bound material as a function of the initial dissolved concentrations to which the solids were exposed. Notably, previous studies showed successive desorption data eventually to trend toward the origin. We believe these data asymptotically coincided with the "true" isotherms as shown in Figure 8 for our model calculations using a relatively low ρ_S (and hence low NSPs concentration). Clearly the effects of nonsettling microparticles and macromolecules can account for these apparent nonideal sorption observations.
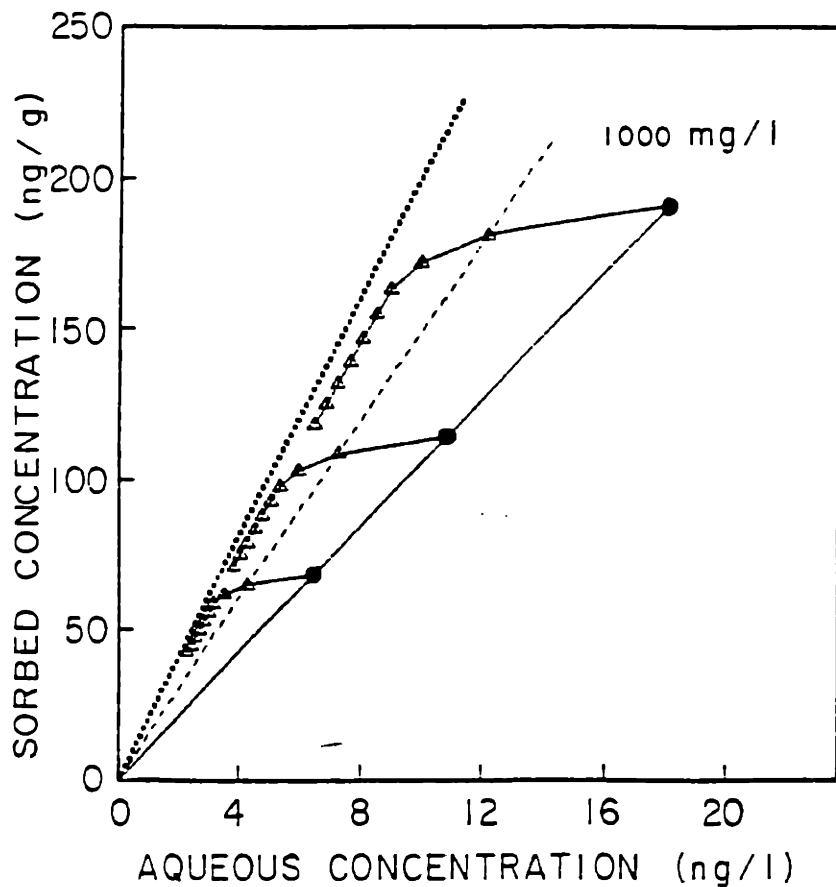
Figure 8. Model predictions for successive desorption
equilibrations (triangles) after initial uptake
experiments using 1000 mg solids per liter of solution
(solid circles). Solid line through uptake data
indicates observed uptake isotherm, while dashed line
through first desorption points demonstrates associated
desorption isotherm. Dotted line reflects uptake
isotherm when NSPs have been eliminated or are
negligible.

Implications

It is clear that precautions must be taken to avoid laboratory artifacts derived from incomplete phase separations. These precautions may consist of either elimination of the nonsettling (or nonfilterable) sorbents by prewashing the solids or by actually measuring the abundance of the NSPs in the otherwise presumed "purely" aqueous phase. Simply centrifuging at greater forces will be helpful, but will not necessarily remove all the sorbents from suspension (especially neutrally bouyant organic macromolecules.)

More importantly, our results support the idea that modelling sorption in the "real world" must include binding to two types of materials, one with and one without appreciable settling velocities. This second sorbing material includes poorly characterized mixture of micro"particles" and "dissolved" macromolecules. This view of three exchanging environmental compartments is necessary not only to predict the actual transport properties of hydrophobic pollutants (i.e. their tendency to be removed from solution by settling to bottom sediments), but also to assess their water column chemical activities. It is likely that, nonpolar compounds sorbed to nonsettling particles (be they humic or fulvic acids, colloidal aggregates, or other neutrally buoyant phases) behave much differently in various environmental processes such as bioconcentration and photo- or bio-degradation than do the truly dissolved molecules. Since much of the DOC in natural waters is polymeric humic substances, measurements of DOC may allow us to roughly quantify nonsettling organic sorbents. Using this information in addition to knowledge of the suspended sediment load, we may more accurately estimate the hydropohobic compound partitioning between the three water column compartments. That is, we may evaluate the "speciation"

of hydrophobic organic compounds with the following:

the dissolved fraction $=$
$$\frac{(1)}{(1 + DOC \cdot K_{oc-NSP} + POC \cdot K_{oc-p})} \quad ,$$

the NSP-sorbed fraction $=$
$$\frac{(DOC \cdot K_{oc-NSP})}{(1 + DOC \cdot K_{oc-NSP} + POC \cdot K_{oc-p})} \quad ,$$

the fraction sorbed to settling particles $=$
$$\frac{(POC \cdot K_{oc-p})}{(1 + DOC \cdot K_{oc-NSP} + POC \cdot K_{oc-p})} \quad .$$

SUMMARY

Our results support the view of Chiou and others that sorption of hydrophobic organic compounds to natural sediments and soils can be viewed as a phase partitioning process, quantifiable with a single K_{oc} equilibrium constant. This constant is the same for uptake or desorption, and does not vary as the "volumes" of the solids and aqueous phases change with respect to one another. Previous experiments suggesting "complex" sorptive behaviors were probably subject to analytical artifacts caused by incomplete phase separations. Our work, taken in the context of recent studies showing sorption to natural microparticles or organic macromolecules, suggests that equilibrium environmental speciation of hydrophobic organic compounds should include three "phases": dissolved, sorbed to nonsettling particles or macromolecules, and sorbed to settling solids. With further work on partition constants appropriate for natural non-settling particles or macromolecules, this three phase equilibration process, possibly using site-specific DOC and POC type-measurements, can be used to greatly improve our predictive capabilities concerning the fate of hydrophobic organic pollutants.

ACKNOWLEDGMENTS

Literature Cited

1. Karickhoff, S.W.; Brown, D.S.; Scott, T.A. Water Res. 1979, 13, 241-248.

2. Means, J.C.; Wood, S.G.; Hassett, J.J.; Banwart, W.L. Environ. Sci. Technol. 1980, 14, 1524-1528.

3. Schwarzenbach, R.P.; Westall, J. Environ. Sci. Technol. 1981, 15, 1360-1367.

4. Chiou, C.T.; Peters, L.J.; Freed, V.H. Science (Washington, D.C.) 1979, 206, 831-832.

5. Chiou, C.T.; Porter, P.E.; Schmedding, D.W. Environ. Sci. Technol. 1983, 17, 227-231.

6. O'Connor, D.J.; Connolly, J.P. Water Res. 1980, 14, 1517-1523.

7. Voice, T.C.; Rice, C.P.; Weber, Jr., W.J., Environ. Sci. Technol. 1983, 17, 513-518.

8. DiToro, D.M.; Horzempa, L.M. Environ. Sci. Technol. 1982, 16, 594-602.

9. Swanson, R.A.; Dutt, G.R. Soil Science Soc. Amer., Proc. 1973, 37, 872-876.

10. Peck, D.E.; Corwin, D.L.; Farmer, W.J. J. Environ. Qual. 1980, 9, 101-106.

11. Carter, C.W.; Suffet, I.H. Environ. Sci. Technol. 1982, 16, 735-740.

12. Johnson, T.C.; Evans, J.E.; Eisenreich, S.J. Limnol. Oceanogr. 1982, 27, 481-491.

13. Menzel, D.W.; Vacarro, R.F. Limnol. Oceanogr. 1964, 9, 138-142.

14. Riley, G.A. Adv. Mar. Biol. 1970, 8, 1-118.

15. Sheldon, R.W.; Sutcliff, W.H.; Prakash, A. Limnol. Oceanogr. 1973, 18, 719-733.

16. Leenheer, J.A.; Stuber, H.A. Environ. Sci. Technol. 1981, 15, 1467-1475.

17. Means, J.C.; Wijayarantne, R. Science (Washington, D.C.) 1982, 215, 968-970.

18. Stevenson, F.J. In "Bound and Conjugated Pesticide Residues", Kaufman, D.D., Still, G.G.; Paulson, G.D.; Bandal, S.K., Eds.; ACS Symposium Series 29: Washington, D.C., 1976; pp 180-207.

19. Karickhoff, S.W., _J. Hydr. Eng._, _A.S.C.E._ 1984 _110_, 707-735.

20. Hsu, T.; Bartha, R. _Soil Sci._ 1974, _116_, 444-452.

21. Hsu, T.; Bartha, R. _J. Agric. Food Chem._ 1976, _24_, 118-122.

22. Appleton, H.T.; Banerjee, S.; Sikka, H.C. In "Dynamics, Exposure, and Hazard Assessment of Toxic Chemicals", Haque, R., Ed.; Ann Arbor Science: Ann Arbor, MI, pp 251-272, 1980.

23. Kenaga, E.E.; Goring, C.A.I. In "Aquatic Toxicology", Eaton, J.G.; Parrish, P.R.; Hendricks, A.C., Eds.; American Society for Testing and Materials: Philadelphia, PA, 1980.

24. Thurman, E.M.; Malcolm, R.L. _Environ. Sci. Technol._ 1981, _15_, 463-466.

25. Stuermer, D.H.; K.E. Peters; Kaplan, I.R. _Geochim. Cosmochim. Acta_ 1978, _42_, 989-997.

Appendix 3 Energy Input by Stirring and Bubbling

During the sorption kinetic experiments with suspended solids, the rate of energy input by mixing or bubbling affects the rate of sorption in two ways. First, vigorous stirring or bubbling creates very small eddies which are comparable to aggregate sizes so that sediment particles will be broken into smaller particles by shearing. Consequently, the size distribution of aggregates will shift to smaller sizes increasing the exposed surface area, decreasing the diffusive pathlength inside, and altimately causing a higher sorption rate. Second, there are stagnant boundary layers of water surrouding suspended particles. The extra time that a sorbate molecule is required to diffuse across this layer by molecular diffusion depends on the thickness of the layer (i.e., the smallest eddy size) which is a function of energy input too.

In this appendix, we will use the smallest eddy size as a criteria to evaluate the effects of mixing by magnetic stirring bar and bubbling in our sorption kinetic experiments.

A 3.1 Energy Input by Magnetic Stirrer

Assuming that the magnetic stirring bar acts as a two-peddle mixer, we estimate the power input by using (Metcalf and Eddy Inc. 1972):

$$P = \frac{C_D \, A \, \rho_w \, v^3}{2} \tag{A3.1}$$

in which P = power input (erg/s), C_D = drag coefficient (= 0.9 for Reynold's number greater than 1000, (Daily and Harleman, 1966)), A = area of paddles, ρ_w = density of water, v = relative velocity of paddles in the water (usually 0.7-0.8 of paddle tip speed). With a 2.5-cm long and 1.3-cm wide oval stirrer bar spinning at 300 times per minute, the energy input is:

$$P = \frac{0.91 \cdot (2.5 \text{ cm}^2)(1 \text{ g/cm}^3)(29 \text{ cm/s})^3}{2}$$

$$= 2.9 \times 104 \text{ g.cm}^2 \cdot s^{-1} \quad (= erg \cdot s^{-1}) \tag{A3.2}$$

The energy dissipated per unit mass, ε, in a 2-L reactor is:

$$\varepsilon = P/(V \cdot \rho_w) = 14 \text{ cm}^2 \cdot s^{-3} \tag{A3.3}$$

where V is the total volume. The length scale of the smallest eddies is given by (Dempsey, 1982):

$$\eta = \frac{v^{3/4}}{\varepsilon^{1/4}} \tag{A3.4}$$

where, η = the length scale of the smallest eddies, v = kinematic viscosity of

the water. ν is 10^{-2} cm^{2}s^{-1} at 20°C. Therefore,

$$\eta = \frac{(10^{-2} \text{ cm}^2\text{s}^{-1})^{3/4}}{(14 \text{ cm}^2\text{s}^{-3})^{1/4}}$$

$$= 0.016 \text{ cm}$$

$$= 160 \text{ } \mu\text{m} \tag{A3.5}$$

A 3.2 Energy Input by Bubbling

The energy generated by a bubble can be estimated by (Schöne, 1970, quoted by Dempsy, 1982):

$$P = \frac{\pi C_D \rho_w R^2 v^3}{2} \tag{A3.6}$$

in which, R = radius of the bubble, v = vertical velocity of the bubble. When the drag force and the buoyant force are balanced, i.e.,

$$(\pi C_D \rho_w R^2 v^3)/2 = (\pi g \rho_w R^3) \cdot 4/3 \tag{A3.7}$$

the velocity of the bubble is given by:

$$v^2 = \frac{8 g R}{3 C_D} \tag{A3.8}$$

where, g = acceration due to gravity (980 cm s^{-2}), $C_D \approx 1$ for spherical bubbles.

At an air flow rate of 90 cm^3/s and an approximate bubble radius of 0.4

cm, there are 336 bubbles generated per second. Their velocity is:

$$v^2 = \frac{8 \cdot (980 \text{ cm s}^{-2})(0.4 \text{ cm})}{3 \times 1}$$

$$v = 32.3 \text{ cm/s} \qquad \text{(A3.9)}$$

The distance between the gas diffuser and the water surface is 11 cm which results in a residence time of bubbles in the water of 0.34 seconds. Consequently, there are 114 bubbles in the water at any time.

The energy dissipation rate, ε, for one bubble is:

$$\varepsilon = \frac{P}{v\rho_w} = \frac{\pi \cdot (0.4 \text{ cm})^2 (32.3 \text{ cm s}^{-1})^3}{2000 \text{ cm}^3}$$

$$= 4.23 \text{ cm}^2/\text{s}^3 \qquad \text{(A3.10)}$$

The total energy dissipation is 484 cm^2/s^3. Using Eq. A.3.4 we obtain the length scale of the smallest eddies in the reactor which is:

$$\eta = 0.0067 \text{ cm}$$

$$= 67 \text{ } \mu\text{m} \qquad \text{(A3.11)}$$

A.3.3. Discussion

The time required for a molecule to diffuse through a smallest eddy (i.e., the stagnant boundary layer) can be approximately estimated by

$$\text{time scale} = \frac{\eta^2}{D_m} \qquad\qquad\qquad \text{(A3.12)}$$

which is about 50 seconds with stirring and 7 seconds with bubbling. This boundary layer diffusion would affect the observed results only in the first few seconds because we applied both bubbling and stirring at the beginning of the experiments. Therefore, we ignored the boundary layer effect when we analysed the results.

Bubbling, with an energy input 35 times higher than mixing, creates quite small eddies (about 67 um) which are smaller than the sizes of half of all particles in the suspensions. Consequently, under continuous bubbling and stirring condition, some particles will break due to shearing by eddies and the size distribution will shift to smaller classes (Fig. 2.3). Under stirring conditions, a much smaller fraction of particles will be larger than the smallest eddies. Thus, less particle breaking is expected. Indeed, only a slight shift of size distribution can be seen (Fig. 2.3). The reason might be that the breaking process is slow if the smallest eddies are comparable or only slightly smaller than the particles. Further research is needed to quantitatively describe this particle breaking phenomenon.

```
REM-                          FINITE DIFFERENCE METHOD
REM-  This program  is for simulation of sorption kinetics with more than
REM-   one particle size group using conventional finite difference method.
REM-   Grid sizes are changeable.
REM-
DEFINT n
DEFDBL a-m,o-z
DIM fs(10),rad(10),ngrid(10),u(10,201),g(10)
DIM dx(10),h(10),ut(10,201),gridsize(10),te(20),num(20),co(20)
DIM sl(10),kl(10),slt(10)                                      '***1
REM------------Entering environmental parameters-----------------------------
REM--------------particle size distribution---------------------------------
PRINT "Please enter environmental parameters."
INPUT "Number of particle classes";ng
  FOR n=1 TO ng
PRINT "Enter fraction, particle radius (cm), and gridsize of class #";n
      INPUT fs(n)
      INPUT rad(n)
      INPUT gridsize(n)
  NEXT n
REM----------------boundary conditions-------------------------------------
  INPUT "Initial concentration in solid (mole/g)";so
  INPUT "Simulation starting time (minute)";te(0)
  INPUT "Printing time step size (minute)";TimeStep
  ncycle=0
    boundary:
          ncycle=ncycle+1
          INPUT "Ending time (minute)";te(ncycle)
          INPUT "Concentration in aqueous phase (mole/ml)";co(ncycle)
          INPUT "Do you want to change concentration in aqueous
phase?";changeC$
    IF LEFT$(changeC$,1)="y" GOTO boundary
REM----------------sorbent concentrations and Kp-----------------------------
  INPUT "Sorbent concentration (g/ml)";solid
  GOSUB KpValue
REM----------------value of Deff-----------------------------------
  GOSUB DeffValue
REM----------------setting coefficients for numerical iterations--------
    p=1.5            'p is the particle bulk density (g/cm^3)
   GOSUB GridNumbersAndTmin
   GOSUB SettingIntervals
   ts=te(0)
   FOR n=1 TO ng
       FOR ni=1 TO ngrid(n)
           u(n,ni)=dx(n)*(ni-1)*so*p
       NEXT ni
   NEXT n
REM-------------setting parameters for 1st order model ****1--------------
FOR nl=1 TO ng
   sl(nl)=so
   kl(nl)=(10.56*solid*Kp+22.7)*d/rad(nl)^2    '**no fraction effect included
```

```
·NEXT n1
sss1=so
REM---------------printing input parameters------------------------
     LPRINT "sorption kinetics simulation with finite difference method
(variable grid size,"
     LPRINT " varible boundary conditions and first--order model
(multi-size))."
     LPRINT "The date is ";DATE$
     LPRINT "The time is ";TIME$
     LPRINT "particle class number=";ng
     LPRINT "fraction","radius(cm)","gridsize(cm)"
     FOR n=1 TO ng
         LPRINT fs(n),rad(n),gridsize(n)
     NEXT n
     LPRINT "sorbent conc. (g/cm^3)=";solid
     LPRINT "Kp=";Kp,"Deff=";d/60;"cm^2/s"
     LPRINT "Initial conc. in solid phase(mole/g)=  ";so
     LPRINT"Time of change            Aqueous conc."
     FOR n=1 TO ncycle
         LPRINT te(n),co(n)
     NEXT n
     LPRINT "Time (log(min))";"        C           ";"         S
   "
OPEN "clip:" FOR OUTPUT AS #1
  GOSUB iteration
CLOSE #1
LPRINT "the time is ";TIME$
END
REM-------------------------------------------------------------
REM      .  Subroutine to estimate the value of Kp
REM-------------------------------------------------------------
KpValue:
    PRINT "What is known?"
    INPUT "Kp(=1), Ce(=2), Koc(=3) or Kow(=4)";k%
  ON k% GOTO Kp,Ce,Koc,Kow
  Kp:
    INPUT "Enter Kp (cm^3/g)";Kp:GOTO fine
  Ce:
    INPUT "Enter Co, Ce."; co(1)
    INPUT ce
    Kp=(co(1)+solid*so-ce)/solid/ce:GOTO fine2
  Koc:
    INPUT "Enter Koc(cm^3/g) and foc(g/g)";Koc
    INPUT foc
    Kp=Koc*foc:GOTO fine
  Kow:
    GOSUB KowToKp
  fine:
  ce=(co(1)+solid*so)/(solid*Kp+1!)
  fine2:
RETURN
```

```
REM------------------------------------------------------------
REM              subroutine to estimate Kp from Kow
REM------------------------------------------------------------
KowToKp:
  INPUT "Enter Kow";Kow
  PRINT "Which equation do you want to use ?"
  PRINT
  PRINT "eq.1: log Koc=log Kow - 0.21"
  PRINT "eq.2: log Koc=0.72 log Kow + 0.49"
  INPUT eq%
  ON eq% GOTO eq1,eq2
    eq1:
      Koc=10^(.4343*LOG(Kow)-.21):GOTO done
    eq2:
      Koc=10^(.72*.4343*LOG(Kow)+.49)
   done:
  INPUT"Enter foc";foc
  Kp=Koc*foc
  RETURN
REM------------------------------------------------------------
REM        subroutine to determine Deff from Dm, porosity,and dry density
REM------------------------------------------------------------
DeffValue:
   INPUT"Do you know the value of Deff";knoDeff$
   IF LEFT$(knoDeff$,1)<>"y" THEN GOTO dodeff
    INPUT "Deff (cm^2/s)";DinSecond
    d=DinSecond*60: GOTO enddeff
    dodeff:
    INPUT "Intraparticle porosity";poro
    INPUT "Dry density";ps
    INPUT "Molecular diffusity (cm^2/sec)";Dm
    d=Dm*poro^2/Kp/(1-poro)/ps*60
    enddeff:
  RETURN
REM------------------------------------------------------------
REM                    subroutine to set grid numbers and maximum time step
REM------------------------------------------------------------
GridNumbersAndTmin:
    tmin=TimeStep
    FOR n=1 TO ng
      ngrid(n)=1+(CINT(rad(n)/gridsize(n))\2)*2
      tmint=.5*rad(n)^2/d/(ngrid(n)-1)^2
      IF tmin>tmint THEN tmin=tmint
      dx(n)=1!/(ngrid(n)-1)
      h(n)=fs(n)*solid*dx(n)^2/p
    NEXT n
  RETURN
REM------------------------------------------------------------
REM                    set time step sizes and coefficients
REM------------------------------------------------------------
```

```
SettingIntervals:
   FOR n=1 TO ng
        g(n)=d*tmin/(rad(n)*dx(n))^2
   NEXT n
RETURN
REM------------------------------------------------------------
REM                  iteration and output of simulation
REM------------------------------------------------------------
iteration:
FOR nc=1 TO ncycle
   c=co(nc)
    num(ncycle)=CINT((te(nc)-te(nc-1))/TimeStep)
   FOR nk=1 TO num(ncycle)
     loop:
       aa=0!
       bb=0!
       FOR ni=1 TO ng
           sumj=0!
               FOR nj=2 TO ngrid(ni)-1
                   ut(ni,nj)=u(ni,nj)+g(ni)*(u(ni,nj+1)-2!*u(ni,nj)+u(ni,nj-1))
                   sumj=sumj+(3+(-1)^nj)*(nj-1)*(ut(ni,nj)-u(ni,nj))
               NEXT nj
           aa=aa+h(ni)*(sumj-(ngrid(ni)-1)*u(ni,ngrid(ni)))
           bb=bb+h(ni)*(ngrid(ni)-1)*Kp*p
       NEXT ni
       ct=(c-aa)/(1!+bb)
       ts=ts+tmin
       c=ct
       FOR nl=1 TO ng
           FOR nm=1 TO ngrid(nl)-1
               u(nl,nm)=ut(nl,nm)
           NEXT nm
           u(nl,ngrid(nl))=Kp*p*c
       NEXT nl
       IF ts<te(nc-1)+TimeStep*nk THEN GOTO loop
       ss=0!
       FOR ni=1 TO ng
           sumk=0!
               FOR nj=2 TO ngrid(ni)-1
                   sumk=sumk+(3+(-1)^nj)*(nj-1)*ut(ni,nj)
               NEXT nj
           ss=ss+fs(ni)*dx(ni)^2*(sumk+(ngrid(ni)-1)*u(ni,ngrid(ni)))
       NEXT ni
       ca!=c
       ssp!=ss/Kp/p
       tl!=ts
       WRITE #1,tl!,ca!,ssp!
       PRINT tl!,ca!,ssp!
       LPRINT tl!,ca!,ssp!
   NEXT nk
NEXT nc
```

```
RETURN
END
```

Appendix 5   Numerical Model for Transfer in Sediment Bed

A5.1 Governing Difference Equation

The governing equation to which the numerical model is based is Eq.4.8

$$\frac{\partial S_b}{\partial t} + \frac{\partial w S_b}{\partial z}$$

$$= \frac{\partial}{\partial z} [D_b \frac{\partial S_b}{\partial z} + D_p n_b \frac{\partial (S_b/R_d)}{\partial z} + D_c n_b \frac{\partial (K_c \rho_c S_b/Rd)}{\partial z}] + f(z) S_b \quad (A5.1)$$

in which

$$w = w_r + \text{other advective processes} \quad (A5.2)$$

The sediment bed is divided into layers. The water column is also a complete mixed layer with depth L_w. The total concentration in water, S_w, is defined as

$$S_w = (1+\rho_w K_{pw}+\rho_{cw} K_{cw}) C_w$$

$$= R_{dw} C_w \quad (A5.3)$$

in which ρ_w and ρ_{cw} are the suspended solid and colloid concentrations (or DOC) in water, respectively, and R_{dw} is the fraction factor in water defined by this equation.

Replacing the partial derivatives with difference expresions:

212

$$\frac{\partial S_b}{\partial z} = \frac{S_b(i+1/2) - S_b(i-1/2)}{\Delta z(i)} \qquad (A5.4)$$

$$\frac{\partial^2 S_b}{\partial z^2} = \frac{1}{\Delta z(i)} \left(\frac{S_b(i+1) - S_b(i)}{0.5(\Delta z(i) + \Delta z(i-1))} - \frac{Sb(i) - Sb(i-1)}{0.5(\Delta z(i) + \Delta z(i+1))} \right) \quad (A5.5)$$

$$f(z) = \frac{w(i+1/2) - w(i-1/2)}{\Delta z(i)} \qquad (A5.6)$$

and using Euler's method to integrate in time we obtain the governing equation in difference form:

$$S_b^{k+1}(i) = S_b^k(i) - \frac{\Delta t [w(i+1/2) S_b^k(i) - w(i-1/2) S_b^k(i-1)]}{\Delta z(i)}$$

$$+ \frac{\Delta t}{\Delta z(i)} \left\{ \left[\frac{D_b(i-1/2)}{0.5(\Delta z(i) + \Delta z(i-1))} + \right. \right.$$

$$\left. \frac{n_b(i-1/2) [D_p(i-1/2) + D_c(i-1/2) K_c(i-1) \rho_c(i-1)]}{0.5 R_d(i-1)(\Delta z(i) + \Delta z(i-1))} \right] S_b^k(i-1)$$

$$- \left[\frac{D_b(i-1/2)}{0.5(\Delta z(i) + \Delta z(i-1))} + \frac{D_b(i+1/2)}{0.5(\Delta z(i) + \Delta z(i+1))} + \right.$$

$$\frac{n_b(i-1/2) [D_p(i-1/2) + D_c(i-1/2) K_c(i) \rho_c(i)]}{0.5 R_d(i)(\Delta z(i) + \Delta z(i-1))} +$$

$$\frac{n_b(i+1/2)[D_p(i+1/2)+D_c(i+1/2)K_c(i)\rho_c(i)]}{0.5R_d(i)(\Delta z(i)+\Delta z(i+1))}]S_b^k(i)$$

$$+[\frac{D_b(i+1/2)}{0.5(\Delta z(i)+\Delta z(i+1))}+$$

$$\frac{n_b(i+1/2)[D_p(i+1/2)+D_c(i+1/2)K_c(i+1)\rho_c(i+1)]}{0.5R_d(i+1)(\Delta z(i)+\Delta z(i+1))}]S_b^k(i+1)\}$$

$$+\frac{\Delta t[w(i+1/2)-w(i-1/2)]R_{dr}(i)}{\Delta z(i)R_d(i)}S_b^k(i) \qquad (A5.7)$$

where k+1 denotes the next time step of k, Δt is the time interval of advance, Δz is the thickness of the layer, i denotes the layer i, i-1 denotes the previous (higher) layer, i+1 denotes the next (lower) layer, i-1/2 indicates the upper boundary of layer i, and i+1/2 indicates the lower boundary of layer i. R_{dr} is the fraction factor of reworked pellets which may be different from R_d of the parent sediments.

At the surface layer there is a source in addition to the advection and diffusion exchange (see 4.2.2):

$$source = w_r[S_w R_{dr}/R_{dw} - \rho_r K_p S_w(1-M(t=t_r)/M_\infty)/R_{dw}$$

$$+ \rho_r K_p S_{br}(1-M(t=t_r)/M_\infty)/R_{dr}] \qquad (A5.8)$$

Therefore, the difference equation is

$$Sb(1)^{k+1} = Sb(1)^{k} + \frac{\Delta t \cdot w(0)}{\Delta z(1)} \{[R_{dr}/R_{dw} - \rho_r K_{pr}(1-M(t=t_r)/M_\infty)/R_{dw}]S_w^{k}$$

$$+ [\rho_r K_{pr}(1-M(t=t_r)/M_\infty)/R_{dr}]S_{br}^{k}\}$$

$$- \frac{\Delta t \cdot w(1+1/2)}{\Delta z(1)} S_b(1)^{k}$$

$$+ \frac{\Delta t}{\Delta z(1)} \{[\frac{D_b(0)}{0.5\Delta z(1)} + \frac{n_b(0)[D_p(0)+D_c(0)K_{cw}\rho_{cw}]}{0.5R_{dw}\Delta z(1)}]S_w^{k}$$

$$-[\frac{D_b(0)}{0.5\Delta z(1)} + \frac{D_b(1+1/2)}{0.5(\Delta z(1)+\Delta z(2))} +$$

$$\frac{n_b(0)[D_p(0)+D_c(0)K_c(1)\rho_c(1)]}{0.5R_d(1)\Delta z(1)} +$$

$$\frac{n_b(1+1/2)[D_p(1+1/2)+D_c(1+1/2)K_c(1)\rho_c(1)]}{0.5R_d(1)(\Delta z(1)+\Delta z(2))}]S_b(1)^{k}$$

$$+[\frac{D_b(1+1/2)}{0.5(\Delta z(1)+\Delta z(2))} +$$

$$\frac{n_b(1+1/2)[D_p(1+1/2)+D_c(1+1/2)K_c(2)\rho_c(2)]}{0.5R_d(2)(\Delta z(1)+\Delta z(2))}]S_b(2)^{k}\}$$

$$+ \frac{\Delta t[w(1+1/2)-w(0)]R_{dr}(1)}{\Delta z(1)R_d(1)} S_b^k(1) \qquad (A5.9)$$

in which (0) denotes the properties on the bed/water interface, subscript r denotes the properties in the reworked pellets, subscript w denotes the properties in the water. The water column receives a flux of desorbed mass (see 4.2.2), therefore, the difference equation is

$$S_w^{k+1} = S_w^k + \frac{\Delta t w(0)}{L_w R_{dr}} (n_{br}+n_{br}\rho_{cr}K_{cr}+\rho_r K_{pr}(M(t=t_r)/M_\infty)) S_{br}^k$$

$$- \frac{\Delta t w(0)}{L_w R_{dw}} (n_{br}+n_{br}\rho_{cr}K_{cr}+\rho_r K_{pr}(M(t=t_r)/M_\infty)) S_w^k$$

$$- \frac{\Delta t}{L_w} \left\{ \frac{D_b(0)}{0.5\Delta z(1)} + \frac{n_b(0)[D_p(0)+D_c(0)K_{cw}\rho_{cw}]}{0.5R_{dw}\Delta z(1)} \right\} S_w^k$$

$$+ \frac{\Delta t}{L_w} \left\{ \frac{D_b(0)}{0.5\Delta z(1)} + \frac{n_b(0)[D_p(0)+D_c(0)K_c(1)\rho_c(1)]}{0.5R_d(1)\Delta z(1)} \right\} S_b^k(1) \quad (A5.10)$$

The solid concentration in the sediment bed is updated by using the following difference equations:

in layer i:

$$\rho(i)^{k+1} = \rho(i)^k + \frac{\Delta t}{\Delta z(i)} \left[\frac{D_b(i-1/2)}{0.5(\Delta z(i) + \Delta z(i-1))} + w(i-1/2) \right] \rho(i-1)^k$$

$$- \frac{\Delta t}{\Delta z(i)} \left[\frac{D_b(i-1/2)}{0.5(\Delta z(i) + \Delta z(i-1))} + \frac{D_b(i+1/2)}{0.5(\Delta z(i) + \Delta z(i+1))} + \right.$$

$$\left. + w(i+1/2) - e(w(i+1/2) - w(i-1/2)) \right] \rho(i)^k$$

$$+ \frac{\Delta t}{\Delta z(i)} \frac{D_b(i+1/2)}{0.5(\Delta z(i) + \Delta z(i+1))} \rho(i+1)^k \tag{A5.11}$$

in the first layer:

$$\rho(1)^{k+1} = \rho(1)^k + \frac{\Delta t \, w(0)}{\Delta z(1)} \rho_r$$

$$- \frac{\Delta t}{\Delta z(1)} \left[\frac{D_b(1+1/2)}{0.5(\Delta z(1) + \Delta z(2))} \right.$$

$$\left. + w(1+1/2) - e(w(1+1/2) - w(0)) \right] \rho(1)^k$$

$$+ \frac{\Delta t}{\Delta z(1)} \frac{D_b(1+1/2)}{0.5(\Delta z(1) + \Delta z(1+1))} \rho(2)^k \tag{A5.12}$$

in which e is the enrichment factor given by

$$e = \rho(\text{reworked})/\rho$$

$$(\text{or} = f_{oc}(\text{reworked})/f_{oc}) \qquad (A5.13)$$

The colloid concentration is modelled with similar equations:

in the layer i:

$$\rho_c^{k+1}(i) = \rho_c^k(i) - \frac{\Delta t [w(i+1/2)\rho_c^k(i) - w(i-1/2)\rho_c^k(i-1)]}{\Delta z(i)}$$

$$+ \frac{\Delta t}{\Delta z(i)} \left\{ \left[\frac{D_b(i-1/2)}{0.5(\Delta z(i)+\Delta z(i-1))} + \frac{n_b(i-1/2)D_c(i-1/2)}{0.5(\Delta z(i)+\Delta z(i-1))} \right] \rho_c^k(i-1) \right.$$

$$- \left[\frac{D_b(i-1/2)}{0.5(\Delta z(i)+\Delta z(i-1))} + \frac{D_b(i+1/2)}{0.5(\Delta z(i)+\Delta z(i+1))} + \right.$$

$$\frac{n_b(i-1/2)D_c(i-1/2)}{0.5(\Delta z(i)+\Delta z(i-1))} + \frac{n_b(i+1/2)D_c(i+1/2)}{0.5(\Delta z(i)+\Delta z(i+1))} \left. \right] \rho_c^k(i)$$

$$\left. + \left[\frac{D_b(i+1/2)}{0.5(\Delta z(i)+\Delta z(i+1))} + \frac{n_b(i+1/2)D_c(i+1/2)}{0.5(\Delta z(i)+\Delta z(i+1))} \right] \rho_c^k(i+1) \right\}$$

$$+ \frac{\Delta t \cdot [w(i+1/2)-w(i-1/2)]}{\Delta z(i)} \rho_c^k(i) \qquad (A5.14)$$

and in the first layer:

$$\rho_c^{k+1}(1) = \rho_c^k(1) + \frac{\Delta t \, w(0)}{\Delta z(1)} \rho_{cw}^k - \frac{\Delta t \, w(1+1/2)}{\Delta z(1)} \rho_c^k(1)$$

218

$$+ \frac{\Delta t}{\Delta z(1)} \left\{ \left[\frac{D_b(0)}{0.5\Delta z(1)} + \frac{n_b(0)D_c(0)}{0.5\Delta z(1)} \right] \rho_{cw}^k \right.$$

$$- \left[\frac{D_b(0)}{0.5\Delta z(1)} + \frac{D_b(1+1/2)}{0.5(\Delta z(1)+\Delta z(2))} + \frac{n_b(0)D_c(0)}{0.5\Delta z(1)} + \right.$$

$$\left. \frac{n_b(1+1/2)D_c(1+1/2)}{0.5(\Delta z(1)+\Delta z(2))} \right] \rho_c^k(1)$$

$$+ \left[\frac{D_b(1+1/2)}{0.5(\Delta z(1)+\Delta z(2))} + \frac{n_b(1+1/2)D_c(1+1/2)}{0.5(\Delta z(1)+\Delta z(2))} \right] \rho_c^k(2) \right\}$$

$$+ \frac{\Delta t \cdot [w(1+1/2)-w(0)]}{\Delta z(1)} \rho_c^k(1) \qquad (A5.15)$$

A5.2 The Computer Program

The computer program to calculate the numerical solution is written in Microsoft BASIC 2.0 for Macintosh (Appendix 6). The environmental parameters can be input from keyboard or from a data file named "transinbed.data". After the first time of data solicitation all information is stored in the file, "transinbed.data". The format and the description of data in the file is as following:

file: transinbed.data

```
dumy,Dm,intraporo,ps,rad
Koc,foc,flag3$
popu1,popu2,rework1,rework2
Lb,ws,Dcol,e,flag1$,flag2$
nb
a(1,1),a(2,1),a(3,1),a(4,1),a(5,1),a(6,1)
a(1,2),a(2,2),a(3,2),a(4,2),a(5,2),a(6,2)
..........................................
..............,a(i,j),.....................
a(1,nb),.........................,a(6,nb)
Endtime
```

notations:

dumy = any number;

Dm = molecular diffusivity, D_m, cm^2/sec;

intrapore = intraparticle porosity, n, cm^3/cm^3;

ps = dry solid density in pellets, ρs, g/cm^3;

rad = particle radius or radius of cross-sectional circle of a
       cylindrical pellet, R, cm;

Koc = K_{oc}

foc = f_{oc}

flag3$: y = using f_{oc} for solid concentration,

         n = using ρ for solid concentration;

popu1 = population density of plow-like animals, cm^{-2};

popu2 = population density of conveyer-belt type animals, cm^{-2};

rework1 = individual reworking rate of "plow-like", cm^3/day;

rework2 = individual reworking rate of "conveyer-belt", cm^3/day;

Lb = mixing depth of "plow-like", cm;

ws = sedimentation rate, cm/year

Dcol = $D_{colloid}$, cm^2/s;

e = enrichment factor (ρ(reworked)/ρ(in the bed));

flag1\$: y = bed surface is equilibrated with the overlying water

(i.e., Db$\neq$0),

n = "Db=0";

flag2\$: y = infinite water volume (L_w=∞ or the concentration in water

is constant),

n = finite water volume;

nb = number of layers in the sediment bed;

a(i,j):

j: 1 = in pellets,

   2 = in water column,

   3 = first layer in the bed,

   4 = second layer in the bed,

   ....;

i: 1 = initial concentration, mol/cm^3;

   2 = porosity, cm^3/cm^3;

   3 = solid concentration, g/cm^3;

   4 = moving coloid concentration, g/cm^3;

   5 = feeding activity, (relative value);

   6 = layer thickness, cm;

Endtime = total simulation time, day.

Other parameters are derived from this basic information set. The

sediment velocity, w(z), is the combination of the sedimentation rate, w_s and

the reworking rate at depth z, i.e.,

$$w(z) = w_s + w_r (\int_0^z f(z)\,dz) / (\int_0^\infty f(z)\,dz) \qquad (A5.16)$$

The residence time, t_r, is calculated from the reworking rate and the diameter

of the pellets,

$$t_r = d/w_r \qquad\qquad\qquad (A5.17)$$

By assuming the geometric and tortuosity facter is n in the pellets with n

equal to 0.13 (see Chapter 2), I obtain the effective diffusivity, D_{eff}, in

the pellets as

$$D_{eff} = \frac{D_m n^2}{K_p(1-n)\rho_s} \qquad\qquad\qquad (A5.18)$$

in which

$$K_p = K_{oc} \cdot f_{oc} \qquad\qquad\qquad (A5.19)$$

The exchange fraction, $M(t=t_r)/M_\infty$, is estimated by using an analytical

solution for a uniform cylinder in an infinite bath (Crank, 1975). The

geometric factor in the sediment bed is also set to be n_b (i.e., i=1). Some

derived parameters are calculated and stored in a temporary matrix b(i,j), in

which

    b(i,j):

    i: 1 = in pellets

       2 = in water

       3 = in first layer

       . . . .

    j = 1 : w(i+1/2)

       2 : $0.5(\Delta z(i-1)+\Delta z(i))$

$3 \ : \ D_b(i-1/2)$

$4 \ : \ D_m \cdot (0.5(n_b(i-1)+n_b(i)))^2$

$5 \ : \ D_{col} \cdot (0.5(n_b(i-1)+n_b(i)))^2$

$6 \ : \ R_d \ (=n_b+e\rho K_p+n_b\rho_c K_c)$

$7 \ : \ R_{dr} \ (=n_b+e\rho K_p+n_b\rho_c K_c)$

The coefficients in the governing equations are calculated and stored in the (nb+2)x(nb+2) matrix m(i,j). The time step size, Δt, is adjusted to let the pivotal coefficient in the first layer, m(3,3), equal to or little larger than 0.5 which will allow a stable iteration.

The concentrations of the solid or the colloids will be updated if the transfer of media is taken into account. The final output including the time course of flux and the final profile will be printed on a line printer and sent to the data file named "clip:" (clipboard) for further processing.

```
REM     PROGRAM TRANSINBED 5.7
REM
DEFDBL a-m,o-z
DEFINT n
REM-------------Input data from file: transinbed.data------------------------
INPUT "Do you want use data stored in data file?",inputchoice$
IF LEFT$(inputchoice$,1)<>"y" GOTO keyinput
OPEN "transinbed.data" FOR INPUT AS #1
INPUT #1,dumb,Dm,intraporo,ps,rad
INPUT #1,Koc,foc,flag3$
INPUT #1,popu1,popu2,rework1,rework2
INPUT #1,Lb,ws,Dcol,e,flag1$,flag2$
INPUT #1,nb
DIM a(7,nb+2),b(7,nb+2),m(nb+2,nb+2),c(4,nb+2),p(nb+2,nb+2),g(nb+2,nb+2)
FOR n=1 TO nb+2
        INPUT #1,a(1,n),a(2,n),a(3,n),a(4,n),a(5,n),a(6,n)
NEXT n
INPUT #1,Endtime
INPUT #1,Flag4$,Flag5$
CLOSE #1
GOTO calpara
REM-------------Input intrparticle diffusion parameters--------------------
keyinput:
INPUT "Molecular diffusivity (cm^2/s)?",Dm
INPUT "Intraparticle porosity?",intraporo
INPUT "Dry solid density (g/cm^3)?",ps
INPUT "Particle or pellet radius (cm)?",rad
GOSUB Kpvalue
REM-------------Input environmental parameters---------------------------
INPUT "Population density of plow-like (#/cm^2)",popu1
INPUT "Population density of conveyer-belt (#/cm^2)",popu2
INPUT "Individual reworking rate by plow-like (cm^3/day)",rework1
INPUT "individual reworking rate by conveyer-belt (cm^3/day)",rework2
INPUT "plow-like bioturbation depth (cm)",Lb
INPUT "Sedimentation rate (cm/year)",ws
INPUT "Diffusivity of colloids (cm^2/s)",Dcol
INPUT "Ingestion enrichment factor",e
INPUT "Is there equilibrium on the interface?",t$
flag1$=LEFT$(t$,1)
INPUT "Infinite water volume?",t$
flag2$=LEFT$(t$,1)
INPUT "Do you want to use foc to represent solid concentration?",t$
flag3$=LEFT$(t$,1)
REM-------------input model setup and initial condition--------------------
INPUT "How many boxes in the sediment bed",nb
DIM a(7,nb+2),b(7,nb+2),m(nb+2,nb+2),c(4,nb+2),p(nb+2,nb+2),g(nb+2,nb+2)
FOR na=6 TO 1 STEP -1
    ON na GOTO one,two,three,four,five,six
        one:
          PRINT "total concentration (cm^-3):":GOTO startA
        two:
          PRINT "porosity:":GOTO startA
        three:
          PRINT "solid density (g/cm^3):":GOTO startA
        four:
          PRINT "DOC (g/cm^3):":GOTO startA
        five:
```

```
        PRINT "reworking activity (relative value):":GOTO startA
      six:
        PRINT "box depth (cm):"
  startA:
  INPUT"In pellets?";a(na,1)
  INPUT"In water?";a(na,2)
  FOR n=3 TO nb+2
      PRINT "box";n-2:INPUT a(na,n)
  NEXT n
NEXT na
INPUT "End time of simulation=?";Endtime
INPUT "Do you want to update solid concentration";t$
Flag4$=LEFT$(t$,1)
INPUT "Do you wnat to update colloid concentration";t$
Flag5$=LEFT$(t$,1)
REM-----------Store input data in file: transinbed.data----------------------
OPEN "transinbed.data" FOR OUTPUT AS #1
WRITE #1,dumb;Dm;intraporo;ps;rad
WRITE #1,Koc;foc;flag3$
WRITE #1,popu1;popu2;rework1;rework2
WRITE #1,Lb;ws;Dcol;e;flag1$;flag2$
WRITE #1,nb
PRINT USING "#.###^^^^    ";dumb;Dm;intraporo;ps;rad
PRINT USING "#.###^^^^    ";Koc;foc
PRINT USING "#.###^^^^    ";popu1;popu2;rework1;rework2
PRINT Lb;ws;Dcol;e;flag1$;flag2$
PRINT USING "#.###^^^^    ";nb
FOR n=1 TO nb+2
        WRITE #1,a(1,n);a(2,n);a(3,n);a(4,n);a(5,n);a(6,n)
        PRINT USING "#.###^^^^    ";a(1,n);a(2,n);a(3,n);a(4,n);a(5,n);a(6,n)
NEXT n
WRITE #1,Endtime
PRINT USING "#.###^^^^    ";Endtime
WRITE #1,Flag4$;Flag5$
PRINT Flag4$;Flag5$
CLOSE #1
GOTO calpara
REM------------Calculate working parameters-------------------------------------
calpara:
REM-------reworking rate and rework-induced sediment velocity----------------
plow=popu1*rework1
IF flag1$="y" THEN plow=0
worm=popu2*rework2
activity=0
FOR n=3 TO nb+2
   activity=activity+a(5,n)*a(6,n)
NEXT n
IF activity=0 THEN activity=1
aty=0
b(1,2)=plow+worm+ws/365
FOR n=3 TO nb+2
   aty=aty+a(5,n)*a(6,n)
   b(1,n)=ws/365+worm*(1-aty/activity)              'total w
NEXT n
REM-------------Calculate Mt-----------------------------------------------------
Kp=Koc*foc
GOSUB Deffvalue
IF flag3$="y" THEN Kp=Koc
wr=popu1*rework1+popu2*rework2   '(cm/day)
tr=rad*2/(wr+1E-10)
```

```
dt=Deff*86400!*tr/rad^2
CALL CylinderOpen(Mt,dt)
REM-------------calculate diffusities-------------------------------------
Db=Lb*popu1*rework1
Kc=Koc
Cw=a(1,2)
FOR n=3 TO nb+2
   b(2,n)=.5*(a(6,n-1)+a(6,n))                          '0.5*(z(i-1)+z(i))
   b(3,n)=Db                                            'Db
   IF a(7,n)>=Lb THEN b(3,n)=0
   b(4,n)=Dm*(.5*(a(2,n-1)+a(2,n)))^2*86400!            'Dp
   b(5,n)=Dcol*(.5*(a(2,n-1)+a(2,n)))^2*86400!          'Dc
   b(6,n)=a(2,n)+a(3,n)*Kp+a(2,n)*a(4,n)*Kc             'Rd
   b(7,n)=a(2,n)+e*a(3,n)*Kp+a(2,n)*a(4,n)*Kc           'Rde
NEXT n
b(2,3)=.5*a(6,3)
IF flag1$<>"y" THEN b(3,3)=0
b(6,2)=a(2,2)+a(3,2)*Kp+a(2,2)*a(4,2)*Kc               'Rd  in water
b(6,1)=a(2,1)+a(3,1)*Kp+a(2,1)*a(4,1)*Kc               'Rd  in pellet
b(6,2)=a(2,2)+a(3,2)*Kp+a(2,2)*a(4,2)*Kc               'Rd  in water
b(6,1)=a(2,1)+a(3,1)*Kp+a(2,1)*a(4,1)*Kc               'Rd  in pellet
a(7,2)=0
a(7,3)=.5*a(6,3)
FOR n=4 TO nb+2
     a(7,n)=a(7,n-1)+b(2,n)
NEXT n
IF flag5$="y" GOTO colloidTime
m33=1/a(6,3)*(b(3,3)/b(2,3)+b(4,3)/b(6,3)/b(2,3)+b(5,3)*Kc*a(4,3)/b(6,3)/b(2,3
))

m33=m33+1/a(6,3)*(b(3,4)/b(2,4)+b(4,4)/b(6,3)/b(2,4)+b(5,4)*Kc*a(4,3)/b(6,3)/b
(2,4))
     m33=m33+1/a(6,3)*b(1,3)+b(7,3)/b(6,3)*t/a(6,3)*(b(1,3)-b(1,2))
GOTO calTime
colloidTime:
m33=1/a(6,3)*(b(3,3)/b(2,3)+b(4,3)/b(6,3)/b(2,3)+b(5,3)/b(2,3))
     m33=m33+1/a(6,3)*(b(3,4)/b(2,4)+b(4,4)/b(6,3)/b(2,4)+b(5,4)/b(2,4))
     m33=m33+1/a(6,3)*b(1,3)+b(7,3)/b(6,3)*t/a(6,3)*(b(1,3)-b(1,2))
calTime:
t=.49/m33
IF t>Endtime/125 THEN t=Endtime/125
REM--------------------set matrix-------------------------------------------
GOSUB SetMatrix
GOSUB ColloidUpdateMatrix
GOSUB MediumUpdateMatrix
REM------------------------iteration----------------------------------------
ts=0
initialmass=0
FOR n=1 TO nb+2
   initialmass=initialmass+a(1,n)*a(6,n)
NEXT n
REM---------------initial medium mass---------------------------------------
nm=3
initialmassM=0
FOR n=1 TO nb+2
   initialmassM=initialmassM+a(nm,n)*a(6,n)
NEXT n
REM-----------------------------------------------------------------------
plottime=Endtime/25
tp=plottime
```

```
Flag6$="n"
IF Flag4$="y" THEN Flag6$="y"
IF Flag5$="y" THEN Flag6$="y"
OPEN "clip:" FOR OUTPUT AS #2
PRINT
PRINT "time          flux"
FOR nt=1 TO 25
  iteration:
  a(1,1)=0
  FOR n=3 TO nb+2
      a(1,1)=a(1,1)+m(1,n)*a(1,n)
  NEXT n
  FOR n=2 TO nb+1
      c(1,n)=0
      FOR na=n-1 TO n+1
          c(1,n)=c(1,n)+m(n,na)*a(1,na)
      NEXT na
  NEXT n
  c(1,3)=c(1,3)+m(3,1)*a(1,1)
  c(1,nb+2)=m(nb+2,nb+1)*a(1,nb+1)+m(nb+2,nb+2)*a(1,nb+2)
  ts=ts+t
  flux=c(1,2)-a(1,2)
  FOR n=1 TO nb+2
      a(1,n)=c(1,n)
  NEXT n
  IF flag2$="y" THEN a(1,2)=Cw
REM
REM----------------------update medium concentration----------------------
REM
IF Flag6$="n" THEN GOTO skip
IF Flag4$="y" THEN GOSUB MediumUpdate
IF Flag5$="y" THEN GOSUB ColloidUpdate
GOSUB SetMatrix
skip:
REM----------------------------------------------------------------------
  IF ts<tp-.00001 THEN GOTO iteration
  fluxp!=flux*a(6,2)/t
  tp=tp+plottime
  tsp!=ts
  WRITE #2,tsp!;fluxp!
  LPRINT USING "   #.###^^^^  ";tsp!;fluxp!
  PRINT USING "#.###^^^^  ";tsp!;fluxp!
NEXT nt
finalmass=0
LPRINT "  depth            conc."
PRINT "depth         conc."
FOR n=2 TO nb+2
   finalmass=finalmass+a(1,n)*a(6,n)
   a7!=a(7,n)
   a1!=a(1,n)
   LPRINT USING"   #.###^^^^  ";a7!;a1!
   PRINT USING"#.###^^^^  ";a7!;a1!
   WRITE #2,a7!;a1!
NEXT n
LPRINT "  Mt= ";Mt
LPRINT "  initial mass= ";initialmass
LPRINT "  final mass= ";finalmass
LPRINT "  time interval= ";t
PRINT "Mt= ";Mt
PRINT "initial mass= ";initialmass
```

```basic
PRINT "final mass= ";finalmass
PRINT "time interval= ";t
REM---------------------------------print medium data----------------------------
finalmassM=0
LPRINT "   depth              conc."
FOR n=1 TO nb+2
    finalmassM=finalmassM+a(nm,n)*a(6,n)
    a7!=a(7,n)
    al!=a(nm,n)
    LPRINT USING"   #.###^^^^   ";a7!;al!
    WRITE #2,a7!;al!
NEXT n
LPRINT "   initial mass= ";initialmassM
LPRINT "   final mass= ";finalmassM
CLOSE #2
END
REM-----------------------------------------------------------------------
REM          Subroutine to estimate the value of Kp
REM-----------------------------------------------------------------------
KpValue:
    PRINT "What is known?"
    INPUT "Koc(=1) or Kow(=2)";k%
  ON k% GOTO Koc,Kow
  Koc:
    INPUT "Enter Koc(cm^3/g) and foc(g/g)";Koc
    INPUT foc
  GOTO fine
  Kow:
    GOSUB KowToKp
  fine:
 RETURN
REM-----------------------------------------------------------------------
REM              subroutine to estimate Kp from Kow
REM-----------------------------------------------------------------------
KowToKp:
  INPUT "Enter Kow";Kow
  PRINT "Which equation do you want to use ?"
  PRINT
  PRINT "eq.1: log Koc=log Kow - 0.21"
  PRINT "eq.2: logKoc=0.72 log Kow + 0.49"
  INPUT eq%
  ON eq% GOTO eq1,eq2
    eq1:
      Koc=10^(.4343*LOG(Kow)-.21):GOTO done
    eq2:
      Koc=10^(.72*.4343*LOG(Kow)+.49)
   done:
  INPUT"Enter foc";foc
  RETURN
REM-----------------------------------------------------------------------
REM          subroutine to determine Deff from Dm, porosity,and dry density
REM-----------------------------------------------------------------------
  DeffValue:
      Deff=Dm*intraporo^2/Kp/e/(1-intraporo)/ps
  RETURN
 REM
 REM---------subroutine for diffusion in cylinder w/open system--------------
 REM
 SUB CylinderOpen(mmt,dt)STATIC
   IF dt>.001 THEN GOTO longrun
```
228

```
        mmt=4!*SQR(dt)/1.77245-3!*dt-.18806*dt^1.5
        GOTO endmtopen
    longrun:
    j(1)=2.40483
    j(2)=5.52008
    j(3)=8.65373
    j(4)=11.79153
    j(5)=14.93092
    j(6)=18.07106
    sum=0!
    FOR nn=1 TO 6
        sum=sum+4!/j(nn)^2*EXP(-dt*j(nn)^2)
    NEXT nn
        mmt=1-sum
endmtopen:
END SUB
REM------------------------------------------------------------------------
REM                         subroutine setting matrix values
REM------------------------------------------------------------------------
SetMatrix:
FOR n=3 TO nb+2
m(1,n)=(b(1,n-1)-b(1,n))/(worm+plow+1E-10)*b(7,n)/b(6,n)
NEXT n
m(2,1)=t/a(6,2)*(worm+plow)*(a(2,1)+a(2,1)*a(4,1)*Kc+a(3,1)*Kp*Mt)/b(6,1)
m(2,2)=1-t/a(6,2)*(worm+plow)*(a(2,1)+a(2,1)*a(4,1)*Kc+a(3,1)*Kp*Mt)/b(6,2)

m(2,2)=m(2,2)-t/a(6,2)*(b(3,3)/b(2,3)+b(4,3)/b(6,2)/b(2,3)+b(5,3)*Kc*a(4,2)/b(
6,2)/b(2,3))
m(2,3)=t/a(6,2)*(b(3,3)/b(2,3)+b(4,3)/b(6,3)/b(2,3)+b(5,3)*Kc*a(4,3)/b(6,3)/b(
2,3))
m(3,1)=t/a(6,3)*(worm+plow)*(1-Mt)*a(3,1)*Kp/b(6,1)
m(3,2)=t/a(6,3)*(worm+plow)*(b(6,1)-(1-Mt)*a(3,1)*Kp)/b(6,2)

m(3,2)=m(3,2)+t/a(6,3)*(b(3,3)/b(2,3)+b(4,3)/b(6,2)/b(2,3)+b(5,3)*Kc*a(4,2)/b(
6,2)/b(2,3))
m(3,3)=1-t/a(6,3)*(b(3,3)/b(2,3)+b(4,3)/b(6,3)/b(2,3)+b(5,3)*Kc*a(4,3)/b(6,3)/
b(2,3))

m(3,3)=m(3,3)-t/a(6,3)*(b(3,4)/b(2,4)+b(4,4)/b(6,3)/b(2,4)+b(5,4)*Kc*a(4,3)/b(
6,3)/b(2,4))
        m(3,3)=m(3,3)-t/a(6,3)*b(1,3)+b(7,3)/b(6,3)*t/a(6,3)*(b(1,3)-b(1,2))
m(3,4)=t/a(6,3)*(b(3,4)/b(2,4)+b(4,4)/b(6,4)/b(2,4)+b(5,4)*Kc*a(4,4)/b(6,4)/b(
2,4))
FOR n=4 TO nb+1
m(n,n-1)=t/a(6,n)*(b(3,n)/b(2,n)+b(4,n)/b(6,n-1)/b(2,n)+b(5,n)*Kc*a(4,n-1)/b(6
,n-1)/b(2,n)+b(1,n-1))
m(n,n)=1-t/a(6,n)*(b(3,n)/b(2,n)+b(4,n)/b(6,n)/b(2,n)+b(5,n)*Kc*a(4,n)/b(6,n)/
b(2,n))

m(n,n)=m(n,n)-t/a(6,n)*(b(3,n+1)/b(2,n+1)+b(4,n+1)/b(6,n)/b(2,n+1)+b(5,n+1)*Kc
*a(4,n)/b(6,n)/b(2,n+1))
        m(n,n)=m(n,n)+t/a(6,n)*(b(7,n)/b(6,n)*(b(1,n)-b(1,n-1))-b(1,n))
m(n,n+1)=t/a(6,n)*(b(3,n+1)/b(2,n+1)+b(4,n+1)/b(6,n+1)/b(2,n+1)+b(5,n+1)*Kc*a(
4,n+1)/b(6,n+1)/b(2,n+1))
NEXT n
n=nb+2
m(n,n-1)=t/a(6,n)*(b(3,n)/b(2,n)+b(4,n)/b(6,n-1)/b(2,n)+b(5,n)*Kc*a(4,n-1)/b(6
,n-1)/b(2,n)+b(1,n-1))
m(n,n)=1-t/a(6,n)*(b(3,n)/b(2,n)+b(4,n)/b(6,n)/b(2,n)+b(5,n)*Kc*a(4,n)/b(6,n)/
b(2,n))
```

```basic
            m(n,n)=m(n,n)+t/a(6,n)*(b(7,n)/b(6,n)*(b(1,n)-b(1,n-1))-b(1,n))
REM
REM-------------------set solid updating matrix-------------------------
REM
MediumUpdateMatrix:
FOR n=3 TO nb+2
p(1,n)=(b(1,n-1)-b(1,n))/(worm+plow+1E-10)*e
NEXT n
p(3,1)=t/a(6,3)*(worm+plow)
p(3,3)=1-t/a(6,3)*b(3,4)/b(2,4)
      p(3,3)=p(3,3)-t/a(6,3)*(b(1,3)-(b(1,3)-b(1,2))*e)
p(3,4)=t/a(6,3)*b(3,4)/b(2,4)
FOR n=4 TO nb+1
p(n,n-1)=t/a(6,n)*(b(3,n)/b(2,n)+b(1,n-1))
p(n,n)=1-t/a(6,n)*(b(3,n)/b(2,n))
      p(n,n)=p(n,n)-t/a(6,n)*(b(3,n+1)/b(2,n+1))
      p(n,n)=p(n,n)+t/a(6,n)*(e*(b(1,n)-b(1,n-1))-b(1,n))
p(n,n+1)=t/a(6,n)*(b(3,n+1)/b(2,n+1))
NEXT n
n=nb+2
p(n,n-1)=t/a(6,n)*(b(3,n)/b(2,n)+b(1,n-1))
p(n,n)=1-t/a(6,n)*(b(3,n)/b(2,n))
      p(n,n)=p(n,n)+t/a(6,n)*(e*(b(1,n)-b(1,n-1))-b(1,n))
RETURN
REM
REM-------------------update solid concentration----------------------
REM
MediumUpdate:
   a(3,1)=0
   FOR n=3 TO nb+2
      a(3,1)=a(3,1)+p(1,n)*a(3,n)
   NEXT n
   FOR n=4 TO nb+1
      c(3,n)=0
      FOR na=n-1 TO n+1
         c(3,n)=c(3,n)+p(n,na)*a(3,na)
      NEXT na
   NEXT n
   c(3,3)=p(3,1)*a(3,1)+p(3,3)*a(3,3)+p(3,4)*a(3,4)
   c(3,nb+2)=p(nb+2,nb+1)*a(3,nb+1)+p(nb+2,nb+2)*a(3,nb+2)
   FOR n=3 TO nb+2
      a(3,n)=c(3,n)
   NEXT n
RETURN
REM
REM-------------------set Colloid updating matrix----------------------
REM
ColloidUpdateMatrix:
FOR n=3 TO nb+2
g(1,n)=(b(1,n-1)-b(1,n))/(worm+plow+1E-10)*e
NEXT n
g(3,1)=t/a(6,3)*(worm+plow)
g(3,3)=1-t/a(6,3)*(b(3,4)/b(2,4)+b(5,3)/b(2,3)+b(5,4)/b(2,4))
     g(3,3)=g(3,3)-t/a(6,3)*(b(1,3)-(b(1,3)-b(1,2))*e)
g(3,4)=t/a(6,3)*(b(3,4)/b(2,4)+b(5,4)/b(2,4))
FOR n=4 TO nb+1
g(n,n-1)=t/a(6,n)*(b(3,n)/b(2,n)+b(5,n)/b(2,n)+b(1,n-1))
g(n,n)=1-t/a(6,n)*(b(3,n)/b(2,n)+b(5,n)/b(2,n))
     g(n,n)=g(n,n)-t/a(6,n)*(b(3,n+1)/b(2,n+1)+b(5,n+1)/b(2,n+1))
     g(n,n)=g(n,n)+t/a(6,n)*(e*(b(1,n)-b(1,n-1))-b(1,n))
```

```
  g(n,n+1)=t/a(6,n)*(b(3,n+1)/b(2,n+1)+b(5,n+1)/b(2,n+1))
NEXT n
n=nb+2
g(n,n-1)=t/a(6,n)*(b(3,n)/b(2,n)+b(5,n)/b(2,n)+b(1,n-1))
g(n,n)=1-t/a(6,n)*(b(3,n)/b(2,n)+b(5,n)/b(2,n))
    g(n,n)=g(n,n)+t/a(6,n)*(e*(b(1,n)-b(1,n-1))-b(1,n))
RETURN
REM
REM-------------------update Colloid concentration-------------------------
REM
ColloidUpdate:
  a(4,1)=0
  FOR n=3 TO nb+2
     a(4,1)=a(4,1)+g(1,n)*a(4,n)
  NEXT n
  FOR n=4 TO nb+1
     c(4,n)=0
     FOR na=n-1 TO n+1
        c(4,n)=c(4,n)+g(n,na)*a(4,na)
     NEXT na
  NEXT n
  c(4,3)=g(3,1)*a(4,1)+g(3,3)*a(4,3)+g(3,4)*a(4,4)
  c(4,nb+2)=g(nb+2,nb+1)*a(4,nb+1)+g(nb+2,nb+2)*a(4,nb+2)
  FOR n=3 TO nb+2
     a(4,n)=c(4,n)
  NEXT n
RETURN
END
```

EN
PLEA